POWERSOUTH
ENERGY COOPERATIVE

Charles R. Lowman Power Plant

Leroy, AL

Structural Stability Summary Report

Unit 1 Bottom Ash Pond

Issued October 2016

CDG Engineers and Associates, Inc.
1840 East Three Notch St.
Andalusia, AL 36421
| cdge.com

POWERSOUTH
ENERGY COOPERATIVE

REPORT

Structural Stability Summary Report
Unit 1 Bottom Ash Pond
Charles R. Lowman Power Plant

October 2016

R. DANIEL WELLS
10/15/16

CDG
Engineering. Environmental. Answers.

TABLE OF CONTENTS

1.0 UNIT 1 BOTTOM ASH POND 2
  1.1 Operator Information 2
  1.2 Location 2
  1.3 Statement of Purpose 2
  1.4 Foundation and Embankments 2
  1.5 Slope Protection and Vegetation 3
  1.6 Spillways and Diversion Systems 3
  1.7 Periodic Safety Factor Assessments 4
  1.8 Engineer's Certification 4

Appendix A

Figure 1- USGS Location Map

Figure 2- Unit 1 Aerial Map of Impoundments

References

CDG Engineers and Associates Inc. (2016). Report of Safety Factor Assessment; Coal Combustion Residuals Impoundment Embankments, Charles R. Lowman Power Plant. Andalusia, AL.

CDG Engineers and Associates, Inc. (2016). History of Construction Unit 1 Bottom Ash Pond, Charles R. Lowman Power Plant. Andalusia, AL.

CDG Engineers and Associates, Inc. (2016). Inflow Design Control Plan Unit 1 Bottom Ash Pond, Charles R. Lowman Power Plant. Andalusia, AL.

1.0 UNIT 1 BOTTOM ASH POND

1.1 Operator Information

Name: Unit 1 Bottom Ash Pond

Owner/Operator: PowerSouth Energy Cooperative, Inc.
Charles R. Lowman Power Plant
Leroy, AL 36458

State ID: None Assigned

1.2 Location

The Unit 1 Bottom Ash Pond is located in Section 18, Township 6N, Range 2 East in Washington, County Alabama and more specifically on the Western bank of the Tombigbee River. Figures 1 and 2 of this report show the location of the Pond.

1.3 Statement of Purpose

The Unit 1 Bottom Ash Pond is currently used as a settling pond for CCR wastes containing bottom ash, fly ash, and other plant wastes. Bottom ash from Unit 1 is transported to the impoundment via wet sluicing. In addition to the bottom ash sluicing operation, the Facility periodically disposes of fly ash and scrubber waste within the impoundment through similar methods.

1.4 Foundation and Embankments

The Unit 1 Bottom Ash Pond was constructed in 1965 in conjunction with Unit 1 of the Charles R. Lowman Power Plant. Based on a review of the available documentation, the Unit 1 Bottom Ash Pond was constructed by excavating below the original ground surface to a depth of ±EL 10' to EL 13'. The excavated soils were used as fill to construct the impoundment embankments. Per the available information shown on the construction plans created by Stanley Engineering Company circa 1965 the pre-construction ground surface elevation within the pond area ranged from ±EL 17' to EL 29'.

The Unit 1 Bottom Ash Pond contains exterior berms located on its northern, southern and eastern sides. The impoundment is bordered to the west by the Facility's entrance road and rail system which serves as an interior berm between the Unit 1 Bottom Ash Pond and the Unit 2/3 Bottom Ash Pond. The northern berm of the Unit 1 Bottom Ash Pond is formed by broad fill placement extending in excess of 200' from the impoundment which contains various Plant infrastructure and systems.

The crest of the embankments range from approximately EL 35' to EL 38'. Based on a review of the impoundment plans and recent topographic survey the embankments were constructed at an inclination of 2(H):1(V) and flatter. The maximum height of exterior embankments is approximately 15 feet, which is located along the eastern embankment.

Based on soil boring information, the Unit 1 Bottom Ash Pond embankments and underlying foundation soils consist of fill, Low Terrace Deposits and Coastal Plain Deposits. Fill thicknesses ranged from approximately 7' to 18'. The fill soils are comprised of silty and clayey, fine to medium-grained sand and fine sandy clay. Standard Penetration Tests (SPT) in the fill indicated a variable consistency with N-values typically ranging from 4 to 23 blows per foot (bpf).

The foundation soils underlying the embankments consist of Low Terrace Deposits and Coastal Plain Deposits. Low Terrace Deposits are water-deposited soils typically resulting from meanderings of rivers and streams. The Charles R. Lowman Power Plant is located along the western bank of the Tombigbee River. Therefore, the Terrace Deposits at this site appear to have resulted from meanderings and flooding of the Tombigbee River.

Based on operational parameters provided by the owner, historical construction data and recent engineering analysis, it is our opinion that the Unit 1 Bottom Ash Pond exhibits suitable stability for its anticipated maximum CCR and CCR wastewater levels. For further information on foundations and embankments refer to the Report for Safety Factor Assessment, dated October 2016.

1.5 Slope Protection and Vegetation

All Unit 1 Bottom Ash Pond slopes are comprised of compacted embankment fill material and an established stand of grass. Vegetation is such that erosion due to surface flows and wave action is resisted and the erosive effects are minimal.

For further information on slope protection and vegetation refer to the History of Construction Unit 1 Bottom Ash Pond, dated October 2016.

1.6 Spillways and Diversion Systems

The Unit 1 Bottom Ash Decant structure is known as the Unit 1 Intake. The Unit 1 Intake consists of two suction lift pumps with a normal operating flow of 800 gpm (1.78 cfs). The pumps are fed by two floating intake hoses that allow for the removal of liquids from the laminar portion of the impounded waters.

The Unit 1 Intake structure is capable of adequately managing the flow from the 1000-yr flood event. The Unit 1 Intake allows for a maximum hydraulic grade (HGL) of 32.4' MSL. This maximum HGL leaves a freeboard of 2.6' in the pond.

There are no hydraulic structures passing through or under any of the pond structural berms.

During high rainfall events, mobile suction lift pumps are utilized at the pond to supplement permanent intake structures to control the flood event and to maintain pool operating levels.

For further information on spillways and diversion systems refer to the Inflow Design Control Plan Unit 1 Bottom Ash Pond, dated October 2016.

1.7 Periodic Safety Factor Assessments

40 CFR 257.73 (e)(1)(i) through (e)(1)(iv) requires that the stability of CCR impoundment embankments be periodically evaluated. A stability evaluation was conducted on the exterior embankments associated with the Unit 1 Bottom Ash Ponds and is detailed in the Report for Safety Factor Assessment, dated October 2016.

The evaluation indicates that the embankments exhibit factors of safety that equal or exceed the required minimum values under the maximum storage pool, maximum surcharge pool and seismic loading scenarios. Additionally, the embankment soils are demonstrated not to be susceptible to liquefaction, and further analyses under the liquefaction loading scenario is not required. Therefore, the embankments are in compliance with the periodic safety factor assessment requirements. The following table summarizes the results of our analyses.

Summary of Analyses Results - Unit 1 Bottom Ash Pond

Loading Condition	Calculated Minimum Factor of Safety	Required Factor of Safety	Conforms to Regulations
Long-Term Maximum Storage Pool	1.6	1.5	Yes
Maximum Surcharge Pool	1.6	1.4	Yes
Seismic	1.0	1.0	Yes
Liquefaction	1.8	1.2	Yes

For further information on the Unit 1 Bottom Ash Pond safety factor assessments please refer to the Report for Safety Factor Assessment, dated October 2016.

The potential for instability in the exterior Unit 1 Bottom Ash Pond embankments was evaluated based on loading associated with rapid drawdown. This potential scenario would involve flooding of the Tombigbee River followed by a subsequent rapid drop in water elevation as the flood waters subside. Based on available data (USGS, Station 02470050), the maximum recession rate of the flood waters occurs relatively slowly at approximately 2.5 feet per day. Excess pore pressures within the primarily granular berm soils are able to dissipate due to the slow drop in flood waters. Therefore, a rapid drawdown condition does not develop within the exterior embankment and further analysis is not warranted.

1.8 Engineer's Certification

The findings in this report were developed from visual observations made by CDG personnel during the preparation of this report and its supporting documents. If significant changes are made to the use of the upstream and downstream areas or capacity of the impoundments, CDG should be allowed to review our findings in light of the changes to determine if an alternate hazard potential classification is warranted. This report was created in accordance with the CCR rule Section 257.73(d) (i) through (vii). All future periodic assessments shall be conducted in accordance with this rule and any of its revisions or additions at the time of the assessment.

Appendix A

Figure 1- Unit 1 Bottom Ash Pond Location Map

Figure 2 – Unit 1 Aerial Map of Impoundments

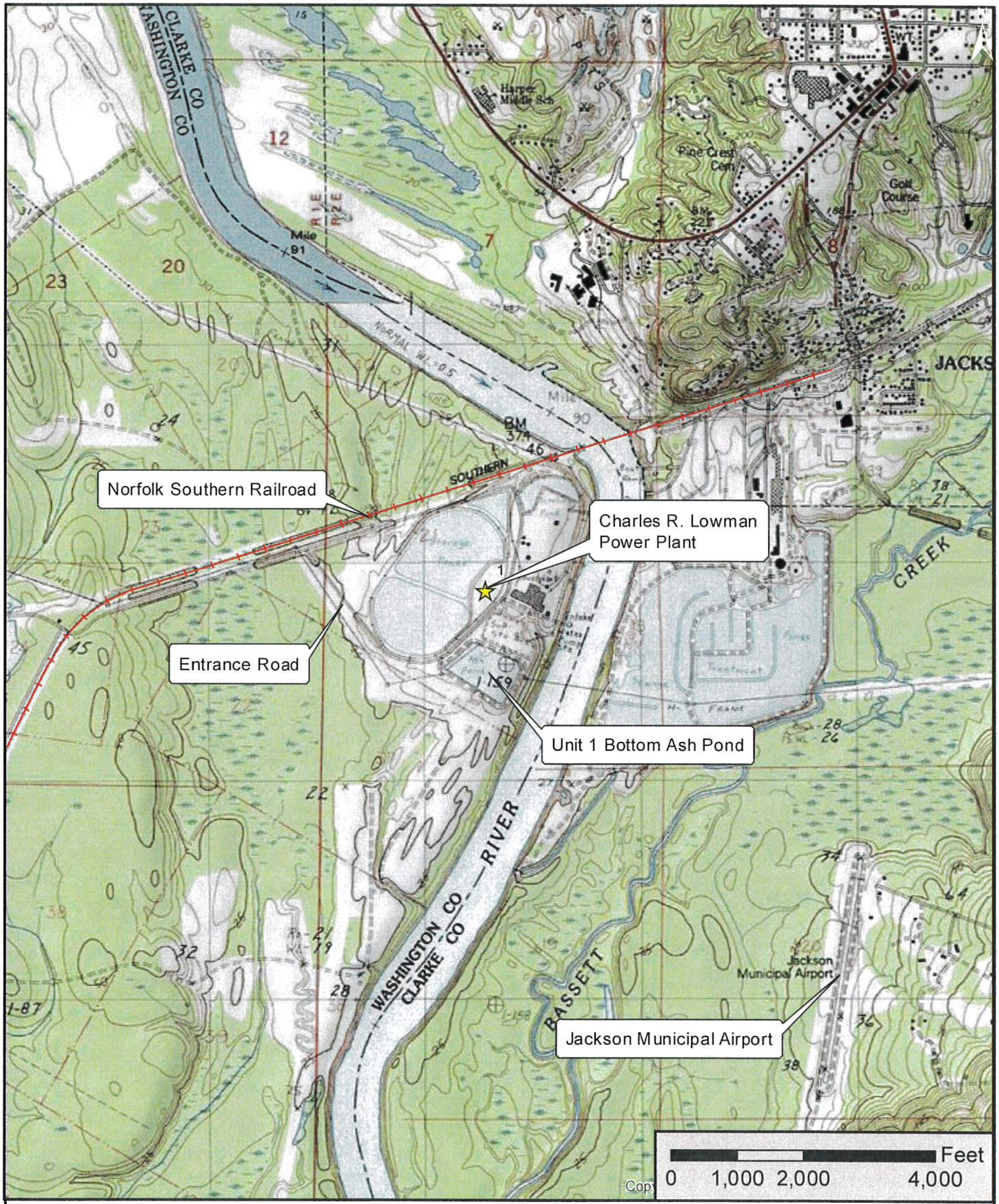

Figure 1 - Unit 1 Bottom Ash Pond Location Map

Charles R. Lowman Power Plant
PowerSouth Energy Cooperative
Leroy, AL

CDG
Engineering. Environmental. Answers.

October 2016

Figure 2 - Unit 1 Aerial Map of Impoundments

Charles R. Lowman Power Plant
PowerSouth Energy Cooperative
Leroy, AL

CDG
Engineering. Environmental. Answers.

October 2016

PowerSouth
ENERGY COOPERATIVE

Charles R. Lowman Power Plant Leroy, AL

Structural Stability Summary Report

Unit 2/3 Bottom Ash Pond

Issued October 2016

CDG Engineers and Associates, Inc.
1840 East Three Notch St.
Andalusia, AL 36421
| cdge.com

POWERSOUTH
ENERGY COOPERATIVE

REPORT
Structural Stability Summary Report
Unit 2/3 Bottom Ash Pond
Charles R. Lowman Power Plant

October 2016

R. DANIEL WEL
12/15/14

CDG
Engineering. Environmental. Answers.

TABLE OF CONTENTS

1.0 UNIT 2/3 BOTTOM ASH POND 2
  1.1 Operator Information 2
  1.2 Location 2
  1.3 Statement of Purpose 2
  1.4 Foundation and Embankments 2
  1.5 Slope Protection and Vegetation 3
  1.6 Spillways and Diversion Systems 3
  1.7 Periodic Safety Factor Assessments 3
  1.8 Engineer's Certification 4

Appendix A

Figure 1- USGS Location Map

Figure 2- Unit 2/3 Aerial Map of Impoundments

References

CDG Engineers and Associates Inc. (2016). Report of Safety Factor Assessment; Coal Combustion Residuals Impoundment Embankments, Charles R. Lowman Power Plant. Andalusia, AL.

CDG Engineers and Associates, Inc. (2016). History of Construction Unit 2/3 Bottom Ash Pond, Charles R. Lowman Power Plant. Andalusia, AL.

CDG Engineers and Associates, Inc. (2016). Inflow Design Control Plan Unit 2/3 Bottom Ash Pond, Charles R. Lowman Power Plant. Andalusia, AL.

1.0 UNIT 2/3 BOTTOM ASH POND

1.1 Operator Information

Name: Unit 2/3 Bottom Ash Pond

Owner/Operator: PowerSouth Energy Cooperative, Inc.
Charles R. Lowman Power Plant
Leroy, AL 36458

State ID: None Assigned

1.2 Location

The Unit 2/3 Bottom Ash Pond is located in Section 18, Township 6N, Range 2 East in Washington, County Alabama and more specifically on the Western bank of the Tombigbee River. Figures 1 and 2 of this report show the location of the Pond.

1.3 Statement of Purpose

The Unit 2/3 Bottom Ash Pond is currently used as a settling pond for CCR wastes containing bottom ash, fly ash, and other plant wastes. Bottom ash from Units 2 and 3 is transported to the impoundment via wet sluicing. In addition to the bottom ash sluicing operation, the Facility periodically disposes of fly ash and scrubber waste within the impoundment through similar methods.

1.4 Foundation and Embankments

The Unit 2/3 Bottom Ash Pond was constructed in 1975-1979 in conjunction with Units 2 and 3 of the Charles R. Lowman Power Plant. Based on a review of the available documentation, the Unit 2/3 Bottom Ash Pond was constructed by excavating below the original ground surface and placing the excavated soils as fill to form the pond floor and surrounding embankments. The original ground surface within the pond area ranged from ±EL 12' to EL 30'. Plans indicate that the pond was excavated to EL 13' and returned to EL 15' with a soil fill described as Type "A" embankment material. Two feet of Type "A" embankment material was also placed on the interior slopes of the embankment.

The Unit 2/3 Bottom Ash Pond contains exterior embankments located on its southern and western sides. A shared, interior embankment is located to the north adjacent to the Scrubber Waste Pond. A shared, interior embankment is located to the east adjacent to the Unit 1 Bottom Ash Pond which serves as the Plant's entrance road. The plans indicated that the embankments were constructed with Type "B" embankment material.

Based on soil boring information, the foundation soils underlying the embankments consist of Low Terrace Deposits and Coastal Plain Deposits. Low Terrace Deposits are water-deposited soils typically resulting from meanderings of rivers and streams. The Charles R. Lowman Power Plant is located along the western bank of the Tombigbee River. Therefore, the Terrace Deposits at this site appear to have resulted from meanderings and flooding of the Tombigbee River.

A toe embankment was constructed along the exterior face of the western embankment in 2015. The toe embankment is approximately 13 feet wide and a maximum of 16 feet in height extending to ±EL

38'. The embankment face was constructed on a ±2.5(H):1(V) inclination or flatter with select, structural fill. The structural fill was placed in thin lifts with individual lifts being moisture conditioned, compacted and tested to ensure a high consistency. The exterior slope of the toe embankment was lined with rip-rap to minimize the potential for erosion and sloughing during flood events of the Tombigbee River

Based on operational parameters provided by the owner, historical construction data and recent engineering analysis, it is our opinion that the Unit 2/3 Bottom Ash Pond exhibits suitable stability for its anticipated maximum CCR and CCR wastewater levels. For further information on foundations and embankments refer to the Report for Safety Factor Assessment, dated October 2016.

1.5 Slope Protection and Vegetation

All Unit 2/3 Bottom Ash Pond slopes are comprised of compacted embankment fill material and rip-rap lined. Rip-rap lining is such that erosion due to surface flows and wave action is resisted and the erosive effects are minimal.

For further information on slope protection and vegetation refer to the History of Construction Unit 2/3 Bottom Ash Pond, dated October 2016.

1.6 Spillways and Diversion Systems

The Unit 2/3 Bottom Ash Intake structure is an enclosed pumping facility. The water from the pond passes over a weir structure and into a concrete sump structure. The water is then pumped out of the sump and into the Scrubber Waste Pond. The Unit 2/3 Intake consists of two suction lift pumps with a normal operating flow of 825 gpm (1.84 cfs).

The Unit 2/3 Bottom Ash Intake structure is capable of adequately managing the flow from the 1000-yr flood event. The Unit 2/3 Bottom Ash Intake allows for a maximum hydraulic grade (HGL) of 40.3' MSL. This maximum HGL leaves a freeboard of 1.7' in the pond.

There are no hydraulic structures passing through or under any of the pond structural berms.

During high rainfall events, mobile suction lift pumps are utilized at the pond to supplement permanent intake structures to control the flood event and to maintain pool operating levels.

For further information on spillways and diversion systems refer to the Inflow Design Control Plan Unit 2/3 Bottom Ash Pond, dated October 2016.

1.7 Periodic Safety Factor Assessments

40 CFR 257.73 (e)(1)(i) through (e)(1)(iv) requires that the stability of CCR impoundment embankments be periodically evaluated. A stability evaluation was conducted on the exterior embankments associated with the Unit 2/3 Bottom Ash Ponds and is detailed in the Report for Safety Factor Assessment, dated October 2016.

The evaluation indicates that the embankments exhibit factors of safety that equal or exceed the required minimum values under the maximum storage pool, maximum surcharge pool and seismic loading scenarios. Additionally, the embankment soils are demonstrated not to be susceptible to liquefaction, and further analyses under the liquefaction loading scenario is not required. Therefore, the embankments are in compliance with the periodic safety factor assessment requirements. The following table summarizes the results of our analyses.

Summary of Analyses Results – Unit 2/3 Bottom Ash Pond			
Loading Condition	**Calculated Minimum Factor of Safety**	**Required Factor of Safety**	**Conforms to Regulations**
Long-Term Maximum Storage Pool	2.0	1.5	Yes
Maximum Surcharge Pool	2.0	1.4	Yes
Seismic	3.4	1.0	Yes
Liquefaction	5.5	1.2	Yes

For further information on the Unit 2/3 Bottom Ash Pond safety factor assessments please refer to the Report for Safety Factor Assessment, dated October 2016.

The potential for instability in the exterior Unit 2/3 Bottom Ash Pond embankments was evaluated based on loading associated with rapid drawdown. This potential scenario would involve flooding of the Tombigbee River followed by a subsequent rapid drop in water elevation as the flood waters subside. Based on available data (USGS, Station 02470050), the maximum recession rate of the flood waters occurs relatively slowly at approximately 2.5 feet per day. Excess pore pressures within the primarily granular berm soils are able to dissipate due to the slow drop in flood waters. Therefore, a rapid drawdown condition does not develop within the exterior embankment and further analysis is not warranted.

1.8 Engineer's Certification

The findings in this report were developed from visual observations made by CDG personnel during the preparation of this report and its supporting documents. If significant changes are made to the use of the upstream and downstream areas or capacity of the impoundments, CDG should be allowed to review our findings in light of the changes to determine if an alternate hazard potential classification is warranted. This report was created in accordance with the CCR rule Section 257.73(d) (i) through (vii). All future periodic assessments shall be conducted in accordance with this rule and any of its revisions or additions at the time of the assessment.

Appendix A

Figure 1- Unit 2/3 Bottom Ash Pond Location Map

Figure 2 – Unit 2/3 Aerial Map of Impoundments

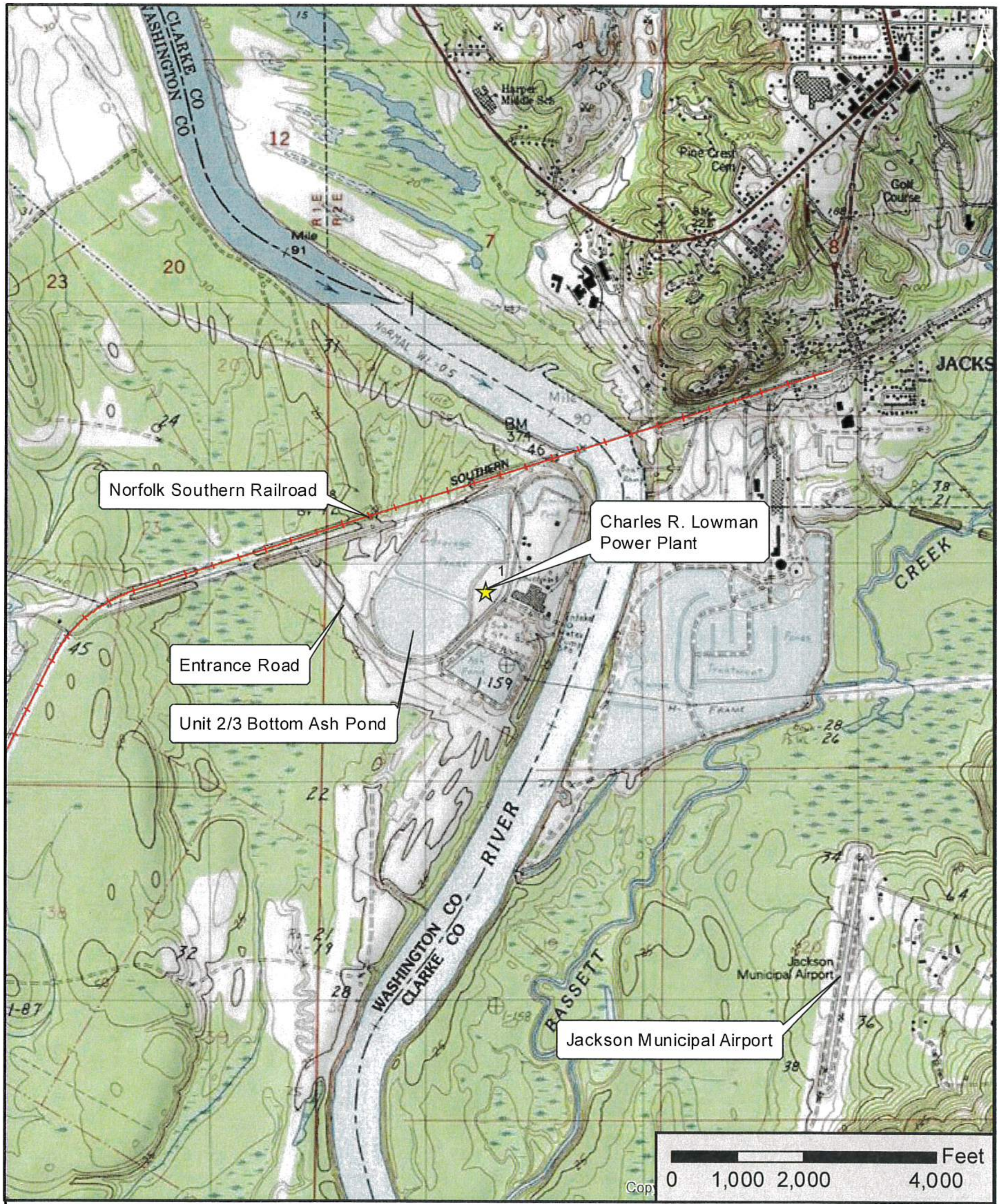

Figure 1 - Unit 2/3 Bottom Ash Pond Location Map

Charles R. Lowman Power Plant
PowerSouth Energy Cooperative
Leroy, AL

Engineering. Environmental. Answers.

October 2016

Figure 2 - Aerial Map of Impoundments

Charles R. Lowman Power Plant
PowerSouth Energy Cooperative
Leroy, AL

CDG
Engineering. Environmental. Answers.

October 2016

PowerSouth
ENERGY COOPERATIVE

Charles R. Lowman Power Plant Leroy, AL

Structural Stability Summary Report

Scrubber Waste Pond

Issued October 2016

CDG Engineers and Associates, Inc.
1840 East Three Notch St.
Andalusia, AL 36421
| cdge.com

PowerSouth
ENERGY COOPERATIVE

REPORT

Structural Stability Summary Report
Scrubber Waste Pond
Charles R. Lowman Power Plant

October 2016

CDG
Engineering. Environmental. Answers.

R. Daniel Wells
12/15/16

TABLE OF CONTENTS

1.0 SCRUBBER WASTE POND 2

1.1 Operator Information 2

1.2 Location 2

1.3 Statement of Purpose 2

1.4 Foundation and Embankments 2

1.5 Slope Protection and Vegetation 3

1.6 Spillways and Diversion Systems 3

1.7 Periodic Safety Factor Assessments 3

1.8 Engineer's Certification 4

Appendix A

Figure 1- USGS Location Map

Figure 2- Scrubber Waste Pond Aerial Map of Impoundments

References

CDG Engineers and Associates Inc. (2016). Report of Safety Factor Assessment; Coal Combustion Residuals Impoundment Embankments, Charles R. Lowman Power Plant. Andalusia, AL.

CDG Engineers and Associates, Inc. (2016). History of Construction Scrubber Waste Pond, Charles R. Lowman Power Plant. Andalusia, AL.

CDG Engineers and Associates, Inc. (2016). Inflow Design Control Plan Scrubber Waste Pond, Charles R. Lowman Power Plant. Andalusia, AL.

1.0 SCRUBBER WASTE POND

1.1 Operator Information

Name: Scrubber Waste Pond

Owner/Operator: PowerSouth Energy Cooperative, Inc.
Charles R. Lowman Power Plant
Leroy, AL 36458

State ID: None Assigned

1.2 Location

The Scrubber Waste Pond is located in Section 18, Township 6N, Range 2 East in Washington, County Alabama and more specifically on the Western bank of the Tombigbee River. Figures 1 and 2 of this report show the location of the Pond.

1.3 Statement of Purpose

The Scrubber Waste Pond is currently used as a settling pond for CCR wastes containing flue gas desulfurization, and other plant wastes.

1.4 Foundation and Embankments

The Scrubber Waste Pond was constructed between 1975-1979 in conjunction with Units 2 and 3 of the Charles R. Lowman Power Plant. Based on a review of the available documentation, the Scrubber Waste Impoundment was constructed by excavating below the original ground surface and placing these soils as compacted fill to form the impoundment floor and surrounding embankments. The original ground surface within the impoundment area ranged from ±EL 12' to EL 27'. Plans indicate that the impoundment was excavated to EL 13' and returned to EL 15' with a soil fill described as Type "A" embankment material. Two feet of Type "A" embankment material was also placed on the interior slopes of the embankment.

The Scrubber Waste Pond contains a single exterior embankment located on its western side. Shared, interior embankments are located to the north adjacent to the Process Waste Pond and to the south adjacent to the Unit 2/3 Bottom Ash Pond. The eastern side of the Scrubber Waste Pond does not contain an embankment with an exposed slope; rather it is formed by an excavation below the existing ground surface.

Based on soil boring information, the Scrubber Waste Pond embankments and underlying foundation soils consist of fill, Low Terrace Deposits and Coastal Plain Deposits. Fill thicknesses ranged from approximately 26' to 33'. The fill soils are comprised of silty and clayey, fine to coarse-grained sand with rock fragments. Standard Penetration Tests (SPT) in the fill indicated a high consistency with N-values ranging from 16 to greater than 50 blows per foot (bpf).

A toe embankment was constructed along the exterior face of the western embankment in 2015. The toe embankment is approximately 13 feet wide and a maximum of 16 feet in height extending to ±EL 35'. The embankment face was constructed on a ±2.5(H):1(V) inclination or flatter with select, structural fill. The structural fill was placed in thin lifts with individual lifts being moisture conditioned, compacted and tested to ensure a high consistency. The exterior slope of the toe embankment was lined with rip-rap to minimize the potential for erosion and sloughing during flood events of the Tombigbee River

Based on operational parameters provided by the owner, historical construction data and recent engineering analysis, it is our opinion that the Scrubber Waste Pond exhibits suitable stability for its anticipated maximum CCR and CCR wastewater levels. For further information on foundations and embankments refer to the Report for Safety Factor Assessment, dated October 2016.

1.5 Slope Protection and Vegetation

All Scrubber Waste Pond slopes are comprised of compacted embankment fill material and rip-rap lining. Rip-rap lining is such that erosion due to surface flows and wave action is resisted and the erosive effects are minimal.

For further information on slope protection and vegetation refer to the History of Construction Scrubber Waste Pond, dated October 2016.

1.6 Spillways and Diversion Systems

The Scrubber Waste Intake consists of two suction lift pumps with a normal operating flow of 1395 gpm (3.11 cfs). The pumps are fed by two floating intake hoses that allow for the removal of liquids from the laminar portion of the impounded waters.

The Scrubber Waste Intake structure is capable of adequately managing the flow from the 1000-yr flood event. The Scrubber Waste Intake allows for a maximum hydraulic grade (HGL) of 39.2' MSL. This maximum HGL leaves a freeboard of 2.8' in the pond.

There are no hydraulic structures passing through or under any of the pond structural berms.

During high rainfall events, mobile suction lift pumps are utilized at the pond to supplement permanent intake structures to control the flood event and to maintain pool operating levels.

For further information on spillways and diversion systems refer to the Inflow Design Control Plan Scrubber Waste Pond, dated October 2016.

1.7 Periodic Safety Factor Assessments

40 CFR 257.73 (e)(1)(i) through (e)(1)(iv) requires that the stability of CCR impoundment embankments be periodically evaluated. A stability evaluation was conducted on the exterior embankments associated with the Scrubber Waste Ponds and is detailed in the Report for Safety Factor Assessment, dated October 2016.

The evaluation indicates that the embankments exhibit factors of safety that equal or exceed the required minimum values under the maximum storage pool, maximum surcharge pool and seismic loading scenarios. Additionally, the embankment soils are demonstrated not to be susceptible to liquefaction, and further analyses under the liquefaction loading scenario is not required. Therefore, the embankments are in compliance with the periodic safety factor assessment requirements. The following table summarizes the results of our analyses.

Summary of Analyses Results – Scrubber Waste Pond			
Loading Condition	**Calculated Minimum Factor of Safety**	**Required Factor of Safety**	**Conforms to Regulations**
Long-Term Maximum Storage Pool	1.9	1.5	Yes
Maximum Surcharge Pool	1.8	1.4	Yes
Seismic	2.1	1.0	Yes
Liquefaction	2.7	1.2	Yes

For further information on the Scrubber Waste Pond safety factor assessments please refer to the Report for Safety Factor Assessment, dated October 2016.

The potential for instability in the exterior Scrubber Waste Pond embankment was evaluated based on loading associated with rapid drawdown. This potential scenario would involve flooding of the Tombigbee River followed by a subsequent rapid drop in water elevation as the flood waters subside. Based on available data (USGS, Station 02470050), the maximum recession rate of the flood waters occurs relatively slowly at approximately 2.5 feet per day. Excess pore pressures within the primarily granular berm soils are able to dissipate due to the slow drop in flood waters. Therefore, a rapid drawdown condition does not develop within the exterior embankment and further analysis is not warranted.

1.8 Engineer's Certification

The findings in this report were developed from visual observations made by CDG personnel during the preparation of this report and its supporting documents. If significant changes are made to the use of the upstream and downstream areas or capacity of the impoundments, CDG should be allowed to review our findings in light of the changes to determine if an alternate hazard potential classification is warranted. This report was created in accordance with the CCR rule Section 257.73(d) (i) through (vii) All future periodic assessments shall be conducted in accordance with this rule and any of its revisions or additions at the time of the assessment.

Appendix A

Figure 1- Scrubber Waste Pond Location Map

Figure 2 – Scrubber Waste Pond Aerial Map of Impoundments

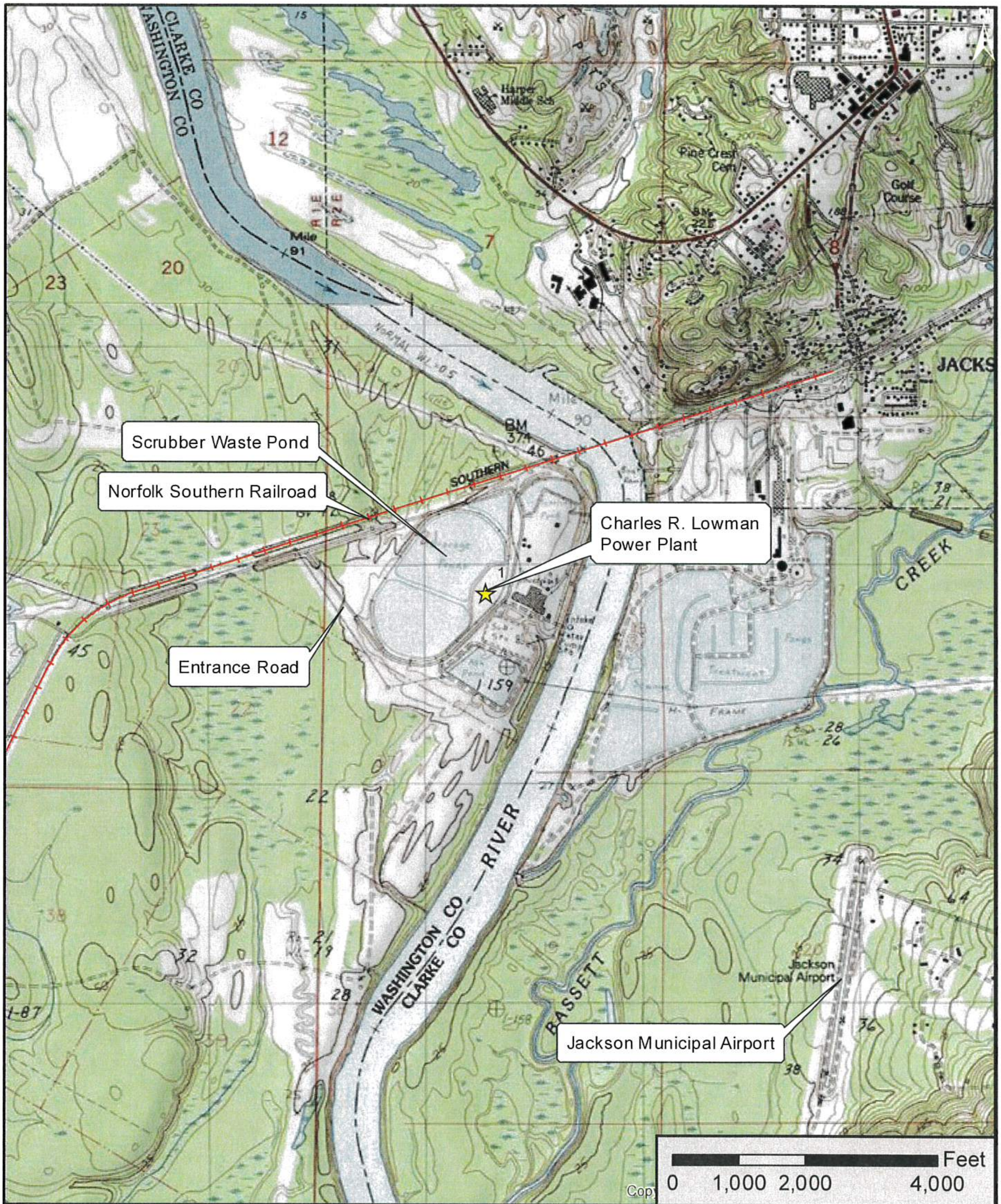

Figure 1 - Scrubber Waste Pond Location Map

Charles R. Lowman Power Plant
PowerSouth Energy Cooperative
Leroy, AL

CDG
Engineering. Environmental. Answers.

October 2016

Figure 2 - Aerial Map of Impoundments

Charles R. Lowman Power Plant
PowerSouth Energy Cooperative
Leroy, AL

CDG
Engineering. Environmental. Answers.

October 2016

Results of the Safety Factor Assessment

Table 11: Summary of Analyses Results

Loading Condition	Calculated Minimum Factor of Safety	Required Minimum Factor of Safety	Conforms to Regulations
Long-Term Maximum Storage Pool	1.6	1.5	Yes
Maximum Surcharge Pool	1.6	1.4	Yes
Seismic	1.0	1.0	Yes
Liquefaction	1.8[1]	1.2	Yes

Note 1: The embankment soils are shown not to be susceptible to liquefaction; therefore, further analysis under the liquefaction loading scenario is not required.

REPORT OF SAFETY FACTOR ASSESSMENT
COAL COMBUSTION RESIDUALS
IMPOUNDMENT EMBANKMENTS

Charles R. Lowman Power Plant
Leroy, Alabama
CDG Project Number: 061521207

October 17, 2016

Prepared for:

Rushton, Stakely, Johnston & Garrett, P.A.
184 Commerce Street
Montgomery, Alabama 36104

Prepared by:

CDG Engineers & Associates, Inc.
1840 East Three Notch Street
Andalusia, AL 36421
Phone: (334) 222-9431
Fax: (334) 222-4018

Engineering. Environmental. Answers.

CDG
Engineering. Environmental. Answers.

CDG Engineers & Associates, Inc.
1830 Hartford Highway
Dothan, AL 36301
Tel (334) 677-9431
Fax (334) 677-9450

www.cdge.com

October 17, 2016

Rushton, Stakely, Johnston & Garrett, P.A.
184 Commerce Street
Montgomery, Alabama 36104

Attention: Mr. J. Theodore Jackson, Jr.

Reference: **Report of Safety Factor Assessment**
Coal Combustion Residuals Impoundment Embankments
Charles R. Lowman Power Plant
Leroy, Alabama
CDG Reference Number: 061521207

Dear Mr. Jackson:

CDG Engineers & Associates, Inc. (CDG) has completed the authorized safety factor assessment for the existing coal combustion residuals (CCR) impoundment embankments at the Charles R. Lowman Power Plant in Leroy, Alabama. Our services were performed in general accordance with *Authorization #RS7 to Engineering Services Contract Master Agreement* dated July 20, 2015.

The purposes of this study were to determine general subsurface conditions at specific soil test boring and cone penetration test locations and to evaluate the stability of the CCR impoundment embankments as required by current federal regulations [40 CFR Part 257.73 (e): *Periodic Safety Factor Assessments*]. This report presents the subsurface information encountered at the test locations, laboratory test results of representative, on-site soil samples, and stability findings associated with the existing embankments.

We appreciate the opportunity to work with you on this project. Please call if you have any questions or need additional information.

Respectfully Submitted,

CDG Engineers & Associates, Inc.

R. Daniel Wells, PE
Project Manager

10/17/16
Danner F. Drake, PE
Senior Engineer

DANNER FRAZER DRAKE

ALBERTVILLE
ANDALUSIA
AUBURN
DOTHAN
GADSDEN
HOOVER
HUNTSVILLE

Table of Contents

1.0 SCOPE OF SERVICES 4

2.0 EMBANKMENT GEOMETRIES AND CRITICAL CROSS-SECTIONS 5

3.0 SUBSURFACE CONDITIONS AND MATERIAL PROPERTIES 7

- 3.1 Surficial Material 7
- 3.2 Previously Placed Fill 7
- 3.3 Low Terrace and Coastal Plain Deposits 8
- 3.4 Groundwater 8

4.0 LABORATORY TEST RESULTS 9

5.0 REQUIRED LOADING CONDITIONS AND FACTORS OF SAFETY 9

6.0 EMBANKMENT STABILITY ANALYSIS 9

- 6.1 Analysis Soil Properties 10
- 6.2 Static, Maximum Storage Pool Stability Analysis 11
- 6.3 Static, Maximum Surcharge Pool Stability Analyses 12
- 6.4 Seismic Stability Analysis Findings 13
- 6.5 Liquefaction Potential 16

7.0 SUMMARY OF STABILITY FINDINGS 17

8.0 GENERAL REMARKS AND CLOSING 18

APPENDIX A – TEST LOCATION PLAN

APPENDIX B – BORING LOGS

APPENDIX C – SUBSURFACE PROFILES

APPENDIX D – STATIC, MAXIMUM STORAGE POOL STABILITY ANALYSIS

APPENDIX E – STATIC, MAXIMUM SURCHARGE POOL STABILITY ANALYSIS

APPENDIX F – CONE PENETRATION TEST LOGS

APPENDIX G – SITE-SPECIFIC SEISMIC HAZARD ANALYSIS

APPENDIX H – MAKDISI AND SEED SEISMIC DEFORMATION ANALYSIS CHARTS

APPENDIX I – SEISMIC STABILITY AND DEFORMATION ANALYSIS

APPENDIX J – LIQUEFACTION POTENTIAL ANALYSIS

EXECUTIVE SUMMARY

Federal regulations (40 CFR 257.73) require that the stability of Coal Combustion Residuals (CCR) impoundment embankments be periodically evaluated. The purpose of this study is to perform the required evaluation for the CCR impoundment embankments at the Charles R. Lowman Power Plant (Lowman). The stability evaluation was conducted on the exterior embankments associated with the Scrubber Waste, Unit 2/3 Bottom Ash, and the Unit 1 Bottom Ash Ponds. Regulations state that the evaluation is to be performed under static long-term maximum storage pool, static maximum surcharge pool and seismic loading scenarios. Additionally, for dikes constructed of soils that have susceptibility to liquefaction, the stability is to be evaluated under liquefaction conditions.

The scope of services performed by CDG Engineers & Associates, Inc. (CDG) consisted of a subsurface exploration, laboratory testing program and analyses of embankment stability under the various required loading scenarios. CDG identified critical cross-sections along each impoundment embankment by evaluating subsurface information and geometric configurations to define locations where failures are most likely to occur.

The stability analyses indicate that the embankments exhibit factors of safety (FS) that equal or exceed the required minimum values under the maximum storage pool, maximum surcharge pool and seismic loading scenarios. Additionally, the embankment soils are demonstrated not to be susceptible to liquefaction, and further analyses under the liquefaction loading scenario is not required. Therefore, the embankments are in compliance with the periodic safety factor assessment requirements. The following table summarizes the results of our analyses.

Summary of Analyses Results

Loading Condition	Calculated Minimum Factor of Safety	Required Minimum Factor of Safety	Conforms to Regulations
Long-Term Maximum Storage Pool	1.6	1.5	Yes
Maximum Surcharge Pool	1.6	1.4	Yes
Seismic	1.0	1.0	Yes
Liquefaction	1.8[1]	1.2	Yes

Note 1: The embankment soils are shown not to be susceptible to liquefaction.

1.0 SCOPE OF SERVICES

The geotechnical evaluation included in-situ sampling and testing to determine the subsurface conditions within and underlying the embankments surrounding the Scrubber Waste Pond, the Unit 2/3 Bottom Ash Pond, and the Unit 1 Bottom Ash Pond at the Lowman Power Plant in Leroy, Alabama. Shared, interior embankments are located between the Scrubber Waste and Unit 2/3 Bottom Ash Ponds and the Unit 2/3 Bottom Ash and Unit 1 Bottom Ash Ponds. The interior embankments serve primarily to separate the impoundments. Their stability provides no contribution to the containment of CCR from the surrounding environment. Therefore, the current scope of services consists of evaluating the exterior embankments. Evaluation of the interior embankments has been excluded.

Laboratory tests were performed to define strength parameters of the actual embankment and foundation materials present at the site. Stability analyses were modeled at various locations throughout the embankments to identify critical cross-sections. The water pool elevations, rail car loading, and CCR fill were varied to determine maximum loading configurations. Maximum storage pool, maximum surcharge pool, seismic and liquefaction loading scenarios were considered. Specifically, our scope of services consisted of the following.

- Field location of soil test borings and cone penetration tests (CPT), review of available geologic data, and mobilization of drilling and CPT rigs.

- Soil test borings along the crest of the embankments surrounding the exterior of the noted impoundments. Borings contained Standard Penetration Tests at regular intervals. Undisturbed samples were obtained at various depths for laboratory testing. The subsurface exploration included 3 soil test borings (T-1 through T-3) performed from August 3 to 10, 2016, 14 soil test borings (S-1 through S-14) performed from November 28 to December 13, 2011 and 13 soil test borings (B-1 through B-13) performed from July 13 to 17, 2009. The borings extended to depths ranging from approximately 40 to 60 feet below the existing ground surface.

- Inspection and materials testing during construction of the toe buttress located along the exterior of the northwest embankment of the Unit 2/3 Bottom Ash and Scrubber Waste Ponds.

- Piezometers were installed in five (5) borings (S-1, S-3, S-7, S-11 and S-13) to determine delayed groundwater levels.

- Cone Penetration Tests (CPT) were performed at the toe of the existing embankments to determine the in-situ characteristics of the foundation soils. CPT data consists of a continuous record of tip resistance, side friction and pore water pressure. The values are correlated with soil type and strength properties. Three (3) CPTs (CPT-1 through CPT-3) were performed on November 29, 2011. CPTs extended to refusal at depths ranging from approximately 45 to 70 feet below the existing ground surface.

- Laboratory tests were performed to determine site-specific soil classification and strength characteristics. Tests included the following: natural moisture content (131 tests), grain size analysis (43 tests), Atterberg limits (44 tests), and consolidated, undrained triaxial shear (6 tests).

- Seismic and liquefaction analysis consisting of the following three step process:
  - Determination of the shear wave velocity within the subsurface stratigraphy at the site;
  - A site-specific hazard analysis including determination of the design ground surface acceleration and synthetic time history for earthquakes corresponding to the 2% and 10% probability of exceedance in 50 years; and
  - Geotechnical analysis of embankment stability under seismic and liquefaction loading conditions based on the site-specific design earthquake record. Rigorous seismic deformation analyses were performed based on the Makdisi and Seed method. The embankment soils were evaluated for liquefaction potential using recommendations by Idriss and Boulanger.

- Evaluation of the information gathered during the subsurface exploration and laboratory testing program and preparation of this report. The report addresses the following items:
  - Description of the existing embankment configurations and critical cross-sections;
  - Subsurface stratigraphy and material properties used in analyses;
  - Summary of loading conditions and required factors of safety;
  - Slope stability analysis of the exterior embankments forming the Scrubber Waste, Unit 2/3 Bottom Ash and Unit 1 Bottom Ash Ponds under the specified loading conditions.

2.0 EMBANKMENT GEOMETRIES AND CRITICAL CROSS-SECTIONS

Embankment geometries were defined by survey data obtained by CDG and by design plans provided by PowerSouth. Design plans were entitled *Alabama Electric Cooperative, Inc.; First Unit – Jackson Station* (Stanley Engineering Company; dated January 20, 1970) and *Tombigbee Generating Plant Units 2 & 3* (Burns & McDonnell; dated June 8, 1976). Survey data was unavailable for the interior of the impoundments below the CCR and water levels present at the time of the field work. Therefore, geometries of interior embankment slopes below the water and CCR levels were based on topographic data obtained from the design plans.

Based on the noted information, the crest elevations of the exterior embankments range from ±EL 35.5' (Unit 1 Bottom Ash Pond) to ±EL 42' (Unit 2/3 Bottom Ash and Scrubber Waste Ponds). Ground surface elevations at the exterior toe of the embankments range from ±EL 19' (Scrubber Waste Pond) to ±EL 35' (Unit 1 Bottom Ash Pond). The embankments exhibit exterior vertical heights ranging from less than 5 feet to a maximum of approximately 21 feet. The exterior face of the perimeter embankments exhibit slope inclinations of ±1.7(H):1(V) and flatter.

Information provided by the client indicates that the maximum elevations of CCR within the impoundments are not strictly defined. However, the CCR is typically maintained a minimum of several feet below the top of the exterior embankments. CCR is sluiced into the impoundments with a maximum elevation defined by the maximum storage pool operating condition. Due to operational considerations, it is only possible for CCR to be mounded above the elevation of the embankment crest on the east side of the Unit 2/3 Bottom Ash Pond – well away from the exterior embankment. Therefore, for analysis purposes, the maximum CCR elevation within the impoundments was modeled at the maximum storage pool water elevation.

A detailed review of the grading and topographic plans was performed to determine the critical cross-sections for the existing embankments. Cross-sections identified for evaluation were selected at numerous locations throughout the embankments to ensure the critical locations were identified. Critical locations for analysis were determined by evaluating subsurface information and geometric configurations of the embankments to define locations exhibiting the greatest driving forces coupled with the smallest resisting forces. Critical slope sections occur at locations exhibiting combinations of unfavorable subsurface conditions, maximum slope heights, and steep slope inclinations.

Our evaluation identified 8 cross-sections where the embankments exhibited critical subsurface conditions and geometries. The critical cross-sections are oriented perpendicular to the face of the embankment slopes. Locations of critical cross-sections are presented on the Test Location Plan (**APPENDIX A**). The following **Table 1** provides a summary of geometric conditions associated with the critical cross-sections identified at the site.

Table 1: Summary of Critical Cross-Sections

Section	Crest Elevation	Toe Elevation	Slope Height	Maximum Inclination
D – D'	±EL 35.5'	±EL 24.5'	±11.0 feet	2.1(H):1(V)
E – E'	±EL 37.1'	±EL 34.9'	±2.2 feet	4.25(H):1(V)
F – F'	±EL 37.9'	±EL 33.5'	±4.4 feet	8.7(H):1(V)
G – G'	±EL 41.0'	±EL 31.6'	±9.4 feet	3.7(H):1(V)
H – H'	±EL 39.5'	±EL 30.0'	±9.5 feet	5.7(H):1(V)
J – J'	±EL 42.7'	±EL 32.0'	±10.7 feet	3.8(H):1(V)
K – K'	±EL 42.7'	±EL 29.2'	±13.5 feet	2.3(H):1(V)
L – L'	±EL 42.7'	±EL 22.0'	±20.7 feet	2.2(H):1(V)

3.0 SUBSURFACE CONDITIONS AND MATERIAL PROPERTIES

The subsurface exploration included 30 soil test borings and 3 cone penetration tests. Details of the conditions encountered at the test locations are contained on the attached Boring Logs (**APPENDIX B**), subsurface profiles (**APPENDIX C**), and CPT Logs (**APPENDIX F**). The stratification lines indicated on the logs and profiles represent the approximate boundaries between soil types. The actual transitions may be gradual.

Test locations were estimated in the field by pacing distances and approximating angles from existing features shown on the available topographic plan (*Facility Map, Charles R. Lowman Plant*; dated May 2009). Therefore, the test locations indicated on the attached Test Location Plan (**APPENDIX A**) are approximate.

In general, the Charles R. Lowman Power Plant site is underlain by terrace deposits associated with the Tombigbee River overlying Coastal Plain Deposits[1]. The embankments are constructed of previously placed fill and undisturbed deposits. Following is a summary of the subsurface conditions encountered in the borings performed along the Scrubber Waste, Unit 2/3 Bottom Ash and Unit 1 Bottom Ash Pond embankments.

3.1 Surficial Material

Borings B-1 to B-6, S-6 to S-12, T-2 and T-3 were performed along an existing rail line and encountered approximately 1½' to 2' of crushed aggregate (railroad ballast) at the ground surface. Borings B-12 and B-13 encountered ±2' of blended silty sand and crushed aggregate at the ground surface. Borings B-10, B-11, S-1 and T-1 initially encountered previously placed soil fill as described in the following section. Borings S-2 to S-5, S-13 and S-14 were performed in vegetated areas and encountered topsoil ranging in thickness from approximately 3 to 12 inches.

3.2 Previously Placed Fill

Underlying the surficial material and at the ground surface at B-10, B-11, S-1 and T-1, the soil test borings encountered previously placed fill associated with the existing embankments. The fill extended to depths ranging from approximately 17 to 32 feet below the existing ground surface along the Scrubber Waste and #2/#3 Bottom Ash Pond embankments and approximately 7 to 18 feet below the existing ground surface along the #1 Bottom Ash Pond embankments. Documentation associated with fill placement procedures and applied compactive effort are unavailable.

The existing fill encountered at the boring locations consisted of silty and clayey, fine to coarse-grained sand and fine sandy clay. The fill contained various amounts of rock fragments. The tested fill exhibited Standard Penetration Test (SPT) N-values ranging from 2 to greater than 50 blows per foot (bpf). N-values typically ranged from 10 to 50 bpf and averaged 29 bpf. The unconfined compressive strength (PP_{qu}) of cohesive samples was determined using a hand-held penetrometer. The samples exhibited PP_{qu} values ranging from less than 0.25 to 1.25 tons per square foot (tsf). The fill exhibited an erratic consistency ranging from very loose to very dense and very soft to very stiff.

---

[1] *Geologic Map of Alabama*; Geologic Survey of Alabama; 1988

Natural moisture contents in samples of the fill ranged from 7% to 27%. Tested samples contained between 7.8% and 83.0% fine-grained (silt and clay size) particles. Atterberg Limits tests indicated the soils were non-plastic (NP) to moderately plastic with Liquid Limits (LL) ranging from NP to 42 and Plasticity Indices (PI) ranging from NP to 25. Based on USCS guidelines, tested samples of the fill are classified as silty sand (SM and SP-SM), sandy clay (CL), clayey sand (SC) and clayey, silty sand (SC-SM).

3.3 Low Terrace and Coastal Plain Deposits

Low terrace deposits are water deposited soils typically resulting from meanderings of rivers and streams. Coastal Plain Deposits are naturally occurring soils that appear to have formed by the gradual deposition of sediment in an ancient marine environment. Low terrace deposits associated with the Tombigbee River and Coastal Plain Deposits were encountered underlying the previously placed fill. The deposits extended to the boring termination depths ranging from approximately 40 to 60 feet below the existing ground surface.

The deposits encountered in the borings generally consisted of silty and clayey, fine to medium-grained sand, gravel and clay with varying amounts of fine sand. SPT N-values in the deposits ranged from Weight of Hammer (WOH) to greater than 50 bpf. N-values typically ranged from 2 to 25 bpf and averaged 13 bpf. WOH material exhibits a very low consistency and is penetrated under the static weight of the hammer and drilling tools. Cohesive samples of the deposits exhibited PP_{qu} values ranging from less than 0.25 tsf to 2.0 tsf. In general, the deposits exhibited very loose to dense and very soft to stiff consistencies.

Natural moisture contents in samples of the deposits ranged from 14% to 38%. Tested samples were non-plastic to highly plastic with LL values ranging from NP to 74 and PI values ranging from NP to 52. The samples contained between 2.3% and 97.7% fine-grained (silt and clay size) particles. Based on the Unified Soil Classification System (USCS), the tested deposits are classified as silty and clayey sand (SM and SM-SC), plastic clay (CH), sandy silt (ML) and silty and fine sandy clay (CL, CL-ML).

3.4 Groundwater

Measurements were made in the open boreholes to determine the depth to groundwater, if present at the time of drilling. Additionally, piezometers were installed in nine (9) borings (B-2, B-5, B-11 and B-13; S-1, S-3, S-7, S-11 and S-13) to determine delayed groundwater levels. Groundwater was encountered at depths ranging from ±9½ feet to ±31 feet below the existing ground surface. The groundwater level was encountered between ±EL11' and ±EL33' at the tested locations. Borings not containing piezometers were backfilled with grout upon completion of drilling operations.

Groundwater depth is highly variable and will often fluctuate due to seasonal variations in precipitation and fluctuations in adjacent bodies of water. Typically, long-term monitoring over several seasons is required to evaluate the stabilized range of depths to groundwater in the upper soils.

4.0 LABORATORY TEST RESULTS

Laboratory tests were performed on representative samples retrieved from the soil test borings. Testing included natural moisture content, Atterberg Limits, and Grain Size Analysis. Results of the laboratory tests and corresponding soil classifications based on USCS guidelines are included on the Boring Logs (**APPENDIX B**).

In addition to the noted laboratory tests, the strength characteristics of representative, in-place and remolded soil samples were determined using consolidated, undrained (CU) triaxial shear tests. The laboratory test results were used in evaluation of the strength characteristics of soils modeled in the stability analysis. A summary of the test results is presented in the following **Table 2**.

Table 2: Soil Strength Test Results

Location	Depth	USCS Classification	Total Stress		Effective Stress	
			Φ	C (psf)	Φ	C (psf)
B-8	21½' – 23½'	CL	12.6°	535	18.7°	449
B-13	11½' – 13½'	SM	31.2°	243	28.3°	651
S-1	10' – 12'	SC	21.8°	1,690	30.1°	398
S-7	26½' – 28½'	CH	0°	1,228		
Dredge Pond, B-1	8' – 10'	SC	21.6°	568	25.0°	484
Dredge Pond, B-1	31.5' – 33.5'	SC	17.7°	384	29.0°	212

5.0 REQUIRED LOADING CONDITIONS AND FACTORS OF SAFETY

Federal regulation 40 CFR Part 257.73 (e) (1) (i) through (iv) specifies loading conditions and corresponding factor of safety (FS) values for CCR impoundment embankments. The following **Table 3** indicates the required minimum FS values for the various loading conditions specified in the regulations.

Table 3: Minimum Required Factors of Safety

Static, Long Term Maximum Storage (Normal) Pool	1.50
Static, Maximum Surcharge Pool (Flood)	1.40
Seismic Condition	1.00
Liquefaction	1.20

6.0 EMBANKMENT STABILITY ANALYSIS

Analyses of maximum storage pool, maximum surcharge pool, seismic and liquefaction loading scenarios were performed at critical locations along the perimeter embankments of the Scrubber Waste, Unit 2/3 Bottom Ash and Unit 1 Bottom Ash Ponds. The stability analyses of the critical embankment cross-sections were performed using the computer software GeoStudio™2012 *version 8.*

The SLOPE/W® module within GeoStudio™2012 was used to assess the rotational and translational stability of the existing embankment configurations. The analysis considers circular, block, and composite slip surfaces using the Spencer Method. The Spencer Method is a factor-of-safety, limit-equilibrium procedure that satisfies both force and moment conditions of equilibrium. The geometry of the cross-sections was imported directly into SLOPE/W® from surfaces generated by the topographic survey data.

6.1 Analysis Soil Properties

The subsurface conditions used in evaluation of the embankment stability are based on the findings of the subsurface exploration and laboratory testing program. The strength characteristics of the fill and in-situ materials were derived from laboratory data, correlations based on USCS soil classifications provided by NAVFAC[2], and our experience with similar soil types. The efficiency of the SPT hammer was measured to be 87.7%.

The embankment and foundation soils have been in-place for many years resulting in dissipation of excess pore water pressures. Therefore, static, maximum storage pool and static, maximum surcharge pool analyses of the embankments were based on drained (effective) soil strength parameters. A nominal effective cohesion value was attributed to granular soils to prevent theoretical surficial slides when modeling slope stability.

Seismic loading can result in development of excess pore pressures. Therefore, undrained (total) soil strength parameters were used in modeling short term, seismic loading in cohesive soils. Additionally, the strength parameters of the on-site soils were conservatively reduced to account for cyclic softening associated with seismic loading conditions. Soil strength parameters (C for cohesive soils and tan Ø for cohesionless soils) were reduced by 20% when modeling seismic loading. Soil properties [Mohr-Coulomb C (cohesion) and Ø (internal friction angle)] used in analyses of the embankments are provided in the following **Table 4**.

---

[2] Navy Facilities Engineering Command; "*Foundations and Earth Structures, Design Manual 7.02*"; dated September 1, 1986; p. 7.2-39.

Table 4: Analysis Soil Properties

Soil Description	γ_{total}	Ø	C (psf)	Ø'	C' (psf)	Reduced Values for Seismic
railroad ballast	105 pcf	n/a	n/a	36°	0 psf	n/a
loose silty sand fill	115 pcf	n/a	n/a	28°	50 psf	Ø' = 23°
medium dense silty sand fill	120 pcf	n/a	n/a	32°	50 psf	Ø' = 26°
dense silty sand fill	125 pcf	n/a	n/a	34°	50 psf	Ø' = 28°
soft sandy clay fill	110 pcf	0°	350 psf	22°	150 psf	C = 280 psf
medium sandy clay fill	115 pcf	0°	500 psf	25°	200 psf	C = 400 psf
stiff sandy clay fill	120 pcf	0°	1,000 psf	27°	400 psf	C = 800 psf
loose clayey sand deposits	115 pcf	n/a	n/a	28°	100 psf	Ø' = 23°
loose silty sand deposits	115 pcf	n/a	n/a	28°	50 psf	Ø' = 23°
medium dense silty sand deposits	120 pcf	n/a	n/a	30°	50 psf	Ø' = 25°
dense silty sand deposits	125 pcf	n/a	n/a	32°	50 psf	Ø' = 26°
soft sandy clay deposits	110 pcf	0°	350 psf	22°	150 psf	C = 280 psf
medium sandy clay deposits	115 pcf	0°	500 psf	25°	200 psf	C = 400 psf
stiff sandy clay deposits	120 pcf	0°	1,000 psf	27°	400 psf	C = 800 psf

The phreatic surface through the embankments was modeled based on the findings of the hydraulic analysis, the subsurface exploration and on horizontally homogenous soil conditions with no toe drain within the embankments. This results in a tailwater depth of ⅓ of the reservoir depth above the embankment toe[3]. Groundwater depth within the embankment was linearly interpolated between the reservoir depth and the tailwater depth.

6.2 Static, Maximum Storage Pool Stability Analysis

Stability analyses were performed at the critical cross-sections under static, maximum storage pool conditions. The static, maximum storage pool represents a long-term condition under typical operation loading parameters. Groundwater levels and pore pressures are assumed to be in equilibrium. The maximum storage pool elevations were defined by the client as detailed in the following **Table 5**.

Table 5: Maximum Storage Pool Elevations

Impoundment Designation	Cross-Section	Top of Embankment	Normal Pool
Unit 1 Bottom Ash	D – D'	±EL 35.5'	EL 31.0'
Unit 1 Bottom Ash	E – E'	±EL 37.1'	EL 31.0'
Unit 1 Bottom Ash	F – F'	±EL 37.9'	EL 31.0'
Unit 2/3 Bottom Ash	G – G'	±EL 43.9'	EL 38.25'
Unit 2/3 Bottom Ash	H – H'	±EL 43.1'	EL 38.25'
Unit 2/3 Bottom Ash	J – J'	±EL 43.1'	EL 38.25'
Scrubber Waste	K – K'	±EL 43.3'	EL 37.5'
Scrubber Waste	L – L'	±EL 43.6'	EL 37.5'

---

[3] US Bureau of Reclamation; *Design of Small Dams*, 1987; p. 191.

40 CFR Part 257.73 (e) (1) (i) states that "The calculated static factor of safety under the long-term, maximum storage pool loading condition must equal or exceed 1.5." The analyses indicate minimum FS values ranging from 1.6 to 6.2 under maximum storage pool conditions. The following **Table 6** provides specific results of the analyses. Detailed results of the static, maximum storage pool analyses are included in **APPENDIX D**.

Table 6: Analyses Results, Static Maximum Storage Pool

Impoundment Designation	Section	Factor of Safety
Unit 1 Bottom Ash	D – D'	1.6
Unit 1 Bottom Ash	E – E'	6.2
Unit 1 Bottom Ash	F – F'	5.7
Unit 2/3 Bottom Ash	G – G'	2.5
Unit 2/3 Bottom Ash	H – H'	2.7
Unit 2/3 Bottom Ash	J – J'	2.0
Scrubber Waste	K – K'	2.3
Scrubber Waste	L – L'	1.9

6.3 Static, Maximum Surcharge Pool Stability Analyses

The maximum surcharge pool is a temporary condition in which the impoundment floods to a level higher than the normal pool. Although the flooding is temporary, the extreme condition of steady-state seepage at the surcharge pool level is typically modeled. Therefore, tailwater depths are adjusted to a higher elevation from the normal condition to reflect the elevated pool within the impoundment.

CDG performed a hydraulic analysis of the subject impoundments through previous authorizations. Results of the analysis are contained in the report entitled *Inflow Design Report for CCR Impoundments* (October, 2016). The hydraulic analysis was based on the specified storm event resulting from a hazard classification rating of "significant" and various water balance scenarios provided by PowerSouth.

The analysis identified the maximum surcharge pool elevations within the impoundments resulting from a 72-hour duration, 1,000-year storm and plant inflows resulting from two scenarios – Normal Operations and Abnormal Operations (e.g. an extended loss of power or pump failure). The maximum hydraulic grade generated from the two plant inflow scenarios was used to evaluate embankment stability for each impoundment.

Our analyses indicate that maximum surcharge pool elevations within the impoundments range from approximately 2.7 feet to 5.1 feet (Unit 1 Bottom Ash Pond) below the top of the embankments (including railroad ballast) at the cross-sections. **Table 7** indicates maximum surcharge pool elevations within the specific impoundments.

Table 7: Maximum Surcharge Pool Elevations			
Impoundment Designation	Cross-Section	Top of Embankment	Maximum Surcharge Pool Elevation[a]
Unit 1 Bottom Ash	D – D′	±EL 35.5′	EL 32.8′
Unit 1 Bottom Ash	E – E′	±EL 37.1′	EL 32.8′
Unit 1 Bottom Ash	F – F′	±EL 37.9′	EL 32.8′
Unit 2/3 Bottom Ash	G – G′	±EL 43.9′	EL 40.3′
Unit 2/3 Bottom Ash	H – H′	±EL 43.1′	EL 40.3′
Unit 2/3 Bottom Ash	J – J′	±EL 43.1′	EL 40.3′
Scrubber Waste	K – K′	±EL 43.3′	EL 39.3′
Scrubber Waste	L – L′	±EL 43.6′	EL 39.3′

Stability analyses under static, maximum surcharge pool conditions were performed at the critical embankment cross-sections. 40 CFR Part 257.73 (e) (1) (ii) states that "The calculated static factor of safety under the maximum surcharge pool loading condition must equal or exceed 1.4." Analyses results indicate FS values ranging from 1.6 to 5.7 as provided in **Table 8**. Details of the analyses are included in **APPENDIX E**.

Table 8: Analyses Results, Maximum Surcharge Pool		
Impoundment Designation	Section	Factor of Safety
Unit 1 Bottom Ash	D – D′	1.6
Unit 1 Bottom Ash	E – E′	5.7
Unit 1 Bottom Ash	F – F′	5.7
Unit 2/3 Bottom Ash	G – G′	2.5
Unit 2/3 Bottom Ash	H – H′	2.5
Unit 2/3 Bottom Ash	J – J′	2.0
Scrubber Waste	K – K′	2.2
Scrubber Waste	L – L′	1.8

6.4 Seismic Stability Analysis Findings

The seismic analysis of embankment stability is performed by estimating permanent displacements rather than calculating a FS based on limit equilibrium principles. The estimated permanent deformation is compared to a tolerable displacement value in light of the potential damage to the final embankment configuration. Based on FEMA guidelines, the amount of allowable deformations along critical failure surfaces is limited to 24 inches[4]. The deformation analysis is performed to determine if potential movements resulting from the design earthquake would produce overtopping of the embankments, or if cracks could form in the embankment or foundation soils that could result in failure by internal erosion. However, for this analysis, we have assumed that permanent deformation is not allowed in the embankments.

---

[4] US Department of Homeland Security – FEMA; *Federal Guidelines for Dam Safety, Earthquake Analyses and Design of*Dams; May 2005; p. 34.

The initial step in the seismic analysis is to assign appropriate dynamic strength parameters (drained or undrained) to the subsurface materials. Reduced soil strengths are applied to soils to model the effect of cyclic loading and undrained shearing that occurs during seismic events. The fine-grained soils were assumed to exhibit 80% of their static cohesion. For non-cohesive soils, the reduced internal friction angle was calculated as $\tan^{-1}(0.8 \times \tan ø)$.

The reduced soil strength parameters were then used in a pseudo-static (seismic coefficient) analysis. Pseudostatic analysis assumes that the earthquake causes an additional horizontal force in the direction of failure due to the motion of the soil mass. The forces are computed as the product of a seismic coefficient and the weight of the soil mass. A FS is determined based on static analysis of driving and resisting forces.

The pseudo-static stability analysis is iteratively performed to evaluate the yield acceleration (k_y) for the individual cross-sections. The yield acceleration represents the smallest horizontal ground acceleration at which a marginally stable condition is produced for a potential slip surface. Therefore, the seismic coefficient that results in a pseudo-static FS of 1.0 represents k_y. Calculations resulted in k_y values ranging from 0.05g to 0.57g at the cross-sections.

The shear wave velocity of the on-site soils was determined using down-hole seismic testing in conjunction with Cone Penetration Tests (**APPENDIX F**). Shear wave testing extended to depths ranging from 45.11 feet to 69.88 feet below the existing ground surface. Measured shear wave velocities at the site ranged from approximately 180 to 1,385 feet per second (fps). Based on the test results and our experience with similar soil conditions, a shear wave velocity of 650 fps was used in the analyses. This value is typical for medium dense sand and also falls within the range of values determined at this site.

The shear wave data was used in formulating a site-specific hazard analysis to determine the ground surface acceleration and synthetic time history for the design earthquake corresponding to the 2% probability of exceedance in 50 years. The seismic hazard analysis determines the near-surface ground effects of the design earthquake. A site response analysis was performed to determine how ground motions attenuate from hard rock up through the overlying column of soil. The ground motions are described by the acceleration response spectra.

The seismic analysis included developing an actual record of earthquake accelerations at the site. In areas of low seismicity such as Alabama, historical records are very limited, requiring derivation of "synthetic" records. For the Lowman site, these records were developed by scaling micro-tremor data and applying information from other locations with similar seismicity. Details of the site-specific hazard analysis are contained in *Development of Design Ground Motions for the Lowman Power Plant* (Pacific Engineering and Analysis; dated 3/27/2012) found in **APPENDIX G**.

The Makdisi and Seed method[5] was used to determine permanent deformations of the embankments at the Lowman site. The Makdisi and Seed method is a rigorous procedure in which the maximum average acceleration (k_{max}) of the critical failure surface is determined as a percentage of the maximum acceleration at the crest of the embankment (uu_{max}). Initially, the reduced shear wave velocity is determined from the damping ratio (λ) and a reduced shear modulus. The three modal periods are then determined based on the embankment height and reduced shear wave velocity. The spectral accelerations corresponding to the model periods are determined from the response spectra (λ = 5%) for the 2,500-year return period (2% probability of exceedance in 50 years). uu_{max} is calculated based on the spectral accelerations.

k_{max} is then determined as the product of uu_{max} and the ratio of the depth of the critical pseudo-static failure surface (y) to the embankment height (H). The critical failure depth exceeded the height of the embankment at the cross-sections. Therefore, the ratio y/H was conservatively assumed to be 1.0. Based on the figure *Variation of Peak Average Acceleration Ratio with Depth of Sliding Mass* (**APPENDIX H**), the ratio of k_{max} to uu_{max} is 0.32 when y/H is 1.0.

Analyses resulted in k_{max} values ranging from 0.047g to 0.061g. Deformations occur whenever k_{max} in an embankment exceeds k_y. Conversely, yielding does not occur and there is zero permanent seismic displacement when k_{max} is less than k_y. For the Lowman site, k_{max} was less than k_y at the cross-sections. 40 CFR Part 257.73 (e) (1) (iii) states that, "The calculated seismic factor of safety must equal or exceed 1.0." Assuming zero allowable permanent displacement, the ratio of k_y/k_{max} represents an equivalent factor of safety under seismic loading.

Permanent deformations are shown not to occur during the design earthquake. Zero displacement indicates equivalent factors of safety ranging from 1.0 to 12.1 at the critical cross sections. Therefore, the embankments conform to the requirements for seismic loading.

Had analyses resulted in k_{max} values in excess of k_y, the magnitude of deformation would then be determined from the figure *Permanent Displacement verses Normalized yield Acceleration for Embankments* (**APPENDIX H**). As indicated on the figure, permanent deformation asymptotically approaches 0.0 as k_y/k_{max} approaches 1.0. The moment magnitude of the design earthquake was selected as 7.5 based on the findings of the site specific hazard analysis. Analyses results are presented in **APPENDIX I** and summarized in **Table 9.**

---

[5] Makdisi, F. I. and Seed, H. B.; "Simplified procedure for estimating dam and embankment earthquake-induced deformations"; *Journal of Geotechnical Engineering Division*, 104(GT7); 1978; pp. 849-868.

Table 9: Seismic Slope Stability Analysis Summary					
Impoundment Designation	Cross-Section	k_y[1]	k_{max}[2]	Deformation[3] (in.)	k_y/k_{max}[4]
Unit 1 Bottom Ash	D – D’	0.05g	0.049g	0.0	1.0
Unit 1 Bottom Ash	E – E’	0.57g	0.047g	0.0	12.1
Unit 1 Bottom Ash	F – F’	0.20g	0.047g	0.0	4.3
Unit 2/3 Bottom Ash	G – G’	0.22g	0.052g	0.0	4.2
Unit 2/3 Bottom Ash	H – H’	0.18g	0.052g	0.0	3.5
Unit 2/3 Bottom Ash	J – J’	0.20g	0.058g	0.0	3.4
Scrubber Waste	K – K’	0.14g	0.058g	0.0	2.4
Scrubber Waste	L – L’	0.13g	0.061g	0.0	2.1

Notes: 1 – Yield acceleration of the critical failure surface.
2 – Maximum average acceleration.
3 – Deformation does not occur when $k_{max} < k_y$.
4 – The ratio of k_y/k_{max} represents an equivalent factor of safety given no allowable permanent displacement.

6.5 Liquefaction Potential

Liquefaction refers to the “quick” condition soils exhibit when rapid motion causes an excessive build-up in pore water pressure. As water pressure increases, soil particles can become suspended within the water and lose particle-to-particle contact. The result is a dramatic drop in shear strength with soils exhibiting a liquid consistency and the potential for significant failures on otherwise stable slopes. Soils most prone to liquefaction are loose sands below the groundwater level.

Liquefaction analysis is performed by first determining potentially liquefiable soil zones within the subsurface profile of the embankment. Secondly, the liquefiable soils are then assigned a residual strength value and the embankment analyzed for stability based on conventional static analysis methods. 40 CFR Part 257.73 (e) (1) (iv) states that, “For dikes constructed of soils that have susceptibility to liquefaction, the calculated liquefaction factor of safety must equal or exceed 1.20.”

The embankment soils were evaluated for liquefaction potential using recommendations by Idriss and Boulanger[6] (2008). That is, the field (or raw) SPT N-values were normalized for overburden pressure, adjusted for a hammer efficiency of 60%, and corrected for fines content and borehole parameters. The design earthquake moment magnitude and resultant peak ground acceleration were determined from the site-specific seismic hazard analysis. The average static shear stress on the horizontal plane was approximate based on elastic theory as presented by Poulos and Davis[7]. The FS for liquefaction of soil layers is calculated as the quotient of the cyclic resistance ratio divided by the cyclic stress ratio.

---

[6] Idriss and Boulanger; *Residual Shear Strength of Liquefied Soils*; University of California, Davis – Department of Civil and Environmental Engineering; 2007.

[7] Poulos, H.G. and Davis, E.H., *Elastic Solutions for Soil and Rock Mechanics; 1974.*

Resultant FS values were a minimum of 1.8. Therefore, the results indicate that the embankments were not constructed of soils that have susceptibility to liquefaction. The following **Table 10** provides the minimum FS at the cross-sections. Details of the liquefaction potential analyses at the cross-sections are included in **APPENDIX J**.

Table 10: Analyses of Liquefaction Potential

Impoundment Designation	Section	Minimum Factor of Safety
Unit 1 Bottom Ash	D – D'	1.8
Unit 1 Bottom Ash	E – E'	Non-liquefiable[1]
Unit 1 Bottom Ash	F – F'	Non-liquefiable[1]
Unit 2/3 Bottom Ash	G – G'	>>5
Unit 2/3 Bottom Ash	H – H'	6.6
Unit 2/3 Bottom Ash	J – J'	5.5
Scrubber Waste	K – K'	2.7
Scrubber Waste	L – L'	>>5

Note: 1 – Sections E and F encountered clay (non-liquefiable) below the water level.

7.0 SUMMARY OF STABILITY FINDINGS

Federal regulations (40 CFR 257.73) require that the stability of CCR impoundment embankments be periodically evaluated. The purpose of this study was to perform the required evaluations for the embankments at the Lowman Power Plant. The stability evaluation was conducted on the exterior embankments associated with the Scrubber Waste, Unit 2/3 Bottom Ash, and the Unit 1 Bottom Ash Ponds.

Regulations state that the evaluation is to be performed under static long-term maximum storage pool, static maximum surcharge pool and seismic loading scenarios. Additionally, for dikes constructed of soils that have susceptibility to liquefaction, the stability is to be evaluated under liquefaction conditions.

Our stability analyses indicate that the embankments exhibit factors of safety that equal or exceed the required minimum values under the maximum storage pool, maximum surcharge pool and seismic loading scenarios. Additionally, the embankment soils are demonstrated not to be susceptible to liquefaction, and further analyses under the liquefaction loading scenario is not required. Therefore, the embankments are in compliance with the periodic safety factor assessment requirements. The following **Table 11** summarizes the results of our analyses.

Table 11: Summary of Analyses Results

Loading Condition	Calculated Minimum Factor of Safety	Required Minimum Factor of Safety	Conforms to Regulations
Long-Term Maximum Storage Pool	1.6	1.5	Yes
Maximum Surcharge Pool	1.6	1.4	Yes
Seismic	1.0	1.0	Yes
Liquefaction	1.8[1]	1.2	Yes

Note 1: The embankment soils are shown not to be susceptible to liquefaction; therefore, further analysis under the liquefaction loading scenario is not required.

8.0 GENERAL REMARKS AND CLOSING

This report has been prepared for the exclusive use of Rushton, Stakely, Johnston & Garrett, P.A. for specific application to the Coal Combustion Residual Impoundment Embankments Stability Evaluation project at Charles R. Lowman Power Plant in Leroy, Alabama and is not transferable to a third party. The recommendations in this report are intended for use on the stated project and should not be used for other purposes.

The analyses and conclusions presented in this report are based upon currently accepted engineering principles, practices, and existing testing standards in the area where the services were provided. No other warranty, expressed or implied, is made.

The findings in this report were developed based on written and verbal information provided by the client and from the limited data obtained from the field and laboratory testing programs. If significant changes are made to the use, capacity or geometry of the embankments and/or impoundments, CDG should be allowed to review our findings in light of the changes to determine if additional testing and revised conclusions are needed.

Appendix A

Test Location Plan

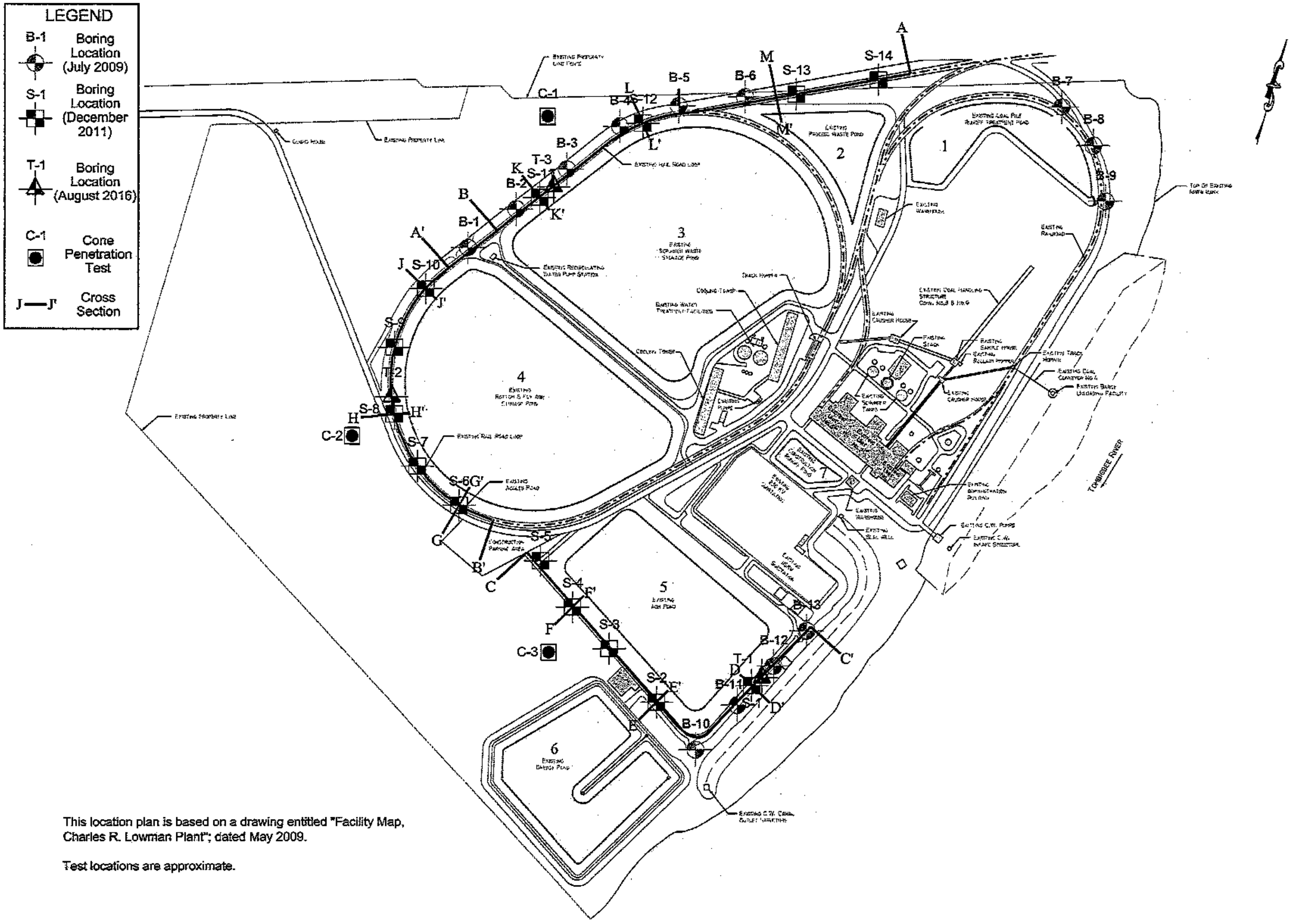

This location plan is based on a drawing entitled "Facility Map, Charles R. Lowman Plant"; dated May 2009.

Test locations are approximate.

Test Location Plan

Safety Factor Assessment
Coal Combustion Residuals Impoundments
Charles R. Lowman Power Plant
Leroy, Alabama
CDG Reference No.: 061521207

Drawn By: JRA
Scale: 1"=+/-500'
Date: 09/20/2016

CDG
Engineering. Environmental. Answers.

Appendix B
Boring Logs

CDG Engineers & associates

Albertville, AL Tel:(256) 891-3458	Andalusia, AL Tel:(334) 222-9431	Birmingham, AL Tel:(205) 733-9431
Hoover, AL Tel:(205) 463-2600	Defuniak Springs, FL Tel:(850) 892-0225	Dothan, AL Tel:(334) 677-9431

BORING LOG

Project Name: Berm Stability Evaluation - Lowman Power Plant
Project Number: 060921201
Boring Number: B-1
Date Drilled: July 15, 2009 Page 1 of 2

Notes: SS = Split Spoon
PPqu = Pocket Penetrometer Unconfined Compressive Strength

Depth (feet)	Approx. Elev. (feet)	Graphic Scale	MATERIAL DESCRIPTION	TYPE	BLOWS/ 6 INCHES	N	CORE REC. (%)	RQD (%)	REMARKS
0	44								
			Crushed aggregate						
			Very dense, red, silty fine to medium SAND, with numerous rock fragments	SS	26-27-28	50+			
5	39								
				SS	20-22-23	45			
			...same	SS	24-24-26	50			
10	34								
			... with numerous rock fragments	SS	29-37-40	50+			
15	29								
			Very dense, silty, coarse-grained SAND, with trace rock fragments	SS	26-38-43	50+			▽ Groundwater encountered at 20 feet at time of boring
20	24								
			Stiff, brown, fine sandy CLAY with gravel	SS	6-6-7	13			
25	19								

BORING LOG

Project Name: Berm Stability Evaluation - Lowman Power Plant
Project Number: 060921201 Phase 3
Boring Number: B-1
Date Drilled: July 15, 2009 Page 2 of 2

Notes: SS = Split Spoon
PPqu = Pocket Penetrometer Unconfined Compressive Strength

Depth (feet)	Approx. Elev. (feet)	Graphic Scale	MATERIAL DESCRIPTION	TYPE	BLOWS/ 6 INCHES	N	CORE REC. (%)	RQD (%)	REMARKS
25	19		Stiff, brown, fine sandy CLAY with gravel (Fill)						
			Medium, grey and tan, fine sandy CLAY	SS	2-3-4	7			
30	14								
			... stiff, grey	SS	3-5-5	10			PPqu = 1.25 tsf
35	9								
			(Low Terrace Deposits)	SS	4-4-7	11			PPqu = 1.25 tsf
40	4		Boring Terminated at 40 feet						
45	-1								
50	-6								Boring backfilled with grout upon completion.

CDG Engineers
& associates

Albertville, AL Tel:(256) 891-3458	Andalusia, AL Tel:(334) 222-9431	Birmingham, AL Tel:(205) 733-9431
Hoover, AL Tel:(205) 463-2600	Defuniak Springs, FL Tel:(850) 892-0225	Dothan, AL Tel:(334) 677-9431

BORING LOG

Project Name: Berm Stability Evaluation - Lowman Power Plant

Project Number: 060921201

Boring Number: B-2

Date Drilled: July 14, 2009

Page 1 of 2

Notes: SS = Split Spoon

Depth (feet)	Approx. Elev. (feet)	Graphic Scale	MATERIAL DESCRIPTION	TYPE	BLOWS/ 6 INCHES	N	CORE REC. (%)	RQD (%)	REMARKS
0	44		Crushed aggregate						
			Dense, red, silty fine to medium SAND	SS	19-20-20	40			LL=18, PL=14, PI=4 Fines Content = 33.5% USCS = SC-SM MC = 8.8%
5	39								
				SS	20-21-22	43			MC = 8.4%
			...very dense, with numerous rock fragments	SS	14-23-30	50+			MC = 10.2%
10	34								∇ Groundwater encountered at +/-11 feet on 8/4/2009.
									∇ Groundwater encountered at 13.5 feet at time of boring
			Dense, tan, silty coarse SAND with numerous rock fragments	SS	21-18-20	38			MC = 13.3%
15	29								
			Medium dense, reddish tan, silty fine SAND with trace rock fragments	SS	7-10-14	24			LL=23, PL=20, PI=3 Fines Content = 25.5% USCS = SM MC = 14.9%
20	24								
			...dense, with gravel	SS	8-13-20	33			MC = 11.3%
25	19								

CDG Engineers
& associates

Albertville, AL
Tel:(256) 891-3458

Andalusia, AL
Tel:(334) 222-9431

Birmingham, AL
Tel:(205) 733-9431

Hoover, AL
Tel:(205) 463-2600

Defuniak Springs, FL
Tel:(850) 892-0225

Dothan, AL
Tel:(334) 677-9431

BORING LOG

Project Name: Berm Stability Evaluation - Lowman Power Plant
Project Number: 060921201
Boring Number: B-2
Date Drilled: July 14, 2009 Page 2 of 2

Notes: SS = Split Spoon

Depth (feet)	Approx. Elev. (feet)	Graphic Scale	MATERIAL DESCRIPTION	TYPE	BLOWS/ 6 INCHES	N	CORE REC. (%)	RQD (%)	REMARKS
25	19		Dense, reddish tan, silty fine SAND, with gravel (Fill)						
			Medium dense, reddish tan, silty fine to coarse-grained SAND	SS	6-12-8	20			MC = 14.2%
30	14								
			Loose, grey, silty fine SAND	SS	2-3-4	7			LL=NP, PL=NP, PI=NP Fines Content = 20.0% USCS = SM MC = 28.3%
35	9								
			... medium dense, with gravel (Low Terrace Deposits)	SS	6-8-8	16			MC = 23.9%
40	4		Boring Terminated at 40 feet						
45	-1								
50	-6								Piezometer installed at the time of boring.

CDG Engineers
& associates

Albertville, AL
Tel:(256) 891-3458

Andalusia, AL
Tel:(334) 222-9431

Birmingham, AL
Tel:(205) 733-9431

Hoover, AL
Tel:(205) 463-2600

Defuniak Springs, FL
Tel:(850) 892-0225

Dothan, AL
Tel:(334) 677-9431

BORING LOG

Project Name: Berm Stability Evaluation - Lowman Power Plant

Project Number: 060921201

Boring Number: B-3

Date Drilled: July 15, 2009

Page 1 of 2

Notes: SS = Split Spoon

Depth (feet)	Approx. Elev. (feet)	Graphic Scale	MATERIAL DESCRIPTION	TYPE	BLOWS/ 6 INCHES	N	CORE REC. (%)	RQD (%)	REMARKS
0	44								
			Crushed aggregate						
			Medium dense, red, silty fine to medium SAND, with numerous rock fragments	SS	7-10-15	25			
5	39								
			... dense	SS	10-18-16	34			
			...reddish tan, with gravel	SS	16-18-18	36			
10	34								
			... very dense, tan, with gravel	SS	24-28-34	50+			
15	29								
			... dense, reddish tan, with trace rock fragments	SS	18-20-29	49			∇ Groundwater encountered at 20 feet at time of boring
20	24								
			...red, with gravel	SS	10-16-22	38			
25	19								

CDG Engineers & associates

Albertville, AL Tel:(256) 891-3458	Andalusia, AL Tel:(334) 222-9431	Birmingham, AL Tel:(205) 733-9431
Hoover, AL Tel:(205) 463-2600	Defuniak Springs, FL Tel:(850) 892-0225	Dothan, AL Tel:(334) 677-9431

BORING LOG

Project Name: Berm Stability Evaluation - Lowman Power Plant

Project Number: 060921201

Boring Number: B-3

Date Drilled: July 15, 2009 Page 2 of 2

Notes: SS = Split Spoon

Depth (feet)	Approx. Elev. (feet)	Graphic Scale	MATERIAL DESCRIPTION	TYPE	BLOWS/ 6 INCHES	N	CORE REC. (%)	RQD (%)	REMARKS
25	19								
			Dense, red, silty fine to medium SAND, with gravel	SS	11-14-11	25			
30	14		(Fill)						
			Stiff, grey and tan, fine sandy CLAY, with gravel	SS	5-6-6	12			
35	9								
			Medium dense, grey and tan, silty fine SAND (Low Terrace Deposits)	SS	5-6-7	13			
40	4		Boring Terminated at 40 feet						
45	-1								
50	-6								Boring backfilled with grout upon completion.

CDG Engineers
& associates

Albertville, AL
Tel:(256) 891-3458

Andalusia, AL
Tel:(334) 222-9431

Birmingham, AL
Tel:(205) 733-9431

Hoover, AL
Tel:(205) 463-2600

Defuniak Springs, FL
Tel:(850) 892-0225

Dothan, AL
Tel:(334) 677-9431

BORING LOG

Project Name: Berm Stability Evaluation - Lowman Power Plant
Project Number: 060921201
Boring Number: B-4
Date Drilled: July 13, 2009

Page 1 of 2

Notes: SS = Split Spoon

Depth (feet)	Approx. Elev. (feet)	Graphic Scale	MATERIAL DESCRIPTION	TYPE	BLOWS/ 6 INCHES	N	CORE REC. (%)	RQD (%)	REMARKS
0	44		Crushed aggregate						
			Dense, red, silty fine to medium SAND	SS	21-24-26	50			MC = 8.4%
5	39								
			...very dense, with gravel	SS	15-25-27	50+			MC = 8.5%
			...medium dense	SS	9-12-15	27			MC = 14.2%
10	34								
			...very dense, reddish brown	SS	30-35-40	50+			MC = 7.3%
15	29								
20	24		...dense, orange and tan	SS	12-14-19	33			MC = 14.7% ∇ Groundwater encountered at 20 feet at time of boring
			...medium dense, red	SS	10-12-15	27			MC = 21.4%
25	+/-19								

CDG Engineers & associates

Albertville, AL Tel:(256) 891-3458	Andalusia, AL Tel:(334) 222-9431	Birmingham, AL Tel:(205) 733-9431
Hoover, AL Tel:(205) 463-2600	Defuniak Springs, FL Tel:(850) 892-0225	Dothan, AL Tel:(334) 677-9431

BORING LOG

Project Name: Berm Stability Evaluation - Lowman Power Plant

Project Number: 060921201

Boring Number: B-4

Date Drilled: July 13, 2009 Page 2 of 2

Notes: SS = Split Spoon

Depth (feet)	Approx. Elev. (feet)	Graphic Scale	MATERIAL DESCRIPTION	TYPE	BLOWS/ 6 INCHES	N	CORE REC. (%)	RQD (%)	REMARKS
25	19		Medium dense, red, silty fine to medium SAND, with gravel						
			Medium dense, tan, silty fine SAND, with gravel	SS	5-7-7	14			MC = 15.3%
30	14		(Fill)						
				SS	2-3-4	7			No recovery
35	9								
			Loose, brown, silty fine SAND (Low Terrace Deposits)	SS	4-3-4	7			MC = 38.2%
40	4		Boring Terminated at 40 feet						
45	-1								
50	-6								Boring backfilled with grout upon completion.

CDG Engineers
& associates

Albertville, AL
Tel:(256) 891-3458

Andalusia, AL
Tel:(334) 222-9431

Birmingham, AL
Tel:(205) 733-9431

Hoover, AL
Tel:(205) 463-2600

Defuniak Springs, FL
Tel:(850) 892-0225

Dothan, AL
Tel:(334) 677-9431

BORING LOG

Project Name: Berm Stability Evaluation - Lowman Power Plant
Project Number: 060921201
Boring Number: B-5
Date Drilled: July 15, 2009

Page 1 of 2

Notes: SS = Split Spoon

Depth (feet)	Approx. Elev. (feet)	Graphic Scale	MATERIAL DESCRIPTION	TYPE	BLOWS/ 6 INCHES	N	CORE REC. (%)	RQD (%)	REMARKS
0	43								
			Crushed aggregate						
			Dense, red, silty fine to coarse SAND, with gravel	SS	10-18-20	38			LL=17, PL=16, PI=1 Fines Content = 21.1% USCS = SM MC = 7.2%
5	38								
			...medium dense	SS	8-12-16	28			MC = 8.3%
			...reddish orange	SS	10-11-12	23			LL=NP, PL=NP, PI=NP Fines Content = 15.3% USCS = SM MC = 8.6%
10	33								
			...same	SS	10-12-16	28			
15	28								
			...same	SS	8-10-14	24			▽ Groundwater encountered at +/-19 feet on 8/4/2009. MC = 13.6%
20	23								
			...dense	SS	15-18-23	41			MC = 15.2%
25	18								

CDG Engineers & associates

Albertville, AL
Tel:(256) 891-3458

Andalusia, AL
Tel:(334) 222-9431

Birmingham, AL
Tel:(205) 733-9431

Hoover, AL
Tel:(205) 463-2600

Defuniak Springs, FL
Tel:(850) 892-0225

Dothan, AL
Tel:(334) 677-9431

BORING LOG

Project Name: Berm Stability Evaluation - Lowman Power Plant
Project Number: 060921201
Boring Number: B-5
Date Drilled: July 15, 2009 Page 2 of 2

Notes: SS = Split Spoon
PPqu = Pocket Penetrometer Unconfined Compressive Strength

Depth (feet)	Approx. Elev. (feet)	Graphic Scale	MATERIAL DESCRIPTION	TYPE	BLOWS/ 6 INCHES	N	CORE REC. (%)	RQD (%)	REMARKS
25	18								
			Reddish orange, silty fine to medium SAND, with gravel (Fill)	SS	6-8-8	16			∇ Groundwater encountered at 30 feet at time of boring
30	13		Stiff, grey, fine sandy CLAY						PPqu = 1.0 tsf
			Medium dense, grey and tan, silty fine SAND	SS	4-6-6	12			LL=23, PL=21, PI=2 USCS = SM MC = 29.7%
35	8								
			...same (Low Terrace Deposits)	SS	4-4-7	11			MC = 28.5%
40	3		Boring Terminated at 40 feet						
45	-2								
50	-7								Piezometer installed at the time of boring.

CDG Engineers
& associates

Albertville, AL
Tel:(256) 891-3458

Andalusia, AL
Tel:(334) 222-9431

Birmingham, AL
Tel:(205) 733-9431

Hoover, AL
Tel:(205) 463-2600

Defuniak Springs, FL
Tel:(850) 892-0225

Dothan, AL
Tel:(334) 677-9431

BORING LOG

Project Name: Berm Stability Evaluation - Lowman Power Plant
Project Number: 060921201
Boring Number: B-6
Date Drilled: July 15, 2009
Page 1 of 2

Notes: SS = Split Spoon

Depth (feet)	Approx. Elev. (feet)	Graphic Scale	MATERIAL DESCRIPTION	TYPE	BLOWS/ 6 INCHES	N	CORE REC. (%)	RQD (%)	REMARKS
0	43								
			Crushed aggregate						
			Medium dense, red, silty fine to medium SAND, with trace gravel	SS	10-11-12	23			
5	38								
				SS	11-14-14	28			
			...red and orange	SS	16-16-14	30			
10	33								▽ Groundwater encountered at 10 feet at time of boring
			... dense, orange with gravel	SS	19-24-26	40			
15	28								
			...medium dense	SS	8-9-10	19			
20	23								
			...same	SS	10-10-12	22			
25	18								

CDG Engineers
& associates

Albertville, AL
Tel:(256) 891-3458

Andalusia, AL
Tel:(334) 222-9431

Birmingham, AL
Tel:(205) 733-9431

Hoover, AL
Tel:(205) 463-2600

Defuniak Springs, FL
Tel:(850) 892-0225

Dothan, AL
Tel:(334) 677-9431

BORING LOG

Project Name:	Berm Stability Evaluation - Lowman Power Plant	
Project Number:	060921201	
Boring Number:	B-6	
Date Drilled:	July 15, 2009	Page 2 of 2

Notes: SS = Split Spoon
PPqu = Pocket Penetrometer Unconfined Compressive Strength

Depth (feet)	Approx. Elev. (feet)	Graphic Scale	MATERIAL DESCRIPTION	TYPE	BLOWS/ 6 INCHES	N	CORE REC. (%)	RQD (%)	REMARKS
25	18		Medium dense, orange, silty fine to medium SAND, with gravel (Fill)						
			Stiff, grey, fine sandy CLAY	SS	5-5-7	12			PPqu = 1.25 tsf
30	13								
			Medium dense, brown, silty fine SAND	SS	6-6-10	16			
35	8								
			...tan and brown (Low Terrace Deposits)	SS	6-8-10	18			
40	3		Boring Terminated at 40 feet						
45	-2								
50	-7								Boring backfilled with grout upon completion.

CDG Engineers
& associates

Albertville, AL
Tel:(256) 891-3458

Andalusia, AL
Tel:(334) 222-9431

Birmingham, AL
Tel:(205) 733-9431

Hoover, AL
Tel:(205) 463-2600

Defuniak Springs, FL
Tel:(850) 892-0225

Dothan, AL
Tel:(334) 677-9431

BORING LOG

Project Name: Berm Stability Evaluation - Lowman Power Plant
Project Number: 060921201
Boring Number: B-7
Date Drilled: July 17, 2009
Page 1 of 2

Notes: SS = Split Spoon

Depth (feet)	Approx. Elev. (feet)	Graphic Scale	MATERIAL DESCRIPTION	TYPE	BLOWS/ 6 INCHES	N	CORE REC. (%)	RQD (%)	REMARKS
0	41								
			Crushed aggregate with silty SAND						
			Medium dense, brown and orange, silty fine to medium SAND, with gravel	SS	12-13-8	21			
5	36								
			... brown and grey, fine - grained	SS	7-12-12	24			
			...dense	SS	10-15-16	31			▽ Groundwater encountered at 10 feet at time of boring
10	31								
			... medium dense, grey	SS	7-9-13	22			
15	26								
			(Fill)						
			Loose, brown, silty fine to medium SAND	SS	2-3-3	6			
20	21								
			...medium dense	SS	5-12-14	26			
25	16								

CDG Engineers & associates

Albertville, AL
Tel:(256) 891-3458

Andalusia, AL
Tel:(334) 222-9431

Birmingham, AL
Tel:(205) 733-9431

Hoover, AL
Tel:(205) 463-2600

Defuniak Springs, FL
Tel:(850) 892-0225

Dothan, AL
Tel:(334) 677-9431

BORING LOG

Project Name: Berm Stability Evaluation - Lowman Power Plant

Project Number: 060921201

Boring Number: B-7

Date Drilled: July 17, 2009

Page 2 of 2

Notes: SS = Split Spoon

Depth (feet)	Approx. Elev. (feet)	Graphic Scale	MATERIAL DESCRIPTION	TYPE	BLOWS/ 6 INCHES	N	CORE REC. (%)	RQD (%)	REMARKS
25	16								
			Medium dense, brown, silty fine to medium SAND	SS	7-8-6	14			
30	11								
			...loose, brown	SS	4-5-5	10			
35	6								
			...medium dense (Low Terrace Deposits)	SS	5-7-7	14			
40	1		Boring Terminated at 40 feet						
45	-4								
50	-9								Boring backfilled with grout upon completion.

CDG Engineers
& associates

Albertville, AL Tel:(256) 891-3458	Andalusia, AL Tel:(334) 222-9431	Birmingham, AL Tel:(205) 733-9431
Hoover, AL Tel:(205) 463-2600	Defuniak Springs, FL Tel:(850) 892-0225	Dothan, AL Tel:(334) 677-9431

BORING LOG

Project Name:	Berm Stability Evaluation - Lowman Power Plant
Project Number:	060921201
Boring Number:	B-8
Date Drilled:	July 17, 2009 Page 2 of 2

Notes: SS = Split Spoon

Depth (feet)	Approx. Elev. (feet)	Graphic Scale	MATERIAL DESCRIPTION	TYPE	BLOWS/ 6 INCHES	N	CORE REC. (%)	RQD (%)	REMARKS
25	16								
			...medium, brown	SS	2-3-3	6			LL=34, PL=15, PI=19 Fines Content = 67.9% USCS = CL MC = 35.6% ▼ Groundwater encountered at +/-31 feet on 8/4/2009.
30	11								
			Medium dense, brown, silty fine SAND	SS	11-15-15	30			MC = 18.6%
35	6								
			...same (Low Terrace Deposits)	SS	5-5-7	12			MC = 31.7%
40	1		Boring Terminated at 40 feet						
45	-4								
50	-9								Piezometer installed at the time of boring.

CDG Engineers & associates

Albertville, AL
Tel:(256) 891-3458

Andalusia, AL
Tel:(334) 222-9431

Birmingham, AL
Tel:(205) 733-9431

Hoover, AL
Tel:(205) 463-2600

Defuniak Springs, FL
Tel:(850) 892-0225

Dothan, AL
Tel:(334) 677-9431

BORING LOG

Project Name: Berm Stability Evaluation - Lowman Power Plant
Project Number: 060921201
Boring Number: B-8
Date Drilled: July 17, 2009

Notes: SS = Split Spoon
UD = Undisturbed Sample

Depth (feet)	Approx. Elev. (feet)	Graphic Scale	MATERIAL DESCRIPTION	TYPE	BLOWS/ 6 INCHES	N	CORE REC. (%)	RQD (%)	REMARKS
0	41								
			Crushed aggregate with silty SAND						
			Dense, greyish brown, silty fine SAND	SS	12-19-20	39			MC = 14.7%
5	36								
			...grey and brown	SS	10-16-20	36			LL=NP, PL=NP, PI=NP Fines Content = 34.5% USCS = SM MC = 7.2%
10	31								∇ Groundwater encountered at 10 feet at time of boring
			... medium dense, brown	SS	5-10-12	22			MC = 11.7%
15	26								
			(Fill)						
			Very loose, brown, silty fine SAND	SS	2-2-2	4			LL=24, PL=20, PI=4 Fines Content = 48.9% USCS = SM-SC MC = 30.0%
20	21								
				UD					
			Stiff, grey, fine sandy CLAY	SS	3-5-5	10			MC = 32.9%
25	16								

CDG Engineers & associates

Albertville, AL Tel:(256) 891-3458	Andalusia, AL Tel:(334) 222-9431	Birmingham, AL Tel:(205) 733-9431
Hoover, AL Tel:(205) 463-2600	Defuniak Springs, FL Tel:(850) 892-0225	Dothan, AL Tel:(334) 677-9431

BORING LOG

Project Name: Berm Stability Evaluation - Lowman Power Plant
Project Number: 060921201
Boring Number: B-9
Date Drilled: July 16, 2009 Page 1 of 2

Notes: SS = Split Spoon

Depth (feet)	Approx. Elev. (feet)	Graphic Scale	MATERIAL DESCRIPTION	TYPE	BLOWS/ 6 INCHES	N	CORE REC. (%)	RQD (%)	REMARKS
0	41								
			Crushed aggregate with silty SAND						
			Dense, grey and brown, silty fine SAND	SS	6-13-20	33			LL=22, PL=19, PI=3 Fines Content = 43.9% USCS = SM MC = 10.9%
5	36								
				SS	14-19-21	40			MC = 8.9%
			...same	SS	14-16-16	32			MC = 10.5% ∇ Groundwater encountered at 10 feet at time of boring
10	31								
			Medium dense, brown, fine SAND with silt	SS	5-6-8	14			LL=NP, PL=NP, PI=NP Fines Content = 7.8% USCS = SM MC = 16.9%
15	26								
			(Fill)						
			Medium, brown, fine sandy CLAY	SS	3-4-3	7			MC = 31.5%
20	21								
			...soft	SS	3-3-2	5			LL=26, PL=21, PI=5 Fines Content = 54.4% USCS = CL MC = 30.3%
25	16								

BORING LOG

Project Name: Berm Stability Evaluation - Lowman Power Plant
Project Number: 060921201
Boring Number: B-9
Date Drilled: July 16, 2009 Page 2 of 2

Notes: SS = Split Spoon

Depth (feet)	Approx. Elev. (feet)	Graphic Scale	MATERIAL DESCRIPTION	TYPE	BLOWS/ 6 INCHES	N	CORE REC. (%)	RQD (%)	REMARKS
25	16								
			...stiff	SS	5-5-5	10			MC = 24.6%
30	11								
			...soft, silty	SS	3-1-3	4			LL=25, PL=18, PI=7 Fines Content = 51.0% USCS = CL-ML MC = 29.8%
35	6								
			...stiff (Low Terrace Deposits)	SS	2-5-7	12			MC = 29.4%
40	1		Boring Terminated at 40 feet						
45	-4								
50	-9								Boring backfilled with grout upon completion.

CDG Engineers & associates

Albertville, AL
Tel:(256) 891-3458

Andalusia, AL
Tel:(334) 222-9431

Birmingham, AL
Tel:(205) 733-9431

Hoover, AL
Tel:(205) 463-2600

Defuniak Springs, FL
Tel:(850) 892-0225

Dothan, AL
Tel:(334) 677-9431

BORING LOG

Project Name: Berm Stability Evaluation - Lowman Power Plant
Project Number: 060921201
Boring Number: B-10
Date Drilled: July 13, 2009 Page 1 of 2

Notes: SS = Split Spoon

PPqu = Pocket Penetrometer Unconfined Compressive Strength

Depth (feet)	Approx. Elev. (feet)	Graphic Scale	MATERIAL DESCRIPTION	TYPE	BLOWS/ 6 INCHES	N	CORE REC. (%)	RQD (%)	REMARKS
0	39								
			Very stiff, red, fine sandy CLAY with numerous rock fragments	SS	3-4-10	14			
5	34		...stiff (Fill)	SS	2-4-5	9			PPqu = 1.25 tsf
			Very stiff, grey and brown, fine sandy CLAY	SS	5-5-9	14			
10	29								
			...stiff, grey	SS	4-4-5	9			
			...medium	SS	2-2-4	6			PPqu = 0.50 tsf ∇ Groundwater encountered at 15 feet at time of boring
15	24								
			Very loose, brown, silty fine to medium SAND	SS	2-1-2	3			
20	19								
				SS	2-1-1	2			
25	14		...same						

CDG Engineers
& associates

Albertville, AL
Tel:(256) 891-3458

Andalusia, AL
Tel:(334) 222-9431

Birmingham, AL
Tel:(205) 733-9431

Hoover, AL
Tel:(205) 463-2600

Defuniak Springs, FL
Tel:(850) 892-0225

Dothan, AL
Tel:(334) 677-9431

BORING LOG

Project Name:	Berm Stability Evaluation - Lowman Power Plant
Project Number:	060921201
Boring Number:	B-10
Date Drilled:	July 13, 2009 Page 2 of 2

Notes: SS = Split Spoon

Depth (feet)	Approx. Elev. (feet)	Graphic Scale	MATERIAL DESCRIPTION	TYPE	BLOWS/ 6 INCHES	N	CORE REC. (%)	RQD (%)	REMARKS
25	14								
				SS	3-2-1	3			
30	9		...brown and grey						
			... loose, grey and orange	SS	3-2-3	5			
35	4								
			...grey (Low Terrace Deposits)	SS	4-3-3	6			
40	-1		Boring Terminated at 40 feet						
45	-6								
50	-11								Boring backfilled with grout upon completion.

CDG Engineers & associates

Albertville, AL
Tel:(256) 891-3458

Andalusia, AL
Tel:(334) 222-9431

Birmingham, AL
Tel:(205) 733-9431

Hoover, AL
Tel:(205) 463-2600

Defuniak Springs, FL
Tel:(850) 892-0225

Dothan, AL
Tel:(334) 677-9431

BORING LOG

Project Name:	Berm Stability Evaluation - Lowman Power Plant
Project Number:	060921201
Boring Number:	B-11
Date Drilled:	July 13, 2009

Page 1 of 2

Notes: SS = Split Spoon

PPqu = Pocket Penetrometer Unconfined Compressive Strength

Depth (feet)	Approx. Elev. (feet)	Graphic Scale	MATERIAL DESCRIPTION	TYPE	BLOWS/ 6 INCHES	N	CORE REC. (%)	RQD (%)	REMARKS
0	39								
			Very stiff, orange and tan, fine sandy CLAY	SS	4-7-10	17			LL=39, PL=18, PI=21 Fines Content = 55.4% USCS = CL
5	34		... stiff	SS	3-4-4	9			LL=36, PL=20, PI=16 Fines Content = 56.5% USCS = CL
			— — — — — — — — — — — —						
			Medium dense, brown, clayey fine to medium SAND with gravel	SS	6-9-14	23			
10	29		...with clay	SS	8-8-9	17			
			(Fill)						▽ Groundwater encountered at +/-13 feet on 8/4/2009.
			Soft, grey, silty CLAY with fine sand	SS	2-2-3	5			LL=40, PL=17, PI=23 Fines Content = 91.6% USCS = CL PPqu < 0.25 tsf
15	24								
20	19		...medium	SS	2-3-3	6			
			— — — — — — — — — — — —						
			Soft, grey, fine sandy CLAY	SS	2-2-3	5			LL=28, PL=20, PI=8 Fines Content = 67.2% USCS = CL MC = 35.3% PPqu < 0.25 tsf
25	14								

BORING LOG

Project Name: Berm Stability Evaluation - Lowman Power Plant
Project Number: 060921201
Boring Number: B-11
Date Drilled: July 13, 2009 Page 2 of 2

Notes: SS = Split Spoon

Depth (feet)	Approx. Elev. (feet)	Graphic Scale	MATERIAL DESCRIPTION	TYPE	BLOWS/ 6 INCHES	N	CORE REC. (%)	RQD (%)	REMARKS
25	14		Soft, grey, fine sandy CLAY						
30	9		Loose, brown, silty fine SAND	SS	3-3-3	6			MC = 26.2%
35	4		...very loose	SS	1-1-1	2			LL=21, PL=20, PI=1 Fines Content = 19.6% USCS = SM MC = 36.9%
40	-1		...loose (Low Terrace Deposits)	SS	7-5-4	9			MC = 27.1%
			Boring Terminated at 40 feet						
45	-6								
50	-11								Piezometer installed at the time of boring.

CDG Engineers
& associates

Albertville, AL
Tel:(256) 891-3458

Andalusia, AL
Tel:(334) 222-9431

Birmingham, AL
Tel:(205) 733-9431

Hoover, AL
Tel:(205) 463-2600

Defuniak Springs, FL
Tel:(850) 892-0225

Dothan, AL
Tel:(334) 677-9431

BORING LOG

Project Name: Berm Stability Evaluation - Lowman Power Plant
Project Number: 060921201
Boring Number: B-12
Date Drilled: July 16, 2009 Page 1 of 2

Notes: SS = Split Spoon
PPqu = Pocket Penetrometer Unconfined Compressive Strength

Depth (feet)	Approx. Elev. (feet)	Graphic Scale	MATERIAL DESCRIPTION	TYPE	BLOWS/ 6 INCHES	N	CORE REC. (%)	RQD (%)	REMARKS
0	39								
			Crushed aggregate with silty SAND						
			Medium dense, orange and tan, silty fine to medium SAND	SS	4-5-6	11			
5	34								
				SS	7-11-11	22			
			(Fill)						
			Medium dense, brown, silty fine to medium SAND	SS	5-8-9	17			
10	29								∇ Groundwater encountered at 10 feet at time of boring
			...grey	SS	7-7-10	17			
15	24								
			Medium, grey, fine sandy CLAY	SS	4-4-4	8			PPqu = 0.75 tsf
20	19								
			...same	SS	3-4-3	7			
25	14								

BORING LOG

Project Name: Berm Stability Evaluation - Lowman Power Plant
Project Number: 060921201
Boring Number: B-12
Date Drilled: July 16, 2009 Page 2 of 2

Notes: SS = Split Spoon
PPqu = Pocket Penetrometer Unconfined Compressive Strength

Depth (feet)	Approx. Elev. (feet)	Graphic Scale	MATERIAL DESCRIPTION	TYPE	BLOWS/ 6 INCHES	N	CORE REC. (%)	RQD (%)	REMARKS
25	14								
			...very soft	SS	2-1-2	3			PPqu < 0.25 tsf
30	9								
			...soft	SS	2-2-3	5			PPqu < 0.25 tsf
35	4								
			Medium dense, grey, clayey fine to medium SAND (Low Terrace Deposits)	SS	7-9-13	22			
40	-1		Boring Terminated at 40 feet						
45	-6								
50	-11								Boring backfilled with grout upon completion.

CDG Engineers & associates

Albertville, AL
Tel:(256) 891-3458

Andalusia, AL
Tel:(334) 222-9431

Birmingham, AL
Tel:(205) 733-9431

Hoover, AL
Tel:(205) 463-2600

Defuniak Springs, FL
Tel:(850) 892-0225

Dothan, AL
Tel:(334) 677-9431

BORING LOG

Project Name:	Berm Stability Evaluation - Lowman Power Plant
Project Number:	060921201
Boring Number:	B-13
Date Drilled:	July 16, 2009

Page 1 of 2

Notes:
SS = Split Spoon
PPqu = Pocket Penetrometer Unconfined Compressive Strength
UD = Undisturbed Sample

Depth (feet)	Approx. Elev. (feet)	Graphic Scale	MATERIAL DESCRIPTION	TYPE	BLOWS/ 6 INCHES	N	CORE REC. (%)	RQD (%)	REMARKS
0	39		Crushed aggregate with silty SAND						
			Stiff, red, fine sandy CLAY	SS	5-7-8	15			LL=42, PL=19, PI=23 Fines Content = 51.6% USCS = CL MC = 13.6%
5	34								
			...hard, with gravel (Fill)	SS	26-28-30	50+			MC = 11.0%
			Medium dense, tan, silty fine to medium SAND		10-10-10	20			MC = 20.2% ▽ Groundwater encountered at 10 feet at time of boring
10	29								
				UD					
				SS	3-3-3	6			No Recovery
15	24								
			Very soft, grey, fine sandy CLAY	SS	1-1-2	3			▽ Groundwater encountered at +/-19 feet on 8/4/2009. MC = 34.0% PPqu < .025 tsf
20	19								
			Very loose, grey, silty fine to medium SAND	SS	2-1-2	3			MC = 31.5%
25	14								

BORING LOG

Project Name:	Berm Stability Evaluation - Lowman Power Plant
Project Number:	060921201 Phase 3
Boring Number:	B-13
Date Drilled:	July 16, 2009

Page 2 of 2

Notes: SS = Split Spoon

Depth (feet)	Approx. Elev. (feet)	Graphic Scale	MATERIAL DESCRIPTION	TYPE	BLOWS/ 6 INCHES	N	CORE REC. (%)	RQD (%)	REMARKS
25	14								
			Very loose, grey, silty fine to medium SAND	SS	2-2-2	4			MC = 34.9%
30	9								
			Loose, brown, fine SAND with silt	SS	3-5-5	10			LL=NP, PL=NP, PI=NP Fines Content = 10.8% USCS = SM MC = 26.0%
35	4								
			...grey (Low Terrace Deposits)	SS	4-4-4	8			MC = 33.4%
40	-1		Boring Terminated at 40 feet						
45	-6								
50	-11								Piezometer installed at the time of boring.

CDG Engineers
& associates

Albertville, AL
Andalusia, AL
Birmingham, AL

Dothan, AL
Huntsville, AL

Boring S-1

Project Name: Lowman Berm Stability Analysis
Project Location: Leroy, Alabama Hammer Type: Automatic
CDG Project Number: 221141100 Method: 3.25"-ID HSA
Date Drilled: 12/1/2011 Approx. Ground Elevation: +/-39 feet

Notes:
+/- 6" of sand/clay at ground surface.

☒ - Split Spoon Sample ■ - Undisturbed Sample

Depth (ft.)	Elev. (ft.)	Material Description	Type	Blows/6" (N-Value)	Rec. % (RQD)	LL	PL	PI	MC	Fines (%)	PPqu (tsf)	Remarks
		Loose, reddish brown, silty fine to medium SAND with rock fragments	☒	4-4-3 (7)								
	35.0											
5		Very soft, tan and red, fine SAND and CLAY	☒	0-1-1 (2)		42	17	25		49.4		USCS = SC
		... brown	☒	1-1-2 (3)								
	30.0		☒	2-3-4 (7)								
10		... medium	■									
	25.0	brown and grey	☒	2-3-3 (6)								▽ Groundwater at +/-EL25 ft. on 12/1/2011.
15		(Fill)										
	20.0											
20		Very loose, grey, silty fine SAND	☒	0-2-2 (4)								
	15.0											
25		... loose, grey and brown	☒	0-2-3 (5)		NP	NP	NP		42.3		USCS = SM
	10.0	... very loose	☒	1-1-1 (2)								

(Continued Next Page)

CDG Engineers & associates

Albertville, AL
Andalusia, AL
Birmingham, AL

Dothan, AL
Huntsville, AL

Boring S-1

Page 2 of 2

Project Name: Lowman Berm Stability Analysis
Project Location: Leroy, Alabama Hammer Type: Automatic
CDG Project Number: 221141100 Method: 3.25"-ID HSA
Date Drilled: 12/1/2011 Approx. Ground Elevation: +/-39 feet

Notes:
+/- 6" of sand/clay at ground surface.

☒ - Split Spoon Sample ■ - Undisturbed Sample

Depth (ft.)	Elev. (ft.)	Graphic Log	Material Description	Type	Blows/6" (N-Value)	Rec. % (RQD)	LL	PL	PI	MC	Fines (%)	PPqu (tsf)	Remarks
			Very loose, grey and brown, silty fine SAND	■									(No Recovery)
35	5.0		...same	☒	0-3-1 (4)								
40	0.0		...loose, grey and tan	☒	1-3-4 (7)								
45	-5.0		... very loose	☒	1-1-3 (4)								
50	-10.0		... loose	☒	1-3-4 (7)								
55	-15.0		... medium dense	☒	4-7-6 (13)		NP	NP	NP		21.4		USCS = SM
													Piezometer Installed.
	-20.0		...tan and light grey (Coastal Plain Deposits)	☒	6-10-8 (18)								

Boring terminated at 60.0 feet.

CDG Engineers & associates

Albertville, AL
Andalusia, AL
Birmingham, AL

Dothan, AL
Huntsville, AL

Boring S-2

Project Name: Lowman Berm Stability Analysis
Project Location: Leroy, Alabama Hammer Type: Automatic
CDG Project Number: 221141100 Method: 3.25"-ID HSA
Date Drilled: 11/30/2011 Approx. Ground Elevation: +/-38 feet

Notes:
+/- 3" of topsoil at ground surface.

PPqu = Unconfined Compressive Strength.

☒ - Split Spoon Sample ■ - Undisturbed Sample

Depth (ft.)	Elev. (ft.)	Graphic Log	Material Description	Type	Blows/6" (N-Value)	Rec. % (RQD)	LL	PL	PI	MC	Fines (%)	PPqu (tsf)	Remarks
	35.0		Medium dense, brown and tan, silty fine to medium SAND	☒	6-6-6 (12)								
5			... loose	☒	3-4-4 (8)								
	30.0		Stiff, brown CLAY with fine sand	☒	4-4-10 (14)							1.0	
10			... same	☒	3-4-6 (10)							1.0	
	25.0		(Fill)										
15			Medium, grey CLAY with fine sand	☒	3-2-5 (7)								
20	20.0		...very soft	☒	0-0-3 (3)							<0.25	
25	15.0		Very loose, brown, silty fine to medium SAND	☒	2-1-2 (3)								▽ Groundwater at +/-EL14 ft. on 11/30/2011.
	10.0		... loose	☒	2-3-5 (8)						15.4		USCS=SM

(Continued Next Page)

CDG Engineers & associates

Albertville, AL
Andalusia, AL
Birmingham, AL

Dothan, AL
Huntsville, AL

Boring S-2

Project Name: Lowman Berm Stability Analysis
Project Location: Leroy, Alabama Hammer Type: Automatic
CDG Project Number: 221141100 Method: 3.25"-ID HSA
Date Drilled: 11/30/2011 Approx. Ground Elevation: +/-38 feet

Notes:
+/- 3" of topsoil at ground surface.

PPqu = Unconfined Compressive Strength.

☒ - Split Spoon Sample ■ - Undisturbed Sample

Depth (ft.)	Elev. (ft.)	Graphic Log	Material Description	Type	Blows/6" (N-Value)	Rec. % (RQD)	LL	PL	PI	MC	Fines (%)	PPqu (tsf)	Remarks
			Loose, light brown, silty fine to medium SAND										
	5.0												
35			...same	☒	2-4-2 (6)								
	0.0												
40			... medium dense, light brown and grey	☒	2-5-9 (14)								
	-5.0												
45			... light grey and tan	☒	4-8-10 (18)								
	-10.0												Borehole backfilled with grout upon completion.
50			... tan (Coastal Plain Deposits)	☒	5-7-15 (22)								
			Boring terminated at 50.0 feet.										
	-15.0												
55													
	-20.0												

CDG Engineers & associates

Albertville, AL
Andalusia, AL
Birmingham, AL

Dothan, AL
Huntsville, AL

Boring S-3

Page 1 of 2

Project Name: Lowman Berm Stability Analysis
Project Location: Leroy, Alabama Hammer Type: Automatic
CDG Project Number: 221141100 Method: 3.25"-ID HSA
Date Drilled: 11/30/2011 Approx. Ground Elevation: +/-38 feet

Notes:
+/- 4" of topsoil at ground surface.

PPqu = Unconfined Compressive Strength.

☒ - Split Spoon Sample ■ - Undisturbed Sample

Depth (ft.)	Elev. (ft.)	Graphic Log	Material Description	Type	Blows/6" (N-Value)	Rec. % (RQD)	LL	PL	PI	MC	Fines (%)	PPqu (tsf)	Remarks
	35.0	▩	Medium dense, red and tan, silty fine to medium SAND with numerous organics	☒	6-5-8 (13)					14			
5		▩	Medium, brown and tan, fine sandy CLAY	☒	4-6-6 (12)					27		0.75	
	30.0	▩	...light brown and light grey	☒	1-3-3 (6)		41	17	24		83.0	0.75	USCS = CL
10		▩	...brown and grey	☒	2-2-3 (5)					24			
	25.0	▩											
15		▩	... grey	☒	0-2-3 (5)								
		▩	(Fill)	■									(No Recovery) ▽ Groundwater at +/-EL21 ft. on 11/30/2011.
	20.0	▨											
20		▨	Very soft, grey, fine sandy CLAY	☒	0-0-2 (2)					33		<0.25	
	15.0	▥											
25		▥	Loose, brown and grey, fine to medium SAND with trace silt	☒	2-3-3 (6)					25			▼ Groundwater at +/-EL14 ft. on 5/1/2012.
	10.0	▥											
		▥	...very loose, light brown and light grey	☒	2-2-2 (4)					25			

(Continued Next Page)

CDG Engineers & associates

Albertville, AL
Andalusia, AL
Birmingham, AL

Dothan, AL
Huntsville, AL

Boring S-3

Page 2 of 2

Project Name: Lowman Berm Stability Analysis
Project Location: Leroy, Alabama Hammer Type: Automatic
CDG Project Number: 221141100 Method: 3.25"-ID HSA
Date Drilled: 11/30/2011 Approx. Ground Elevation: +/-38 feet

Notes:
+/- 4" of topsoil at ground surface.

PPqu = Unconfined Compressive Strength.

☒ - Split Spoon Sample ■ - Undisturbed Sample

Depth (ft.)	Elev. (ft.)	Graphic Log	Material Description	Type	Blows/6" (N-Value)	Rec. % (RQD)	LL	PL	PI	MC	Fines (%)	PPqu (tsf)	Remarks
			Very loose, tan, fine to medium SAND with trace silt										
	5.0												
			...loose	☒	3-4-3 (7)		NP	NP	NP	28	4.1		USCS = SM
35													
	0.0												
			...very loose	☒	1-1-4 (5)					27			
40													
	-5.0												
			...same	☒	1-1-2 (3)								
45													
	-10.0												
			...loose, light grey and tan (Coastal Plain Deposits)	☒	3-4-4 (8)		NP	NP	NP	16	4.5		USCS = SM Piezometer Installed.
50													
			Boring terminated at 50.0 feet.										
	-15.0												
55													
	-20.0												

CDG Engineers & associates

Albertville, AL
Andalusia, AL
Birmingham, AL

Dothan, AL
Huntsville, AL

Boring S-4

Project Name: Lowman Berm Stability Analysis
Project Location: Leroy, Alabama Hammer Type: Automatic
CDG Project Number: 221141100 Method: 3.25"-ID HSA
Date Drilled: 11/30/2011 Approx. Ground Elevation: +/-38 feet

Notes:
+/- 4" of topsoil at ground surface.

PPqu = Unconfined Compressive Strength.

☒ - Split Spoon Sample ■ - Undisturbed Sample

Depth (ft.)	Elev. (ft.)	Graphic Log	Material Description	Type	Blows/6" (N-Value)	Rec. % (RQD)	LL	PL	PI	MC	Fines (%)	PPqu (tsf)	Remarks
			Medium dense, red and tan, silty fine to medium SAND	☒	5-5-8 (13)								
	35.0												
5			...loose, brown and grey	☒	3-3-4 (7)								
			... same	☒	2-2-4 (6)								
	30.0												
10			Medium, grey and brown, fine sandy CLAY	☒	2-3-5 (8)							1.25	
	25.0												
15			... same	☒	2-4-5 (9)							1.0	
			(Fill)										
	20.0												
20			Medium, grey and brown CLAY with fine sand	☒	2-2-3 (5)								
	15.0												
25			...soft	☒	0-1-2 (3)								▽ Groundwater at +/-EL12 ft. on 11/30/2011.
	10.0												
			Loose, brown and grey, clayey fine to medium SAND with trace rock fragments	☒	1-3-2 (5)								

(Continued Next Page)

CDG Engineers & associates

Albertville, AL
Andalusia, AL
Birmingham, AL
Dothan, AL
Huntsville, AL

Boring S-4

Project Name: Lowman Berm Stability Analysis
Project Location: Leroy, Alabama Hammer Type: Automatic
CDG Project Number: 221141100 Method: 3.25"-ID HSA
Date Drilled: 11/30/2011 Approx. Ground Elevation: +/-38 feet

Notes:
+/- 4" of topsoil at ground surface.

PPqu = Unconfined Compressive Strength.

☒ - Split Spoon Sample ■ - Undisturbed Sample

Depth (ft.)	Elev. (ft.)	Graphic Log	Material Description	Type	Blows/6" (N-Value)	Rec. % (RQD)	LL	PL	PI	MC	Fines (%)	PPqu (tsf)	Remarks
		▨	Loose, brown and grey, clayey fine to medium SAND with trace rock fragments										
	5.0	▨											
35		▨	... tan	☒	2-4-4 (8)								
	0.0												
40			Very loose, brown and grey, fine to medium SAND with trace silt	☒	3-2-2 (4)						4.1		
	-5.0												
45			...medium dense	☒	12-8-10 (18)								
	-10.0												Borehole backfilled with grout upon completion.
50			... loose, light grey and tan (Coastal Plain Deposits)	☒	7-6-4 (10)								
			Boring terminated at 50.0 feet.										
	-15.0												
55													
	-20.0												

CDG Engineers & associates

Albertville, AL
Andalusia, AL
Birmingham, AL

Dothan, AL
Huntsville, AL

Boring S-5

Page 1 of 2

Project Name: Lowman Berm Stability Analysis
Project Location: Leroy, Alabama Hammer Type: Automatic
CDG Project Number: 221141100 Method: 3.25"-ID HSA
Date Drilled: 11/29/2011 Approx. Ground Elevation: +/-40 feet

Notes:
+/- 4" of topsoil at ground surface.

☒ - Split Spoon Sample ■ - Undisturbed Sample

Depth (ft.)	Elev. (ft.)	Graphic Log	Material Description	Type	Blows/6" (N-Value)	Rec. % (RQD)	LL	PL	PI	MC	Fines (%)	PPqu (tsf)	Remarks
			Medium dense, red, brown and tan, silty fine to medium SAND with trace organics	☒	7-8-11 (19)								
5	35.0		... dark grey and light brown	☒	6-5-6 (11)								
			...very loose, brown and grey	☒	1-2-2 (4)								
10	30.0		...grey	☒	1-2-2 (4)								
			... loose, grey and brown	☒	4-3-3 (6)								
15	25.0												
			(Fill)										
			Medium, grey and brown CLAY with fine sand	☒	0-3-2 (5)								
20	20.0												
			Loose, light grey and tan, silty fine SAND	☒	2-2-5 (7)								
25	15.0												
			... very loose, grey and tan	☒	1-2-2 (4)								

(Continued Next Page)

Boring S-5

Project Name: Lowman Berm Stability Analysis
Project Location: Leroy, Alabama Hammer Type: Automatic
CDG Project Number: 221141100 Method: 3.25"-ID HSA
Date Drilled: 11/29/2011 Approx. Ground Elevation: +/-40 feet

Notes:
+/- 4" of topsoil at ground surface.

☒ - Split Spoon Sample ■ - Undisturbed Sample

Depth (ft.)	Elev. (ft.)	Graphic Log	Material Description	Type	Blows/6" (N-Value)	Rec. % (RQD)	LL	PL	PI	MC	Fines (%)	PPqu (tsf)	Remarks
			Very loose, grey and tan, silty fine SAND										
35	5.0		... loose, tan	☒	3-4-6 (10)								
40	0.0		... medium dense	☒	5-6-9 (15)								
45	-5.0		...same	☒	5-6-13 (19)								
50	-10.0		... same (Coastal Plain Deposits)	☒	13-12-13 (25)								Borehole caved prior to groundwater measurement.Borehole backfilled with grout upon completion.
			Boring terminated at 50.0 feet.										
55	-15.0												

CDG Engineers & associates

Albertville, AL
Andalusia, AL
Birmingham, AL

Dothan, AL
Huntsville, AL

Boring S-6

Page 1 of 2

Project Name: Lowman Berm Stability Analysis
Project Location: Leroy, Alabama Hammer Type: Automatic
CDG Project Number: 221141100 Method: Mud-Rotary
Date Drilled: 12/13/2011 Approx. Ground Elevation: +/-42 feet

Notes:
+/- 18" of railroad ballast at ground surface.

PPqu = Unconfined Compressive Strength.

☒ - Split Spoon Sample ■ - Undisturbed Sample

Depth (ft.)	Elev. (ft.)	Graphic Log	Material Description	Type	Blows/6" (N-Value)	Rec. % (RQD)	LL	PL	PI	MC	Fines (%)	PPqu (tsf)	Remarks
	40.0		Loose, red, silty fine to medium SAND	☒	0-4-5 (9)								
5			...medium dense	☒	10-9-10 (19)								
	35.0		...very dense	☒	26-29-30 (59)								
10			... red and tan, with trace rock	☒	24-26-28 (54)								
	30.0												
15			... dense, tan and grey with rock fragments	☒	12-20-28 (48)								▽ Groundwater at +/-EL28 ft. on 12/13/2011.
	25.0												
20			...very dense, tan	☒	14-34-36 (70)								
	20.0												
25			... red (Fill)	☒	15-31-35 (66)								
	15.0												
			Stiff, red and grey CLAY with fine sand and rock fragments	☒	6-7-7 (14)							1.25	

(Continued Next Page)

CDG Engineers
& associates

Albertville, AL
Andalusia, AL
Birmingham, AL

Dothan, AL
Huntsville, AL

Boring S-6

Page 2 of 2

Project Name: Lowman Berm Stability Analysis
Project Location: Leroy, Alabama Hammer Type: Automatic
CDG Project Number: 221141100 Method: Mud-Rotary
Date Drilled: 12/13/2011 Approx. Ground Elevation: +/-42 feet

Notes:
+/- 18" of railroad ballast at ground surface.
PPqu = Unconfined Compressive Strength.
☒ - Split Spoon Sample ■ - Undisturbed Sample

Depth (ft.)	Elev. (ft.)	Graphic Log	Material Description	Type	Blows/6" (N-Value)	Rec. % (RQD)	LL	PL	PI	MC	Fines (%)	PPqu (tsf)	Remarks
		▨	Stiff, red and grey CLAY with fine sand and rock fragments										
	10.0	▨											
		▨	... same	☒	5-7-6 (13)							2.0	
35		▨											
	5.0	▨											
		▨	... soft, light grey and tan	☒	3-3-3 (6)		41	17	24			0.5	USCS=CL
40		▨											
	0.0	▨											
		▨	... medium, light grey and brown	☒	3-4-4 (8)							0.5	
45		▨											
	-5.0	▥											
		▥	Medium dense, grey, silty fine SAND	☒	9-14-13 (27)								
50		▥											
	-10.0	▥											
		▥	... grey and tan	☒	9-10-12 (22)								
55		▥											
	-15.0	▥											Borehole backfilled with grout upon completion.
		▥	...same (Coastal Plain Deposits)	☒	12-14-14 (28)								

Boring terminated at 60.0 feet.

CDG Engineers & associates

Albertville, AL
Andalusia, AL
Birmingham, AL

Dothan, AL
Huntsville, AL

Boring S-7

Project Name: Lowman Berm Stability Analysis
Project Location: Leroy, Alabama Hammer Type: Automatic
CDG Project Number: 221141100 Method: Mud-Rotary
Date Drilled: 11/30/2011 Approx. Ground Elevation: +/-42 feet

Notes:
+/- 18" of railroad ballast at ground surface.

PPqu = Unconfined Compressive Strength.

☒ - Split Spoon Sample ■ - Undisturbed Sample

Depth (ft.)	Elev. (ft.)	Graphic Log	Material Description	Type	Blows/6" (N-Value)	Rec. % (RQD)	LL	PL	PI	MC	Fines (%)	PPqu (tsf)	Remarks
	40.0	▩	Medium dense, silty fine to medium SAND with rock fragments	☒	0-7-10 (17)		NP	NP	NP		27.7		USCS = SM
5		▩	... red, brown and tan, with trace rock fragments	☒	10-13-14 (27)								
	35.0	▩	... very dense, reddish tan with numerous rock fragments	☒	18-27-30 (57)								
10		▩	... dense, reddish brown and tan with trace rock fragments	☒	11-15-16 (31)		NP	NP	NP		24.9		USCS = SM
	30.0	▩											
15		▩	... medium dense, reddish tan with rounded rock fragments	☒	5-6-11 (17)								∇ Groundwater at +/-EL27.5 ft. on 11/30/2011.
	25.0	▩											▼ Groundwater at +/-EL25.5 ft. on 5/1/2012.
20		▩	Medium dense, grey, clayey SAND with trace rock fragments	☒	7-9-12 (21)		30	20	10		28.4		USCS = SC
	20.0	▩		■									(No Recovery)
25		▩	...very loose, grey and tan (Fill)	☒	2-2-2 (4)								
	15.0	▨		■									
		▨	Stiff, red and grey CLAY with fine sand	☒	3-6-7 (13)							1.5	

(Continued Next Page)

CDG Engineers & associates

Albertville, AL
Andalusia, AL
Birmingham, AL

Dothan, AL
Huntsville, AL

Boring S-7

Project Name: Lowman Berm Stability Analysis

Project Location: Leroy, Alabama   Hammer Type: Automatic

CDG Project Number: 221141100   Method: Mud-Rotary

Date Drilled: 11/30/2011   Approx. Ground Elevation: +/-42 feet

Notes:
+/- 18" of railroad ballast at ground surface.

PPqu = Unconfined Compressive Strength.

☒ - Split Spoon Sample ■ - Undisturbed Sample

Depth (ft.)	Elev. (ft.)	Graphic Log	Material Description	Type	Blows/6" (N-Value)	Rec. % (RQD)	LL	PL	PI	MC	Fines (%)	PPqu (tsf)	Remarks
			Stiff, red and grey CLAY with fine sand										
	10.0			■									
35			...same	☒	8-11-13 (24)							2.0	
	5.0												
40			... light grey and brown	☒	3-5-7 (12)							1.5	
	0.0												
45			...grey and tan	☒	4-6-8 (14)							1.25	
	-5.0												
50			...same	☒	2-2-3 (5)								
	-10.0												
55			Very dense, silty fine to medium SAND with numerous rock fragments	☒	28-38-40 (78)								
	-15.0												
			... with rounded rock fragments (Coastal Plain Deposits)	☒	30-30-28 (58)								Piezometer Installed.

Boring terminated at 60.0 feet.

Boring S-8

Project Name: Lowman Berm Stability Analysis
Project Location: Leroy, Alabama Hammer Type: Automatic
CDG Project Number: 221141100 Method: Mud-Rotary
Date Drilled: 12/12/2011 Approx. Ground Elevation: +/-42 feet

Notes:
+/- 18" of railroad ballast at ground surface.

PPqu = Unconfined Compressive Strength.

☒ - Split Spoon Sample ■ - Undisturbed Sample

Depth (ft.)	Elev. (ft.)	Graphic Log	Material Description	Type	Blows/6" (N-Value)	Rec. % (RQD)	LL	PL	PI	MC	Fines (%)	PPqu (tsf)	Remarks
	40.0		Dense, red and brown, silty fine to medium SAND with trace organics	☒	11-20-21 (41)								
5			...red	☒	17-15-17 (32)								
	35.0		... with trace rock fragments	☒	17-20-20 (40)								
10			...very dense, reddish tan with numerous rock fragments	☒	28-30-50 (80)								▽ Groundwater at +/-EL32 ft. on 12/12/2011.
	30.0												▼ Groundwater at +/-EL30 ft. on 12/14/2011.
			... red and grey	☒	50/5"								
15													
	25.0		(Fill)										
20			Loose gravel fragments	☒	5-4-3 (7)						2.3		
	20.0												
25			... with clay	☒	3-4-3 (7)								
	15.0												
			Stiff, red and grey CLAY with fine sand	☒	3-6-8 (14)							1.25	

(Continued Next Page)

CDG Engineers & associates

Albertville, AL
Andalusia, AL
Birmingham, AL

Dothan, AL
Huntsville, AL

Boring S-8

Project Name: Lowman Berm Stability Analysis
Project Location: Leroy, Alabama Hammer Type: Automatic
CDG Project Number: 221141100 Method: Mud-Rotary
Date Drilled: 12/12/2011 Approx. Ground Elevation: +/-42 feet

Notes:
+/- 18" of railroad ballast at ground surface.

PPqu = Unconfined Compressive Strength.

☒ - Split Spoon Sample ■ - Undisturbed Sample

Depth (ft.)	Elev. (ft.)	Graphic Log	Material Description	Type	Blows/6" (N-Value)	Rec. % (RQD)	LL	PL	PI	MC	Fines (%)	PPqu (tsf)	Remarks
			Stiff, red and grey CLAY with fine sand										
	10.0												
			...same	☒	3-4-5 (9)		71	21	50			1.0	USCS=CH
35													
	5.0												
			...same	☒	5-6-7 (13)							1.25	
40													
	0.0												
			Very dense, tan, silty fine SAND	☒	14-22-28 (50)								
45													
	-5.0												
			Dense, tan, clayey fine SAND	☒	12-20-20 (40)								
50													
	-10.0												
			Dense gravel fragments	☒	14-16-18 (34)								
55													
	-15.0												
			...very dense, with fine sand (Coastal Plain Deposits)	☒	18-24-28 (52)								Borehole backfilled with grout upon completion.

Boring terminated at 60.0 feet.

CDG Engineers
& associates

Albertville, AL
Andalusia, AL
Birmingham, AL
Dothan, AL
Huntsville, AL

Boring S-9

Project Name: Lowman Berm Stability Analysis
Project Location: Leroy, Alabama Hammer Type: Automatic
CDG Project Number: 221141100 Method: Mud-Rotary
Date Drilled: 12/6/2011 Approx. Ground Elevation: +/-42 feet

Notes:
+/- 18" of railroad ballast at ground surface.

PPqu = Unconfined Compressive Strength.

☒ - Split Spoon Sample ■ - Undisturbed Sample

Depth (ft.)	Elev. (ft.)	Graphic Log	Material Description	Type	Blows/6" (N-Value)	Rec. % (RQD)	LL	PL	PI	MC	Fines (%)	PPqu (tsf)	Remarks
	40.0	▩	Medium dense, red and brown, silty fine to medium SAND with trace organics										
5		▩	... red	☒	19-14-14 (28)								
	35.0	▩	... dense	☒	10-14-17 (31)								
10		▩	... medium dense, red and tan with trace rock fragments	☒	11-12-13 (25)								▽ Groundwater at +/-EL32.5 ft. on 12/6/2011.
	30.0	▩											
15		▩	... very dense, red	☒	14-40-50 (90)								
		▩	(Fill)										
	25.0	▧											
20		▧	Very stiff, brown and grey, fine sandy CLAY	☒	9-13-20 (33)								
	20.0	▥											
25		▥	Loose, grey, silty fine SAND	☒	2-2-3 (5)								
	15.0	▨											
		▨	Medium, grey CLAY with fine sand	☒	2-3-4 (7)								

(Continued Next Page)

Boring S-9

Project Name: Lowman Berm Stability Analysis
Project Location: Leroy, Alabama Hammer Type: Automatic
CDG Project Number: 221141100 Method: Mud-Rotary
Date Drilled: 12/6/2011 Approx. Ground Elevation: +/-42 feet

Notes:
+/- 18" of railroad ballast at ground surface.

PPqu = Unconfined Compressive Strength.

☒ - Split Spoon Sample ■ - Undisturbed Sample

Depth (ft.)	Elev. (ft.)	Graphic Log	Material Description	Type	Blows/6" (N-Value)	Rec. % (RQD)	LL	PL	PI	MC	Fines (%)	PPqu (tsf)	Remarks
			Medium, grey CLAY with fine sand										
	10.0			■									(No Recovery)
			... red and grey	☒	2-3-3 (6)								
35													
	5.0			■									(No Recovery)
			... stiff	☒	2-5-6 (11)							1.5	
40													
	0.0												
			...soft, grey	☒	2-2-2 (4)							<0.25	
45													
	-5.0												
			... same	☒	2-4-5 (9)							0.25	
50													
	-10.0												
			...hard, grey and tan	☒	40-50-6 (56)								
55													
	-15.0												
			Very dense, tan, clayey fine to medium SAND with rock fragments (Coastal Plain Deposits)	☒	30-36-40 (76)								Borehole backfilled with grout upon completion.

Boring terminated at 60.0 feet.

CDG Engineers
& associates

Albertville, AL
Andalusia, AL
Birmingham, AL

Dothan, AL
Huntsville, AL

Boring S-10

Project Name: Lowman Berm Stability Analysis
Project Location: Leroy, Alabama Hammer Type: Automatic
CDG Project Number: 221141100 Method: Mud-Rotary
Date Drilled: 12/6/2011 Approx. Ground Elevation: +/-42 feet

Notes:
+/- 18" of railroad ballast at ground surface.
PPqu = Unconfined Compressive Strength.
☒ - Split Spoon Sample ■ - Undisturbed Sample

Depth (ft.)	Elev. (ft.)	Graphic Log	Material Description	Type	Blows/6" (N-Value)	Rec. % (RQD)	LL	PL	PI	MC	Fines (%)	PPqu (tsf)	Remarks
	40.0		Dense, red and black, silty fine to medium SAND	☒	0-17-23 (40)								
5			... same	☒	13-23-24 (47)								
	35.0		... red	☒	18-19-20 (39)								
10			...very dense	☒	26-25-30 (55)								∇ Groundwater at +/-EL32.5 ft. on 12/6/2011.
	30.0												
15			... with rock fragments	☒	11-24-28 (52)								
	25.0												
20			... same	☒	18-23-29								
			(Fill)		(52)								
	20.0												
25			Medium dense, brown, silty fine to medium SAND	☒	9-9-8 (17)								
	15.0			■									(No Recovery)
			Stiff, grey and red CLAY with fine sand	☒	3-4-5 (9)							1.0	

(Continued Next Page)

CDG Engineers
& associates

Albertville, AL
Andalusia, AL
Birmingham, AL

Dothan, AL
Huntsville, AL

Boring S-10

Page 2 of 2

Project Name: Lowman Berm Stability Analysis
Project Location: Leroy, Alabama Hammer Type: Automatic
CDG Project Number: 221141100 Method: Mud-Rotary
Date Drilled: 12/6/2011 Approx. Ground Elevation: +/-42 feet

Notes:
+/- 18" of railroad ballast at ground surface.

PPqu = Unconfined Compressive Strength.

☒ - Split Spoon Sample ■ - Undisturbed Sample

Depth (ft.)	Elev. (ft.)	Graphic Log	Material Description	Type	Blows/6" (N-Value)	Rec. % (RQD)	LL	PL	PI	MC	Fines (%)	PPqu (tsf)	Remarks
		▨	Stiff, grey and red CLAY with fine sand										
	10.0	▨		■									(No Recovery)
35		▨	... grey	☒	2-4-5 (9)		74	22	52			1.5	USCS=CH
	5.0	▨		■									(No Recovery)
40		▨	... same	☒	4-5-7 (12)							1.0	
	0.0	▨											
45		▨	... same	☒	5-6-7 (13)							1.5	
	-5.0	▨											
50		▨	... same	☒	4-5-5 (10)							1.75	
	-10.0	▨											
55		▨	... soft	☒	2-2-3 (5)							0.5	
	-15.0	▥											Borehole backfilled with grout upon completion.
		▥	Dense, light brown and tan, silty fine to medium SAND (Coastal Plain Deposits)	☒	15-18-31 (49)								

Boring terminated at 60.0 feet.

CDG Engineers
& associates

Albertville, AL
Andalusia, AL
Birmingham, AL

Dothan, AL
Huntsville, AL

Boring S-11

Project Name: Lowman Berm Stability Analysis
Project Location: Leroy, Alabama Hammer Type: Automatic
CDG Project Number: 221141100 Method: Mud-Rotary
Date Drilled: 12/8/2011 Approx. Ground Elevation: +/-42 feet

Notes:
+/- 18" of railroad ballast at ground surface.

☒ - Split Spoon Sample ■ - Undisturbed Sample

Depth (ft.)	Elev. (ft.)	Graphic Log	Material Description	Type	Blows/6" (N-Value)	Rec. % (RQD)	LL	PL	PI	MC	Fines (%)	PPqu (tsf)	Remarks
	40.0		Medium dense, red and black, silty fine to medium SAND with rock fragments	☒	0-0-18 (18)								
5			...dense, red	☒	29-21-24 (45)								
	35.0		...medium dense	☒	18-15-13 (28)								
10			...very dense, red and tan, with numerous rock fragments	☒	28-30-31 (61)								▽ Groundwater at +/-EL32.5 ft. on 12/8/2011.
	30.0												
15			...dense	☒	10-23-23 (46)								
	25.0												
20			... very dense, reddish tan	☒	14-28-30 (58)								
	20.0												
25			... dense, red and tan with numerous rock fragments	☒	14-17-18 (35)								▼ Groundwater at +/-EL17 ft. on 5/1/2012.
	15.0												
			... medium dense, red	☒	8-16-14 (30)								

(Continued Next Page)

CDG Engineers & associates

Albertville, AL
Andalusia, AL
Birmingham, AL

Dothan, AL
Huntsville, AL

Boring S-11

Project Name: Lowman Berm Stability Analysis
Project Location: Leroy, Alabama Hammer Type: Automatic
CDG Project Number: 221141100 Method: Mud-Rotary
Date Drilled: 12/8/2011 Approx. Ground Elevation: +/-42 feet

Notes:
+/- 18" of railroad ballast at ground surface.

☒ - Split Spoon Sample ■ - Undisturbed Sample

Depth (ft.)	Elev. (ft.)	Graphic Log	Material Description	Type	Blows/6" (N-Value)	Rec. % (RQD)	LL	PL	PI	MC	Fines (%)	PPqu (tsf)	Remarks
			Medium dense, red, silty fine to medium SAND with numerous rock fragments (Fill)										
	10.0												
			Stiff, red and grey CLAY with fine sand	☒	6-9-9 (18)		68	22	46				USCS=CH
35													
				■									
	5.0												
			...grey and tan	☒	6-8-9 (17)								
40													
				■									
	0.0												
			Medium dense, grey and tan, silty fine SAND	☒	10-14-15 (29)								
45													
	-5.0												
			... same	☒	6-6-12 (18)						24.7		USCS=SM
50													
	-10.0												
			... tan with rock fragmnets	☒	5-9-10 (19)								
55													
	-15.0												
													Piezometer Installed.
			... grey and tan (Coastal Plain Deposits)	☒	10-10-11 (21)								

Boring terminated at 60.0 feet.

CDG Engineers & associates

Albertville, AL
Andalusia, AL
Birmingham, AL

Dothan, AL
Huntsville, AL

Boring S-12

Page 1 of 2

Project Name: Lowman Berm Stability Analysis
Project Location: Leroy, Alabama Hammer Type: Automatic
CDG Project Number: 221141100 Method: Mud-Rotary
Date Drilled: 12/5/2011 Approx. Ground Elevation: +/-42.5 feet

Notes:
+/- 18" of railroad ballast at ground surface.

PPqu = Unconfined Compressive Strength.

☒ - Split Spoon Sample ■ - Undisturbed Sample

Depth (ft.)	Elev. (ft.)	Graphic Log	Material Description	Type	Blows/6" (N-Value)	Rec. % (RQD)	LL	PL	PI	MC	Fines (%)	PPqu (tsf)	Remarks
	40.0	▩	Very dense, red and black, silty fine to medium SAND with rock fragments	☒	34-40-50 (90)		NP	NP	NP		30.2		USCS = SM
5		▩	... red	☒	23-35-35 (70)								
	35.0	▩	... with trace rock fragments	☒	20-31-25 (56)								
10		▩	Very dense, red and tan, fine to medium SAND with trace silt	☒	20-27-30 (57)		NP	NP	NP		8.4		USCS = SP-SM ▽ Groundwater at +/-EL33 ft. on 12/6/2011.
	30.0	▩											
15		▩	...medium dense, reddish tan with trace rock fragments	☒	10-16-20 (36)								
	25.0	▩											
20		▩	Dense, red and grey, clayey fine to medium SAND	☒	11-21-22 (43)								▼ Groundwater at +/-EL23 ft. on 12/13/2011.
	20.0	▩											
25		▩	...medium dense, red	☒	5-11-16 (27)								
		▩	(Fill)										
	15.0	▨											
		▨	Stiff, grey CLAY with trace fine sand	☒	4-5-6 (11)		67	24	43		97.7	1.25	USCS = CH

(Continued Next Page)

Boring S-12

Project Name: Lowman Berm Stability Analysis
Project Location: Leroy, Alabama Hammer Type: Automatic
CDG Project Number: 221141100 Method: Mud-Rotary
Date Drilled: 12/5/2011 Approx. Ground Elevation: +/-42.5 feet

Notes:
+/- 18" of railroad ballast at ground surface.
PPqu = Unconfined Compressive Strength.
☒ - Split Spoon Sample ■ - Undisturbed Sample

Depth (ft.)	Elev. (ft.)	Graphic Log	Material Description	Type	Blows/6" (N-Value)	Rec. % (RQD)	LL	PL	PI	MC	Fines (%)	PPqu (tsf)	Remarks
			Stiff, grey CLAY with trace fine sand										
	10.0												
			... medium	☒	3-3-6 (9)							0.5	
35													
	5.0												
			Loose, grey, silty fine to medium SAND	☒	2-3-3 (6)		NP	NP	NP		29.7		USCS = SM
40													
	0.0												
			... medium dense, light grey and tan with rock fragments	☒	7-9-10 (19)								
45													
	-5.0												
			... same	☒	5-6-7 (13)								
50													
	-10.0												
			Medium dense, light grey and tan, fine to medium SAND with trace silt	☒	9-15-12 (27)		NP	NP	NP		6.8		USCS = SP-SM
55													
	-15.0												Borehole backfilled with grout upon completion.
			... tan (Coastal Plain Deposits)	☒	5-8-6 (14)								

Boring terminated at 60.0 feet.

CDG Engineers & associates

Albertville, AL
Andalusia, AL
Birmingham, AL

Dothan, AL
Huntsville, AL

Boring S-13

Project Name: Lowman Berm Stability Analysis
Project Location: Leroy, Alabama   Hammer Type: Automatic
CDG Project Number: 221141100   Method: 3.25"-ID HSA
Date Drilled: 11/28/2011   Approx. Ground Elevation: +/-42 feet

Notes:
+/- 12" of topsoil at ground surface.
PPqu = Unconfined Compressive Strength.
☒ - Split Spoon Sample ■ - Undisturbed Sample

Depth (ft.)	Elev. (ft.)	Graphic Log	Material Description	Type	Blows/6" (N-Value)	Rec. % (RQD)	LL	PL	PI	MC	Fines (%)	PPqu (tsf)	Remarks
	40.0		Medium dense, red and black, silty fine to medium SAND	☒	6-7-7 (14)								
5			...very loose, tan and red	☒	5-1-3 (4)								
	35.0		... medium dense, reddish brown	☒	5-5-6 (11)								
10			Stiff, red and grey CLAY with fine sand	☒	3-4-8 (12)							1.0	
	30.0												
15			Medium dense, red and grey, silty fine to medium SAND (Fill)	☒	9-6-7 (13)								
	25.0												
20			Loose, light brown, silty fine to medium SAND	☒	2-2-3 (5)								
	20.0												
25			... light brown and tan	☒	2-3-4 (7)								
	15.0												
			... same	☒	2-3-4 (7)								▽ Groundwater at +/-EL12.5 ft. on 5/1/2012.

(Continued Next Page)

CDG Engineers
& associates

Albertville, AL
Andalusia, AL
Birmingham, AL

Dothan, AL
Huntsville, AL

Boring S-13

Project Name: Lowman Berm Stability Analysis
Project Location: Leroy, Alabama Hammer Type: Automatic
CDG Project Number: 221141100 Method: 3.25"-ID HSA
Date Drilled: 11/28/2011 Approx. Ground Elevation: +/-42 feet

Notes:
+/- 12" of topsoil at ground surface.
PPqu = Unconfined Compressive Strength.
☒ - Split Spoon Sample ■ - Undisturbed Sample

Depth (ft.)	Elev. (ft.)	Graphic Log	Material Description	Type	Blows/6" (N-Value)	Rec. % (RQD)	LL	PL	PI	MC	Fines (%)	PPqu (tsf)	Remarks
			Loose, light brown and tan, silty fine to medium SAND										
	10.0												
35			...very loose	☒	3-2-2 (4)								
	5.0												
40			...loose, light brown and tan	☒	3-3-5 (8)								
	0.0												
45			... medium dense	☒	6-7-7 (14)								
	-5.0												
													Piezometer Installed.
50			...loose (Coastal Plain Deposits)	☒	2-3-3 (6)								
			Boring terminated at 50.0 feet.										
	-10.0												
55													
	-15.0												

CDG Engineers & associates

Albertville, AL
Andalusia, AL
Birmingham, AL

Dothan, AL
Huntsville, AL

Boring S-14

Page 1 of 2

Project Name: Lowman Berm Stability Analysis
Project Location: Leroy, Alabama Hammer Type: Automatic
CDG Project Number: 221141100 Method: 3.25"-ID HSA
Date Drilled: 11/29/2011 Approx. Ground Elevation: +/-42 feet

Notes:
+/- 12" of topsoil at ground surface.

PPqu = Unconfined Compressive Strength.

☒ - Split Spoon Sample ■ - Undisturbed Sample

Depth (ft.)	Elev. (ft.)	Graphic Log	Material Description	Type	Blows/6" (N-Value)	Rec. % (RQD)	LL	PL	PI	MC	Fines (%)	PPqu (tsf)	Remarks
	40.0		Medium dense, red, silty fine to medium SAND with rock fragments	☒	5-6-8 (14)								
5			... with trace rock fragments	☒	5-7-8 (15)								
	35.0		... same	☒	5-5-7 (12)								
10			... red and tan	☒	8-8-7 (15)								
	30.0												
15			... same	☒	7-9-14 (23)								
			(Fill)										
	25.0												
20			Very soft, grey and tan, CLAY with fine sand	☒	1-1-1 (2)								
	20.0												
25			... medium, grey	☒	2-2-4 (6)								
	15.0												
			Loose, brown, silty fine SAND	☒	2-3-4 (7)								

(Continued Next Page)

CDG Engineers & associates

Albertville, AL
Andalusia, AL
Birmingham, AL

Dothan, AL
Huntsville, AL

Boring S-14

Page 2 of 2

Project Name: Lowman Berm Stability Analysis
Project Location: Leroy, Alabama Hammer Type: Automatic
CDG Project Number: 221141100 Method: 3.25"-ID HSA
Date Drilled: 11/29/2011 Approx. Ground Elevation: +/-42 feet

Notes:
+/- 12" of topsoil at ground surface.

PPqu = Unconfined Compressive Strength.

☒ - Split Spoon Sample ■ - Undisturbed Sample

Depth (ft.)	Elev. (ft.)	Graphic Log	Material Description	Type	Blows/6" (N-Value)	Rec. % (RQD)	LL	PL	PI	MC	Fines (%)	PPqu (tsf)	Remarks
			Loose, brown, silty fine SAND	■									(No Recovery)
	10.0												
			... brown, tan and grey	☒	2-3-5 (8)								
35													
	5.0	▨	Soft, grey and tan CLAY with fine sand	☒	1-2-4 (6)							0.25	
40													
	0.0		Medium dense, tan, silty fine to medium SAND	☒	5-9-10 (19)								
45													
	-5.0												
			...loose	☒	2-3-4 (7)								
50													
	-10.0												
			...same (Coastal Plain Deposits)	☒	3-3-5 (8)								Borehole caved prior to groundwater measurement.Borehole backfilled with grout upon completion.
55			Boring terminated at 55.0 feet.										
	-15.0												

CDG
Engineering. Environmental. Answers.

Albertville, AL
Andalusia, AL
Birmingham, AL

Dothan, AL
Huntsville, AL

Boring T-1

Page 1 of 3

Project Name: Lowman CCR Rule Phase I
Project Location: Leroy,AL
Hammer Type: Automatic
CDG Project Number: 061521207
Method: Diedrich D-50 Mud Rotary
Date Drilled: 8/3/2016
Approx. Ground Elevation: +/-39.0 feet

Notes:
No topsoil present at ground surface

☒ - Split Spoon Sample

Depth (ft.)	Approx. Elev. (ft.)	Graphic Log	Material Description	Type	Blows/6" (N-Value)	Rec. % (RQD)	LL	PL	PI	MC	Fines (%)	PPqu (tsf)	Remarks
	35.0	░											
5		░	Loose, reddish brown, silty fine to medium SAND with rock fragment	☒	3-3-2 (5)								
	30.0	▨											
10		▨	Very soft, brown, fine sandy CLAY with rock fragment	☒	2-2-2 (4)							<0.25	
	25.0	▨											
15		▨	...soft (Fill)	☒	2-2-2 (4)		29	18	11		72.3	0.5	USCS=CL
	20.0	▨											
20		▨	Soft, brown, sandy CLAY with trace organics	☒	2-3-4 (7)							0.5	
	15.0	▨											
25		▨	...very soft	☒	1-0-0 (WOH)		42	21	21		77.8	0.25	USCS=CL

(Continued Next Page)

Boring T-1

Project Name: Lowman CCR Rule Phase I
Project Location: Leroy,AL Hammer Type: Automatic
CDG Project Number: 061521207 Method: Diedrich D-50 Mud Rotary
Date Drilled: 8/3/2016 Approx. Ground Elevation: +/-39.0 feet

Notes:
No topsoil present at ground surface

☒ - Split Spoon Sample

Depth (ft.)	Approx. Elev. (ft.)	Graphic Log	Material Description	Type	Blows/6" (N-Value)	Rec. % (RQD)	LL	PL	PI	MC	Fines (%)	PPqu (tsf)	Remarks
			...very soft *(Continued from previous page)*										
	10.0												
30			...with fine sand	☒	0-0-0 (WOH)							0.25	
	5.0												
35			Very loose, gray and tan, fine sandy SILT	☒	1-1-1 (2)		NP	NP	NP		54.9		USCS=ML
	0.0												
40			Very soft, gray and brown, fine sandy CLAY	☒	0-0-0 (WOH)		30	21	9		66.8	0.25	USCS=CL
	-5.0												
45			Loose, gray, silty fine SAND	☒	4-4-4 (8)								
	-10.0												
50													
			...medium dense	☒	5-7-11 (18)								

(Continued Next Page)

Boring T-1

Project Name: Lowman CCR Rule Phase I
Project Location: Leroy,AL   Hammer Type: Automatic
CDG Project Number: 061521207   Method: Diedrich D-50 Mud Rotary
Date Drilled: 8/3/2016   Approx. Ground Elevation: +/-39.0 feet

Notes:
No topsoil present at ground surface

☒ - Split Spoon Sample

Depth (ft.)	Approx. Elev. (ft.)	Graphic Log	Material Description	Type	Blows/6" (N-Value)	Rec. % (RQD)	LL	PL	PI	MC	Fines (%)	PPqu (tsf)	Remarks
			...medium dense *(Continued from previous page)*										
55	-15.0		...same	☒	5-3-8 (11)								
60	-20.0		...loose, with few pebbles (Coastal Plain Deposits)	☒	3-2-7 (9)								Borehole backfilled with grout upon completion.
			Boring terminated at 60.0 feet.										
65	-25.0												
70	-30.0												
75	-35.0												

Engineering. Environmental. Answers.

Albertville, AL
Andalusia, AL
Birmingham, AL

Dothan, AL
Huntsville, AL

Boring T-2

Page 1 of 3

Project Name: Lowman CCR Rule Phase I
Project Location: Leroy,AL Hammer Type: Automatic
CDG Project Number: 061521207 Method: Diedrich D-50 Mud Rotary
Date Drilled: 8/9/2016 Approx. Ground Elevation: +/-42.0 feet

Notes:
+/- 18" of railroad ballast at ground surface

☒ - Split Spoon Sample

Depth (ft.)	Approx. Elev. (ft.)	Graphic Log	Material Description	Type	Blows/6" (N-Value)	Rec. % (RQD)	LL	PL	PI	MC	Fines (%)	PPqu (tsf)	Remarks
	40.0												
5			Dense, red and tan, silty fine to medium SAND with rock fragments	☒	11-27-23 (50)								
	35.0												
10													
			...medium dense	☒	7-7-8 (15)								
	30.0												
15													
			...same (Fill)	☒	1-12-14 (26)		NP	NP	NP		20.1		USCS=SM Small amount of Costal Plain Deposits observed in sample
	25.0												
			Dense, gray, silty fine to medium SAND	☒	8-17-18 (35)								
20													
	20.0												
25			...loose	☒	3-4-6 (10)		NP	NP	NP		14.7		USCS=SM

(Continued Next Page)

Boring T-2

Project Name: Lowman CCR Rule Phase I
Project Location: Leroy,AL Hammer Type: Automatic
CDG Project Number: 061521207 Method: Diedrich D-50 Mud Rotary
Date Drilled: 8/9/2016 Approx. Ground Elevation: +/-42.0 feet

Notes:
+/- 18" of railroad ballast at ground surface

☒ - Split Spoon Sample

Depth (ft.)	Approx. Elev. (ft.)	Graphic Log	Material Description	Type	Blows/6" (N-Value)	Rec. % (RQD)	LL	PL	PI	MC	Fines (%)	PPqu (tsf)	Remarks
	15.0	⁙	...loose *(Continued from previous page)*										
30		▨	Stiff, light gray and brown, plastic CLAY with fine sand	☒	3-3-4 (7)							1.25	
	10.0	▨											
35		▨	...same	☒	4-4-6 (10)							1.25	
	5.0	▨											
40		▨	...trace sand	☒	4-5-5 (10)		70	25	45		97.6	1.0	USCS=CH
	0.0	▨											
45		▨	...same	☒	5-4-5 (9)							1.25	
	-5.0	▨											
50		▨	...medium, with trace organics	☒	3-3-3 (6)							0.75	

(Continued Next Page)

Boring T-2

Project Name: Lowman CCR Rule Phase I
Project Location: Leroy,AL Hammer Type: Automatic
CDG Project Number: 061521207 Method: Diedrich D-50 Mud Rotary
Date Drilled: 8/9/2016 Approx. Ground Elevation: +/-42.0 feet

Notes:
+/- 18" of railroad ballast at ground surface

☒ - Split Spoon Sample

Depth (ft.)	Approx. Elev. (ft.)	Graphic Log	Material Description	Type	Blows/6" (N-Value)	Rec. % (RQD)	LL	PL	PI	MC	Fines (%)	PPqu (tsf)	Remarks
		▨	...medium, with trace organics *(Continued from previous page)*										
55		▨	...light gray, with trace organics	☒	4-2-3 (5)							0.5	
	-15.0												
60		⁘	Dense, tan, silty fine to medium SAND with few rock fragments (Coastal Plain Deposits)	☒	16-20-18 (38)								Borehole backfilled with grout upon completion.
	-20.0												
65													
	-25.0												
70													
	-30.0												
75													
	-35.0												

Boring terminated at 60.0 feet.

Boring T-3

Project Name: Lowman CCR Rule Phase I
Project Location: Leroy,AL Hammer Type: Automatic
CDG Project Number: 061521207 Method: Diedrich D-50 Mud Rotary
Date Drilled: 8/10/2016 Approx. Ground Elevation: +/-42.0 feet

Notes:
+/- 18" of railroad ballast at ground surface

☒ - Split Spoon Sample

Depth (ft.)	Approx. Elev. (ft.)	Graphic Log	Material Description	Type	Blows/6" (N-Value)	Rec. % (RQD)	LL	PL	PI	MC	Fines (%)	PPqu (tsf)	Remarks
	40.0												
5			Medium dense, red, silty fine to medium SAND	☒	3-6-14 (20)								
	35.0												
10			...same	☒	8-12-11 (23)								
	30.0												
15			Dense, red, silty fine to coarse SAND with rock fragments	☒	11-16-15 (31)		NP	NP	NP		10.3		USCS=SP-SM
	25.0												
20			...medium dense	☒	11-15-12 (27)								
	20.0												
25			...dense	☒	15-17-20 (37)								

(Continued Next Page)

CDG
Engineering. Environmental. Answers.

Albertville, AL
Andalusia, AL
Birmingham, AL

Dothan, AL
Huntsville, AL

Boring T-3

Project Name: Lowman CCR Rule Phase I
Project Location: Leroy,AL Hammer Type: Automatic
CDG Project Number: 061521207 Method: Diedrich D-50 Mud Rotary
Date Drilled: 8/10/2016 Approx. Ground Elevation: +/-42.0 feet

Notes:
+/- 18" of railroad ballast at ground surface

☒ - Split Spoon Sample

Depth (ft.)	Approx. Elev. (ft.)	Graphic Log	Material Description	Type	Blows/6" (N-Value)	Rec. % (RQD)	LL	PL	PI	MC	Fines (%)	PPqu (tsf)	Remarks
			...dense *(Continued from previous page)*										
	15.0												
30			...medium dense	☒	10-9-7 (16)								
	10.0												
35			(Fill)	☒	1-1-1 (2)		66	22	44		84.4	<0.25	USCS=CH
			Very soft, gray, plastic CLAY with trace of root fragment										
	5.0												
40													
			...soft	☒	2-3-4 (7)							0.50	
	0.0		Loose, gray, silty fine SAND										
45			...medium dense	☒	5-4-7 (11)								
	-5.0												
50			...same	☒	6-7-8 (15)								

(Continued Next Page)

CDG
Engineering. Environmental. Answers.

Albertville, AL
Andalusia, AL
Birmingham, AL
Dothan, AL
Huntsville, AL

Boring T-3

Project Name: Lowman CCR Rule Phase I
Project Location: Leroy,AL Hammer Type: Automatic
CDG Project Number: 061521207 Method: Diedrich D-50 Mud Rotary
Date Drilled: 8/10/2016 Approx. Ground Elevation: +/-42.0 feet

Notes:
+/- 18" of railroad ballast at ground surface

☒ - Split Spoon Sample

Depth (ft.)	Approx. Elev. (ft.)	Graphic Log	Material Description	Type	Blows/6" (N-Value)	Rec. % (RQD)	LL	PL	PI	MC	Fines (%)	PPqu (tsf)	Remarks
			...same *(Continued from previous page)*										
55				☒	8-10-12 (22)								
	-15.0												
			...same (Coastal Plain Deposits)	☒	8-11-11 (22)								Borehole backfilled with grout upon completion.
60			Boring terminated at 60.0 feet.										
	-20.0												
65													
	-25.0												
70													
	-30.0												
75													
	-35.0												

Appendix C

Subsurface Profiles

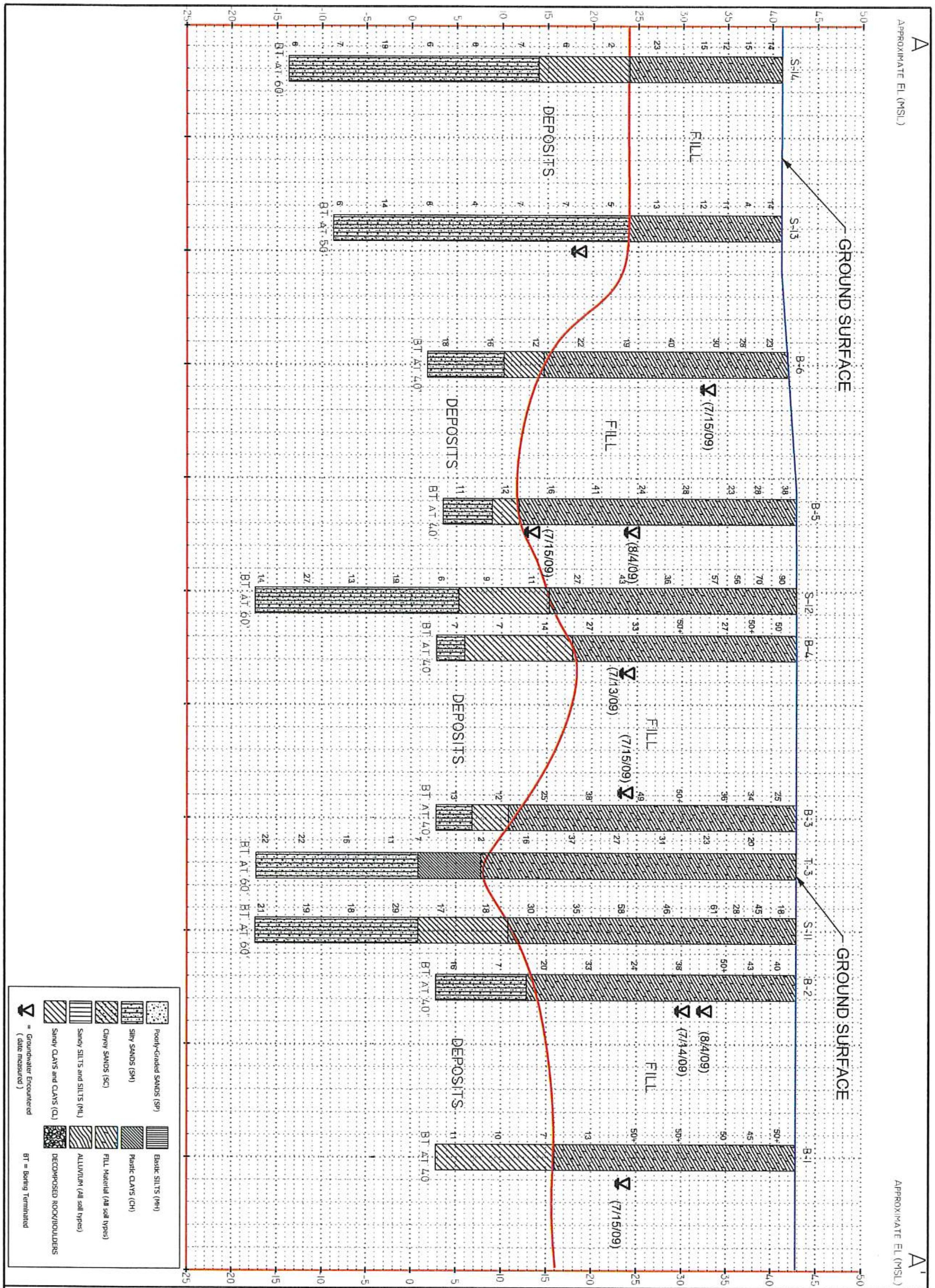

CDG
Engineering. Environmental. Answers.

Subsurface Profile
A - A'

Drawn By: JDA

Scale:
(H):1"=+/-160'
(V): 1"=+/-10'

Date: 09/22/2016

Saftey Factor Assessment
Coal Combustion Residuals Impoundments
Charles R. Lowman Power Plant
Leroy, Alabama
CDG Reference No. : 061521207

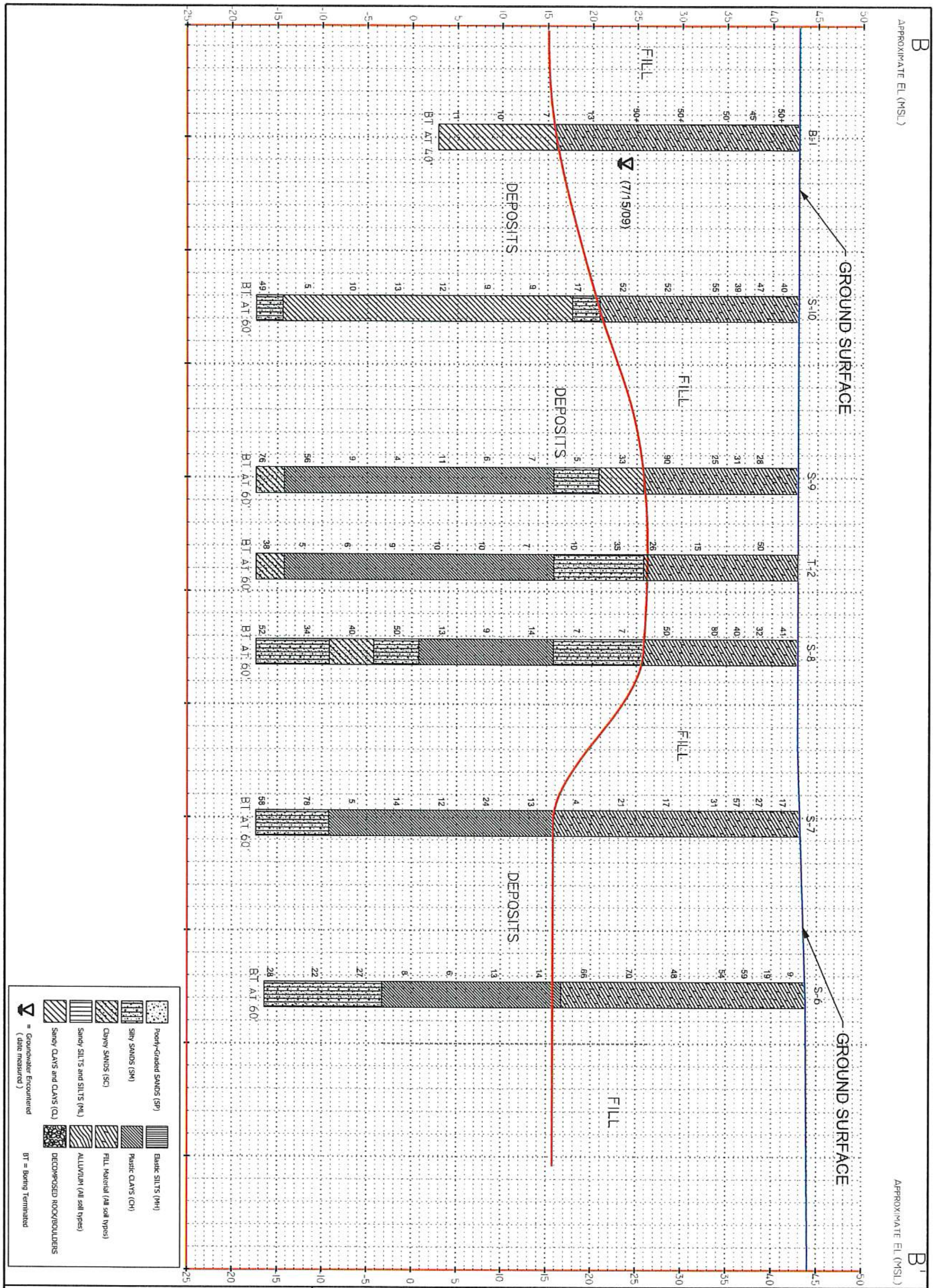

CDG
Engineering. Environmental. Answers.

Subsurface Profile
B - B'

Drawn By: JDA
Scale:
(H):1"=+/-160'
(V): 1"=+/-10'
Date: 09/22/2016

Saftey Factor Assessment
Coal Combustion Residuals Impoundments
Charles R. Lowman Power Plant
Leroy, Alabama
CDG Reference No. : 061521207

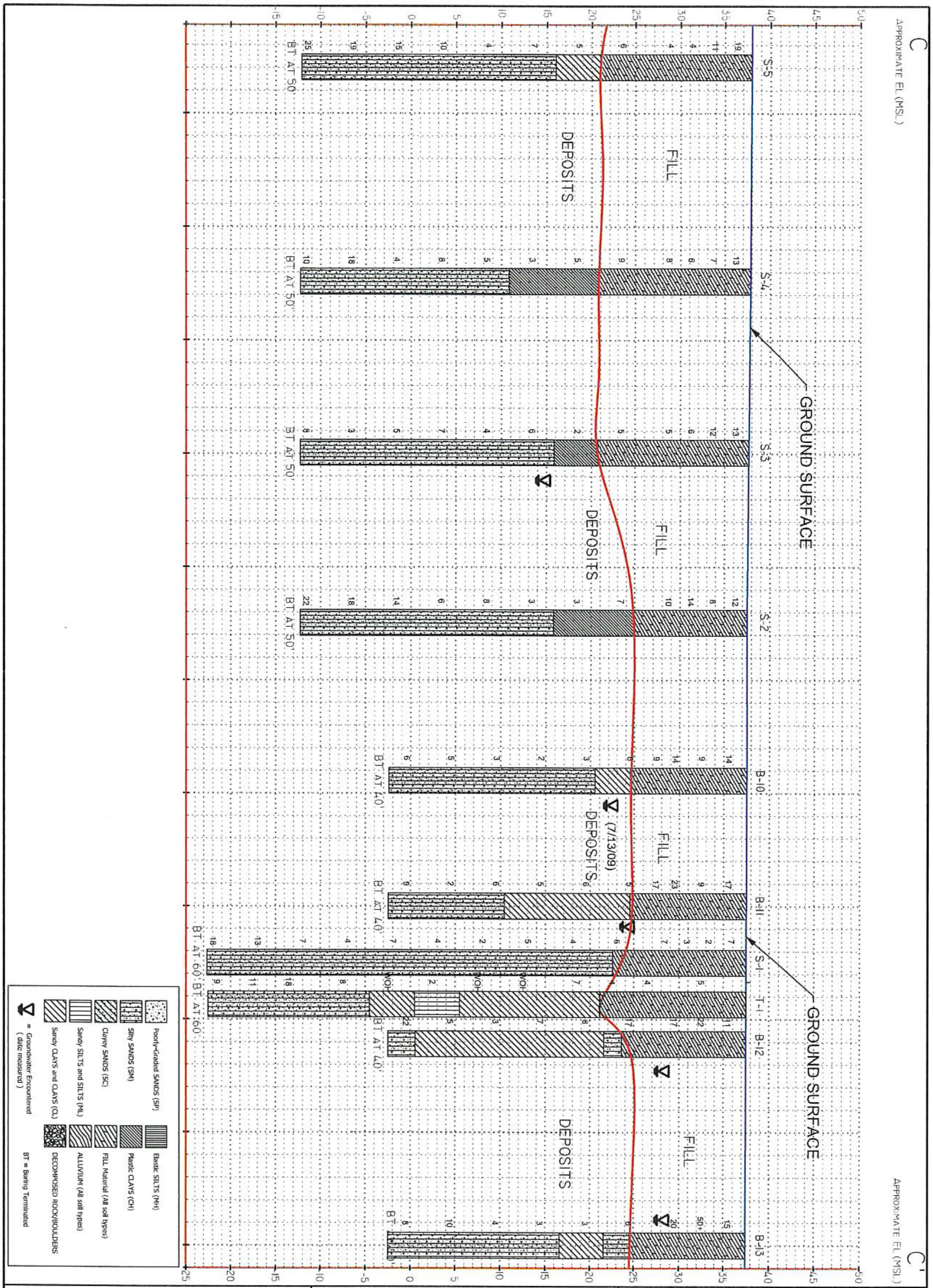

CDG

Engineering. Environmental. Answers.

Subsurface Profile
C - C'

Drawn By: JDA	Scale: (H):1"=+/-160' (V): 1"=+/-10'	Date: 09/22/2016

Saftey Factor Assessment
Coal Combustion Residuals Impoundments
Charles R. Lowman Power Plant
Leroy, Alabama
CDG Reference No. : 061521207

Appendix D

Static, Maximum Storage Pool Stability Analysis

Method: Spencer

Calculated Factor of Safety: 1.625

Required Minimum Factor of Safety: 1.5

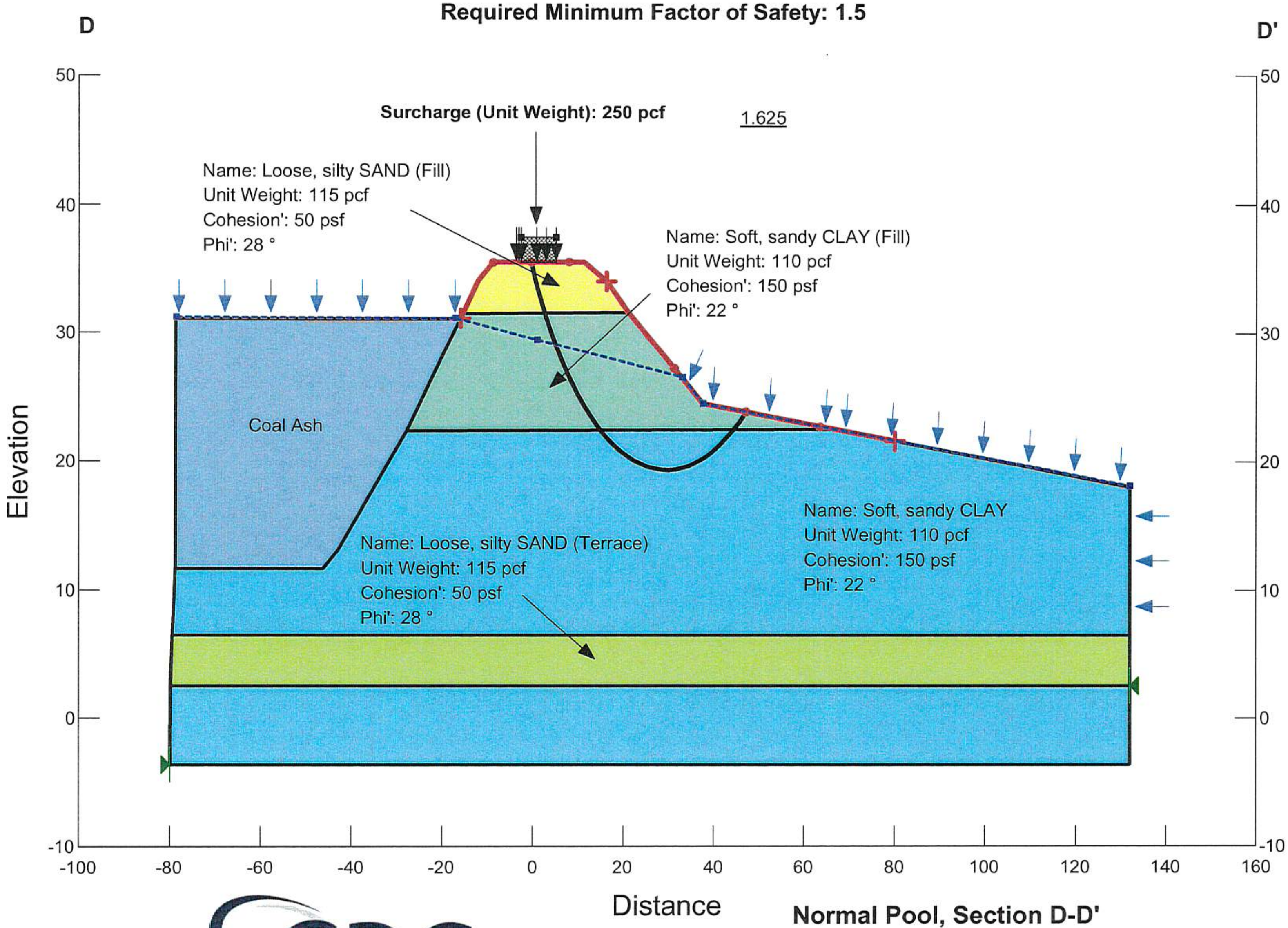

Engineering. Environmental. Answers.

Normal Pool, Section D-D'

Unit 1 Impoundment

Charles R. Lowman Power Plant

CDG Project No. 061521207

Scale: As Shown

Method: Spencer

Calculated Factor of Safety: 6.215

Required Minimum Factor of Safety: 1.5

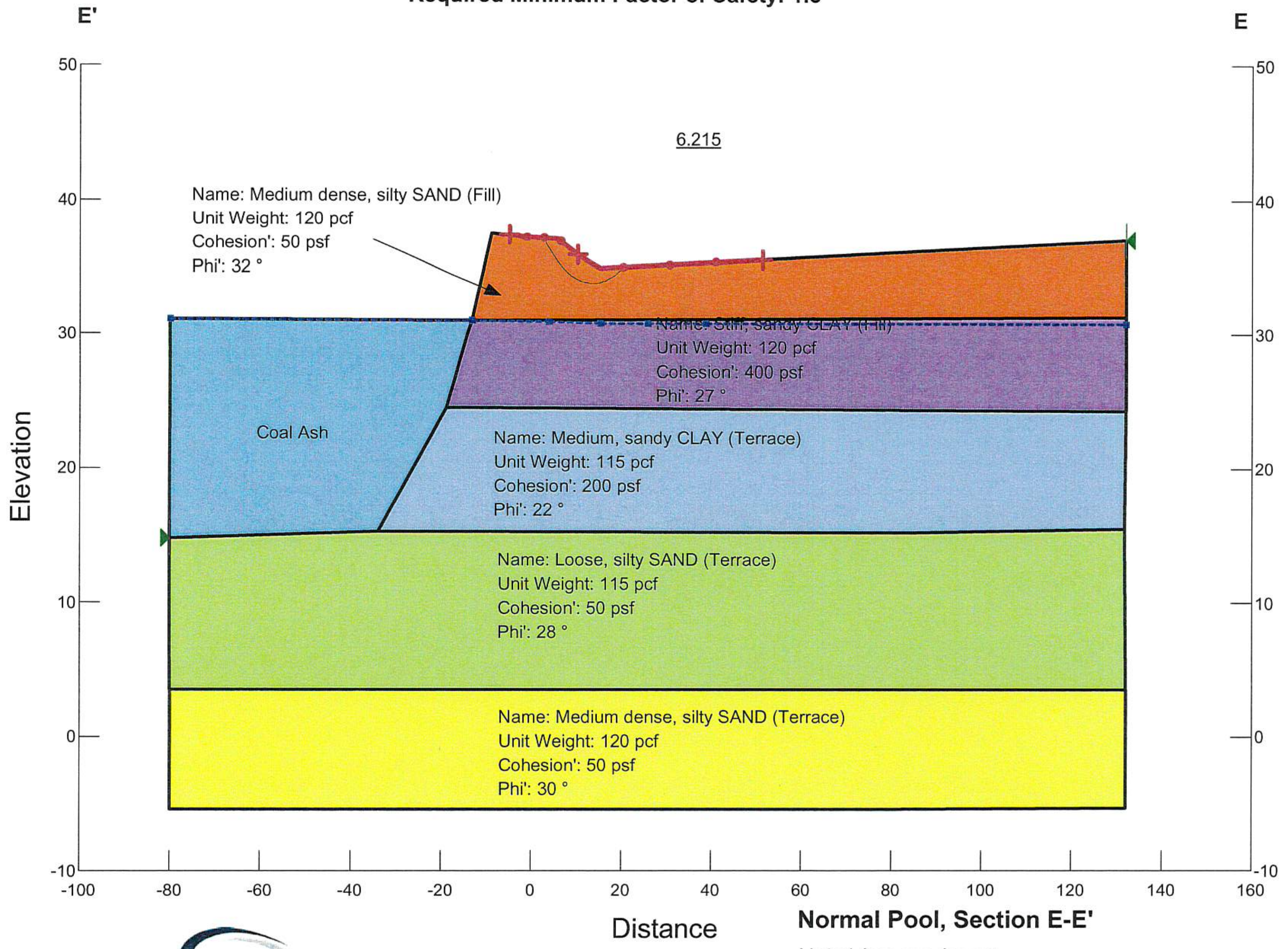

Normal Pool, Section E-E'

Unit 1 Impoundment
Charles R. Lowman Power Plant
CDG Project No. 061521207
Scale: As Shown

CDG
Engineering. Environmental. Answers.

Method: Spencer

Calculated Factor of Safety: 5.739

Required Minimum Factor of Safety: 1.5

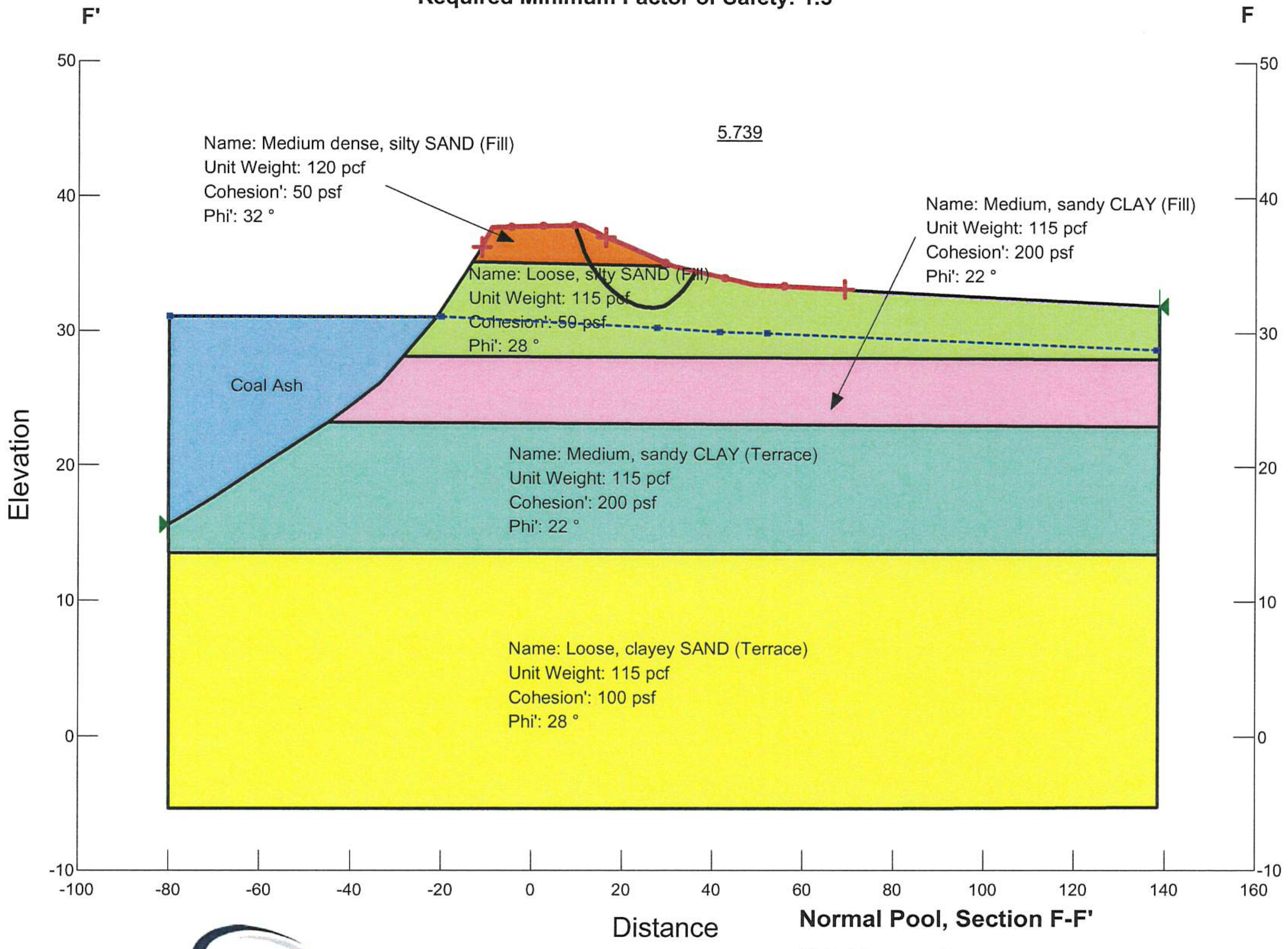

Normal Pool, Section F-F'

Unit 1 Impoundment
Charles R. Lowman Power Plant
CDG Project No. 061521207
Scale: As Shown

CDG
Engineering. Environmental. Answers.

Method: Spencer

Calculated Factor of Safety: 2.491

Required Minimum Factor of Safety: 1.5

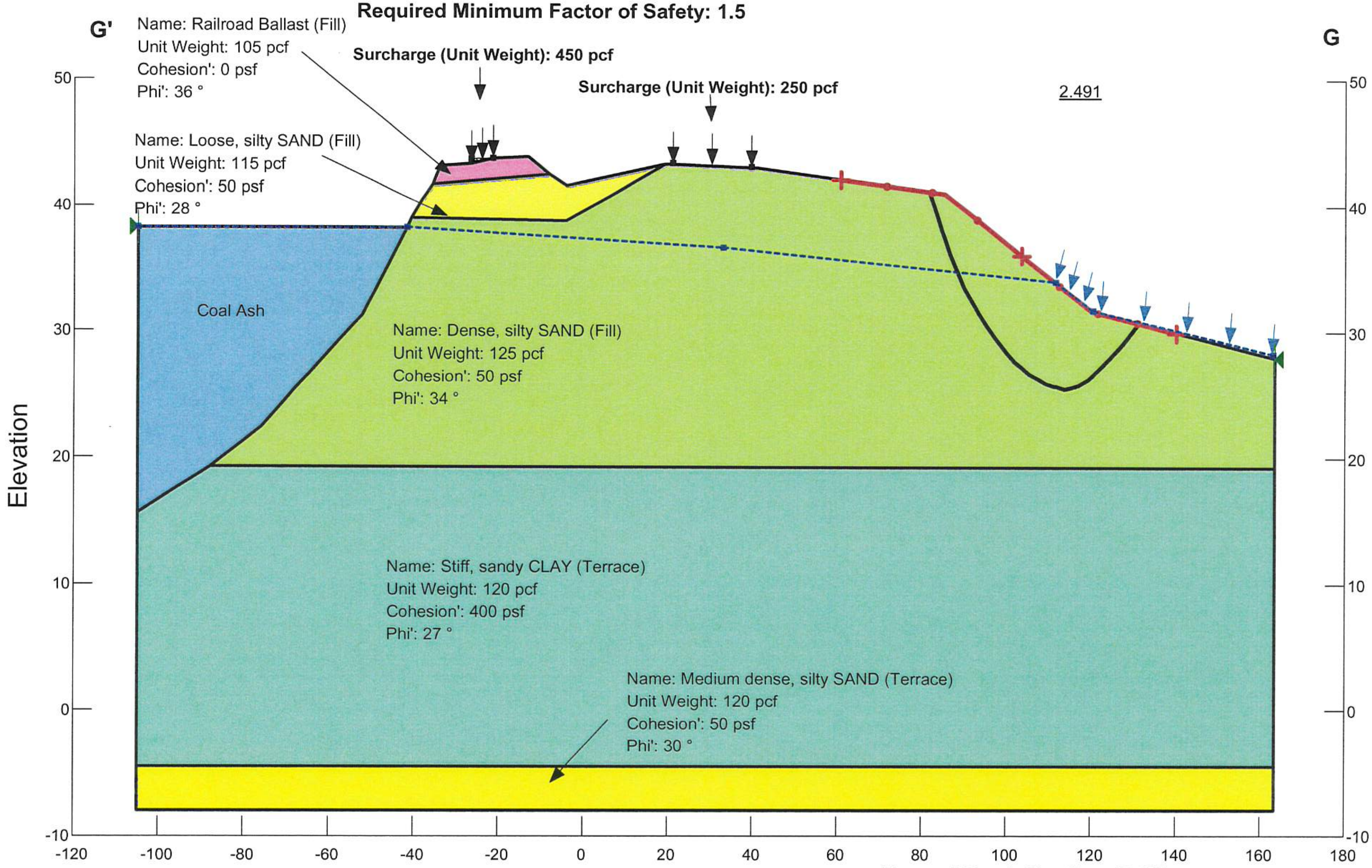

Normal Pool, Section G-G'

Unit 2/3 Impoundment
Charles R. Lowman Power Plant
CDG Project No. 061521207
Scale: As Shown

Engineering. Environmental. Answers.

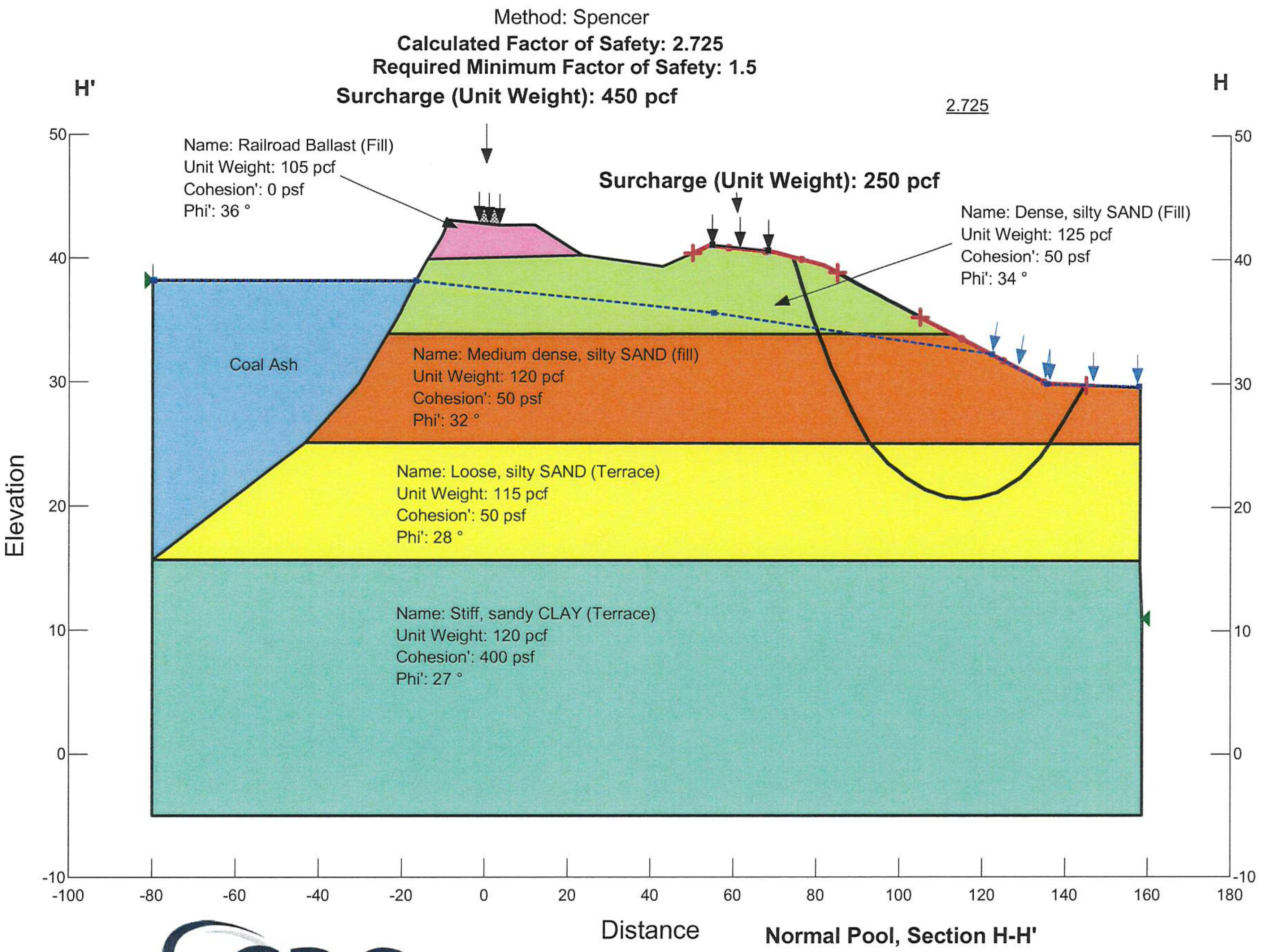

CDG
Engineering. Environmental. Answers.

Normal Pool, Section H-H'

Unit 2/3 Impoundment
Charles R. Lowman Power Plant
CDG Project No. 061521207
Scale: As Shown

Method: Spencer

Calculated Factor of Safety: 1.993

Required Minimum Factor of Safety: 1.5

Surcharge (Unit Weight): 450 pcf

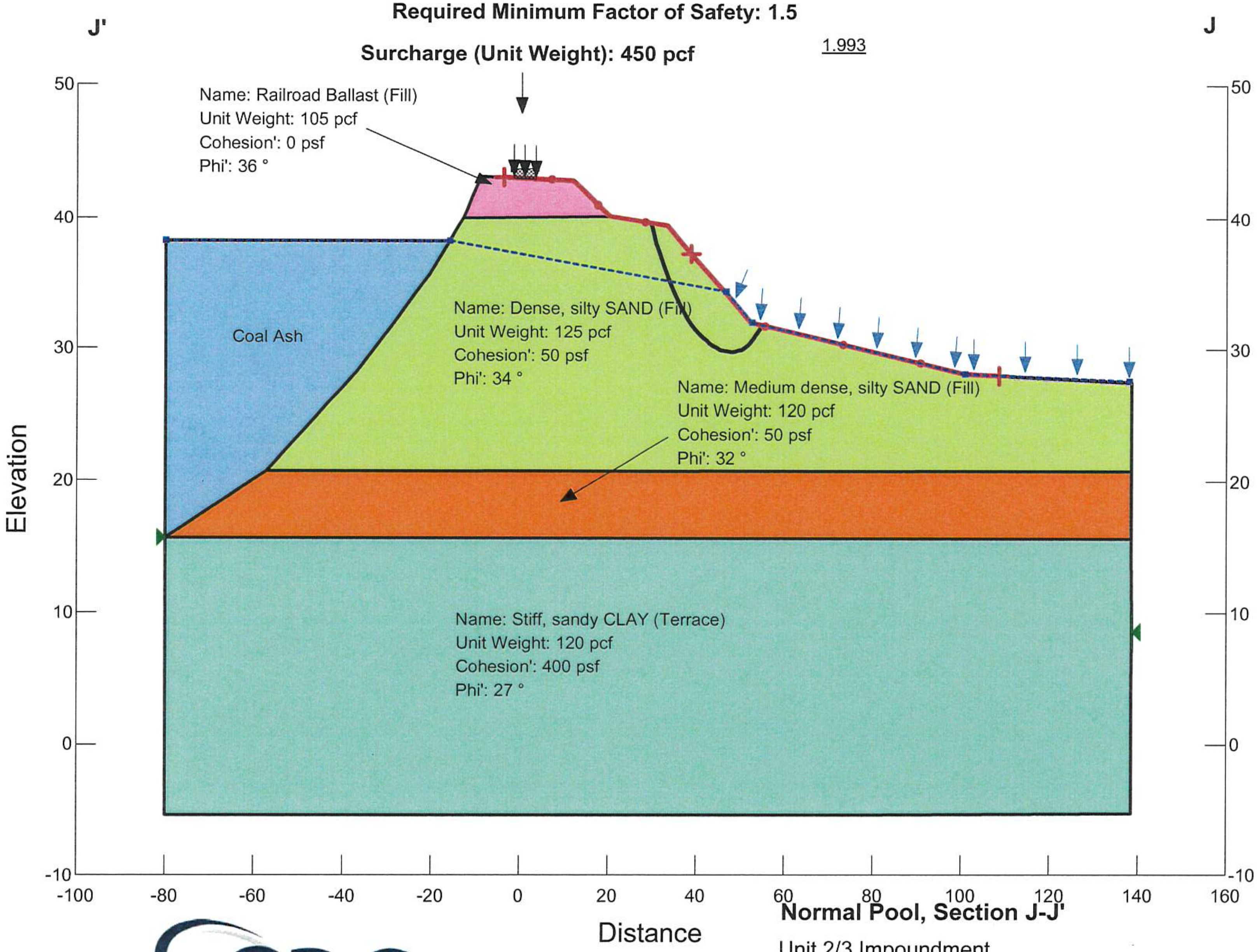

Normal Pool, Section J-J'

Unit 2/3 Impoundment
Charles R. Lowman Power Plant
CDG Project No. 061521207
Scale: As Shown

CDG
Engineering. Environmental. Answers.

Method: Spencer

Calculated Factor of Safety: 2.336

Required Minimum Factor of Safety: 1.5

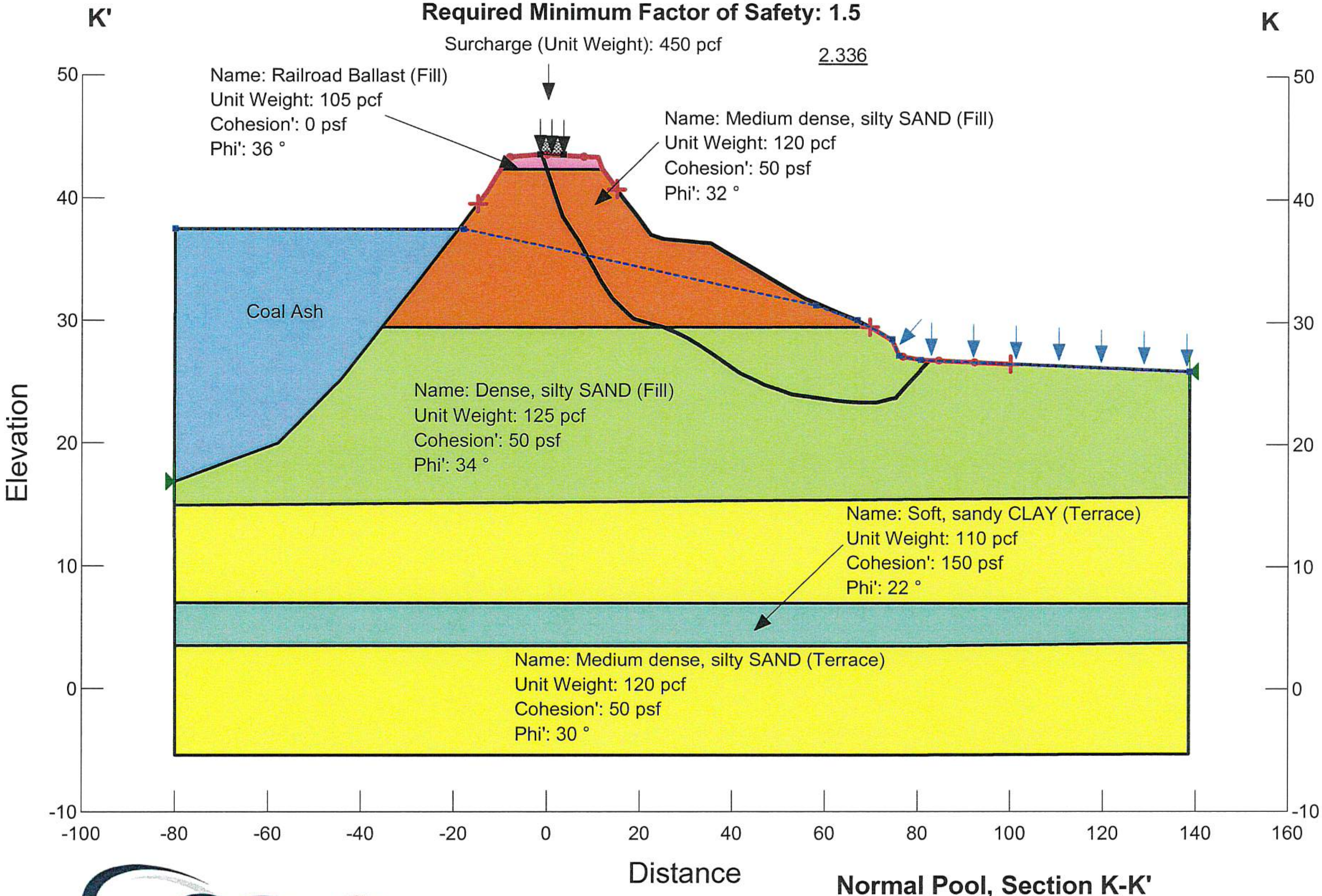

Engineering. Environmental. Answers.

Normal Pool, Section K-K'

FGD Impoundment

Charles R. Lowman Power Plant

CDG Project No. 061521207

Scale: As Shown

Method: Spencer

Calculated Factor of Safety: 1.888

Required Minimum Factor of Safety: 1.5

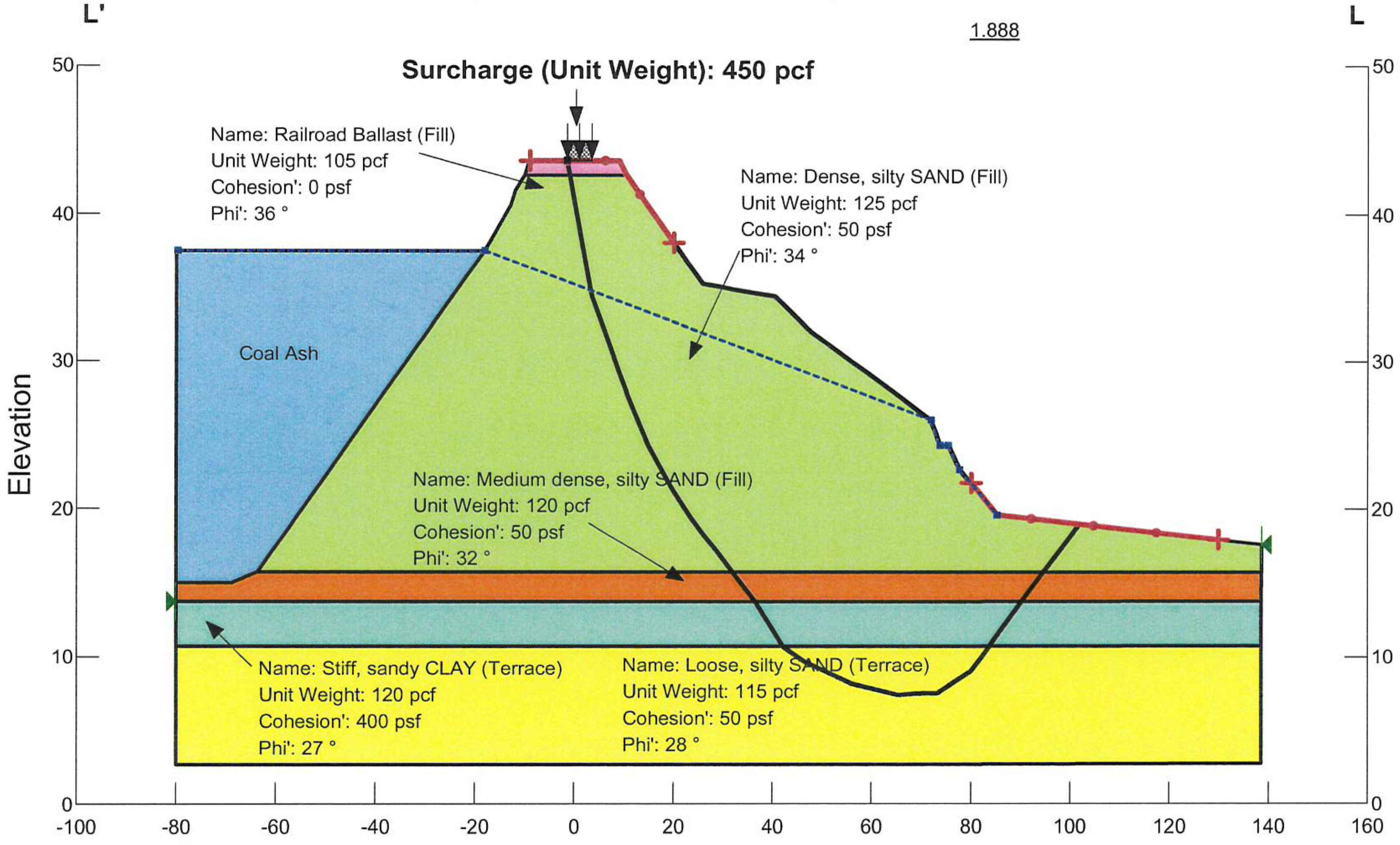

Engineering. Environmental. Answers.

Normal Pool, Section L-L'

FGD Impoundment
Charles R. Lowman Power Plant
CDG Project No. 061521207
Scale: As Shown

Method: Spencer

Calculated Factor of Safety: 1.506

Required Minimum Factor of Safety: 1.4

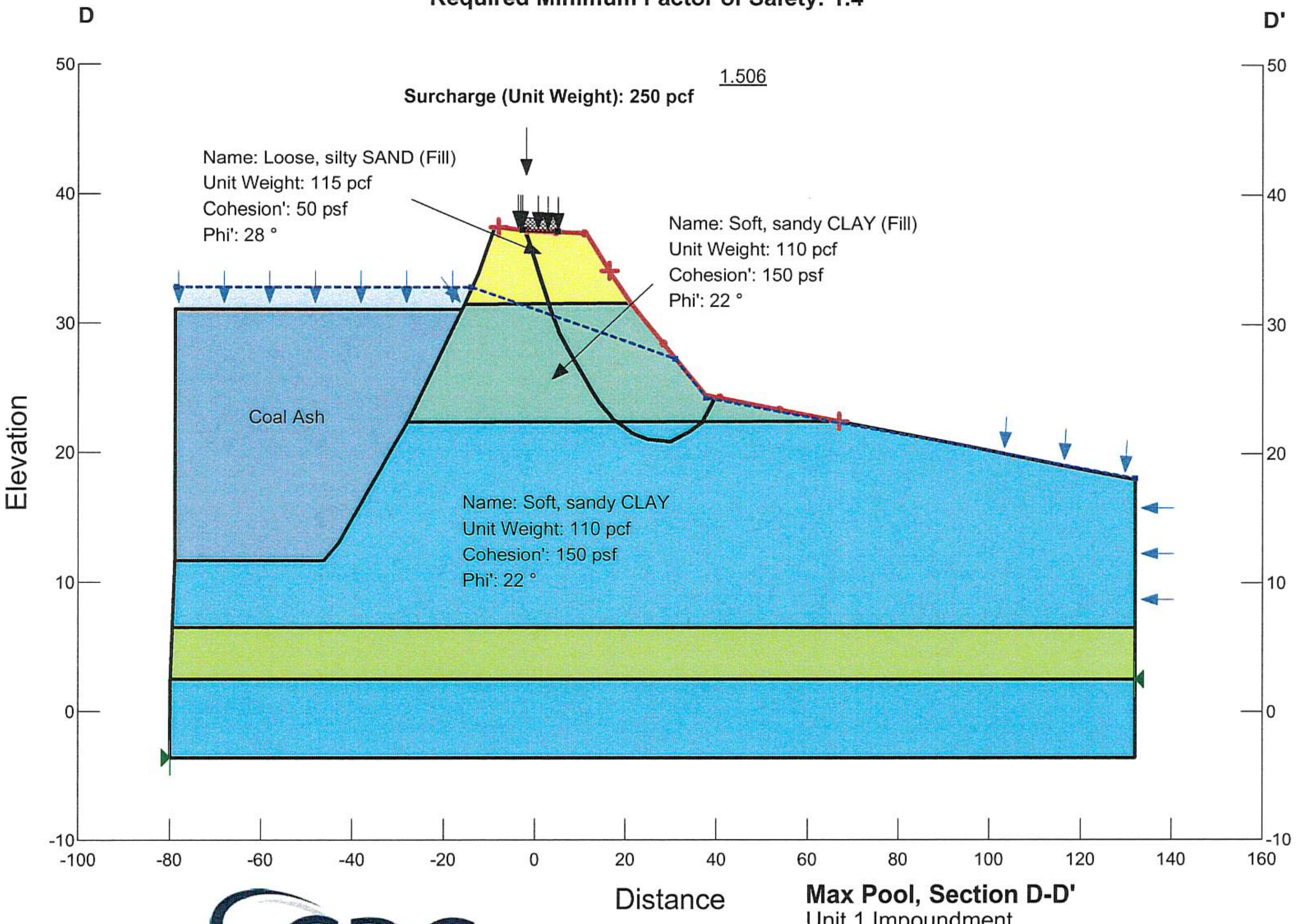

Engineering. Environmental. Answers.

Max Pool, Section D-D'
Unit 1 Impoundment
Charles R. Lowman Power Plant
CDG Project No. 061521207
Scale: As Shown

Appendix E

Static, Maximum Surcharge Pool Stability Analysis

Method: Spencer

Calculated Factor of Safety: 1.562

Required Minimum Factor of Safety: 1.4

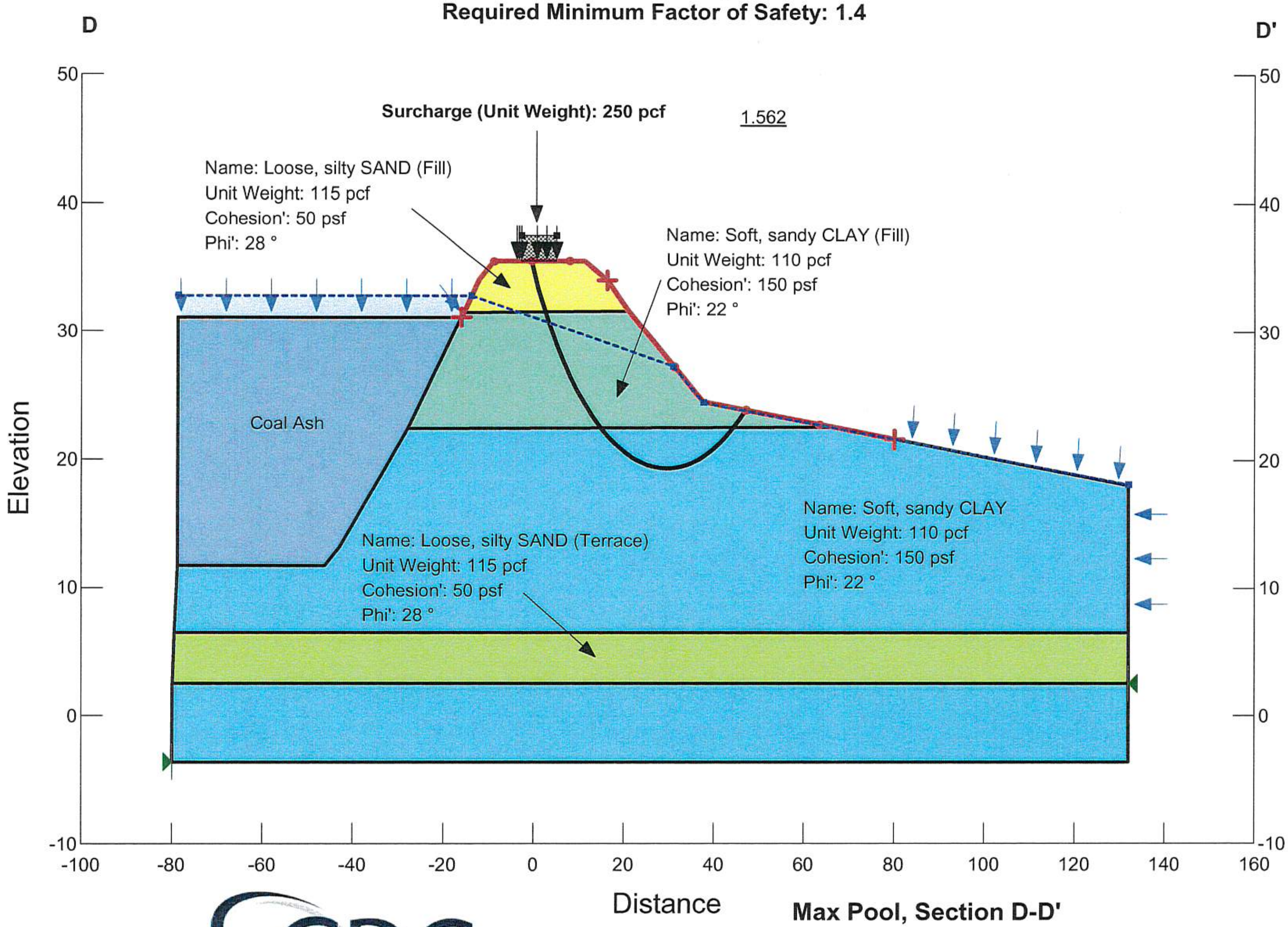

Engineering. Environmental. Answers.

Max Pool, Section D-D'

Unit 1 Impoundment

Charles R. Lowman Power Plant

CDG Project No. 061521207

Scale: As Shown

Method: Spencer

Calculated Factor of Safety: 5.721

Required Minimum Factor of Safety: 1.4

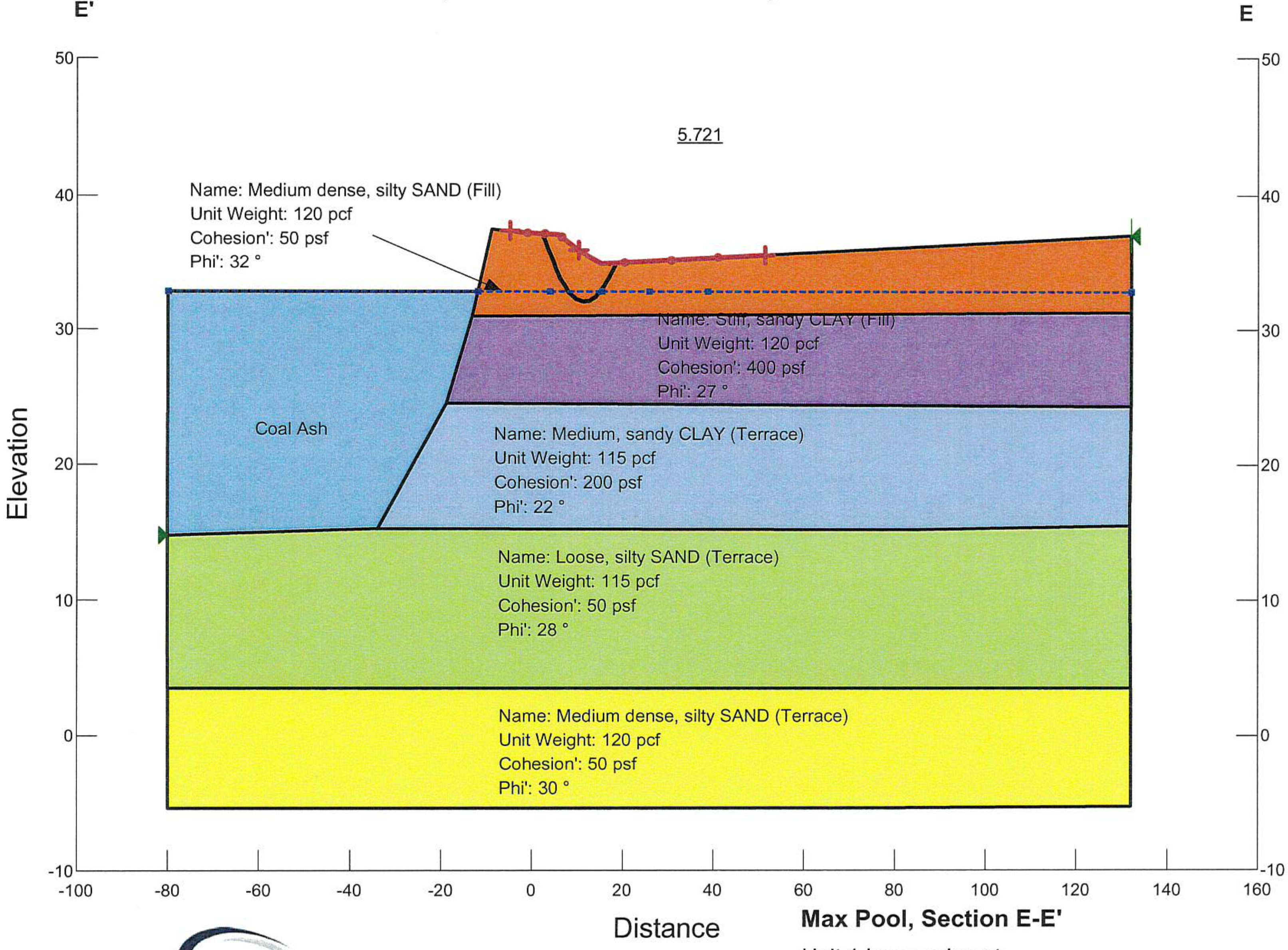

Max Pool, Section E-E'

Unit 1 Impoundment
Charles R. Lowman Power Plant
CDG Project No. 061521207
Scale: As Shown

CDG
Engineering. Environmental. Answers.

Method: Spencer

Calculated Factor of Safety: 5.739

Required Minimum Factor of Safety: 1.4

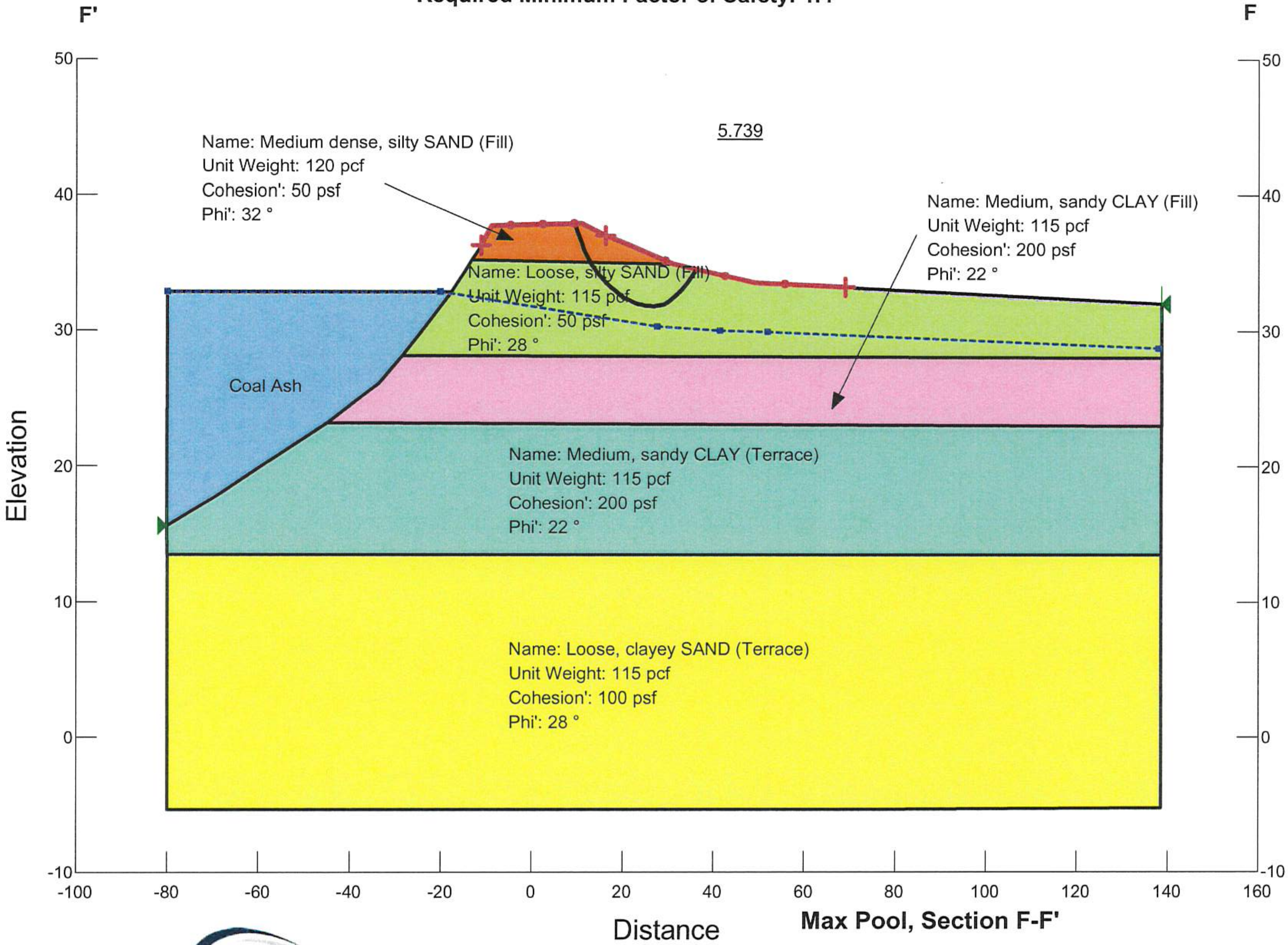

Max Pool, Section F-F'

Unit 1 Impoundment
Charles R. Lowman Power Plant
CDG Project No. 061521207
Scale: As Shown

Engineering. Environmental. Answers.

Method: Spencer

Calculated Factor of Safety: 2.491

Required Minimum Factor of Safety: 1.4

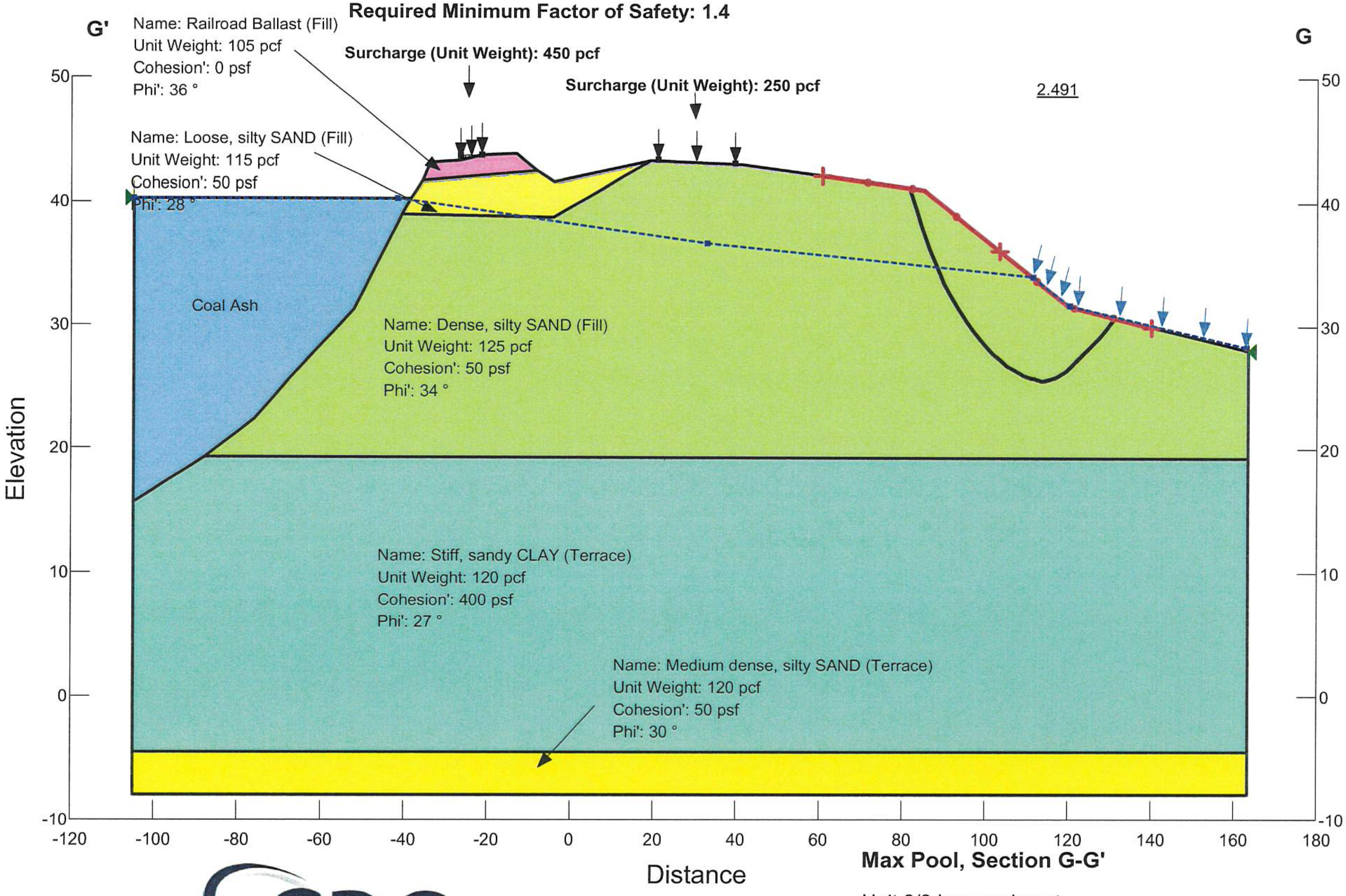

Max Pool, Section G-G'

Unit 2/3 Impoundment
Charles R. Lowman Power Plant
CDG Project No. 061521207
Scale: As Shown

CDG
Engineering. Environmental. Answers.

Method: Spencer

Calculated Factor of Safety: 2.485

Required Minimum Factor of Safety: 1.5

Surcharge (Unit Weight): 450 pcf

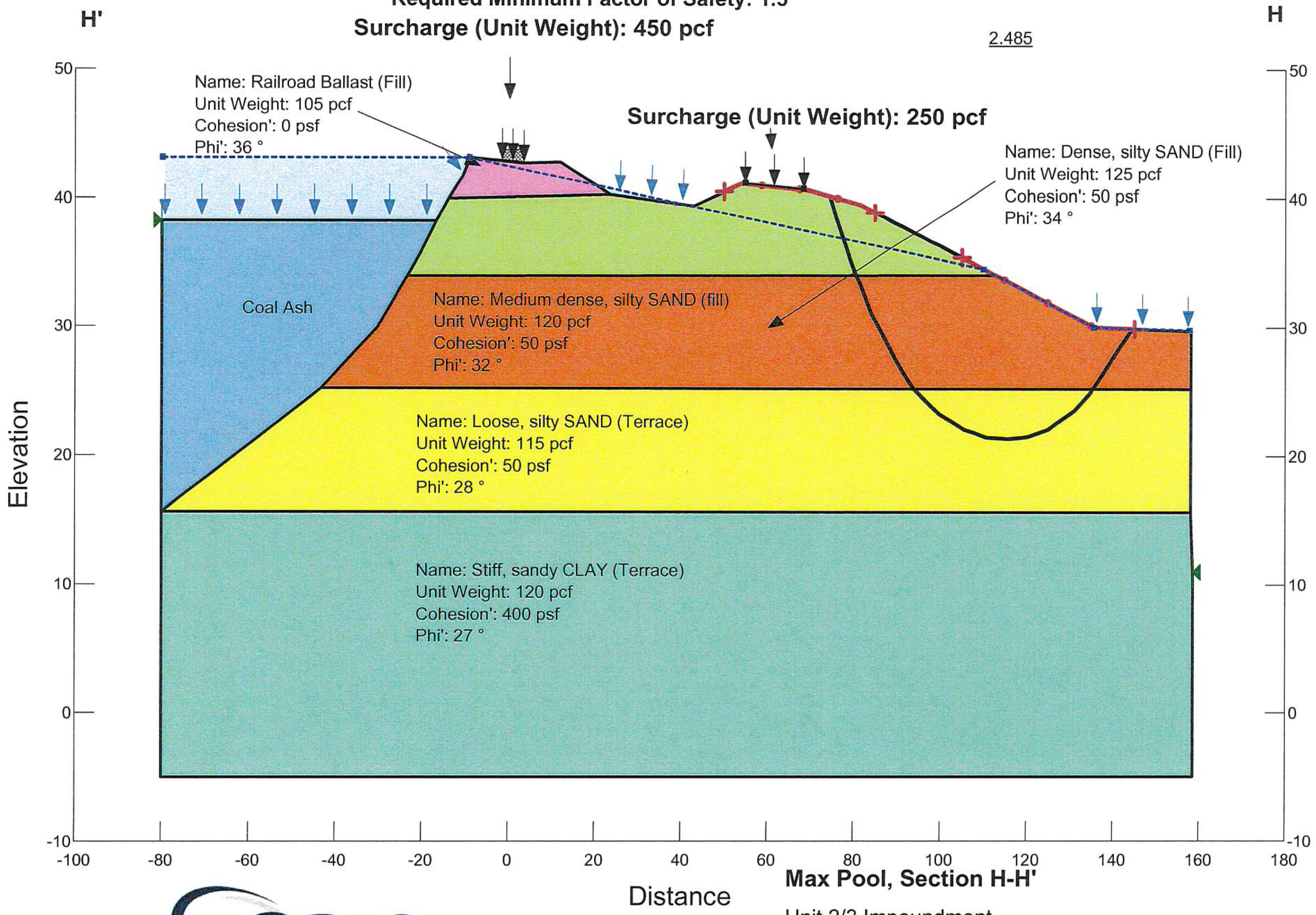

Max Pool, Section H-H'

Unit 2/3 Impoundment
Charles R. Lowman Power Plant
CDG Project No. 061521207
Scale: As Shown

Engineering. Environmental. Answers.

Method: Spencer

Calculated Factor of Safety: 1.951

Required Minimum Factor of Safety: 1.4

Surcharge (Unit Weight): 450 pcf

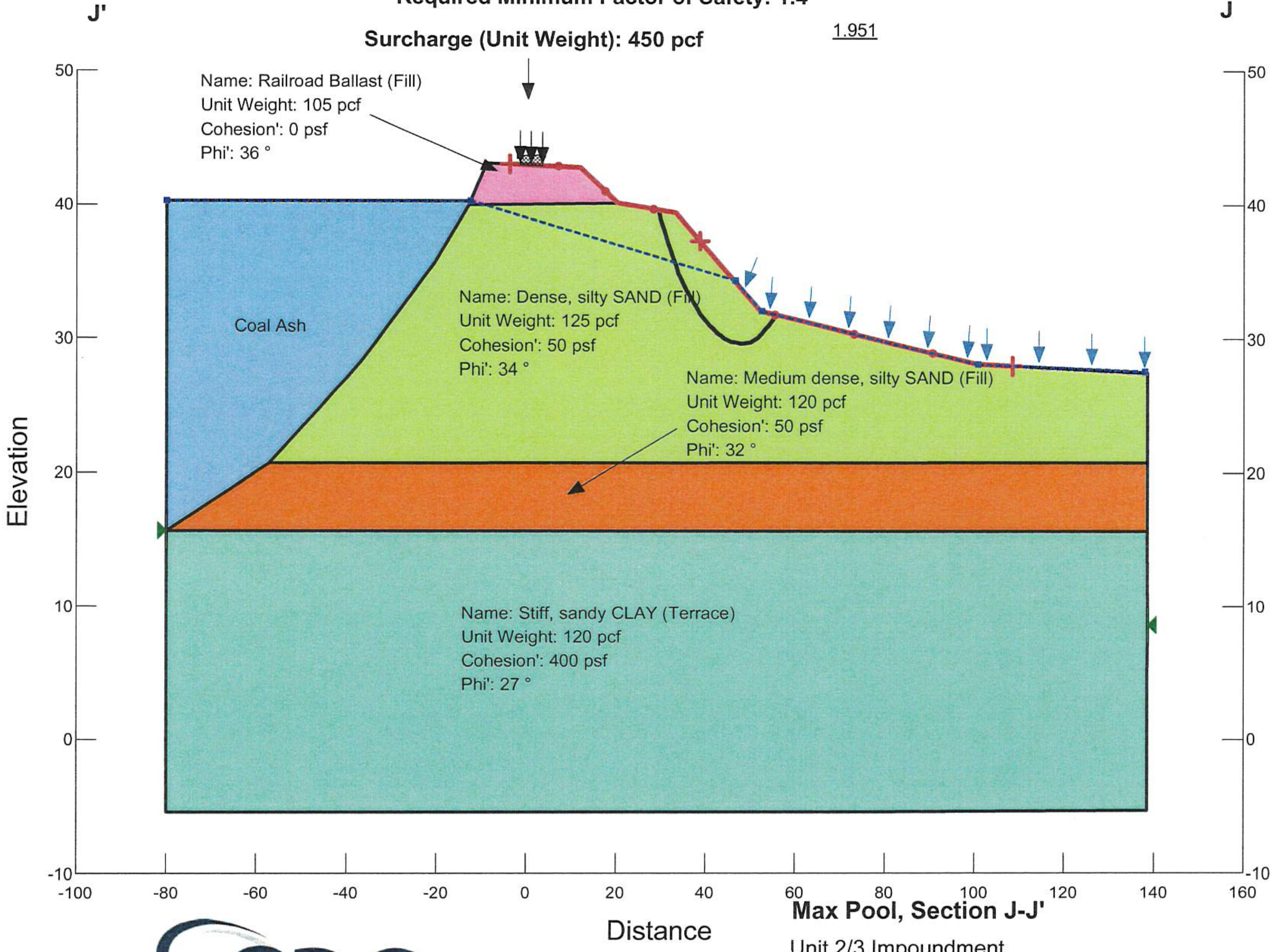

Max Pool, Section J-J'

Unit 2/3 Impoundment
Charles R. Lowman Power Plant
CDG Project No. 061521207
Scale: As Shown

CDG

Engineering. Environmental. Answers.

Methoc pencer

Calculated Factor of Safety: 2.201

Required Minimum Factor of Safety: 1.5

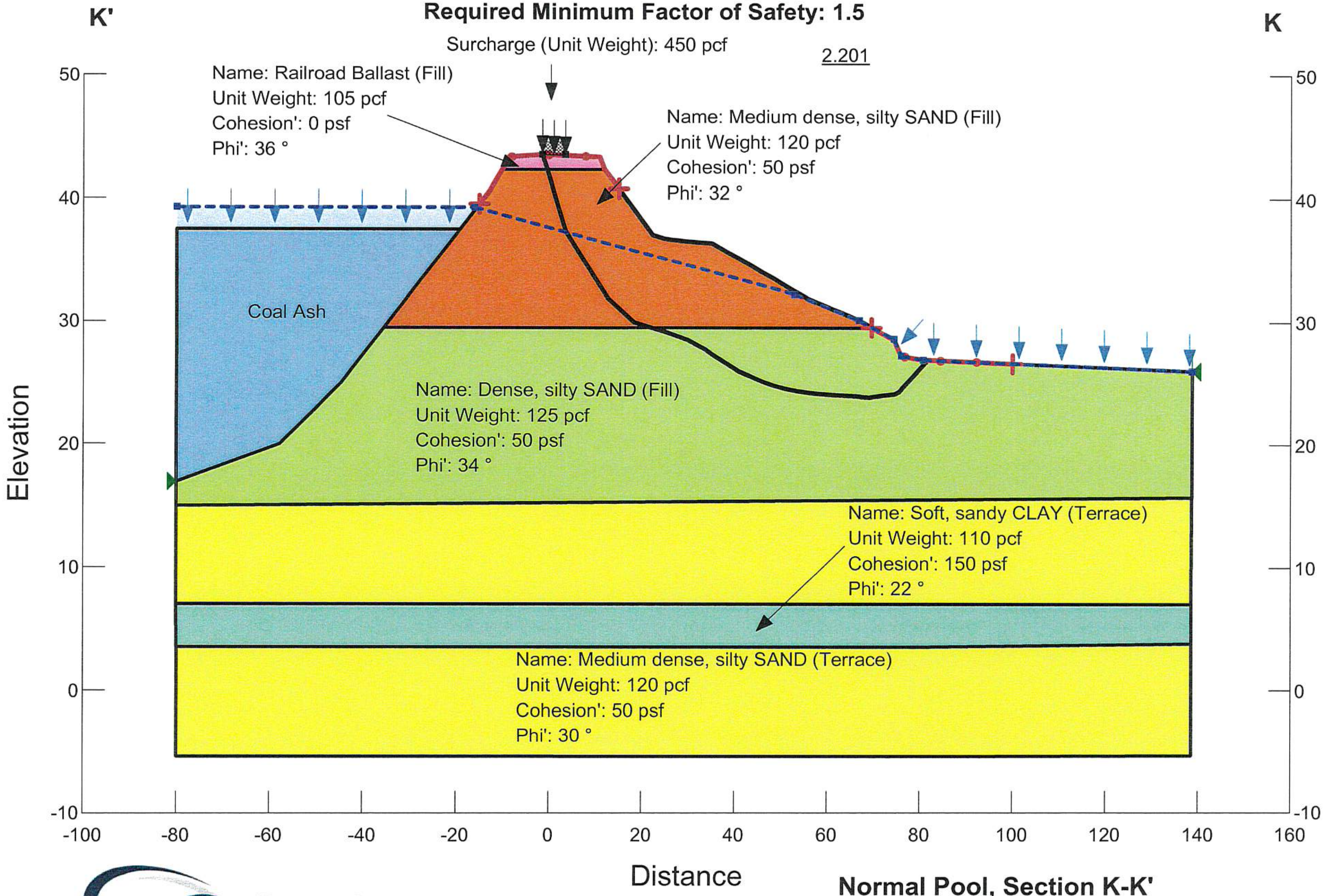

Normal Pool, Section K-K'
FGD Impoundment
Charles R. Lowman Power Plant
CDG Project No. 061521207
Scale: As Shown

CDG

Engineering. Environmental. Answers.

Method: Spencer

Calculated Factor of Safety: 1.804

Required Minimum Factor of Safety: 1.4

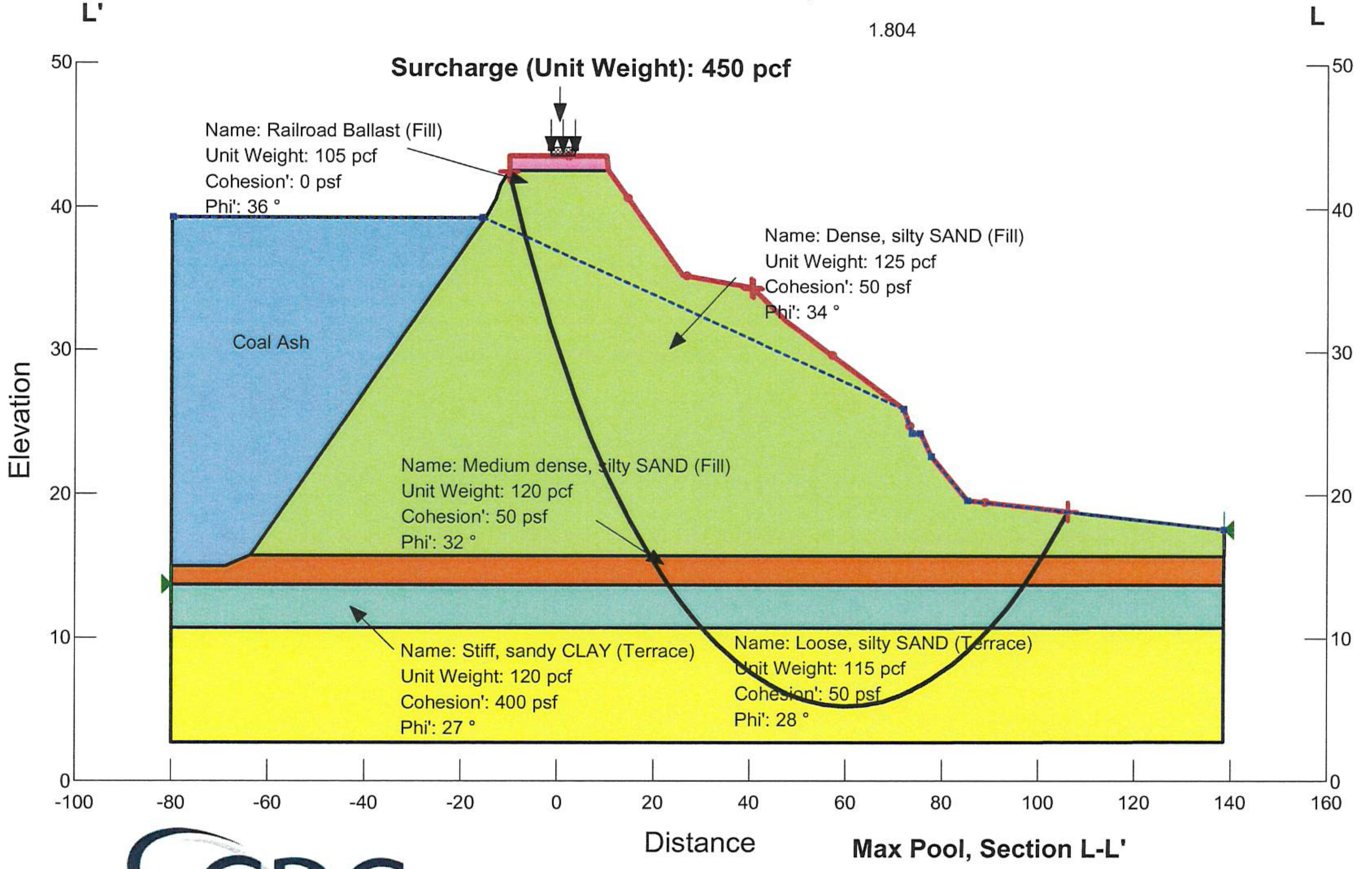

Engineering. Environmental. Answers.

Max Pool, Section L-L'
FGD Impoundment
Charles R. Lowman Power Plant
CDG Project No. 061521207
Scale: As Shown

Appendix F

Cone Penetration Test Logs

SOUTHERN EARTH SCIENCES, INC.

Operator: DANNY HINES
Sounding: SCPT-1
Cone Used: DDG0892

CPT Date/Time: 11/29/2011 10:34:38 AM
Location: LOWMAN POWER PLANT
Job Number: M11-372

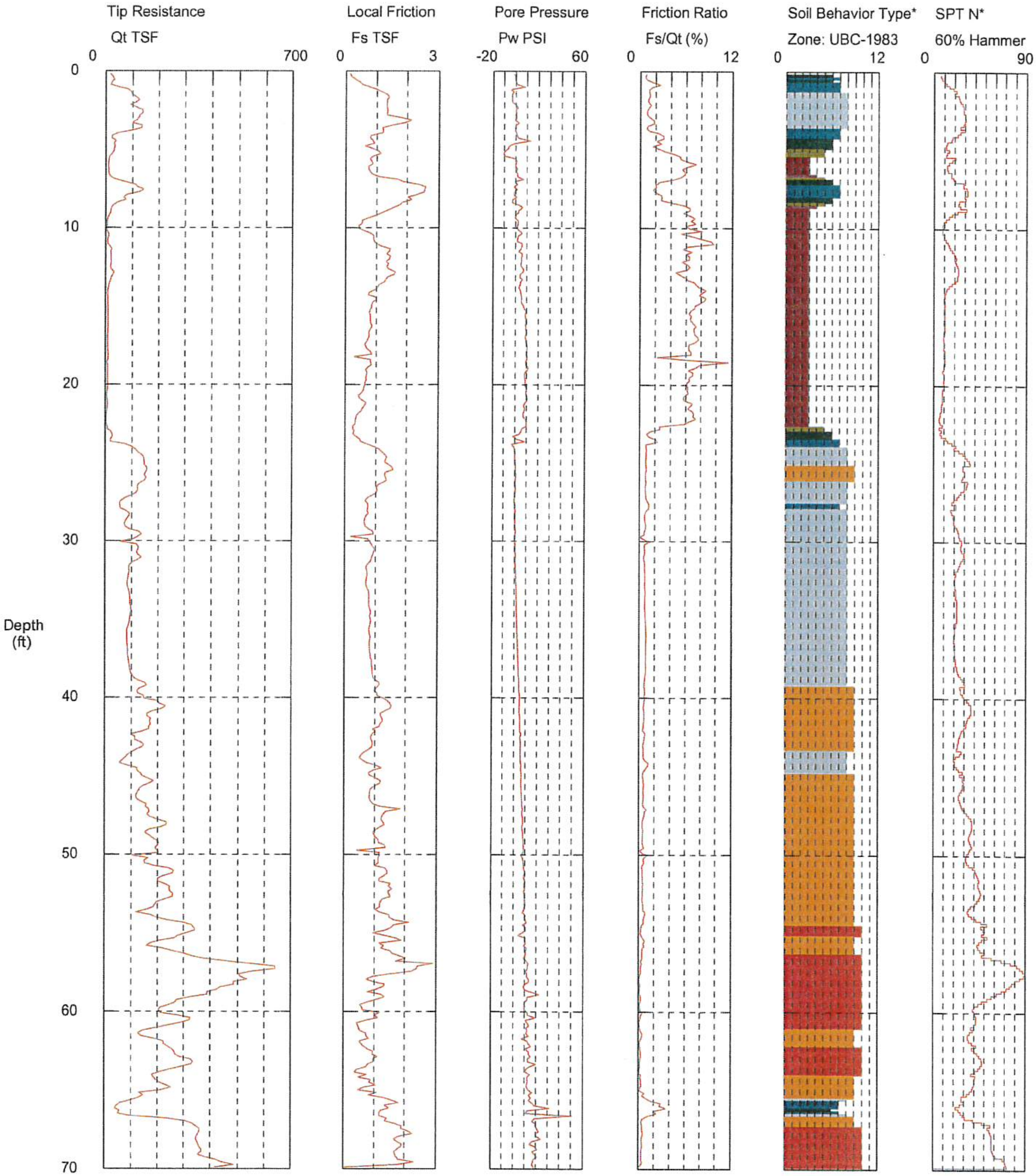

Maximum Depth = 69.88 feet

Depth Increment = 0.164 feet

- 1 sensitive fine grained
- 2 organic material
- 3 clay
- 4 silty clay to clay
- 5 clayey silt to silty clay
- 6 sandy silt to clayey silt
- 7 silty sand to sandy silt
- 8 sand to silty sand
- 9 sand
- 10 gravelly sand to sand
- 11 very stiff fine grained (*)
- 12 sand to clayey sand (*)

N31.48424 W87.91472
SOUTHERN EARTH SCIENCES

GROUNDWATER: SOUNDING WET AND COLLAPSED AT 0.5 FEET

*Soil behavior type and SPT based on data from UBC-1983

SOUTHERN EARTH SCIENCES, INC.

Operator: DANNY HINES
Sounding: SCPT-1
Cone Used: DDG0892

CPT Date/Time: 11/29/2011 10:34:38 AM
Location: LOWMAN POWER PLANT
Job Number: M11-372

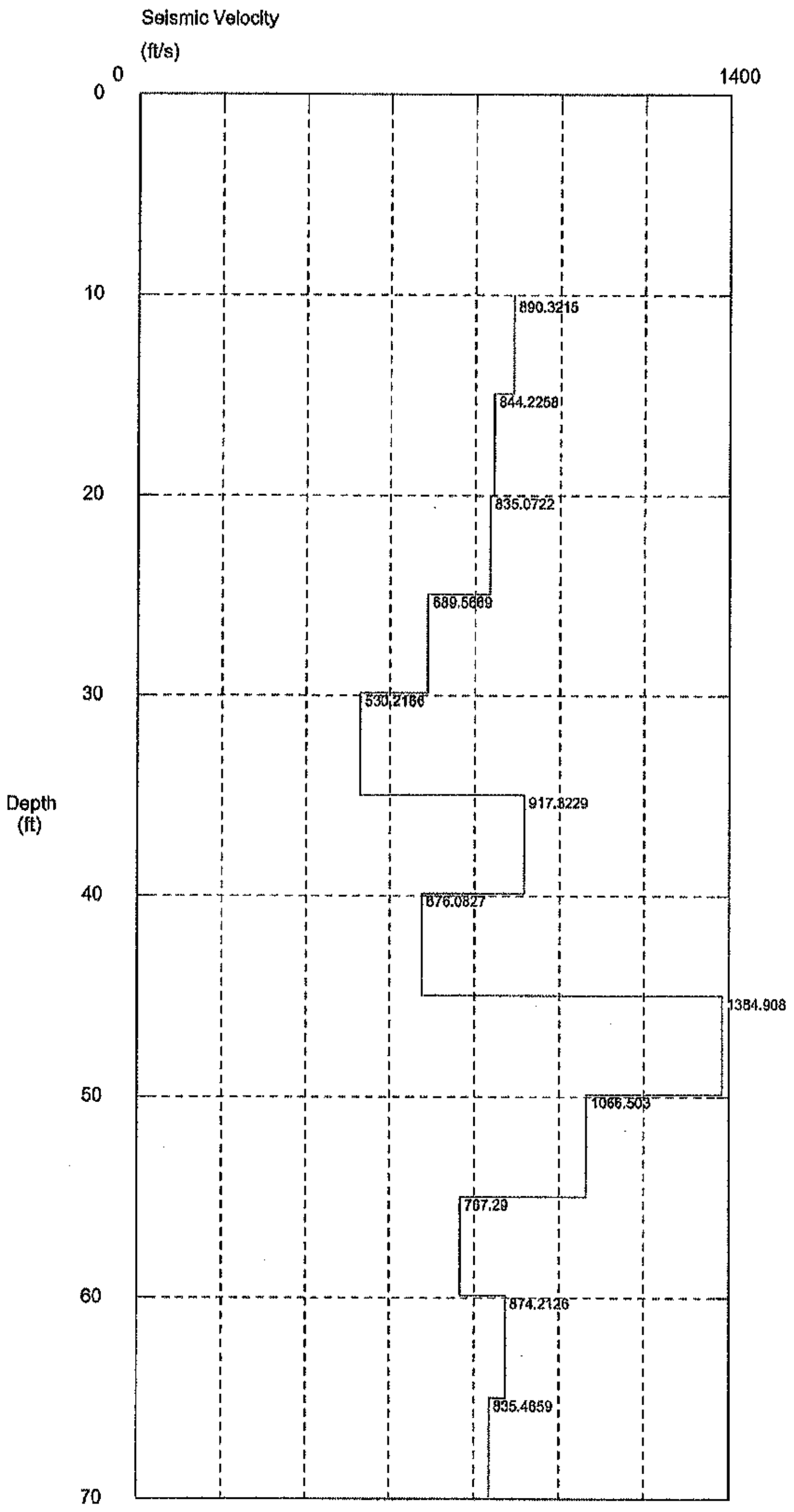

Maximum Depth = 69.88 feet

Depth Increment = 0.164 feet

N31.48424 W87.91472
SOUTHERN EARTH SCIENCES

GROUNDWATER: SOUNDING WET AND COLLAPSED AT 0.5 FEET

SOUTHERN EARTH SCIENCES, INC.

Operator: DANNY HINES
Sounding: SCPT-2
Cone Used: DDG0892

CPT Date/Time: 11/29/2011 12:02:16 PM
Location: LOWMAN POWER PLANT
Job Number: M11-372

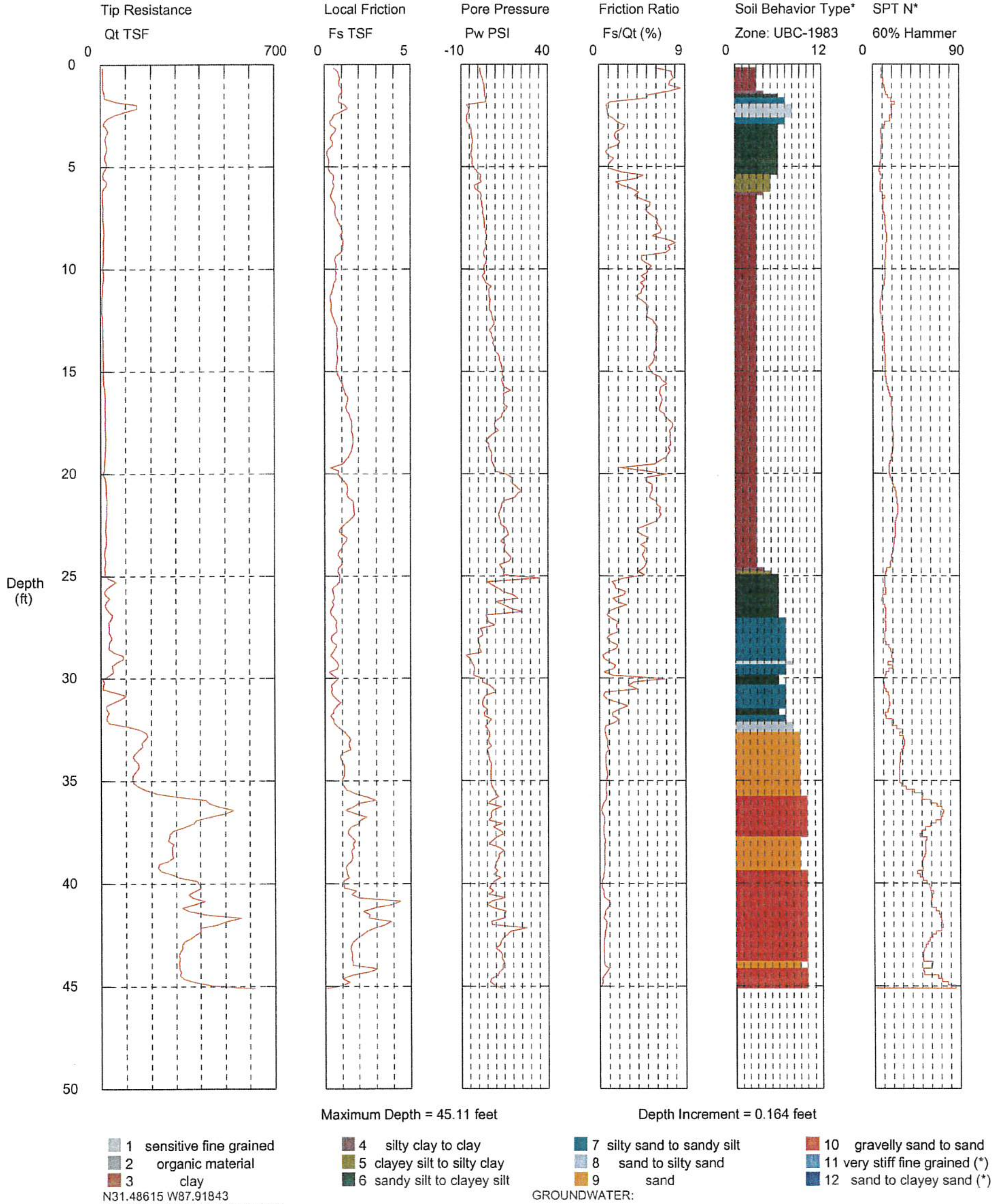

Maximum Depth = 45.11 feet

Depth Increment = 0.164 feet

N31.48615 W87.91843

SOUTHERN EARTH SCIENCES

GROUNDWATER:

*Soil behavior type and SPT based on data from UBC-1983

SOUTHERN EARTH SCIENCES, INC.

Operator: DANNY HINES
Sounding: SCPT-2
Cone Used: DDG0892

CPT Date/Time: 11/29/2011 12:02:16 PM
Location: LOWMAN POWER PLANT
Job Number: M11-372

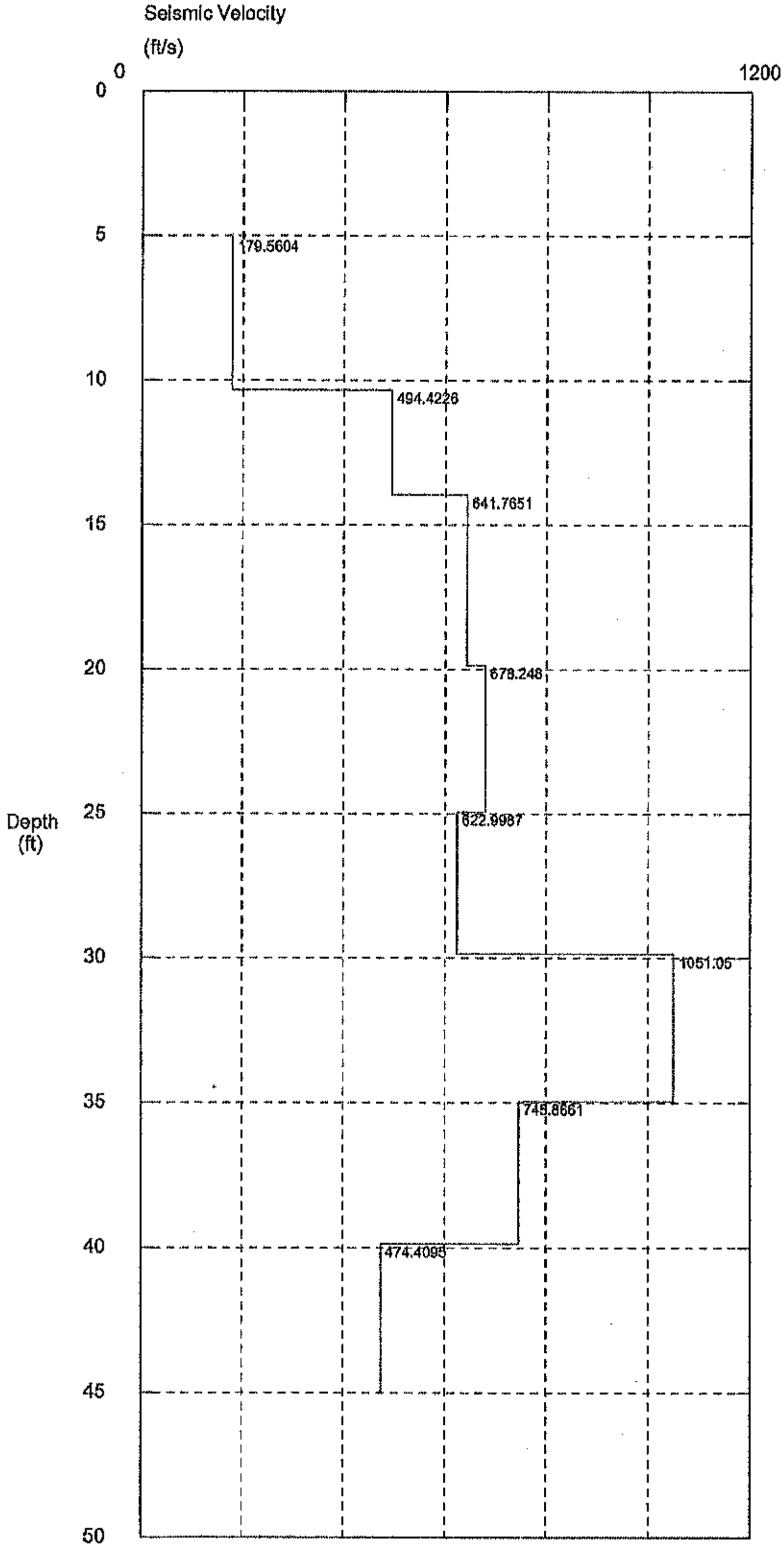

Maximum Depth = 45.11 feet

Depth Increment = 0.164 feet

N31.48615 W87.91843
SOUTHERN EARTH SCIENCES

GROUNDWATER:

SOUTHERN EARTH SCIENCES, INC.

Operator: DANNY HINES
Sounding: SCPT-3A
Cone Used: DDG0892

CPT Date/Time: 11/29/2011 2:20:34 PM
Location: LOWMAN POWER PLANT
Job Number: M11-372

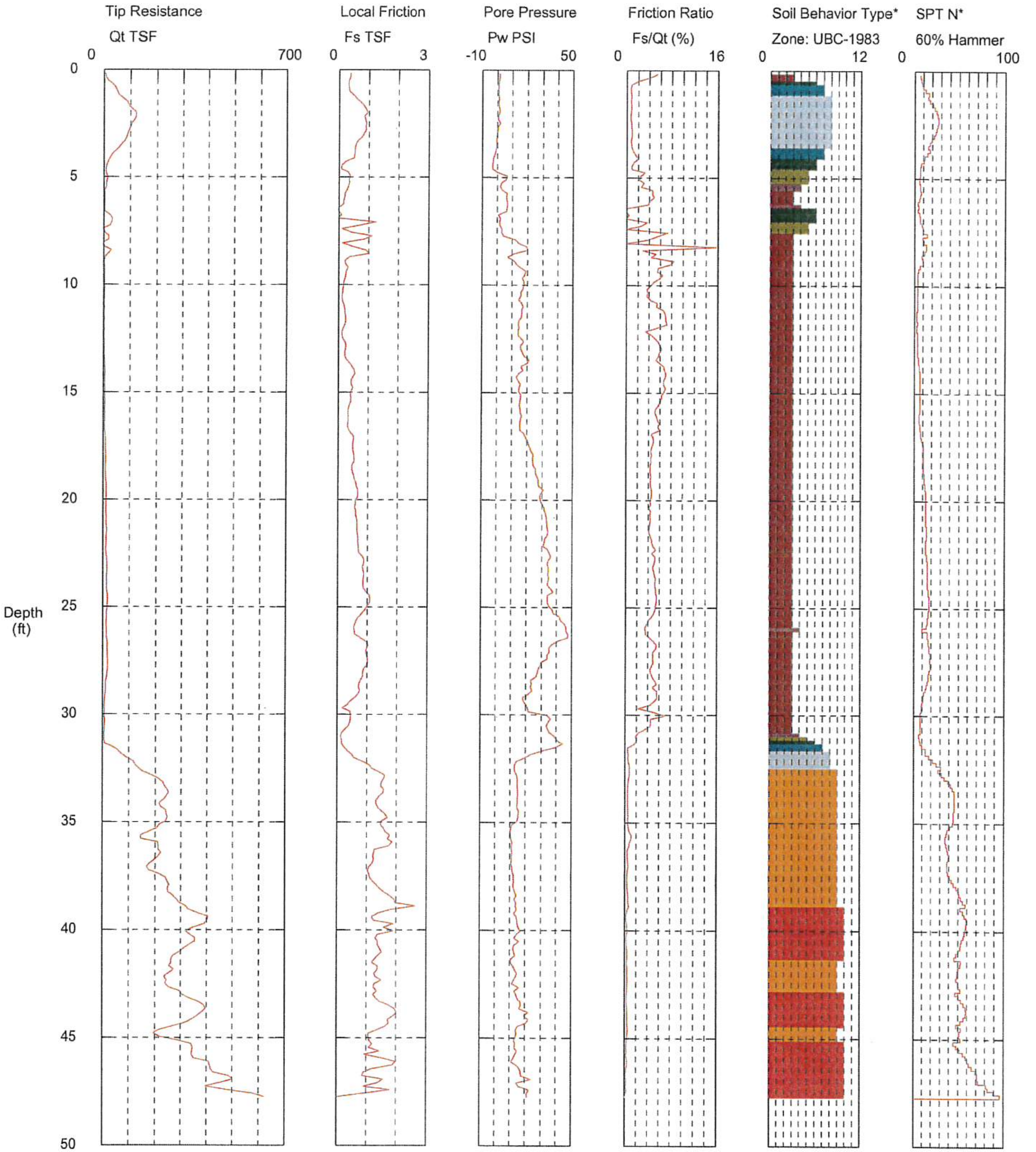

Maximum Depth = 47.74 feet

Depth Increment = 0.164 feet

▨ 1 sensitive fine grained
▨ 2 organic material
▨ 3 clay

▨ 4 silty clay to clay
▨ 5 clayey silt to silty clay
▨ 6 sandy silt to clayey silt

▨ 7 silty sand to sandy silt
▨ 8 sand to silty sand
▨ 9 sand

▨ 10 gravelly sand to sand
▨ 11 very stiff fine grained (*)
▨ 12 sand to clayey sand (*)

N31.49008 W87.91789
SOUTHERN EARTH SCIENCES

GROUNDWATER:

*Soil behavior type and SPT based on data from UBC-1983

SOUTHERN EARTH SCIENCES, INC.

Operator: DANNY HINES
Sounding: SCPT-3A
Cone Used: DDG0892

CPT Date/Time: 11/29/2011 2:20:34 PM
Location: LOWMAN POWER PLANT
Job Number: M11-372

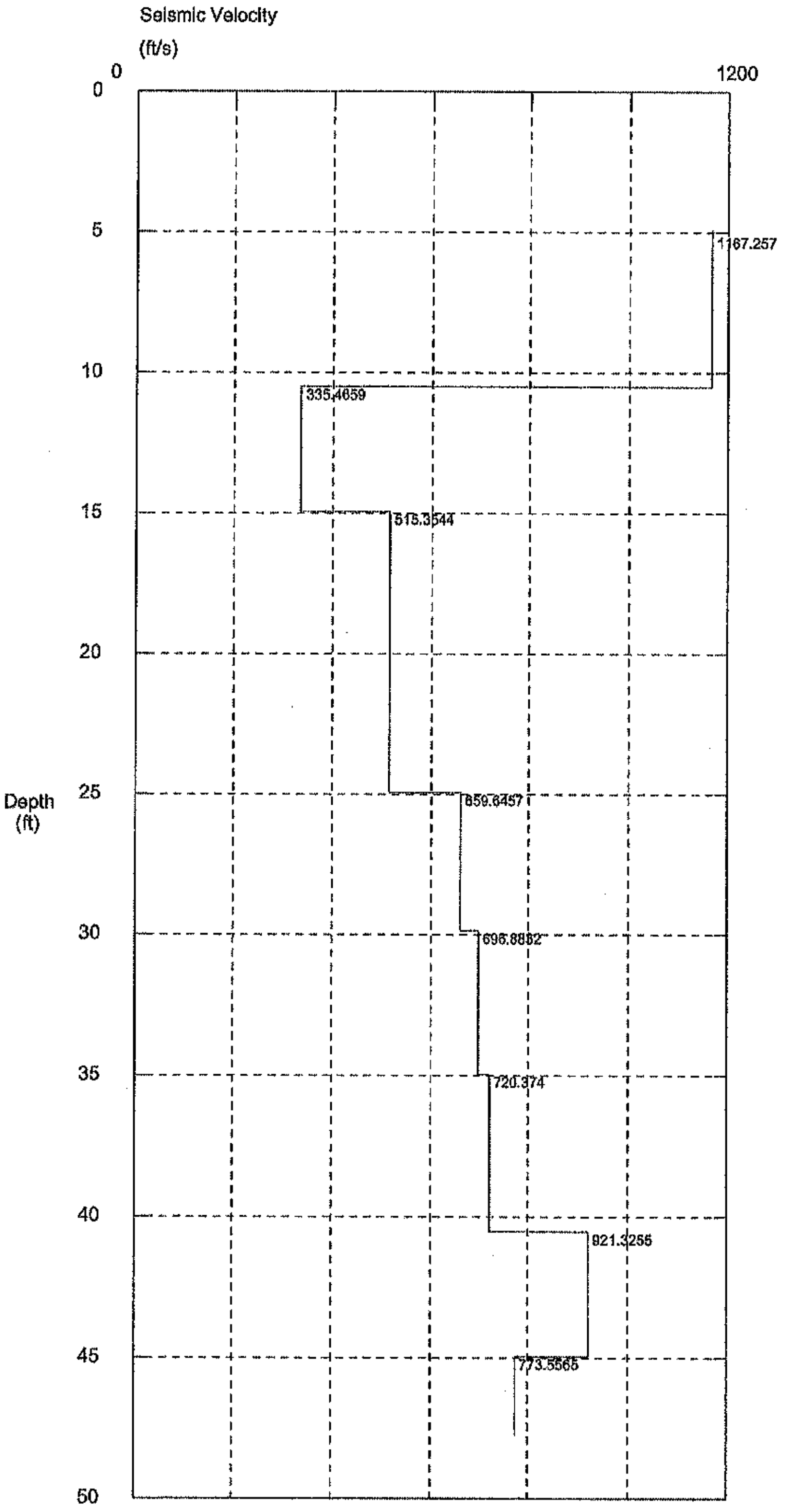

Maximum Depth = 47.74 feet

Depth Increment = 0.164 feet

N31.49008 W87.91789
SOUTHERN EARTH SCIENCES

GROUNDWATER:

Appendix G

Site Specific Seismic Hazard Analysis

DEVELOPMENT OF DESIGN GROUND MOTIONS FOR THE LOWMAN POWER PLANT

Final Report
3/27/2012
Pacific Engineering and Analysis
Prepared by
Walter Silva
Bob Darragh

Prepared for:

CDG Engineers & Associates
1830 Hartford Highway, Dothan, Alabama 36301

TABLE OF CONTENTS

1.0	Introduction	1
2.0	Development of Hard Rock Outcrop Motions	2
2.1	Uniform Hazard	2
2.2	Approach to Probabilistic Seismic Hazard Evaluation	3
2.3	CEUS Earthquake Occurrence	4
2.3.1	Non-Characteristic Earthquakes	5
2.3.2	Characteristic Earthquakes	8
2.3.2.1	New Madrid Sources	8
2.3.2.2	Charleston Sources	10
2.3.2.3	Wabash Valley Sources	11
2.4	Hard Rock Ground Motion Attenuation Models	12
2.5	Lowman Power Plant Hard Rock Seismic Hazard and Deaggregations	13
3.0	Development of Horizontal Hazard Consistent Site-Specific Soil Motions	17
3.1	Site-Specific Profile	16
3.1.1	Kappa	16
3.2	Equivalent-Linear Properties	17
3.3	Development of Transfer Functions	18
3.3.1	Site Aleatory Variability	18
3.3.2	Point-Source Model Parameters	19
3.3.3	Horizontal Amplification Factors	20
3.4	Soil Surface Design Motions	21
3.41	Design Time Histories	22
References		23

TABLES

Table 1:	Seismicity Parameters For Non-Characteristic Background Source Areas.	27
Table 2a:	b-Value Used For The Non-Uniform Hazard Model.	28
Table 2b:	Mmax Used For The Non-Uniform Hazard Model.	28
Table 3:	Finite Fault Parameters For New Madrid Scenarios.	29
Table 4:	Alternate Characteristic Magnitudes Considered For The Charleston Source.	30
Table 5:	Hard Rock Ground Motion Attenuation Models Used In This Study.	31
Table 6a:	Uniform Hazard Spectral Acceleration (G's) For 10% Probability Of Exceedance in 50 Years (AEF 2 x 10^{-3}); Hard Rock Site Conditions.	32
Table 6b:	Uniform Hazard Spectral Acceleration (G's) For 2% Probability Of Exceedance in 50 Years (AEF 4 x 10^{-4}); Hard Rock Site Conditions.	33
Table 7a:	Earthquake Hazard Disaggregation Mean Magnitude And Distance For PGA And 1-Hz for 10% Probability Of Exceedance In 50 Years	34

(AEF 2 x 10^{-3})
Table 7b: Earthquake Hazard Disaggregation Mean Magnitude And Distance For PGA And 1-Hz for 2% Probability Of Exceedance In 50 Years (AEF 4 x 10^{-4}) 34
Table 8: Base-Case Shear-Wave Velocity Profiles. 35
Table 9: Point Source Parameters. 37
Table 10: Weights. 38
Table 11: Uniform Hazard Spectral Acceleration (G's) For 10% Probability Of Exceedence In 50 Years (AEF 2 x 10^{-3}): Horizontal, Surface (Top-of-Soil). 39
Table 12: Uniform Hazard Spectral Acceleration (G's) For 2% Probability Of Exceedence In 50 Years (AEF 4 x 10^{-4}): Horizontal, Surface (Top-of-Soil). 40
Table 13: Basis Time History Used In Spectral Match. 41

FIGURES

Figure 1: Historic and instrumental seismicity for the CEUS (Chapman, 1998). All magnitudes are m_{blg}, either measured or inferred from Modified Mercalli Intensities of historic earthquakes. One of the four Charleston seismic zones used in this study is shown. 42
Figure 2: Circles indicate the epicenters of earthquakes with magnitudes greater than 3.0 contained in the USGS catalog for eastern North America (Mueller et al., 1997) (*http://geohazards.cr.usgs.gov/eq/html/catdoc.html*). 43
Figure 3: Source areas defined for non-characteristic events are indicated by the polygons. The triangle indicates the project location. 44
Figure 4: Characteristic earthquake source scenario for the New Madrid seismic zone involving three fault segments (Table 3). 45
Figure 5: Characteristic earthquake source scenario for the New Madrid seismic zone involving 6 fault segments (Table 3). 46
Figure 6: Hard rock horizontal component mean UHS computed at the Lowman Power Plant Site (Tables 6a and 6b) for AEF 4 x 10^{-4} (2,500 yrs), and AEF 2 x 10^{-3} (500 yrs). 47
Figure 7: Magnitude and distance disaggregation at AEF 2 x 10^{-3} (500 year) for structural frequencies 100.0 Hz (PGA) and 1.0 Hz at the Lowman Power Plant Site. 48
Figure 8: Magnitude and distance disaggregation at AEF 4 x 10^{-4} (2,500 year) for structural frequencies 100.0 Hz (PGA) and 1.0 Hz at the Lowman Power Plant Site. 50
Figure 9: Shear-wave velocity profiles used in the analyses. Profiles (P1 and P2) consist of about 6,500 feet (2,000m) of soils and soft rock above crystalline basement. 52
Figure 10: Generic G/Gmax and hysteretic damping curves for cohesionless soil (EPRI, 1993). 54
Figure 11: Example plot of median and ± 1 sigma amplification factors computed for the Lowman Power Plant profile P1 (Figure 9) with M = 7.5, single 55

corner frequency source model, and Peninsular Range (PR) G/G_{max} and hysteretic damping curves. Distances were adjusted to obtain the target hard rock median peak acceleration values: Surface motions.

Figure 12: Example plot of median and ± 1 sigma amplification factors computed for the Lowman Power Plant profile P2 (Figure 9) with M = 7.5, single corner frequency source model, and Peninsular Range (PR) G/G_{max} and hysteretic damping curves. Distances were adjusted to obtain the target hard rock median peak acceleration values. Surface motions. 57

Figure 13: Comparison of site-specific soil UHS (top-of-soil) with the hard rock UHS, logarithmic and linear Sa axes. 59

Figure 14: Comparison of site-specific soil UHS (top-of-soil) with the hard rock UHS for AEF 4×10^{-4} (2,500 year), logarithmic and linear Sa axes. 61

Figure Set 15: Spectral match acceleration, velocity, and displacement time histories followed by response spectra (target and spectral match, logarithmic and linear Sa axes) and ratios of time history spectra over target spectra for the horizontal component at the surface for AEF 2×10^{-3}. 63

Figure Set 16: Spectral match acceleration, velocity, and displacement time histories followed by response spectra (target and spectral match, logarithmic and linear Sa axes) and ratios of time history spectra over target spectra for the horizontal component at the surface (top-of-soil) for AEF 4×10^{-4}. 67

APPENDICES

Appendix A Development Of Regional Hard Rock Attenuation Relations For Central And Eastern North America, Mid-Continent And Gulf Coast Areas A-1

Appendix B Site Response Analysis Method B-1

Appendix C Stochastic Ground Motion Model Description C-1

Appendix D Approaches To Develop Site-Specific Hazard D-1

DEVELOPMENT OF DESIGN GROUND MOTIONS
FOR THE LOWMAN POWER PLANT

1.0 INTRODUCTION

Site-specific design ground motions (average horizontal 5% damped response spectrum and spectrally matched time history) were developed for the Lowman Power Plant, Alabama (31.4858°N, 87.9176°W). Site-specific horizontal motions were computed assuming vertically propagating shear-waves with material nonlinearity approximated through equivalent-linear site response analyses. The approach taken follows state-of-practice in central and eastern North America (CENA) in that an initial hazard analysis was performed for the site location using horizontal component (average) attenuation relations appropriate for hard rock outcropping (2.83 km/sec; EPRI, 1993). This reference site condition was assumed to exist beneath the local soils and soft-to-firm rock. In developing the fully probabilistic UHS design spectra, accommodation for the effects of the local materials above hard rock conditions was made by developing site-specific horizontal component UHS design spectra using approaches which properly accommodate aleatory (randomness) and epistemic (uncertainty) variabilities in site-specific dynamic material properties. The approach implemented preserves the desired exceedence probability of the hard rock hazard (Bazzurro and Cornell 2004). The hard rock hazard analyses represent hazard curves as well as uniform hazard spectra computed for 2% and 10% exceedence probability in 50 years (annual exceedence frequencies, AEF = 4 x 10^{-4} and AEF = 2 x 10^{-3}, respectively). Site-specific UHS were computed at the soil surface to provide control motions for follow-on analyses where horizontal time histories were spectrally matched to the design spectra at the soil surface for both 2% and 10% exceedance probability in 50 years. The site-specific UHS developed at soil surface were computed at the desired hard rock hazard level defined as an of AEF 4 x 10^{-4} (2% in 50 years (2,475 year)) and as an AEF 2 x 10^{-3} (10% in 50 years (500 year)). The site-specific UHS were developed using an approach that accommodates both epistemic and aleatory variabilities in both the hard rock attenuation relations as well as site-specific dynamic material properties.

The regional attenuation relations and their uncertainties are discussed in Appendix A. These regional relations were developed for hard rock (e.g. reference site) conditions and are used in the probabilistic seismic hazard analysis. Subsequent to the hard rock hazard analysis, site-specific hazard curves were developed using a fully probabilistic approach. This approach accommodates the effects of the local soils in terms of mean or base-case dynamic material properties as well as their variabilities, while maintaining the desired hazard levels of the hard rock hazard analysis. Appendix B contains a detailed discussion of the site response analysis methodology and Appendix C discusses the numerical model used to simulate the motions used in developing the attenuation relations. Appendix D discusses fully probabilistic approaches to developing site-specific hazard.

2.0 DEVELOPMENT OF HARD ROCK OUTCROP MOTIONS

Eastern U.S. regional seismicity is illustrated in Figures 1 and 2. Figure 1 shows historical and instrumental seismicity through 1996. Figure 2 shows all earthquakes near the study region with magnitude estimates exceeding 3.0 through 1994. Most events shown in Figure 2 are pre-instrumental earthquakes, with magnitude estimates derived from intensity data. The earthquake catalog assembled by the U.S. Geological Survey (Mueller et al., 1997) was used to establish the recurrence relations for the various source zones used in this study.

2.1 Uniform Hazard

The purpose of this task was to provide site-specific hard rock outcrop uniform hazard spectra and soil motions for the Lowman Power Plant. Criteria specified for the ground motion assessment in this study were 2% and 10% probability of exceedance of ground motions in a 50-year period (annual exceedence frequency (AEF) of 4 x $10^{-4}$and 2 x 10^{-3}, respectively).

The scope of this task was to perform a probabilistic hazard assessment considering published information on earthquake occurrence in the central and eastern U.S. (CEUS), available earthquake catalogs, and inferences from paleoseismic data collected along the central U.S. and the eastern seaboard. Depending on local site and subsurface conditions, predicted probabilistic motions may differ significantly at other sites. The scope of this study does not include site-specific geologic or seismologic investigations relevant to the detection or delineation of geologic faults in the vicinity of the site.

2.2 Approach to Probabilistic Seismic Hazard Evaluation

The analysis methods used in this study are based on the approach developed by Cornell (1968). Basically, the earthquake processes that might potentially affect the project site are modeled stochastically in both time and space. Seismic sources are also defined. Within these sources, earthquakes are assumed to occur randomly, in terms of their epicentral locations, as well as in terms of their occurrence times. Temporally, the earthquakes are assumed to follow a simple Poisson process. The Poisson model is the most tractable model that can be applied to this type of analysis, and has been employed as a "standard" model for hazard analysis for many years. The most important assumption is that earthquakes associated with a given source have no "memory" of past earthquakes. The Poisson model is an approximation. Large earthquakes have been shown to occur in a time-dependent manner: i.e., the probability of a large shock in fact depends upon the time elapsed since the last large shock on a given fault, or in a given source area.

The seismicity model used to generate hazard in the central and eastern U.S. consists of two components. The first component uses a characteristic earthquake to model the recurrence of the "1811-1812-type" New Madrid, "1886-type" Charleston and Wabash Valley Seismic Zone (WVSZ, Zone 2 in Figure 3) earthquakes within a specified source zone.

The New Madrid, Charleston and Wabash Valley seismic zones are delineated on the basis of historical seismicity and geophysical and paleoseismic inference. Earthquake occurrence rates are determined by paleoseismicity, evidenced by relic liquefaction features at magnitude thresholds of about 6. Recurrence rates for both the New Madrid and Charleston seismic zones are 500-600 years, consistent with the latest paleoseismic data for those areas.

The second component is based on historic seismicity, alternative models for the rates of seismicity based on historic occurrence of earthquakes are used to compute seismic hazard. One model (discussed below) uses a uniform distribution for the central and eastern U.S. The model has the potential disadvantage of "smoothing out" significant local variation of the seismic hazard, while alternate models assign spatially dependent rates of seismicity. Hence this approach to modeling earthquake recurrence gives higher weights to spatially dependent historic rates over uniform distributions of earthquakes. Seismotectonic zonation or sources placed on specific faults would require an understanding of the earthquake process that is beyond the state of current knowledge.

Variabilities in specific seismic source and ground motion models are addressed (aleatory variabilities) as well as uncertainties in the models (epistemic variabilities). No effort is made to explore or include all available models in the literature, but only those that are judged reasonable. Judgments on reasonableness are also reflected in weight assignments for the various models and parameters. Variabilities were included for the following models and parameters: (1) source configuration, maximum magnitude and recurrence rate for the New Madrid, Charleston and Wabash Valley sources; (2) maximum magnitude and b-value for the non-uniform zone; and (3) ground motion attenuation models.

A logic tree expresses the range of possible models reflecting the uncertainties in the model. Models are developed by sampling every combination possible in the logic tree. Depending on the combination of weights, each hazard model has an associated total weight. Finally, a weighted mean hazard model is computed along with a mean earthquake magnitude and distance disaggregation. The uniform hazard spectrum is computed by selecting the weighted mean AEF for each structural frequency at the selected exceedance level.

2.3 CEUS Earthquake Occurrence

Over much of central and eastern North America, the specific geological features (faults) that are causally related to seismicity are not well defined. Hence, area sources based primarily on seismic history were used for analysis of non-characteristic events. Larger magnitude characteristic events with potential to occur in the upper Mississippi Embayment (New Madrid), Wabash and Charleston regions are modeled with a combination of area and fault sources. Within the various area sources, earthquakes are assumed to occur with uniform probability in space, their locations having no dependence upon magnitude. Figure 3 shows the area sources defined for the non-characteristic "background" events.

The historical seismicity of the central United States is dominated by the earthquake history of the upper Mississippi Embayment, in an area referred to as the "New Madrid" seismic zone. Three major earthquakes occurred in 1811 and 1812, with magnitudes in the range 7.5 to 8.2 (Johnston, 1996; Hough et al., 2000). The seismogenic faults responsible for those shocks are delineated by the modern seismicity, shown in Figures 1 and 2. This is the site of the most frequent earthquakes in the eastern U.S, and for this study, it is represented by the area source indicated as "NM" in Figure 3. The Charleston seismic zone produced a significant earthquake in 1886 (Figure 1).

The immediately surrounding area of New Madrid represents a geologic feature known as the Reelfoot Rift. This is a Late Precambrian- Early Cambrian feature that developed as a result of extensional stresses (e.g., Wheeler, 1997). The Reelfoot Rift area also exhibits an elevated level of seismicity, compared to the eastern U.S. average, and is represented as an area source termed "Reelfoot" in Figure 3.

There is also an extensive area including southeastern Missouri, southern Illinois and southwestern Indiana that exhibits a level of seismicity comparable to the Reelfoot Rift, excluding the seismically intense New Madrid area. Two source areas for **M**<6.5 background seismicity have been defined to represent this region. Source 1 (Figure 3) includes southeastern Missouri and southwestern Illinois, and Source 2 (Figure 3) includes most of southern Illinois, southwestern Indiana and parts of western Kentucky.

The tectonic style that defines the Reelfoot Rift changes in western Kentucky. Northeast trending faults of the Reelfoot rift change to an easterly trend in that area and form what is known as the Rough Creek Fault system. Also, this area exhibits a lower level of historical seismicity than the Reelfoot Rift area, and no paleoseismic evidence for large prehistoric shocks has been found to date. Treatment of this geologically complex area involves significant uncertainty for any study dealing with the central U.S. seismic hazard (see, e.g., Wheeler, 1997). Insufficient data exist to apply a characteristic earthquake model for this source, although the region is part of the continental margin and has experienced a deformational history similar to the New Madrid region. For that reason, maximum magnitude for this source is taken to be **M**=7.5 for analysis. However, the area will be treated as a part of the background seismicity, using a conventional Gutenberg-Richter recurrence model. This source is shown in Figure 3 as "Rough Creek".

2.3.1 Non-Characteristic Earthquakes

This study treats smaller earthquakes, with moment magnitudes between 5.0 and 6.5-7.5 (depending on geologic setting) differently than larger shocks in three other specific areas. There is consensus of expert opinion that magnitude 6.5 and smaller shocks can occur on relatively small, inconspicuous features that exist throughout the North American continental craton. For that reason, such shocks are treated as forming a seismicity "background" in the central United States. In areas representing the Paleozoic and Mesozoic accreted margin of North America, the maximum magnitude of such background seismicity is considered to be somewhat larger. In this study, a value of moment magnitude **M**=7.5 is assumed to represent the maximum magnitude of shocks in areas of the continental margin affected by late Precambrian- early Paleozoic and Mesozoic rifting. Those latter areas are treated as background as well, because of the large source to site distances. The seismic hazard due to the background is estimated using a standard approach assuming a truncated Gutenberg-Richter recurrence model and area sources. In three areas such treatment is not adequate. The New Madrid, Charleston, and Wabash Valley areas have exhibited earthquakes both historically and in the geologic record indicating that the historical record of smaller shocks does not adequately represent the likelihood of future large shocks. In those areas, a different (characteristic earthquake) approach is used to handle shocks with magnitudes greater than 6.5 (see Section 2.3.2).

The Eastern Tennessee area exhibits an elevated level of seismicity, compared to the eastern U.S. average, and is represented as an area source termed "ETN" in Figure 3. The Appalachian region lies within the extended continental crust (as does New Madrid, Rough Creek and parts of zone 2 sources (Wabash Valley)). The Alabama (AL), Southern Appalachian Zone (SA) and Piedmont (Pied) sources are treated as background in similar fashion to the Eastern Tennessee (ETN) source, using a maximum moment magnitude Mmax=7.5 (Table 1).

The source areas described above dominate the hazard presented by the background seismicity at the project site. The calculations involve other, less important, contributions to hazard from other seismic sources to distances of 500 km from the site. Much of the central U.S region to the north, west and south of the sources described above exhibits a very low level of historical earthquake activity, and presents minimal hazard (e.g. Sibol et al., (1987). Numbers 3, 4 and 5 in Figure 3 indicate these source areas. Also, frequent earthquakes have occurred in western Ohio, near Anna. Distances and activity rates are such that these sources do not contribute significantly to hazard, and are included only for completeness.

To estimate the background hazard, earthquakes with magnitudes smaller than the maximum moment magnitude Mmax are treated as occurring at random according to the Gutenberg-Richter recurrence model within source areas that were defined largely on the basis of the observed rate of historical and recent instrumentally recorded seismicity. The seismic hazard presented to the project by these sources is directly proportional to the seismicity rate per unit area within the source and inversely proportional to the distance of the source from the project.

Table 1 lists, for each background source area, the parameters defining the Gutenberg-Richter recurrence model. The model is

$$\text{Log } N = a - b\,m, \qquad (1)$$

where N is the number of earthquakes per year with magnitude greater than m. The parameters a and b are estimated from the historical record of pre-instrumental earthquakes, as well as from the catalog of more recent instrumentally recorded earthquakes. The Gutenberg-Richter model implies an exponential probability density function for earthquake magnitude. In this study, this density function is truncated at an upper (Mmax) and lower (Mmin) bounds.

There are several different magnitude scales in use. Two types are used in this study. The scale developed by Nuttli (1973) is based on the amplitude of the short-period Lg phase. It is the magnitude scale generally used in eastern North America for shocks recorded at regional distances. It is referred to in this study as m_{blg}. It is the magnitude scale adopted for most eastern U.S. earthquake catalogs. The recurrence relationships used in this study are developed in terms of this magnitude.

The moment magnitude scale (Hanks and Kanamori, 1979) is based on seismic moment and is a better estimate of the true size of an earthquake in a geological sense. Here, it is used in the equations for ground motion prediction, and in the definition of characteristic earthquakes (see below) as well as the upper and lower truncation limits of the magnitude probability density functions.

Earthquakes with moment magnitude less than Mmin = 5.0 are not considered, as they do not produce damaging ground motions. The upper truncation magnitude Mmax is a critical parameter for the analysis, and depends on the particular source under consideration. The values of a and b listed in Table 1 are in terms of mblg magnitude. The following conversion (Frankel et al., 1996; Johnston 1996) was used to convert from mblg to moment magnitude **M**:

$$\mathbf{M} \text{ (moment magnitude)} = 3.45 - 0.473 \text{ mblg} + 0.145\text{mblg}^2. \qquad (2)$$

For the remaining areas not defined by the region specific background source zones listed in Table 1 and shown in Figure 3, the hazard is specified by a combination of four models of the historical earthquake catalog (Frankel et al., 1996). Those models are based on: (1) spatially smoothed $m_{bLg} \geq 3$ occurring since 1924; (2) spatially smoothed $m_{bLg} \geq 4$ occurring since 1860; (3) spatially smoothed $m_{bLg} \geq 5$ occurring since 1700; and (4) a regional background zone. In models 1 through 3, a 0.1 degree grid spacing was used to count events of the specified magnitude and larger to determine a grid a-value. The grid of a-values for each model was smoothed using a Gaussian function. The fourth model is a large background zone that covers the southeastern U.S. and employed a uniform weighting scheme to count earthquakes. A b-value of 0.95 (Table 2a) and a maximum magnitude (Mw_{max}) of 7.5 (Table 2b) were used for models 1 through 4.

An adaptive weighting scheme was used to derive the final grid a-values. Models 1, 2 and 3 were weighted by 0.5, 0.25, and 0.25 respectively to compute grid a-values. Where the weighted grid a-value was less than the background zone rate (model 4), weights of 0.4, 0.2, 0.2, and 0.2 were used for models 1-4 respectively. The adaptive weighting scheme matches the seismicity rates in regions of high seismicity but tends to increase seismicity slightly above historical rates in regions of low seismicity. With the exception of the Charleston and New Madrid source zones, the modeling of earthquake occurrence used the truncated exponential model (Equation 1 with cut-off at Mw_{max}). Other magnitude distributions are possible; however, Anderson and Luco (1983) have shown that the truncated exponential model is conservative at the largest magnitudes.

2.3.2 Characteristic Earthquakes

A characteristic earthquake model was employed for the New Madrid, Charleston, and Wabash Valley sources.

2.3.2.1 New Madrid Sources

The New Madrid seismic zone has received considerable attention from the seismological community in recent years (see, e.g., Johnston and Schweig, 1996). Wheeler and Perkins (2000) summarize important considerations for seismic hazard assessment in the region. Cramer (2001a, 2001b) discusses the important elements of the hazard model, in terms of uncertainties and their impact on hazard calculation. Basically, the elements that must be quantified involve the maximum magnitudes of potential earthquakes, the locations of the faults where such earthquakes may occur, and the temporal behavior (recurrence intervals) of the larger shocks.

Issues related to recurrence involve the paleoearthquake chronology that has been developed in recent years from age-dating prehistoric liquefaction features (Tuttle and Schweig, 2000). This work indicates a mean recurrence interval of 458 years for liquefaction inducing earthquakes in the New Madrid seismic zone. However, there is considerable uncertainty involved in those estimates and the possibility exists that a longer recurrence interval (e.g., 1000 years) is appropriate for hazard calculations. The approach used in this analysis is to use both values, with more weight given to the 458-year scenario, on the basis of the best-estimate results from the recent paleoseismic investigations of liquefaction features. The weighting scheme adopted here is similar to that currently being considered for the 2002 update of the National Seismic hazard maps (Cramer, 2001a, b; see also, documentation for the August 2002 Draft National Seismic Hazard Maps,*http://geohazards.cr.usgs.gov/eq/2002draftAug/DocAugust2002REV.html*).

The magnitude estimates of the 1811-1812 events as well as all paleoearthquakes are very uncertain. Johnston (1996) proposed that the magnitudes of the principle shocks of 1811-12 were as high as 8.3. Recently, Hough et al., (2000) have suggested that the 1811-1812 magnitudes were in the range 7.0 to 7.5. In the hazard calculations, the magnitudes of the characteristic earthquakes are treated as two mutually exclusive and exhaustive scenarios: 1) 7.0 to 7.5 and 2) 7.5 to 8.0 (Moment magnitude). The calculations incorporate, for each characteristic magnitude scenario, the two alternative recurrence intervals: 1) 458 years and 2) 1000 years with relative weights of 0.9 and 0.1 respectively (Table 3).

The locations of the faults that ruptured in 1811-1812 are generally believed to be illuminated by the modern seismicity pattern which occurs generally in the Reefloot zone in Figure 3. There are 3 major fault segments, involving two northeast trending strike-slip faults separated by a compressional stepover on a major southeast striking reverse fault. One scenario for the locations of future characteristic New Madrid earthquakes is to assume that they can only occur independently on these 3 faults. Figure 4 illustrates this scenario. However, large prehistoric events may have occurred on currently aseismic faults in the Reelfoot Rift. The possibility exists that future large shocks could occur elsewhere in the Rift, nearer to the project. Figure 5 illustrates a second New Madrid fault scenario, which places the characteristic events on 6 parallel strike-slip faults. In the hazard calculations, both source configurations are given equal weight, consistent with the fact that the potential source locations of future large earthquakes within the Reelfoot Rift are currently uncertain.

Finite fault rupture is modeled in the hazard calculations. This implies that the source to site distance is a function of earthquake magnitude. The Wells and Coppersmith (1994) magnitude-area scaling relationship is used in the hazard code to estimate the rupture area for a given magnitude. In addition, the magnitude-fault width relationship of Wells and Coppersmith (1994) is used to estimate the fault width. The resulting ratio of fault area divided by fault width (not to exceed the total fault width) gives the estimate of the fault length for a given magnitude.

For the 3 fault scenario, earthquake magnitudes spanning the non-characteristic range **M** 6.5 to 7.0 (scenario 1) or **M** 6.5 to 7.5 (scenario 2) are modeled as occurring on the faults using the Gutenberg Richter recurrence relation for source area NM in Table 3. The activity is divided equally among the 3 faults. For the 6-fault scenario, earthquakes in the magnitude range 6.5 to 7.0 (or 6.5 to 7.5, depending on characteristic magnitude scenario) are modeled using the combined Gutenberg-Richter recurrence models for sources NM and Reelfoot Rift (with a = 3.31), and with the activity divided equally among the 6 faults. Finite fault recurrence is summarized in Table 3.

2.3.2.2 Charleston Sources

The Charleston model assumes a weighted magnitude of Mw 7.2 (Table 4) with a frequency of 1/550 yr^{-1} occurring randomly in time. The magnitude range is based on the mean of the 1886 Charleston earthquake magnitude using intensity data (Johnston, 1996) and the analyses of Bakun and Harper, 2002. The earthquake frequency is established on the basis of recent geologic investigations on dates of relic liquefaction features (Amick et al., 1991, Obermeier et al., 1990, Talwani and Schaeffer, 2001).

Two different source configurations for the Charleston source were incorporated in this hazard assessment. A large zone (Figure 1) that incorporates the historic seismicity and locations of relic liquefaction is given the weight of 0.50. A more refined fault zone area extends to the northeast and accounts for possible stream channel irregularities (Marple and Talwani, 1990) was given a weight of 0.5. This characterization follows the source model used in the current USGS national hazard maps (Petersen et al., 2008).

2.3.2.3 Wabash Valley Sources

The seismic history to the east of the project area involves moderate earthquake activity in southern Illinois and southwestern Indiana. Nuttli and Herrmann (1978), Nutlli (1979) and Nuttli and Brill (1981) discussed the seismicity of this area and defined a general boundary for a "Wabash Valley seismic zone" (WVSZ).

In contrast to the seismic zone of the same name, the Wabash Valley fault zone (WVFZ) is a zone of northeast trending normal and strike-slip faults along the border of Illinois, Kentucky and Indiana, lying within the larger region referred to as the Wabash Valley seismic zone (WVSZ). The WVFZ has long been suspected of being related to seismicity in the WVSZ. However, the seismicity does not correlate with mapped faults of the WVSZ. Tectonic relationships of the WVFZ to the more active Reelfoot Rift and New Madrid seismic zone are not clear, and are controversial (see for example, discussion in Kolata and Hildenbrand, 1997; Wheeler, 1997; Wheeler and Cramer, 2001).

Recent geologic investigations in Indiana and Illinois have found evidence of major (M>6.5) prehistoric earthquakes in the WVSZ (Obermeier 1991; Obermeier et al. 1992; Munson et al. 1992, 1997; Pond and Martin 1997; Obermeier 1998, McNulty and Obermeier 1999). Six large (M>6.5) earthquakes have occurred within the last 12,000 years in the WVSZ. Two of these events may have exceeded magnitude 7.0.

Gravity and magnetic data reveal a major feature (Commerce Geophysical Lineament, or CGL) trending along the western margin of the Reelfoot Rift northeastward across southern Illinois and western Indiana. Langenheim and Hildenbrand (1997) interpreted the CGL as a mafic intrusive structure within Precambrian basement and proposed that it may be seismogenic. Hildenbrand and Ravat (1997) suggested that the CGL was probably reactivated during formation of the Reelfoot

Rift and Rough Creek graben. The feature correlates spatially with moderate magnitude historical shocks as well as the inferred locations of prehistoric shocks in the WVSZ.

The seismic hazard model for earthquakes with magnitudes larger than 6.5 in the Wabash Valley Seismic Zone (WVSZ, Zone 2 in Figure 3) involves 2 scenarios for source configuration. In scenario 1, **M**>6.5 shocks are assumed to occur throughout area source 2. The recurrence rate is constrained by the Paleoseismic results suggesting the occurrence of 6 **M**>6.5 events in the last 12,000 years. A truncated Gutenberg-Richter recurrence model was used, with lower (moment) magnitude bound of 6.5 and an upper (moment) magnitude bound of 7.5. In terms of mblg magnitude, the recurrence model is

$$\text{Log N} = 2.95 - 0.96 \text{ mblg} \qquad (3)$$

For the second scenario, the area wherein **M**>6.5 shocks are assumed to occur is reduced to include a region approximately 120 km wide centered on the CGL. Equation 3 is again used to model the recurrence of large shocks.

2.4 Hard Rock Ground Motion Attenuation Models

The hazard evaluation used three earthquake magnitude-dependent attenuation models for eleven structural frequencies and 5% damped spectral peak acceleration and their standard deviations. Region specific hard rock attenuation relations and their uncertainties have recently been developed for the central and eastern U.S. (Appendix A). These relations were developed for applications to the midcontinent and reflect region specific influences (Appendix A). The three attenuation models reflect uncertainty in modeling strong ground motion in the eastern U.S. Attenuation of ground motion from single-corner source models (Toro et al., 1997; EPRI, 1993) is developed in Appendix A. Magnitude dependent stress drop, a recent finding for WUS sources (Silva and Darragh, 1995; Atkinson and Silva, 1997; Silva et al., 1997) is also developed in Appendix A. The two-corner model is also considered appropriate (Atkinson and Boore, 1997) (Appendix A). Weights for the relations were taken as 0.4 for the variable stress drop and 0.4 for the single constant stress drop and 0.2 two-corner for source models (Table 5). To accommodate variability in mean (epistemic) stress drop for the single corner model; medium, low, and high mean stress drop attenuation relations are used (Appendix A). The median stress drop is taken as 110 bars (EPRI, 1993) with the aleatory variability about the median at 0.5 $\sigma_{\ln}$, appropriate for

WUS (Silva et al., 1997). The range in median stress drops was adjusted to give a total variability of 0.7 (Appendix A and EPRI, 1993). The relations are appropriate for basement hard rock outcropping for use as input to site-specific soil column analyses. Table 5 summarizes the selected attenuation models and weighting scheme.

2.5 Lowman Power Plant Hard Rock Seismic Hazard and Deaggregations

Analysis of earthquake hazard requires information on geographic distribution of earthquakes, rupture parameters, ground motion attenuation, and source zone activity. This information is needed so that the ground motion can be estimated for any given earthquake and summed according to the frequency of earthquakes of different sizes and locations.

For spatial modeling of characteristic earthquakes considered in the ground motion evaluations, our procedure is to randomly orient vertical faults whose locations and lengths are constrained by the geometry of the area source and by the rupture length-magnitude relationship applied in this study. For the non-uniform source, the approach is to integrate the contributions from the grid of incremental a-values over the entire source. For the characteristic earthquake sources, source-to-site distance is defined as the closest distance to randomly oriented vertical faults. The faults are centered on each of a grid of points, the strikes are randomized and then the closest distance is used in the hazard analysis. Hazard from each of the grid points, or faults is then averaged. Note that this algorithm allows rupture to extend as much as ½ of a fault length beyond the dimensions of the source zone. Following recommendations by Bender (1984), the one-to-one relation between magnitude and mean rupture length (rather than the median rupture length determined from the regression) is used to avoid laborious analysis of the uncertainty in magnitude-fault length relationships. The Wells and Coppersmith (1994) correlation between earthquake magnitude and subsurface fault length was used in this study. For the area sources and maximum magnitudes considered in this study, fault lengths did not exceed the maximum linear dimension of the area source. A minimum magnitude (m_{bLg}) of 5 was considered in the hazard calculations.

The 5% damped hard rock uniform hazard spectra for 10% and 2% exceedance in 50 years are listed in Tables 6a and 6b, and are shown in Figure 6. Disaggregation of the hazard by earthquake magnitude and distance was conducted. Table 7 lists the mean earthquake magnitudes and distances controlling the hazard for the site location. Figure 7 illustrates the disaggregation for

PGA and 1 second for 10% exceedance in 50 years. Figure 8 illustrates the disaggregation for PGA and 1 second for 2% exceedance in 50 years. For both AEFs, at high frequency (e.g. PGA) the nearby Alabama, Piedmont, and background areal sources (Figure 3) are dominant contribution to the hazard along with the New Madrid seismic zone (e.g. Figures 1-5). At periods of 1 second and longer the New Madrid seismic zone is the major contributor to the hazard.

3.0 DEVELOPMENT OF HORIZONTAL HAZARD CONSISTENT SITE-SPECIFIC SOIL MOTIONS

Design performance goals for the Lowman Power Plant were based on a probabilistic design spectrum at an annual probability of exceedence of 2% and 10% in 50 years (2,475 year, AEF 4 x 10^{-4} and 500 year, AEF 2 x 10^{-3}). Achievement of these performance goals for soil surface was assured through computation of site-specific design motions with a fully probabilistic methodology that incorporates both aleatory (randomness) and epistemic (uncertainty) variability in dynamic material properties. The fully probabilistic approach maintains the hazard level (desired exceedence frequency) of the hard rock UHS (Bazzuro and Cornell, 2004; Appendix D, Approach 3) while incorporating variability in site-specific dynamic material properties for the soil surface design motions.

As a result, horizontal design spectra reflect similar exceedence frequencies while maintaining the desired hazard levels and structural performance goals. To provide a basis for follow-on analyses, horizontal motions were developed at the soil surface for both 2% and 10% exceedance in 50 years.

The fully probabilistic approach to developing a site-specific soil UHS while both maintaining the hard rock hazard level (hazard consistent) and incorporating site variabilities is a fairly recent development. The approach was first introduced in 1998 in a Nuclear Regulatory Commission research project (NUREG/CR-6728, 6769), and has been applied at several DOE and nuclear facilities as well as several smaller projects. The approach will likely become state-of-practice as it reflects the only method of achieving desired hazard levels across structural frequency in developing site-specific design motions. An unfortunate aspect of a fully probabilistic approach is the large number of site response analyses required to achieve statistically stable estimates of desired hazard levels. Typically, for each case of dynamic material properties, thirty site response analyses are performed to develop statistically stable estimates of median and standard deviations of amplification factors ($Sa(f)_{soil}/Sa(f)_{hard\ rock}$), both of which are used in the fully probabilistic approach (Bazzurro and Cornell, 2004). Additionally, because the soil hazard at any exceedence frequency has contributions from the hard rock or reference hazard at all exceedence frequencies, suites of amplification factors are required covering a wide range in reference ground motions, typically peak accelerations ranging from 0.01g to 1.50g by varying control motion distances (Table 9).

The amplification factors were developed using the conventional equivalent-linear approximation to nonlinear soil response along with vertically propagating shear-waves for horizontal motions. In the site response approach implemented here, time histories were not used. Instead, a frequency domain random vibration theory (RVT) approach was implemented which requires only the uniform hazard spectra. The methodology is discussed in Appendix B. Control motions used to drive the soil columns were generated with the point-source model discussed in Appendix C.

Because controlling earthquake magnitudes typically change with structural frequency and hazard level in a probabilistic seismic hazard analysis, amplification factors must be developed for multiple magnitudes to cover the magnitude ranges across both structural and exceedence frequency. As an additional complicating factor, there currently exists large epistemic variability (uncertainty) in large magnitude (**M** > 5.5) source processes in the CENA captured in single-verses double-corner source models (Appendix A). Conditional on magnitude, soil site amplification factors can differ significantly due to the differences in loading levels between single- and double-corner source models (NUREG/CR-6728). As a result, for magnitudes greater than about **M** 5.5, separate amplification factors were computed using single- and double-corner source models. The resulting hazard curves were then weighted (Table 10) and combined over exceedence frequency.

To properly accommodate epistemic variability, uncertainty in mean dynamic material properties, e.g. G/G_{max} and hysteretic damping curves, separate analyses must be performed for each case of mean curves, resulting in distinct sets of hazard curves. These are then averaged with weights over probability, thereby achieving desired exceedence frequencies.

3.1 Site-Specific Profile

To develop a site-specific shear-wave velocity profile, CDG Engineers & Associates provided CPT logs and SCPT logs (Southern Earth Sciences, Inc.). The deepest profiles extend to a depth of about a depth of about 70 ft. CDG Engineers & Associates reviewed and summarized the local geology. The Lowman Power Plant site is in the Coastal Plain Geomorphic Province and on the down-throw side of the Mobile graben. The site is underlain by relatively recent water-deposited alluvial, coastal and low terrace deposits (sandy clay and silty sand). The deeper lithology is very complex due to the presence of salt domes (Klepac and Louann) and the near-by Jackson fault line. The top of the Louann is at approximately 11,000 ft. Depth to basement rock is estimated at about 20,000 ft. Unit weights for the soft to medium and loose soils and medium dense to very dense soils were taken as 115 and 120 psf respectively (CDG Engineers & Associates).

Two profiles were adopted to reflect uncertainty in the velocities beneath the top 100 feet (Figure 9). The top 100 ft of Profiles P1 and P2 is based on measured shear-wave velocities in SCPT-2. Below a depth of 100 ft each profile (P1 and P2) was based on measured shear-wave velocities in similar sedimentary materials (Fukushima et al., 1995) and extends to depths where they reach hard basement rock defined as a shear-wave velocity of 2.83 km/sec (Table 8). Hard basement material was placed at a depth of 6,562 ft (2,000 m), a depth that considers amplification beyond the longest period of interest at the site. Table 8 lists the profiles and Table 10 shows the relative weights used in the hazard analyses, assumed equal for profiles P1 and P2.

3.1.1 Kappa

For frequencies exceeding about 1 Hz, a major constraint in motions at low loading levels is the overall shallow (1 km to 2 km) crustal damping parameterized through kappa (Anderson and Hough, 1986; EPRI, 1993; Silva and Darragh, 1995; Silva et al., 1997). Analyses of WNA recorded motions have shown average kappa values of about 0.04 s at both soft rock and deep soil sites (Anderson and Hough, 1986). At rock or very shallow soil sites, kappa has been shown to vary with rock quality or stiffness approaching 0.06 s at highly weathered soft rock sites to 0.004 s at very hard rock sites in the CENA (Silva and Darragh, 1995). Because the profile consists of about twenty thousand feet of sedimentary rock, a kappa value of 0.04 sec was assumed for the profile. This value is typical for soft rock in the WNA.

To accommodate randomness in the base case shear-wave velocity profiles, they were randomized using a model based upon an analysis of variance of about 500 measured shear-wave velocity profiles (Appendix B). Depth to hard rock was taken as 6,562 ft (2,000 m) and randomized ± 1,000 ft. This process was intended to accommodate both uncertainty in mean values as well as variability over the site area. In developing the suites of amplification factors (Section 3.3) the ensemble average motion (mean log) then reflects the best estimate ground motion and its variability (standard deviation) for that base-case profile accommodates site-specific randomness in the base case profile throughout the site.

3.2 Equivalent-Linear Properties

Generic soil G/Gmax and hysteretic damping curves were used (EPRI, 1993). These curves were intended to capture nonlinearity in shallow cohesionless and low plasticity soils, as well as nonlinearity in soft as well as firm rock. They have been validated by modeling recorded motions at soil and rock sites in western North America (Silva et al, 1997). The profile was constrained to be linear in response at depths exceeding 500 ft (Silva et al., 1996) The EPRI (1993) G/Gmax and hysteretic damping curves are shown in Figure 10. Two sets of curves were used in the site-specific analyses to capture epistemic variability (uncertainty in mean or base-case curves). One set was taken as the original EPRI (1993) suite shown in Figure 10. To consider the possibility that the local soils may behave more linearly, a subset of the EPRI (1993) curves, developed by modeling recorded motions at firm cohesionless soil sites (Silva et al., 1997), was also used for each profile. The second set, termed Peninsular Range curves (PR), use the EPRI (1993) 51 to 120 ft curves for 0 to 50 ft and the 501 to 1,000 ft curves for deeper materials. The two sets of curves were given equal weights (Table 10).

As with the shear-wave velocity profiles, the G/G_{max} and hysteretic curves were randomized (Appendix B) to accommodate aleatory variability over the site area.

3.3 Development of Transfer Functions

Transfer functions include spectral ratios (5% damping) of horizontal soil motions to hard rock motions (amplification factors). Amplification factors were computed for each soil profile for a suite of expected hard rock (reference) peak accelerations (0.01 to 1.50g; Table 9). The amplification factors were developed for the soil surface.

To approximate nonlinear soil response, for horizontal motions, an RVT based equivalent-linear approach was used (EPRI 1993; Silva et al., 1997). The approach has been validated by modeling strong ground motions recorded at over 500 sites and 19 earthquakes for a wide range in site conditions and loading levels (up to 1g) (EPRI 1993; Silva et al., 1997). Comparisons with fully nonlinear codes for loading levels up to 1g showed the equivalent-linear approach adequately captured both high- and low-frequency soil response in terms of 5% damped response spectra. The validations revealed that the equivalent-linear approach significantly underestimated durations (time domain) of high-frequency motions at high loading levels compared to both fully nonlinear analysis as well as recorded motions. However, for 5% damped response spectra the equivalent-linear approach performed as well as fully nonlinear codes and was somewhat conservative near the fundamental column resonance (EPRI 1993).

3.3.1 Site Aleatory Variability

To accommodate random fluctuations in velocity, depth to basement, G/G_{max}, and hysteretic damping values across a site, multiple realizations (30) were developed for dynamic material properties. The profile randomization scheme for shear-wave velocity is based on a variance analysis of over 500 measured shear-wave velocity profiles and varies both velocity and layer thickness (EPRI, 1993; Silva et al., 1997). The model includes a velocity distribution at depth coupled with a velocity correlation with depth. The depth correlation is intended to eliminate unnatural velocity variations at a given depth that are independent of realizations above and below. Driven by measured velocities, the correlation length (distance) increases with depth with a corresponding decrease in the velocity COV at a given depth. Profiles vary less as depth increases and become more uniform, on average.

To capture random fluctuations in modulus reduction and damping curves, values are randomized assuming a log-normal distribution consistent with shear-wave velocity and material damping (EPRI, 1993). Based on random variations in laboratory dynamic testing for soils of the same type or classification (EPRI, 1993) a σ_{ln} of 0.15 and 0.3 is used for G/G_{max} and hysteretic damping respectively. These standard deviations are taken at a cyclic shear-strain of 0.03%, where the G/G_{max} curves typically show significant reduction. Suites of curves are generated by sampling the distribution, applying the random perturbation to the base-case (initial) curve at 0.03% shear strain, and preserving the shape of the base case curve to generate an entire random curve. Bounds are placed at ± 2σ over the entire strain range to prevent nonphysical excursions.

Shear-wave damping is separately (independently) randomized following the same procedure. The randomization code can accommodate coupling or correlation of any degree (-1 to 1) between modulus reduction and hysteric damping, which is expected to occur between mean or base-case curves reflecting different material type curves. However, for random fluctuations within the same material type the correlation is likely low; that is, a randomly linear curve is not necessarily associated with a randomly low damping. Additionally, because modulus reduction is far more significant than material damping in site response (Silva, 1992), the issue is not significant.

3.3.2 Point-Source Model Parameters

The omega-square point-source model (Boore, 1983; Atkinson, 1993; Silva et al., 1997) was used to generate hard rock outcrop as well as site-specific soil motions for a range in expected hard rock peak acceleration values (0.01 to 1.50g; Table 9).

To accommodate potential effects of control motion spectral shape (magnitude) on nonlinear site response, amplification factors were computed for **M** 5.5 and **M** 7.5, based on the magnitude deaggregations (Section 2.5, Tables 7a and 7b, and Figures 7 and 8). Additionally, because large **M** CENA source processes may be significantly different than those of WNA in spectral shape, typified by an intermediate frequency spectral sag or two corner frequencies (Atkinson, 1993), transfer functions were computed for this source model as well (Tables 5 and 10). The hard rock crustal model used to generate the horizontal component reference site motions is listed on Table 9 with the remaining point-source parameters (stress drop, Δσ; Q, and kappa) also listed on Table 9.

To include the effects of the change in magnitude contributions to the reference site hazard with both structural and exceedence frequency for the site-specific UHS, indicated in the **M** deaggregations (Section 2.5), weights were assigned to the respective amplification factors according to Table 10. This weighting then accommodates potential effects of control motion spectral shape due to magnitude on the soil surface amplification factors.

3.3.3 Horizontal Amplification Factors

Horizontal amplification factors (median and sigma estimates) for 5% damped response spectra, soil surface relative to hard rock, were developed for each base-case set of properties as well as magnitude (**M**, Table 9). For **M** 7.5 amplification factors were also developed using both single- and double-corner source models (Tables 9 and 10). The base-case site properties include two profiles (P1 and P2; Figure 9, Table 8) and two sets of modulus reduction and hysteretic damping curves (EPRI, 1993 and PR, Silva et al., 1997). The site epistemic variability then comprises four sets of mean site-specific properties resulting in four sets of amplification factors for each magnitude as well as single- and double-corner source models for **M** 7.5 (Table 10). Including the three different sources results in twelve sets of amplification factors. For eleven levels of loading (0.01g to 1.50g, Table 9) and thirty realizations for each case as well as loading level results in nearly four thousand site response calculations. As previously mentioned, a fully probabilistic site-specific analysis, fully accommodating all aleatory and epistemic variability to achieve desired hazard as well as fractile levels, can result in extensive analyses.

As an example of the horizontal amplification factors, Figures 11 and 12 show median and $\pm$ 1σ estimates computed at the soil surface for profiles P1 and P2 respectively (Figure 9) with **M** 7.5 control motions (single-corner source model, Table 9) for the site using the Peninsular Range (Silva et al., 1996) G/G_{max} and hysteretic damping curves (Section 3.2). The mean depth of the profile is 6,562 ft to basement material with a shear-wave velocity of about 9,300 ft/sec (Table 9). PGA's reflect expected hard rock values ranging from 0.01g to 1.50g (Table 9). The amplification of the deep soil and soft-rock profile (Figures 11 and 12, Table 8) is apparent in the low-frequency amplification ($\leq$ 1 Hz) at all loading levels. At higher frequency the low loading levels (0.01g) show low amplification resulting from a combination of damping due to kappa (Section 3.1.1) and amplification of the deep soft rock profile along with the shallow soils. At higher loading levels, Figures 11 and 12 clearly shows the effects of nonlinearity, with high-frequency factors decreasing with increasing loading levels. For example, at 1.5g and 30 Hz, the median factors decrease to about 0.2. Such a large deamplification may represent a shortcoming of the equivalent-linear approach that reflects a frequency independent softening. However, careful validations with recorded motions at high loading levels (EPRI, 1993; Silva et al., 1997) showed no indication of equivalent-linear inadequacy in modeling overall levels of response spectra of recorded motions, particularly at high frequency. While these local particular soils were not sampled in the validations, the overall adequacy of the equivalent-linear approach has been validated for deamplification to levels approaching 0.5, which is set as a lower bound in all analyses.

3.4 Soil Surface Design Motions

Horizontal site-specific soil UHS were computed using an approach that correctly preserves the desired hazard level of the hard rock PSHA. In developing the probabilistic site-specific UHS, distributions (median and sigma estimates) of the amplification factors were integrated with the hard rock hazard curves. This process correctly accommodates the site-specific randomness (aleatory variability) of dynamic material properties across the site in the development of site-specific (soil) hazard curves (Bazzuro and Cornell, 2004; Appendix D, Approach 3). Additionally, this method properly accommodates site epistemic variability or uncertainty in mean or base-case properties, such as G/G_{max} and hysteretic damping curves, kappa values, underlying rock conditions, as well as differences in site response due to single- and double-corner source models as control motions. For each suite of base-case properties (epistemic variability), site-specific mean hazard curves were developed which properly include randomness (aleatory variability) about the base-case properties. The resultant hazard curves, one for each base-case, are then averaged over exceedence frequency resulting in a single site-specific hazard curve at each structural frequency. In the averaging process, weights were employed reflecting the likelihood of in-situ conditions for modulus reduction and hysteretic damping curves, soft rock beneath the soil (profiles P1 and P2, Figure 9), as well as source process for single- versus double-corner source models. The relative weights are listed in Table 10. Also listed in Table 10 are the magnitude distributions verses structural and exceedence frequency used in developing the site-specific UHS. As previously discussed, achievement of an accurate exceedence frequency for soil hazard requires integration of the hard rock hazard curves with the site amplification factors to exceedence frequencies significantly lower than desired for the soil (Section 3.0 and Appendix D Approach 3). For example, in developing the UHS at AEF 4 x 10^{-4}, integrations of the hard rock hazard was performed to AEF 10^{-6}. The relative weights were based on deaggregations performed at AEF 2 x 10^{-3} (Figure 7) and AEF 4 x 10^{-4} (Figure 8).

The site-specific mean 5% damped horizontal UHS developed soil for the soil surface compared to the hard rock UHS are shown in Figure 13 for AEF 2 x 10^{-3} (500 year) with the soil spectra listed in Table 11. For AEF 4 x 10^{-4} (2,475 year), the site-specific mean 5% damped horizontal UHS developed for the soil surface compared to the hard rock UHS are shown in Figure 14 with the soil spectra listed in Table 12. As with the amplification factors (Figures 11 and 12) the surface UHS reflects the low-frequency amplification of the soil and soft rock profile while the high-frequency deamplification is due largely to the damping (kappa, Section 3.1.1) in the deep soft rock profile.

3.4.1 Design Time Histories

To provide control motions for potential follow-on analyses, spectrally matched horizontal component time histories were developed for the smoothed design spectrum at the surface (top-of-soil) for AEF 2 x 10^{-3} and AEF 4 x 10^{-4}. The spectral matching approach adjusts the Fourier amplitude spectrum of an input (basis) time history such that its response spectrum matches that of a target (Silva and Lee, 1987). The resulting time history has its phase spectrum largely unaltered, preserving the nonstationarity of the basis time history as well as relative phasing between components, both of which may be important for structural analyses.

For both AEFs, the same basis time history was used (Table 13) that reflects an actual recording. To represent the range in magnitudes and distances in the deaggregations (Figures 7 and 8) as well as possible rupture distances as closely as possible, the recorded motion from the Landers earthquake listed in Table 13 was selected.

The final soil surface spectral matches as well as acceleration, velocity, and displacement time histories are shown in Figure Sets 15 and 16 for AEF 2 x 10^{-3} and 4 x 10^{-4} respectively. Each set includes the suite of three-component records. Also included are plots of spectral ratios, target over time history response spectrum, which clearly illustrate the degree of fit. Guidelines generally followed were those of the NRC (NUREG/CR-6728, ASCE 43-05) which recommend matches be within 0.9 and 1.3 of the targets from 0.2 Hz to 25.0 Hz. As the ratio plots show, the matches follow the guidelines throughout most of the frequency range.

REFERENCES

Amick, D., R. Gelinas and K. Cato (1991). "Magnitudes, locations, and return periods of large prehistoric earthquakes occurring in Coastal South Carolina." *Seis. Res. Letters*, 62(3), pp. 161.

Anderson, J.G. and J.E. Luco (1983). "Consequences of slip rate constraints on earthquake occurrence relations." *Bulletin of the Seismological Society of America*, 73, pp. 471-496.

Atkinson, G.M. and D.M. Boore (1997). "Some Comparisons Between Recent Ground Motion Relations." *Seis. Res. Lett.*, 68(1), pp. 24-40.

Atkinson, G.M and W.J. Silva (1997). "An empirical study of earthquake source spectra for California earthquakes." *Bull. Seism. Soc. Am.* 87(1), 97-113.

Bakun, W.H. and M.G. Harper (2002). The 1811-1812 New Madrid, Missouri, and the 1886 Charleston, South Carolina, earthquakes, preprint.

Bazzurro, Paolo and C.A. Cornell (2004). "Nonlinear soil-site effects in probabilistic seismic-hazard analysis." *Bulletin of Seismological Society of America*, 94(6), 2110-2123.

Bender, B. (1984). "Seismic hazard estimation using a finite-fault rupture model." *BSSA*, 74, pp. 1899-1923.

Chapman, M.C. (1998). Personal transmittal of Virginia Polytechnic Institute earthquake catalog complete through Dec. 31, 1996.

Cornell, C.A. (1968). "Engineering seismic risk analysis." *Bull. Seism. Soc. Am.*, 58, 1583-1606.

Cramer, C.H. (2001a). "The New Madrid seismic zone: capturing variability in seismic hazard analysis." *Seis. Res. Letts.*, 72(6), 664-672.

Cramer, C.H. (2001b). "A seismic hazard uncertainty analysis for the New Madrid seismic zone." *Engineering Geology*, 62, 251-266.

Electric Power Research Institute (1993). "Guidelines for determining design basis ground motions." Palo Alto, Calif: Electric Power Research Institute, vol. 1-5, EPRI TR-102293.
vol. 1: Methodology and guidelines for estimating earthquake ground motion in eastern North America.
vol. 2: Appendices for ground motion estimation.
vol. 3: Appendices for field investigations.
vol. 4: Appendices for laboratory investigations.
vol. 5: Quantification of seismic source effects.

Frankel, A., C. Mueller, T. Barnhard, D. Perkins, E.V. Leyendecker, N. Dickman, S. Hanson, and M. Hopper (1996). "National Seismic Hazard Maps: Documentation, June 1996." *U.S. Geological Survey* Open-File Report 96-532.

Hanks, T.C., and H. Kanamori (1979). "A moment magnitude scale." *J. Geophys. Res.*, 84, 2348-2350.

Hildenbrand, T.G. and D. Ravat (1997). "Geophysical setting of the Wabash valley fault system." *Seism. Res. Lett.*, 68, 567-585.

Hough, S.E., J.G. Armbruster, L. Seeber, and J.F. Hough (2000). On the Modified Mercalli intensities and magnitudes of the 1811-12 New Madrid earthquakes, J. Geophys. Res., v.105, pp 23,839-23,864.

Johnston, A. (1996). "Seismic moment assessment of stable continental earthquakes, Part 3: 1811-1812 New Madrid, 1886 Charleston, and 1755 Lisbon." *Geophys. J. Int.* vol. 125, 639-678.

Johnston, A.C., and E.S. Schweig (1996). "The enigma of the New Madrid earthquakes of 1811-1812." *Ann. Rev. Earth Planet. Sci,* 24, 339-384.

Kolata, D.R. and T.G. Hildenbrand (1997). "Structural Underpinnings and Neotectonics of the Southern Illinois Basin: An Overview." *Seism. Res. Lett.*, 68, 499-510.

Langenheim, V.E. and T.G. Hildenbrand (1997). "Commerce geophysical lineament; its source, geometry and relation to the Reelfoot Rift and New Madrid seismic zone." *Geol. Soc. Am. Bull.*, 109, 580-595.

Marple, R.T. and P. Talwani (1990). "Field investigations of the Woodstock lineament." (abs.) Program and Abstracts, 62nd Annual Meeting Eastern Section Seismological Society of America, Blacksburg, VA.

McNulty, W.E. and S.F. Obermeier (1999). "Liquefaction evidence for at least two strong Holocene Paleo-earthquakes in central and southwestern Illinois, USA." *Environmental and Engineering Geoscience* V, 133-146.

Mueller, C., M. Hopper and A. Frankel (1997). "Preparation of earthquake catalogs for the national seismic-hazard maps - contiguous 48 states." *U.S. Geological Survey* Open-File Report 97-464, 36p.

Munson, P.J., S.F. Obermeier, C.A. Munson and E.R. Hajic (1997). "Liquefaction evidence for Holocene and latest Pliestocene seismicity in the southern halves of Indiana and Illinois--A preliminary overview." *Seism. Res. Lett.* 68, 521-536.

Munson, P.J., C.A. Munson, N.K. Bleuer and M.D. Labitzke (1992). "Distribution and dating of prehistoric earthquake liquefaction in the Wabash Valley of the central U.S." *Seism. Res. Lett.*, 63, 337-342.

NRC NUREG/CR-6728 (2001). "Technical basis for revision of regulatory guidance on design ground motions: hazard- and risk-consistent ground motions spectra guidelines." Prepared for Division of Engineering Technology, Washington, DC.

Nuttli, O.W. and K.G. Brill (1981). "Earthquake source zones in the central US determined from historical seismicity in Approach to seismic zonation for siting nuclear electric power generating facilities in the eastern US." edited by N. Barstow, K.G. Brill, O.W. Nuttli, and P.W. Pomeroy, USNRC Report NUREG/CR 1577, 98-143.

Nuttli, O.W. (1979). "The Relation of Sustained Maximum Ground Acceleration and Velocity to Earthquake Intensity and Magnitude." U.S. Army Waterways Experimental Station, Vicksburg, MS., Misc. Paper S-73-1, Rept. 16.

Nuttli, O.W. and R.B. Herrmann (1978). "State-of-the-art for assessing earthquake hazards in the United States, Report 12, Credible earthquakes for the central United States." U. S. Army Corps of Engineers, Waterways Experiment Station Misc. Pap. S-73-1, 103 p.

Nuttli, O.W. (1973). "Seismic wave attenuation and magnitude relations for eastern North America." *J. Geophys. Res.*, 78, 876-885.

Obermeier, S.F. (1998). "Liquefaction evidence for strong earthquakes of Holocene and latest Pleistocene ages in the states of Indiana and Illinois, USA." *Eng. Geo. 50*, 227-254.

Obermeier, S.F., P.J. Munson, C.A. Munson, J.R. Martin, A.D. Frankel, T.L. Youd and E.C. Pond (1992). "Liquefaction evidence for strong Holocene earthquakes(s) in the Wabash Valley of Indiana-Illinois." *Seism. Res. Lett.* 63, 321-335.

Obermeier, S.F. and many others (1991). "Evidence of strong earthquake shaking in the lower Wabash Valley from prehistoric liquefaction features." *Science,* 251, 1061-1062.

Obermeier, S.F., R.B. Jacobson, J.P. Smoote, R.E. Weems, G.S. Gohn, J.E. Monroe, and D.S. Powers (1990). "Earthquake-induced liquefaction features in the coastal setting of South Carolina and in the fluvial setting of the New Madrid seismic zone." *U.S. Geological Survey*, Prof. Paper 1504, 44pp.

Petersen, M.D., A.D. Frankel, S.C. Harmsen, C.S. Mueller, K.M. Haller, R.L. Wheeler, R.L. Wesson, Y. Zeng, O. S. Boyd, D. M. Perkins, N. Luco, E. H. Field, C. J. Wills, and K. S. Rukstales (2008). "Documentation for the 2008 update of the United States National seismic hazard maps." *U.S. Geological Survey, Open-File Report* 2008-1128.

Pond, E.C. and J.R. Martin (1997). "Estimated magnitudes and ground-motion characteristics associated with prehistoric earthquakes in the Wabash Valley region of the central United States." *Seism. Res. Lett.,* 68, 611-623.

Sibol, M.S., G.A. Bollinger, and E.C. Mathena (1987). "Seismicity of the southeastern United States: July 1, 1986-December 31, 1986." *Southeastern U.S. Seismic Network Bull.*, no. 19, 64 pp.

Silva, W.J., N. Abrahamson, G. Toro, and C. Costantino (1997). "Description and validation of the stochastic ground motion model." Submitted to Brookhaven National Laboratory, Associated Universities, Inc. Upton, New York.

Silva, W.J. and R. Darragh (1995). "Engineering characterization of earthquake strong ground motion recorded at rock sites." Palo Alto, California: Electric Power Research Institute, TR-102261.

Silva, W.J. and K. Lee (1987) "WES RASCAL code for synthesizing earthquake ground motions" State-of-the-Art for Assessing Earthquake Hazards in the United States, Report 24, U.S. Army Engineers Waterways Experiment Station, Misc. Paper S-73-1.

Talwani, P., and Schaeffer, W.T. (2001). "Recurrence rates of large earthquakes in the South Carolina Coastal Plain based on paleoliquefaction data", *Journal of Geophysical Research*, 106: 6621-6642.

Toro, G.R., N.A. Abrahamson, and J.F. Schneider (1997). "Model of strong ground motions from earthquakes in Central and Eastern North America: Best estimates and uncertainties." Seismological Research Let., 68(1), 41-57.

Tuttle, M.P. and E.S. Schweig (2000). Earthquake potential of the New Madrid seismic zone, EOS, Trans. Am. Geophys. Union, v. 81, 308-309.

Wells, D.J. and K.J. Coppersmith (1994). "New empirical relationships among magnitude, rupture length, rupture width, rupture area, and surface displacement." *BSSA*, 84(4), 974-1002.

Wheeler, R.L. and C.H. Cramer (2001). "Updated seismic hazard in the southern Illinois basin-Geological and geophysical foundations." *submitted to Seism. Res. Lett.*, 2001.

Wheeler, R.L. and D.M. Perkins (2000). "Research, methodology, and applications of probabilistic seismic-hazard mapping of the central and eastern United States - Minutes of a workshop on June 13-14, 2000, at Saint Louis University." *USGS Open- File Report* 00-0390, 18 pp.

Wheeler, R.L (1997). "Boundary separating the seismically active Reelfoot Rift from the sparsely seismic Rough Creek graben, Kentucky and Illinois." *Seism. Res. Lett.*, 68, 586-598.

Table 1
Seismicity Parameters For Non-Characteristic Background Source Areas

	Area km^2	a	b	Mmax	
				m_{blg}	**M**
1 SE Missouri, W Illinois	53,000	3.00	0.96	6.50	6.50
2 S Illinois, S Indiana (Wabash Valley)	92,110	2.95	0.96	6.50	6.50
3 E. Indiana, S Ohio, NE Kentucky	91,880	2.38	0.96	6.50	6.50
4 Iowa, N Illinois, N. Indiana, N Ohio	331,474	2.62	0.96	6.50	6.50
5 Missouri, Arkansas, Mississippi, Tenn	408,384	2.82	0.96	6.50	6.50
NM New Madrid	6,773	3.13	0.96	6.50	6.50
Reelfoot Rift	34,580	2.79	0.96	6.50	6.50
Rough Creek	12,800	2.09	0.96	7.162	7.50
Anna, Ohio	4,843	2.32	0.96	6.50	6.50
Piedmont	35,648	0.468	0.84	7.162	7.50
SA Southern Appalachian Zone	75,715	2.42	0.84	7.162	7.50
ETN Eastern Tennessee Seismic Zone	37,345	2.72	0.90	7.162	7.50
AL Alabama	52,466	1.80	0.84	7.162	7.50

Table 2a.

b-Value Used For The Non-Uniform Hazard Model

b-Value	Weight
0.95	1.00

Table 2b.

Mmax Used For The Non-Uniform Hazard Model

Mmax (Mw)	Weight
7.5	1.00

Table 3
Finite Fault Parameters For New Madrid Scenarios

Fault	b-value	Min Mag	Max Mag (Wt)	Recurrence Period[1] (years) (Wt)
Scenario 3-1	0.96	6.5	7.0 (0.33) 7.5 (0.34) 8.0 (0.33)	458 (0.9) 1,000 (0.1)
Scenario 3-2	0.96	6.5	7.0 (0.33) 7.5 (0.34) 8.0 (0.33)	458 (0.9) 1,000 (0.1)
Scenario 3-3	0.96	6.5	7.0 (0.33) 7.5 (0.34) 8.0 (0.33)	458 (0.9) 1,000 (0.1)
Scenario 6-1	0.96	6.5	7.0 (0.33) 7.5 (0.34) 8.0 (0.33)	458 (0.9) 1,000 (0.1)
Scenario 6-2	0.96	6.5	7.0 (0.33) 7.5 (0.34) 8.0 (0.33)	458 (0.9) 1,000 (0.1)
Scenario 6-3	0.96	6.5	7.0 (0.33) 7.5 (0.34) 8.0 (0.33)	458 (0.9) 1,000 (0.1)
Scenario 6-4	0.96	6.5	7.0 (0.33) 7.5 (0.34) 8.0 (0.33)	458 (0.9) 1,000 (0.1)
Scenario 6-5	0.96	6.5	7.0 (0.33) 7.5 (0.34) 8.0 (0.33)	458 (0.9) 1,000 (0.1)
Scenario 6-6	0.96	6.5	7.0 (0.33) 7.5 (0.34) 8.0 (0.33)	458 (0.9) 1,000 (0.1)

---

[1] Note that recurrence rate was equally divided between the faults in each of the New Madrid scenarios.

Table 4
Alternate Characteristic Magnitudes Considered For The Charleston Source

Source	Magnitude (Mw)	Weight
Charleston Zone	7.5	0.15
	7.3	0.45
	7.1	0.20
	6.8	0.20

Table 5

Hard Rock Ground Motion Attenuation Models Used In This Study

Model	Stress Drop (Bars)	Weight
Single Corner	Variable – medium (120)	0.24
	Variable – low (60)	0.08
	Variable – high (240)	0.08
Single Corner	Constant – medium (120)	0.12
	Constant – low (60)	0.04
	Constant – high (240)	0.04
Single Corner	Constant with saturation– medium (120)	0.12
	Constant with saturation– low (60)	0.04
	Constant with saturation– high (240)	0.04
Double Corner	N/A	0.20

Table 6a

Uniform Hazard Spectral Acceleration (G's) For 10% Probability Of Exceedances In 50 Years (AEF 2 x 10^{-3}); Hard Rock Site Conditions

Frequency (Hz)	10% Exceedance (g's)
.100	.00700
.200	.00203
.333	.00428
.500	.00669
.625	.00814
1.000	.01000
1.333	.01285
2.000	.01601
2.500	.01942
3.333	.02197
5.000	.02911
6.667	.03231
10.000	.03841
14.286	.03967
25.000	.03868
50.000	.03582
100.000 (PGA)	.01785

Table 6b

Uniform Hazard Spectral Acceleration (G's) For 2% Probability Of Exceedances In 50 Years (AEF 4 x 10^{-4}); Hard Rock Site Conditions

Frequency (Hz)	2% Exceedance (g's)
.100	.00307
.200	.00777
.333	.01380
.500	.02116
.625	.02533
1.000	.02945
1.333	.03866
2.000	.04851
2.500	.05828
3.333	.06604
5.000	.08998
6.667	.10341
10.000	.12491
14.286	.13203
25.000	.13532
50.000	.13172
100.000 (PGA)	.06063

Table 7a

Earthquake Hazard Disaggregation
Mean Magnitude And Distance For PGA And 1-Hz
10% Probability Of Exceedance In 50 Years

POE in 50 yrs	Frequency(Hz)	Mag (M)	Distance (km)
10%	PGA (100.0)	6.31	227.48
10%	1.0	6.98	385.22

Table 7b

Earthquake Hazard Disaggregation
Mean Magnitude And Distance For PGA And 1-Hz
2% Probability Of Exceedance In 50 Years

POE in 50 yrs	Frequency(Hz)	Mag (M)	Distance (km)
2%	PGA (100.0)	6.15	111.69
2%	1.0	7.07	295.35

Table 8
Base Case Shear-Wave Velocity Profiles

Profile 1		Profile 2	
Thickness (ft)	Shear-Wave Velocity (ft/sec)	Thickness (ft)	Shear-Wave Velocity (ft/sec)
10.0	500.0	10.0	500.0
20.0	700.0	20.0	700.0
49.25	850.0	49.25	850.0
70.0	1200.0	20.8	1200.0
50.0	1600.0	6.0	1551.9
25.0	2200.0	13.0	1801.9
25.0	2212.0	11.0	1981.9
30.0	2223.0	20.0	2181.9
20.0	2238.3	18.0	2421.9
20.0	2251.4	29.0	2621.9
20.0	2264.5	55.0	2781.9
20.0	2273.3	68.0	2981.9
20.0	2282.0	100.0	3151.9
20.0	2290.8	82.0	3224.0
20.0	2299.5	85.0	3281.0
20.0	2308.3	91.9	3367.8
20.0	2317.0	67.3	3403.1
20.0	2325.8	96.5	3458.0
20.0	2334.5	98.8	3521.6
20.0	2343.3	86.6	3587.7
20.0	2352.0	160.0	3664.5
20.0	2360.8	100.0	3822.6
20.0	2369.5	100.0	3894.4
20.0	2378.3	100.0	3937.2
20.0	2387.0	100.0	4002.8
20.0	2395.8	100.0	4068.4
20.0	2404.5	100.0	4134.1
20.0	2413.3	100.0	4199.7
10.0	2417.7	100.0	4265.3
40.0	2435.2	100.0	4330.9
40.0	2452.7	100.0	4396.5
40.0	2470.2	100.0	4429.4
40.0	2487.7	100.0	4495.0
40.0	2505.2	100.0	4560.6
40.0	2522.7	100.0	4626.2
40.0	2540.2	100.0	4691.8
40.0	2557.7	75.0	4757.5
40.0	2575.2	500.0	4921.5

Table 8
Base Case Shear-Wave Velocity Profiles (continued)

Profile 1		Profile 2	
Thickness (ft)	Shear-Wave Velocity (ft/sec)	Thickness (ft)	Shear-Wave Velocity (ft/sec)
40.0	2592.7	500.0	5249.6
40.0	2610.2	500.0	5577.7
40.0	2627.7	500.0	5905.8
40.0	2645.2	500.0	6233.9
100.0	2688.9	1300.0	6562.0
100.0	2732.7		9285.0 *
100.0	2776.4		
100.0	2820.2		
100.0	2863.9		
100.0	2907.7		
100.0	2951.5		
100.0	2995.2		
100.0	3038.9		
80.0	3082.7		
4773.0	3281.0		
	9285.0 *		

* Hard rock half space (2.83 km/sec)

Table 9
Point Source Parameters

M 5.5, M 7.5 1c, M 7.5 2c

G(g)	Distance (km)			Depth (km)		
1.50	0.00	3.99	7.28	2.40	8.00	8.00
1.25	0.00	7.26	9.70	2.90	8.00	8.00
1.00	0.00	10.52	12.70	3.60	8.00	8.00
0.75	0.00	14.49	17.58	4.70	8.00	8.00
0.50	0.00	22.32	26.01	6.70	8.00	8.00
0.40	2.00	27.46	30.83	8.00	8.00	8.00
0.30	6.50	34.22	39.66	8.00	8.00	8.00
0.20	12.50	47.13	53.00	8.00	8.00	8.00
0.10	23.00	81.00	92.00	8.00	8.00	8.00
0.05	38.00	144.00	157.00	8.00	8.00	8.00
0.01	115.00	427.00	410.00	8.00	8.00	8.00

Notes:
1c = single corner source model (Boore, 1983; Silva et al., 1997)
2c = double corner source model (Atkinson and Boore, 1997)
$Q = 670 f^{0.33}$
$\Delta\sigma$ (1c) = 110 bars
κ = 0.006 sec, hard rock

Hard Rock Crustal Model (EPRI, 1993)

th (km)	V_s (km/sec)	V_p (km/sec)	ρ (cgs)
1	2.83	4.90	2.52
11	3.52	6.10	2.71
28	3.75	6.50	2.78
	4.62	8.00	3.35

Table 10
Weights
Amplification Factors

	(AEF 2 x 10^{-3})		**(AEF 4 x 10^{-4})**	
Frequency (Hz)	Weights		Weights	
	M 5.5	**M** 7.5	**M** 5.5	**M** 7.5
0.10	0.10	0.90	0.00	1.00
0.20	0.10	0.90	0.00	1.00
0.33	0.10	0.90	0.00	1.00
0.50	0.20	0.80	0.15	0.85
0.62	0.20	0.80	0.15	0.85
1.00	0.30	0.70	0.30	0.70
1.33	0.375	0.70	0.30	0.70
2.00	0.375	0.625	0.45	0.55
2.50	0.45	0.625	0.45	0.55
3.33	0.45	0.55	0.60	0.40
5.00	0.45	0.55	0.60	0.40
6.67	0.50	0.50	0.60	0.40
10.0	0.50	0.50	0.65	0.35
14.29	0.50	0.50	0.65	0.35
25	0.50	0.50	0.65	0.35
50	0.50	0.50	0.70	0.30
100	0.50	0.50	0.70	0.30

Source Model

Single Corner	0.8
Double Corner	0.2

Profiles

Profile	Weight
P1	0.5
P2	0.5

Modulus Reduction and Hysteretic Damping Curves

Curves	Weights
EPRI	0.5
Peninsular Range	0.5

Table 11
Uniform Hazard Spectral Acceleration (G's)
For 10% Probability Of Exceedence In 50 Years (AEF 2 x 10^{-3}):
Horizontal, Surface (Top-of-Soil)

Frequency (Hz)	Soil Surface
.10000E+00	.17964E-02
.20000E+00	.48080E-02
.33333E+00	.10795E-01
.50000E+00	.17397E-01
.62500E+00	.21474E-01
.10000E+01	.34198E-01
.13333E+01	.50782E-01
.20000E+01	.57573E-01
.25000E+01	.60076E-01
.33333E+01	.61213E-01
.50000E+01	.80778E-01
.66667E+01	.79105E-01
.10000E+02	.71164E-01
.14286E+02	.62356E-01
.25000E+02	.54517E-01
.50000E+02	.40540E-01
.10000E+03	.40540E-01

Table 12
Uniform Hazard Spectral Acceleration (G's)
For 2% Probability Of Exceedence In 50 Years (AEF 4 x 10^{-4}):
Horizontal, Surface (Top-of-Soil)

Frequency (Hz)	Soil Surface
.10000E+00	.80241E-02
.20000E+00	.18602E-01
.33333E+00	.36946E-01
.50000E+00	.56764E-01
.62500E+00	.68596E-01
.10000E+01	.10657E+00
.13333E+01	.15543E+00
.20000E+01	.16613E+00
.25000E+01	.17319E+00
.33333E+01	.18068E+00
.50000E+01	.22871E+00
.66667E+01	.22319E+00
.10000E+02	.18666E+00
.14286E+02	.15283E+00
.25000E+02	.11849E+00
.50000E+02	.99921E-01
.10000E+03	.99921E-01

Table 13
Basis Time History Used In Spectra Matches

Earthquake Name	Date	**M**	Station Name	Component	Site	Rupture Distance (km)
Landers, Ca	June 1992	7.3	17852 Serrano Avenue, Village Park, CA	270 degrees	Deep Soil	133

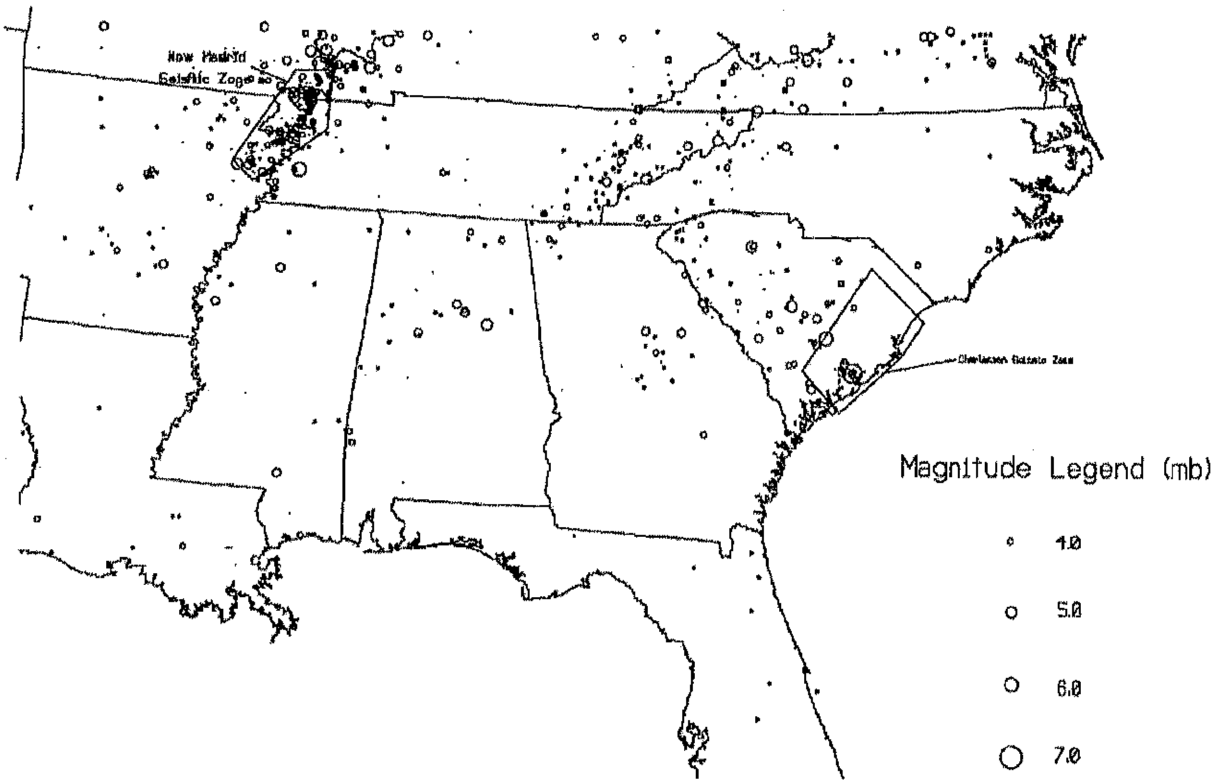

Figure 1. Historic and instrumental seismicity for the CEUS (Chapman, 1998). All magnitudes are mblg, either measured or inferred from Modified Mercalli Intensities of historic earthquakes. One of the four Charleston seismic zones used in this study is shown.

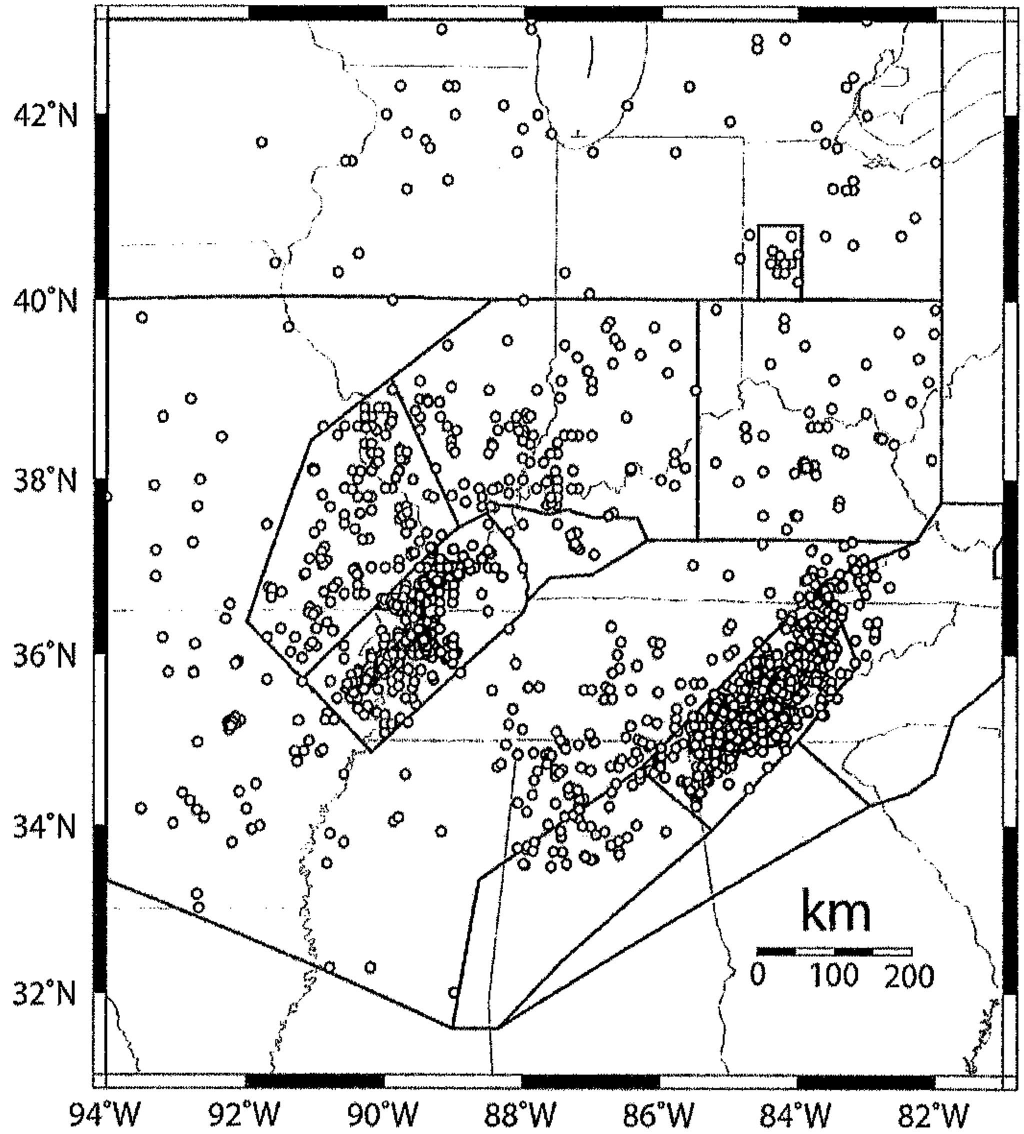

Figure 2. Circles indicate the epicenters of earthquakes with magnitudes greater than 3.0 contained in the USGS catalog for eastern North America (Mueller et al., 1997) (*http://geohazards.cr.usgs.gov/eq/html/catdoc.html*).

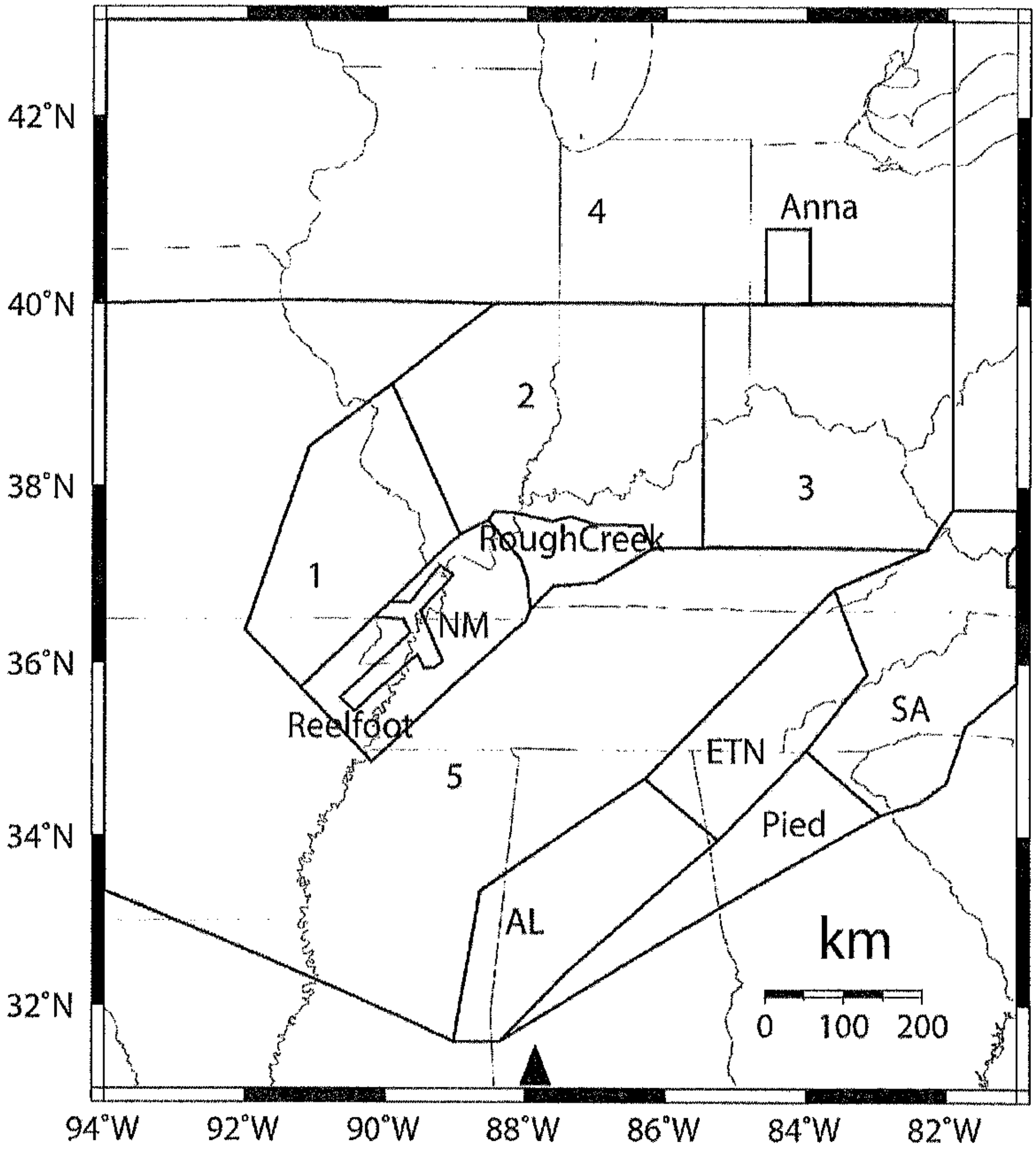

Figure 3. Source areas defined for non-characteristic events are indicated by the polygons. The triangle indicates the project location.

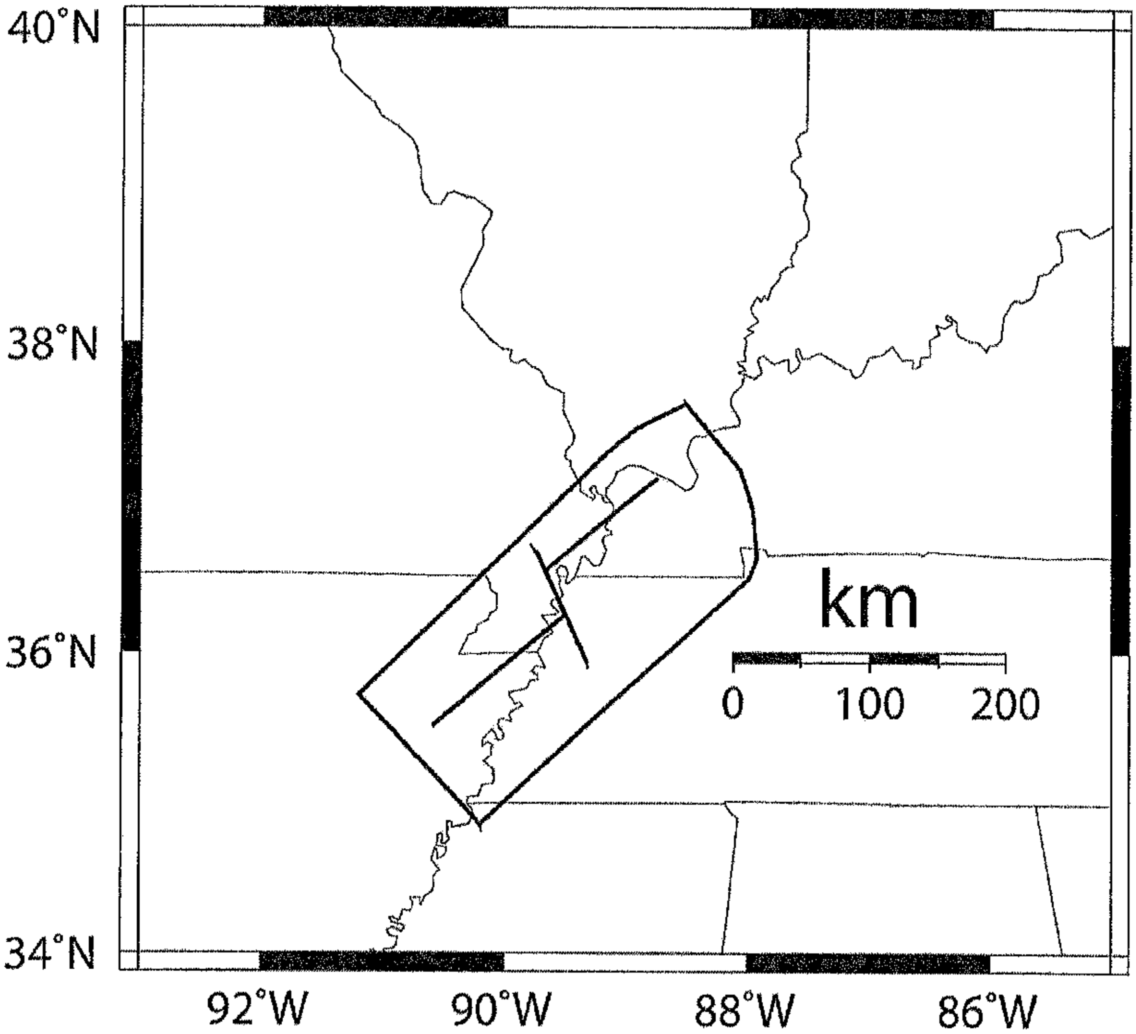

Figure 4. Characteristic earthquake source scenario for the New Madrid seismic zone involving three fault segments (Table 3).

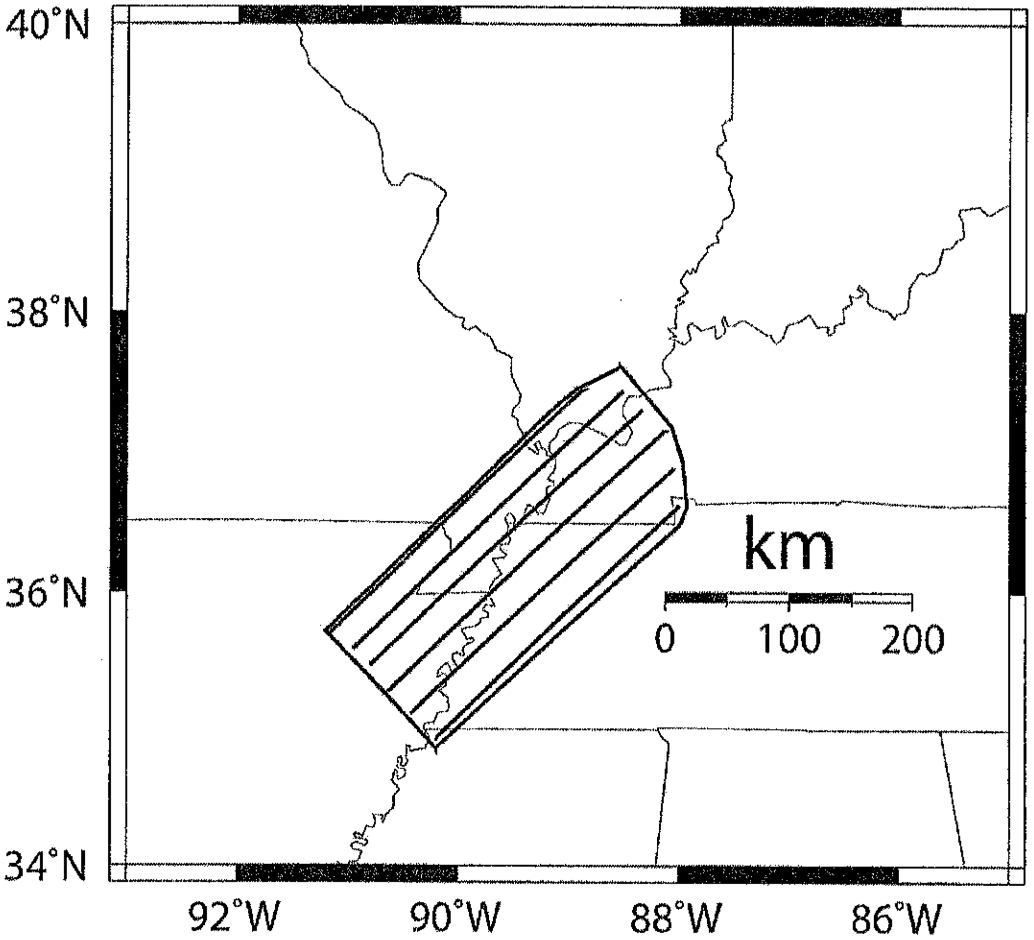

Figure 5. Characteristic earthquake source scenario for the New Madrid seismic zone involving 6 fault segments (Table 3).

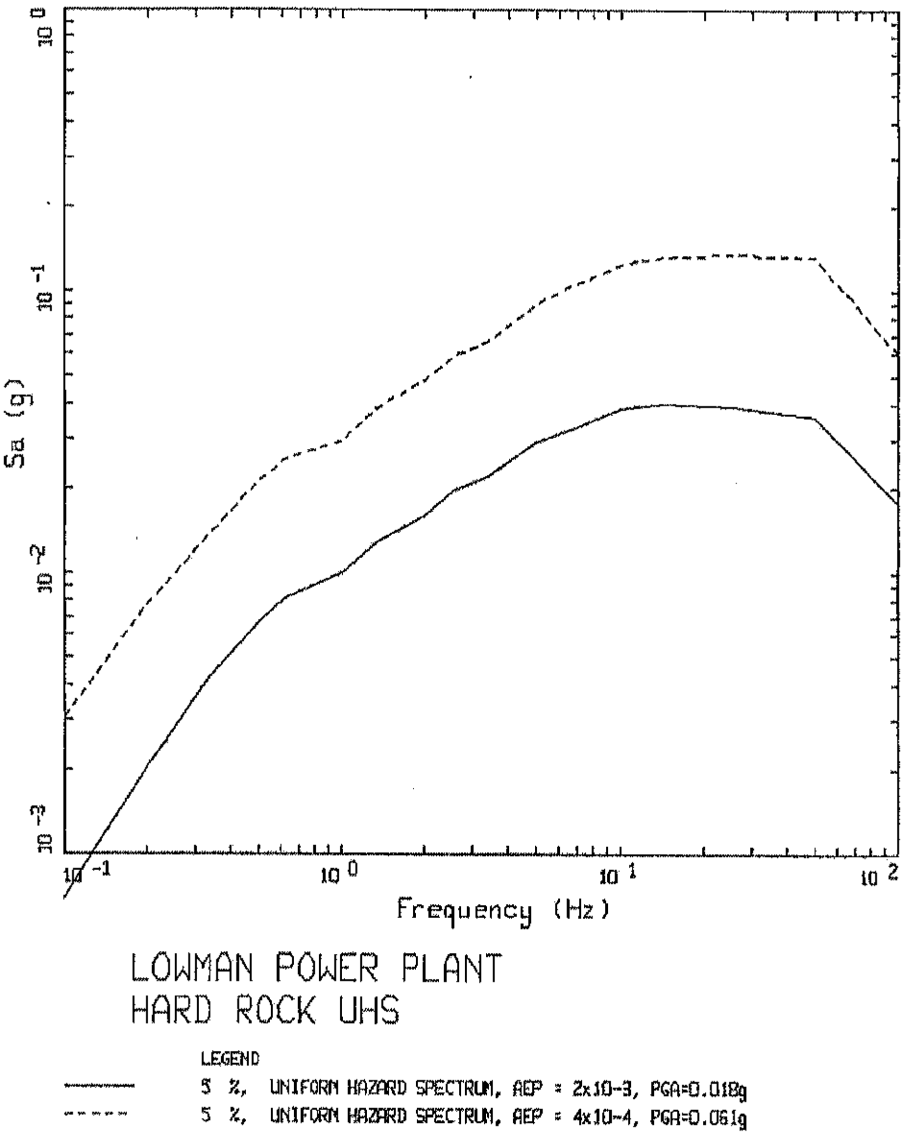

Figure 6. Hard rock horizontal component mean UHS computed at the Lowman Power Plant Site (Tables 6a and 6b) for AEF 4 x 10^{-4} (2,500 yrs), and AEF 2 x 10^{-3} (500 yrs).

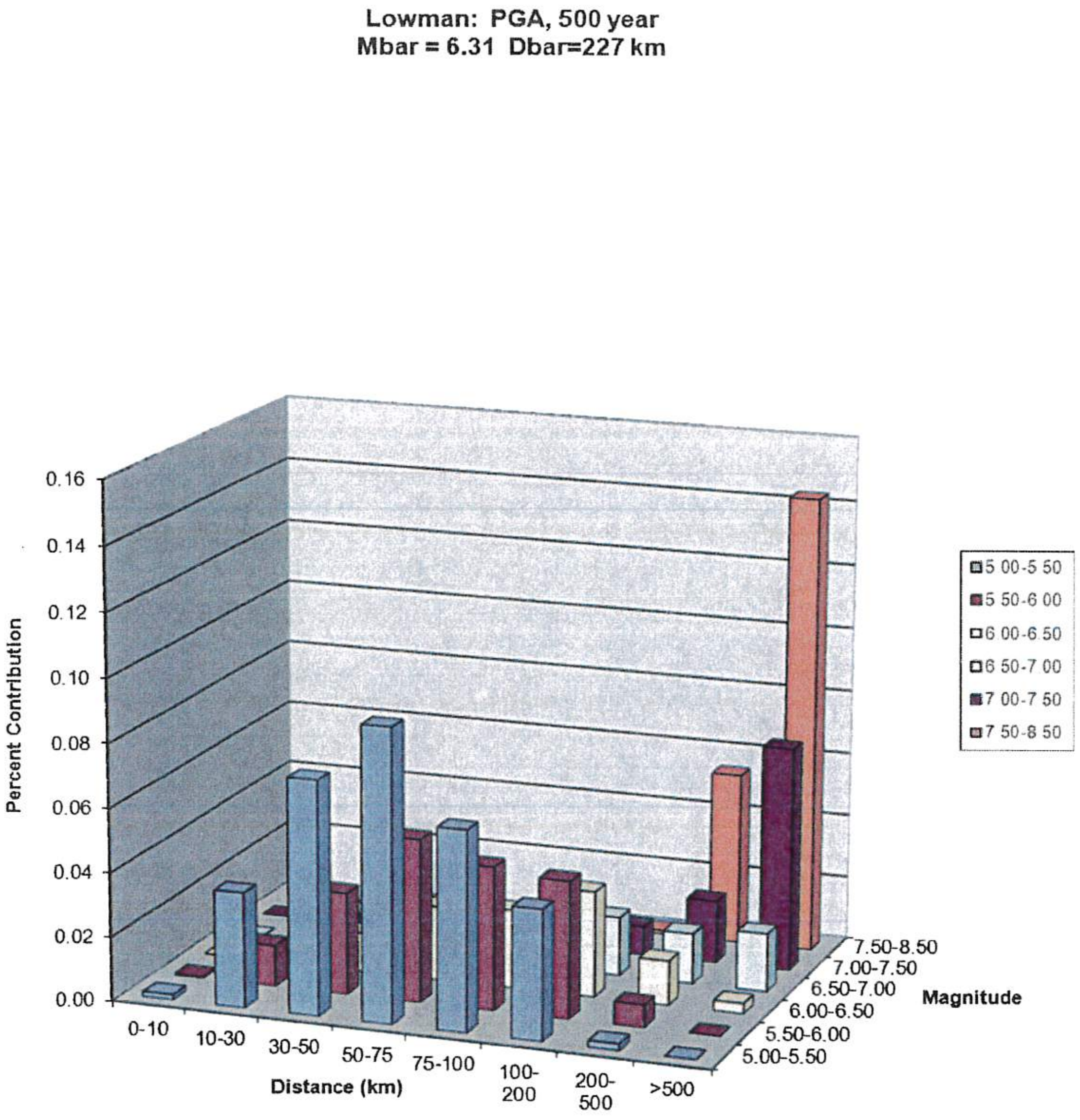

Figure 7. Magnitude and distance disaggregation at AEF 2 x 10^{-3} (500 yrs) for structural frequencies 100.0 Hz (PGA) and 1.0 Hz at the Lowman Power Plant Site.

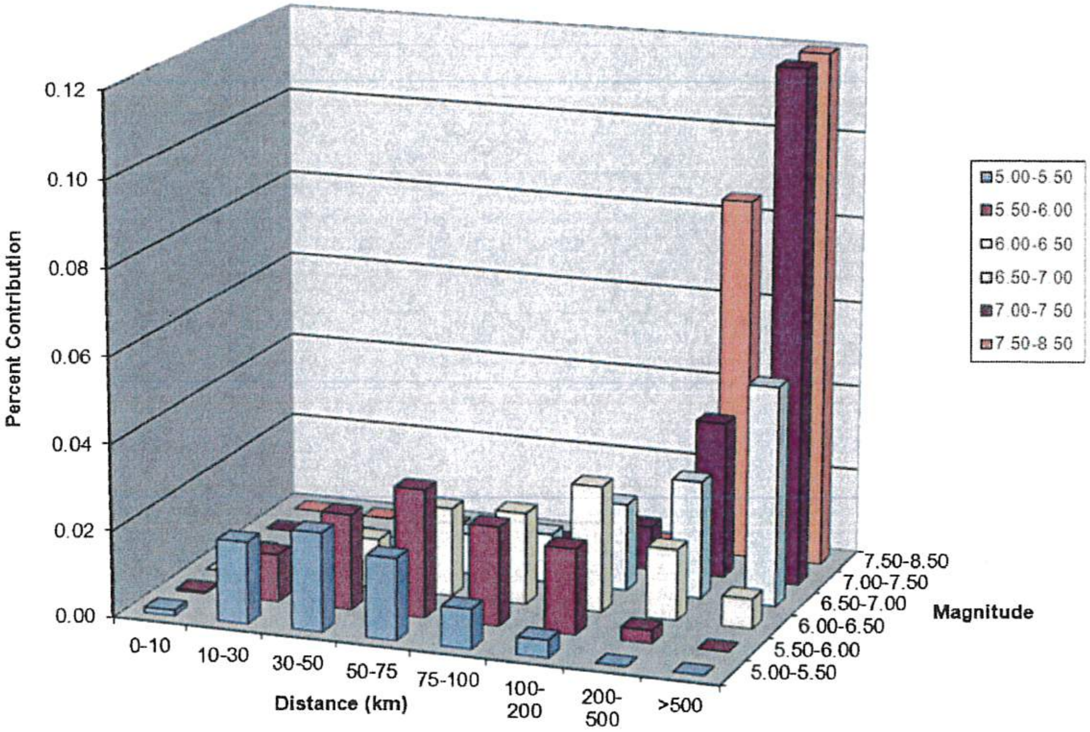

Lowman T=1.0sec, 500 year
Mbar = 6.98 Dbar = 385 km

Figure 7. (cont.)

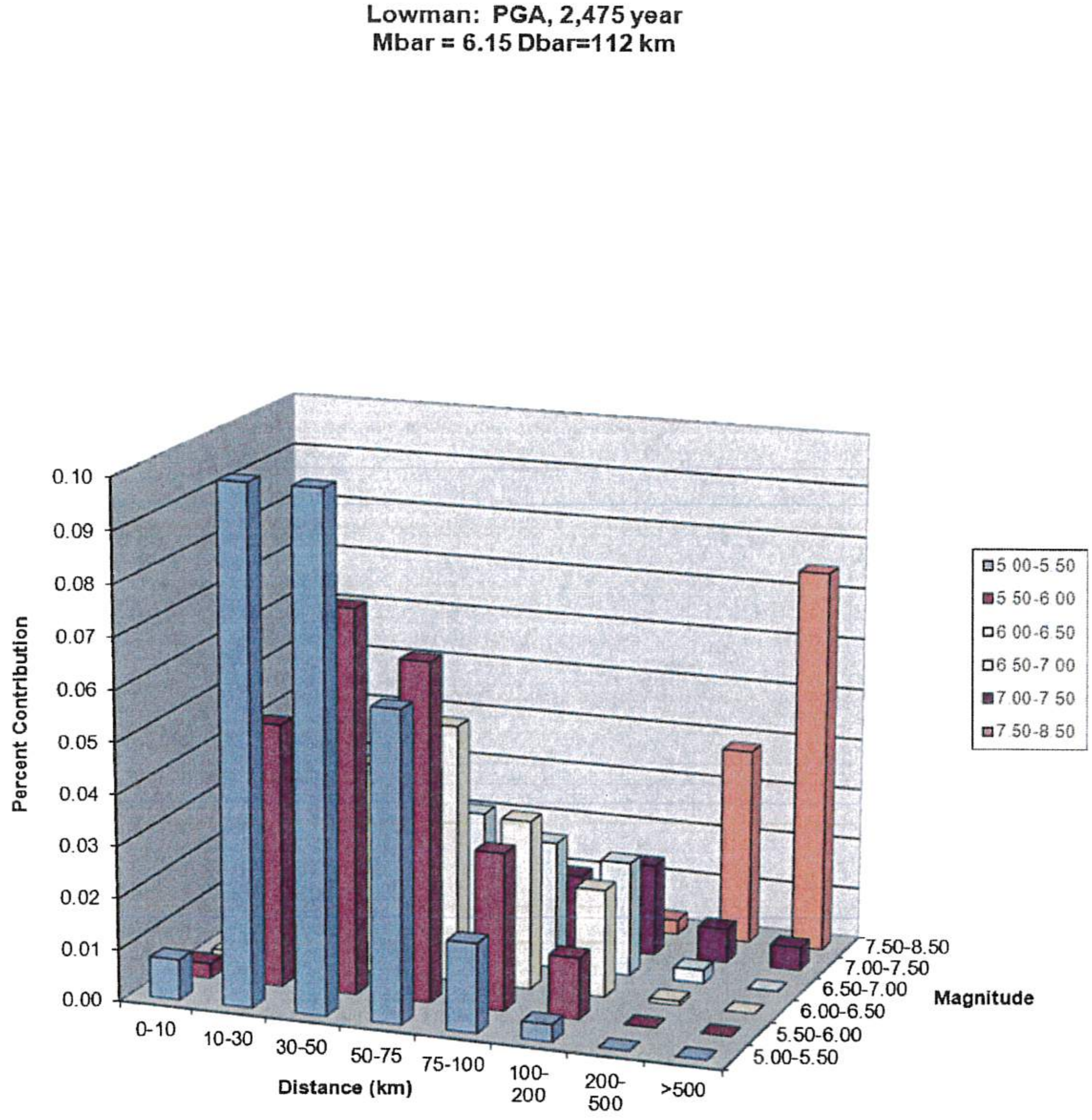

Figure 8. Magnitude and distance disaggregation at AEF 4 x 10^{-4} (2,500 yrs) for structural frequencies 100.0 Hz (PGA) and 1.0 Hz at the Lowman Power Plant Site.

Lowman T=1.0sec, 2,475 year
Mbar = 7.07 Dbar = 295 km

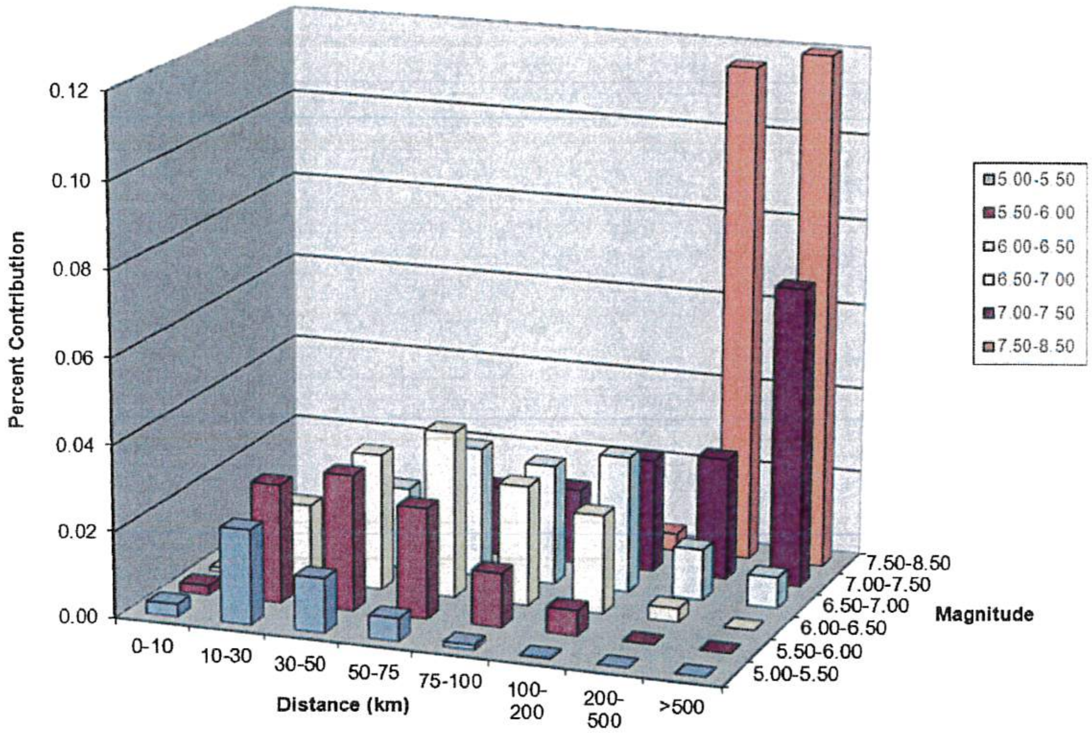

Figure 8 (cont.)

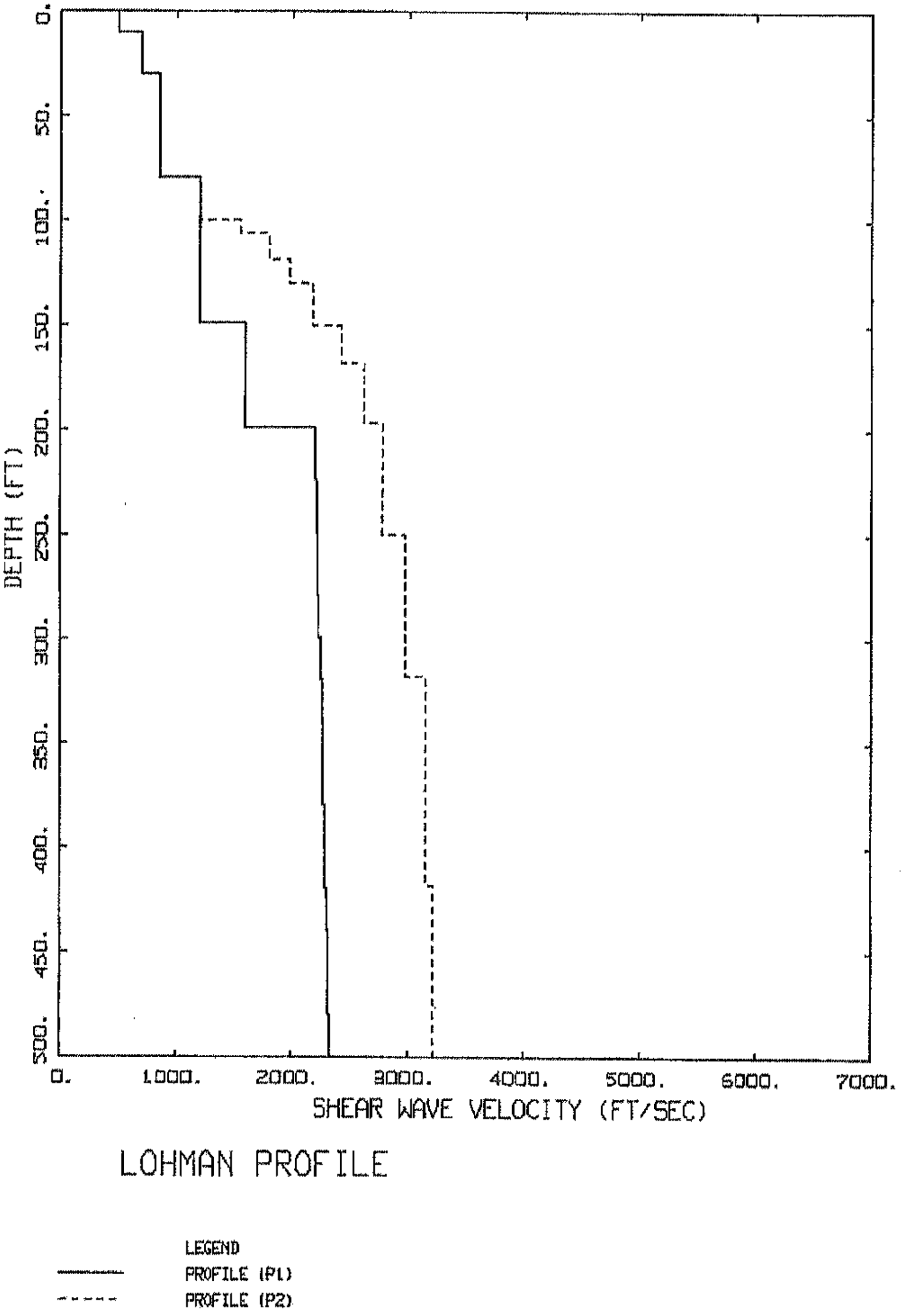

Figure 9. Shear-wave velocity profiles used in the analyses. Profiles (P1 and P2) consist of about 6,500 feet (2,000m) of soils and soft rock above crystalline basement.

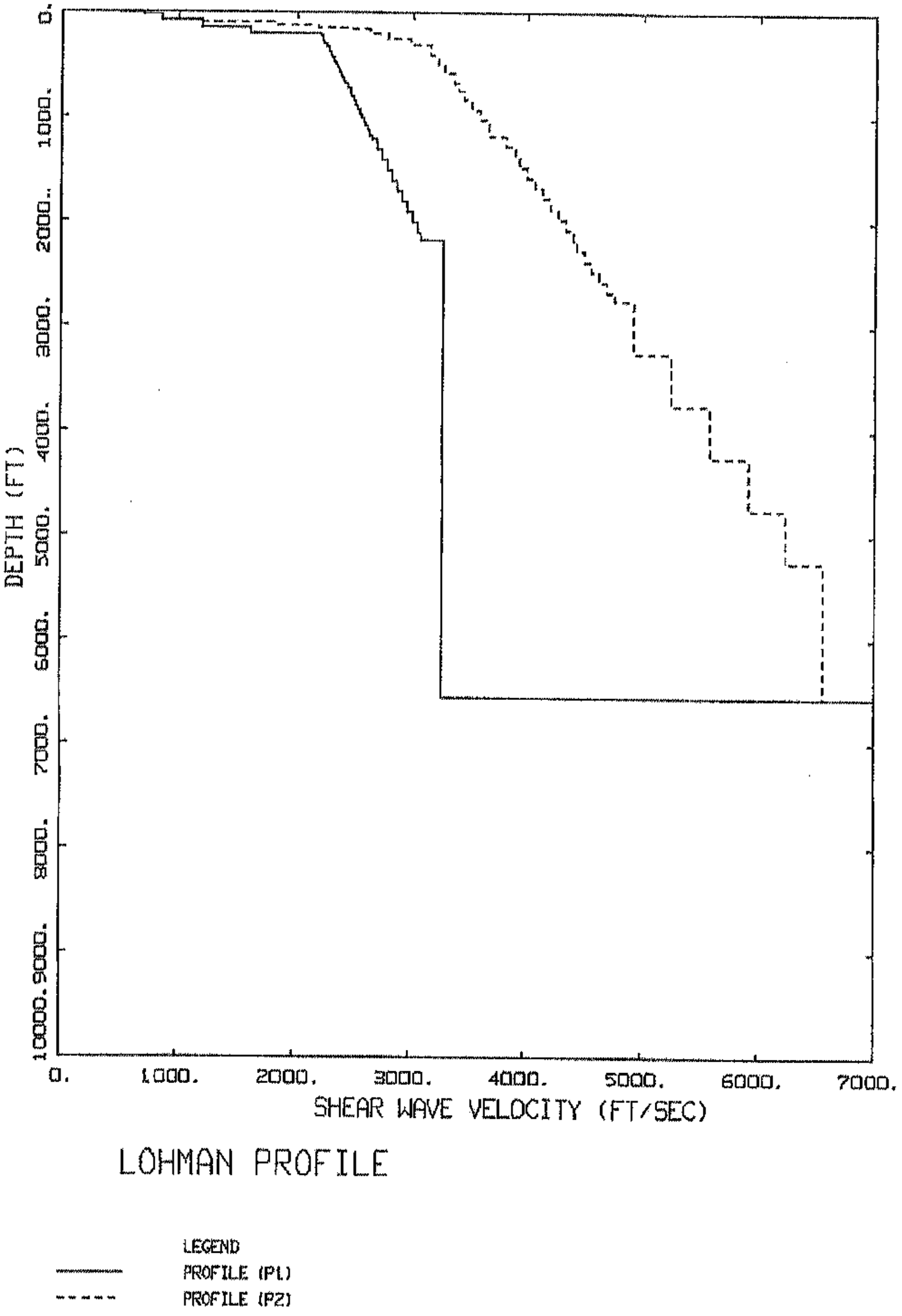

Figure 9. (cont.)

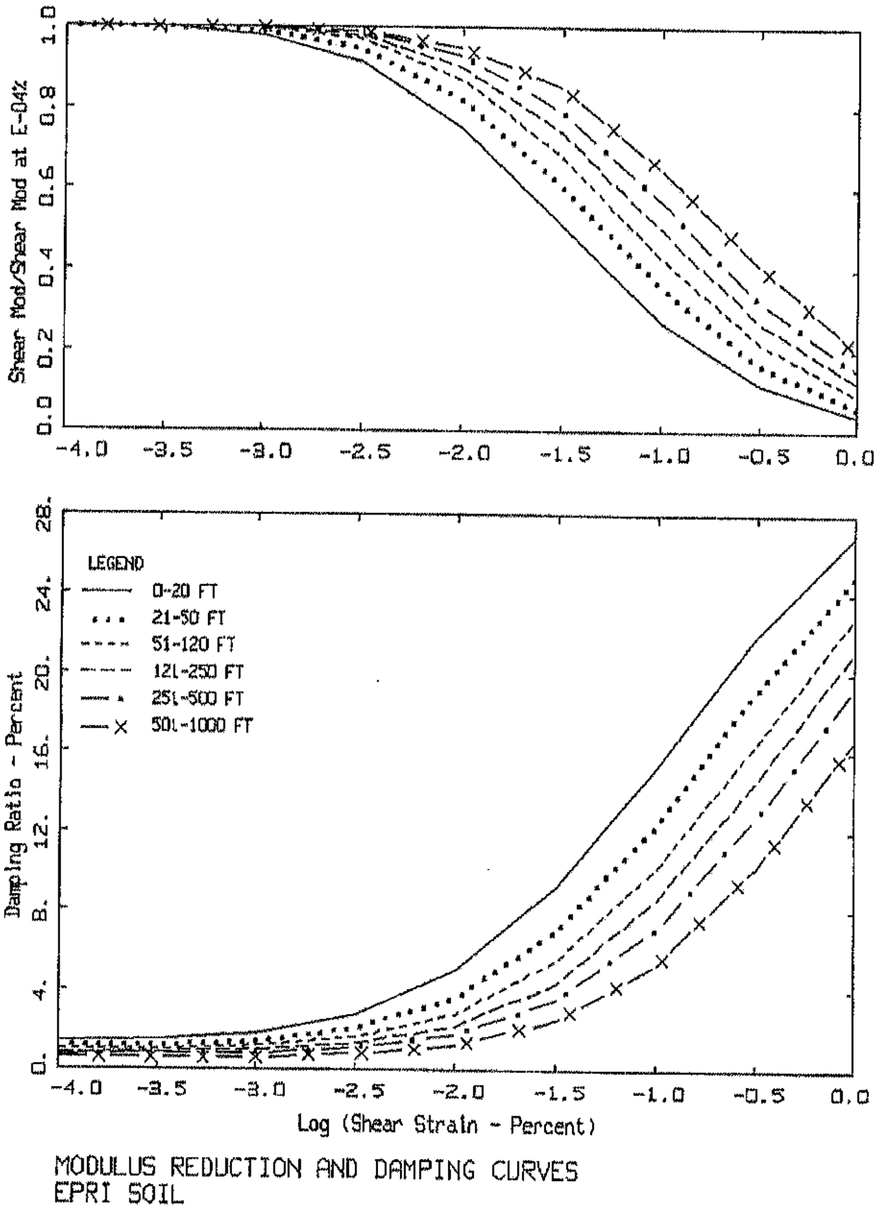

Figure 10. Generic G/Gmax and hysteretic damping curves for cohesionless soil (EPRI, 1993).

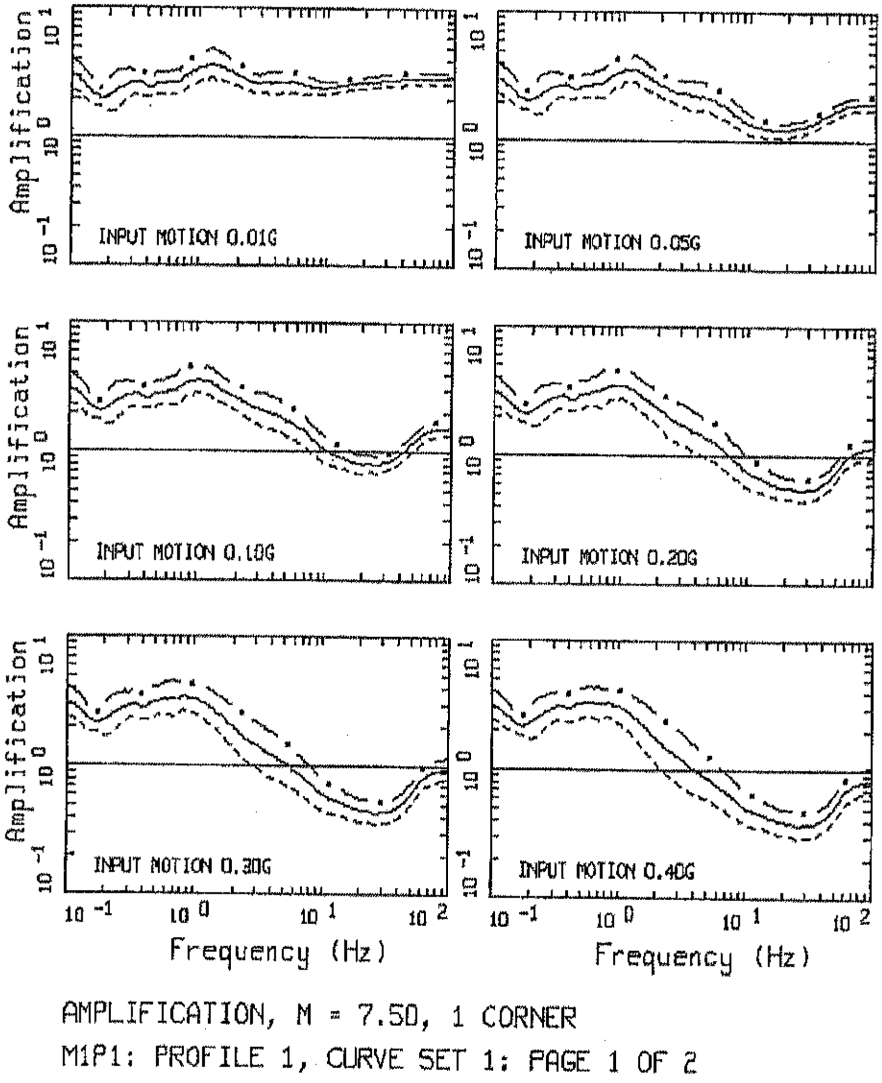

Figure 11. Example plot of median and ± 1 sigma amplification factors computed for the Lowman Power Plant profile P1 (Figure 9) with M = 7.5, single corner frequency source model, and Peninsular Range (PR) G/G_{max} and hysteretic damping curves. Distances were adjusted to obtain the target hard rock median peak acceleration values: Surface motions.

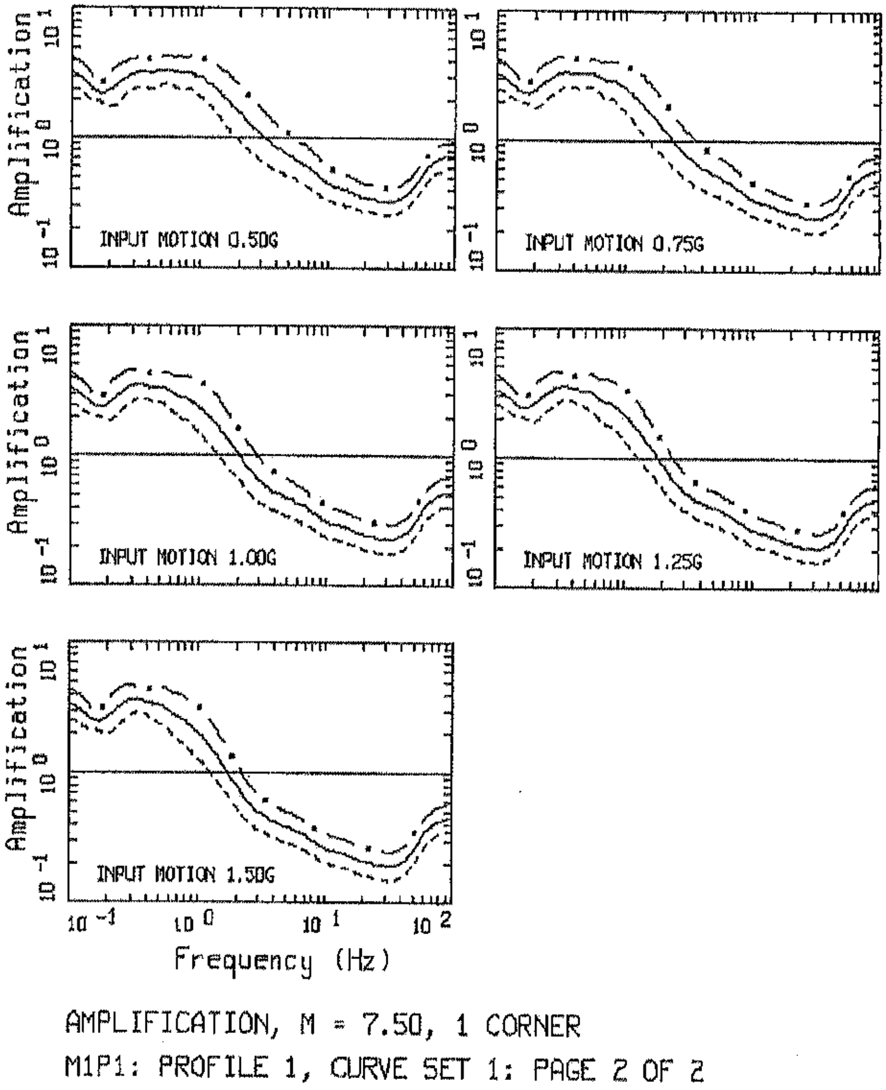

Figure 11. (cont.)

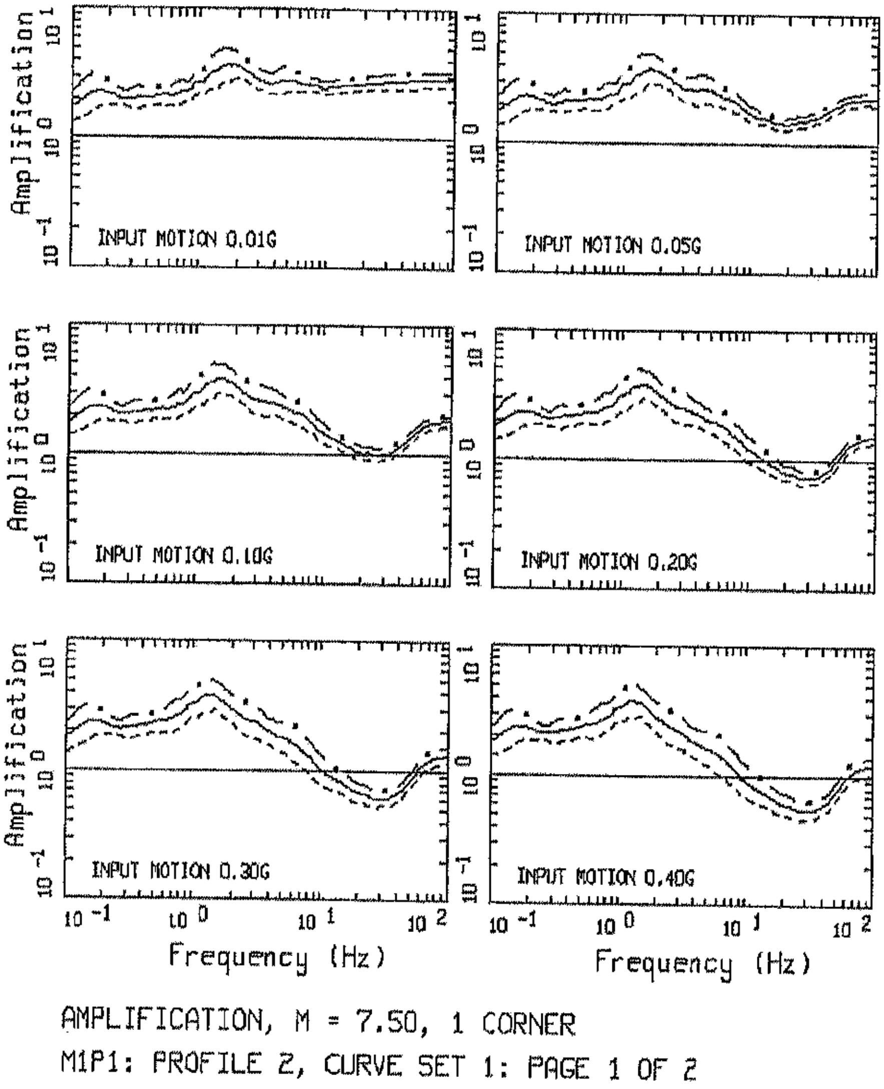

Figure 12. Example plot of median and ± 1 sigma amplification factors computed for the Lowman Power Plant profile P2 (Figure 9) with M = 7.5, single corner frequency source model, and Peninsular Range (PR) G/G_{max} and hysteretic damping curves. Distances were adjusted to obtain the target hard rock median peak acceleration values: Surface motions.

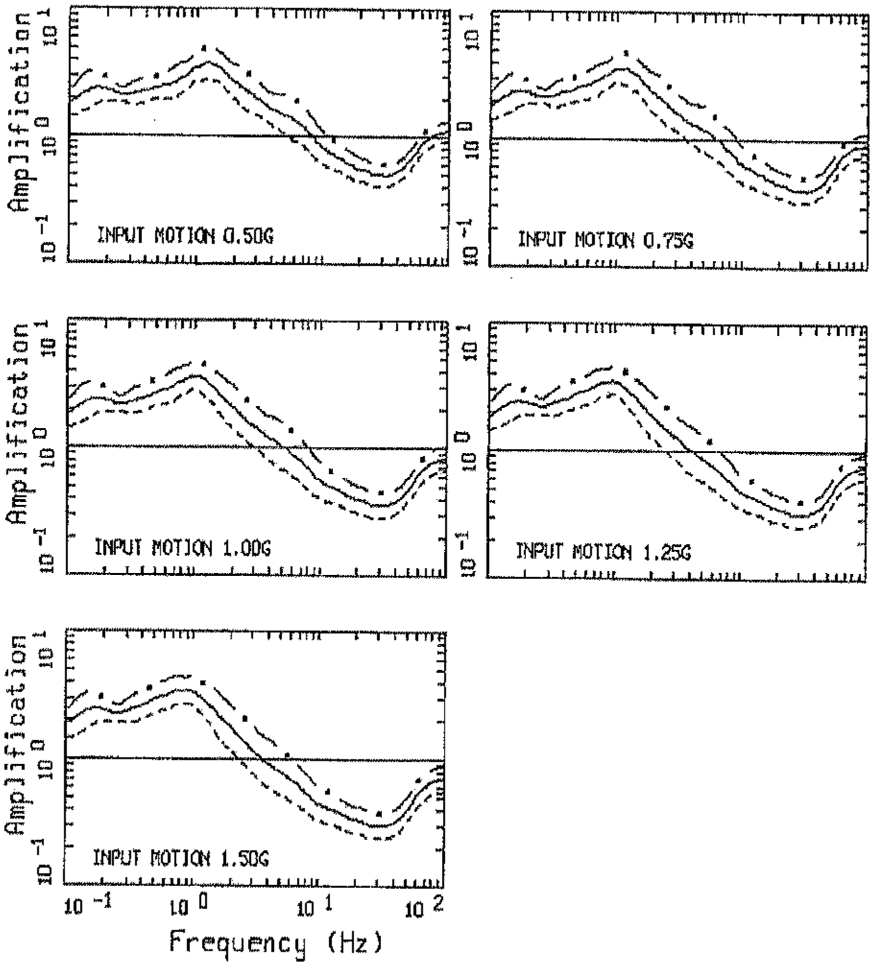

AMPLIFICATION, M = 7.50, 1 CORNER
M1P1: PROFILE 2, CURVE SET 1: PAGE 2 OF 2

Figure 12. (cont.)

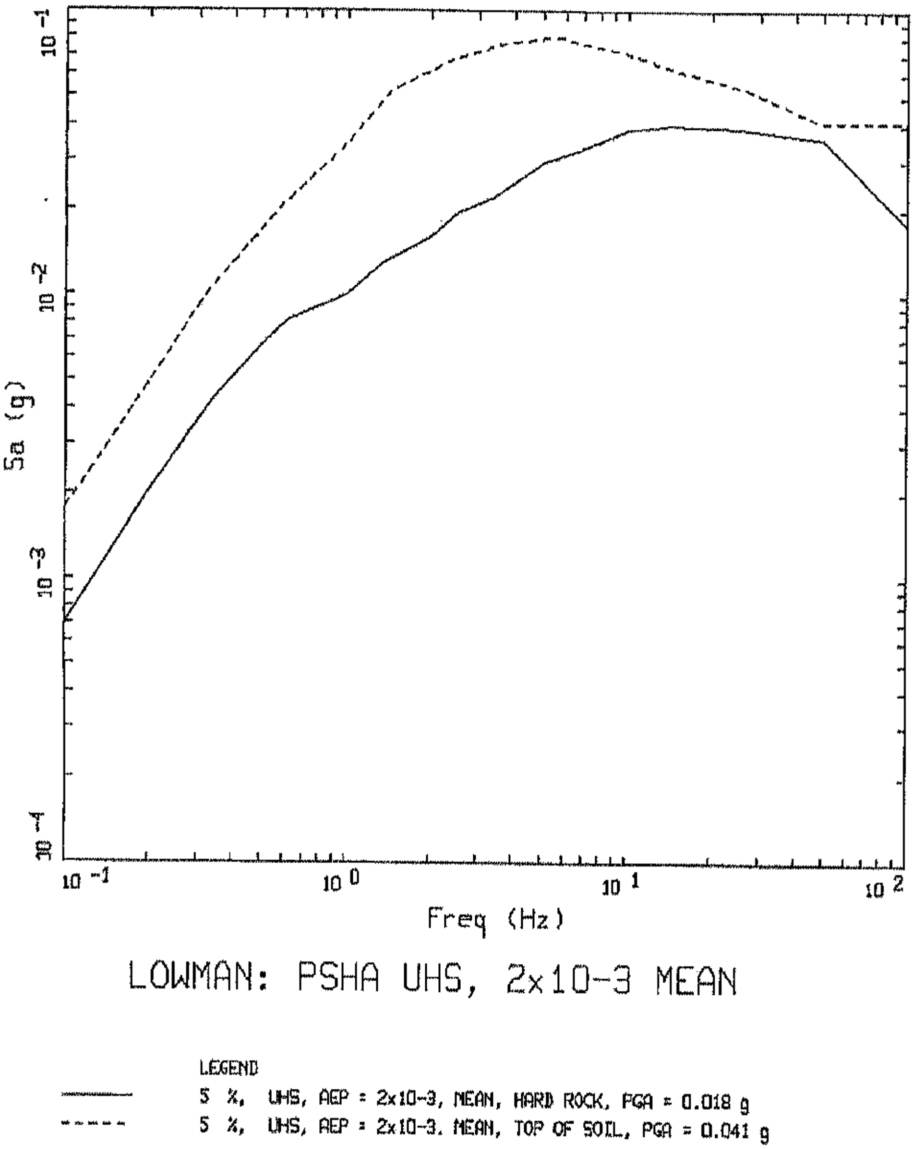

Figure 13. Comparison of site-specific soil UHS (top-of-soil) with the hard rock UHS, logarithmic and linear Sa axes.

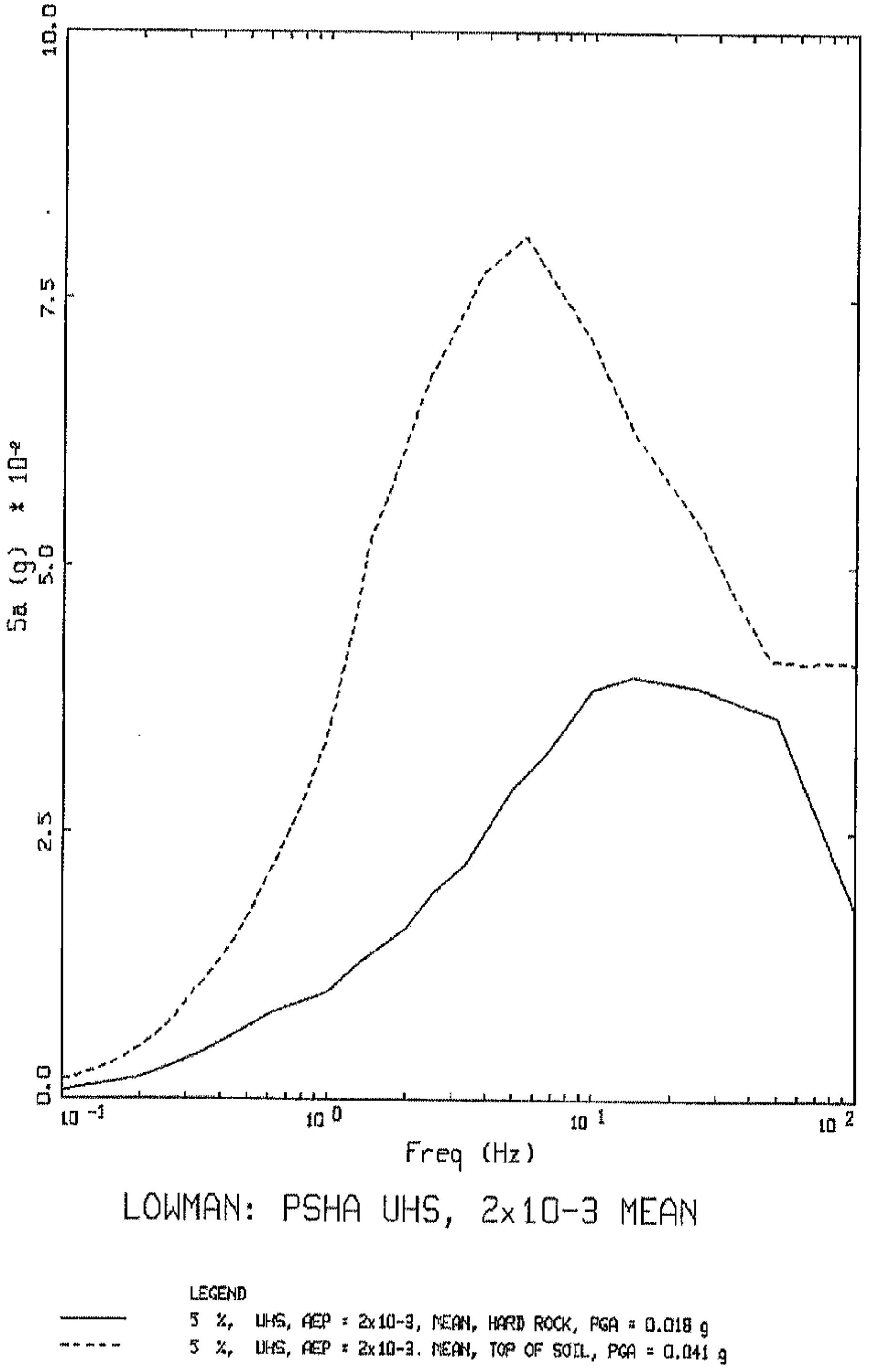

Figure 13. (cont.)

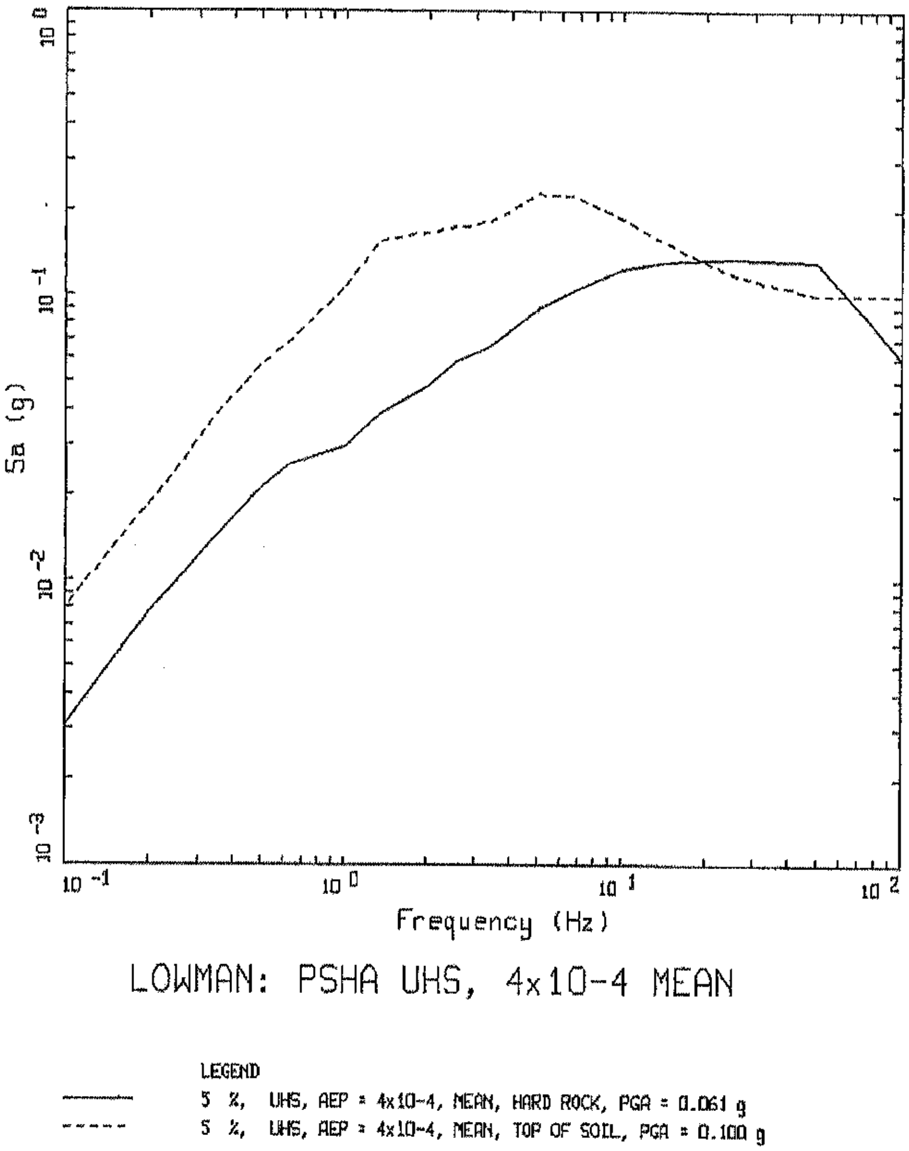

Figure 14. Comparison of site-specific soil UHS (top-of-soil) with the hard rock UHS, logarithmic and linear Sa axes.

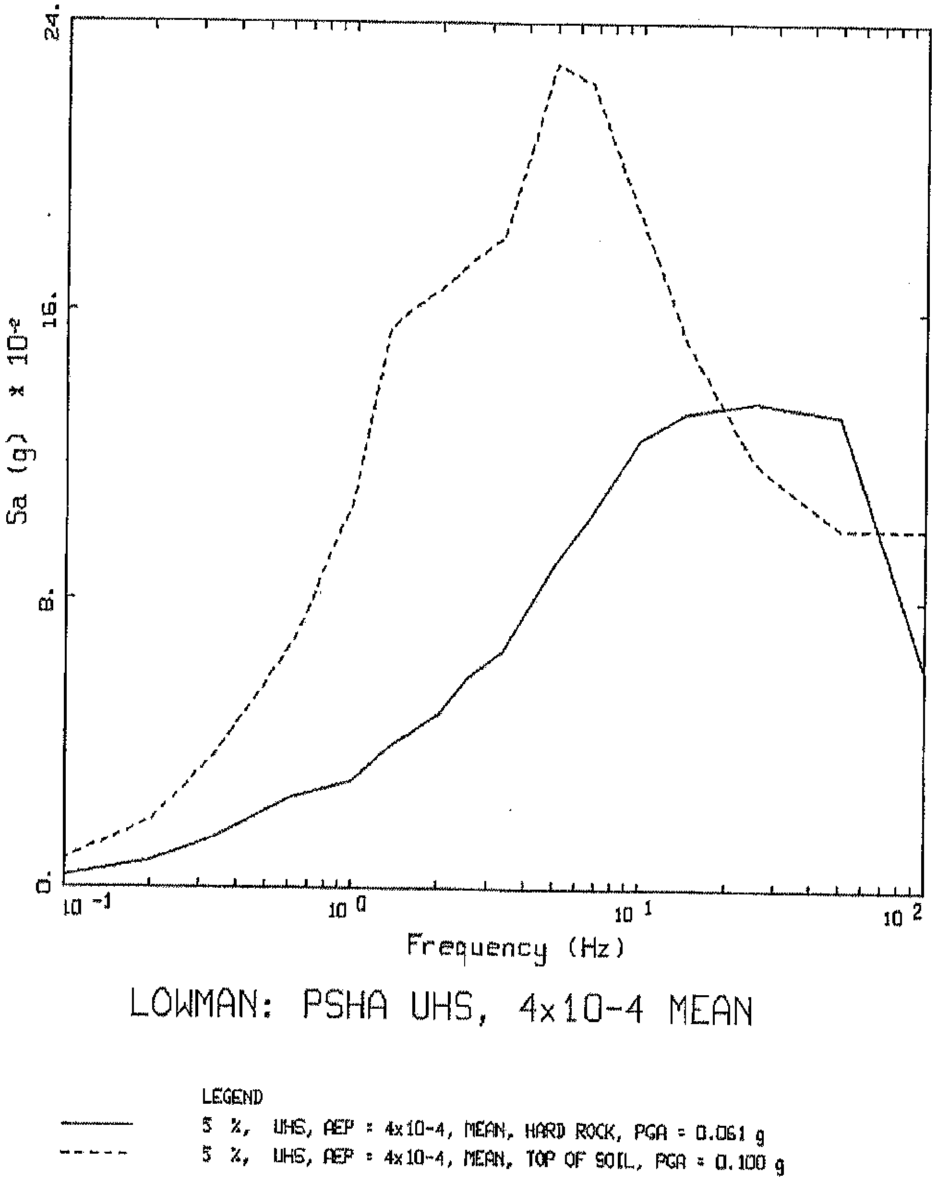

Figure 14. (cont.)

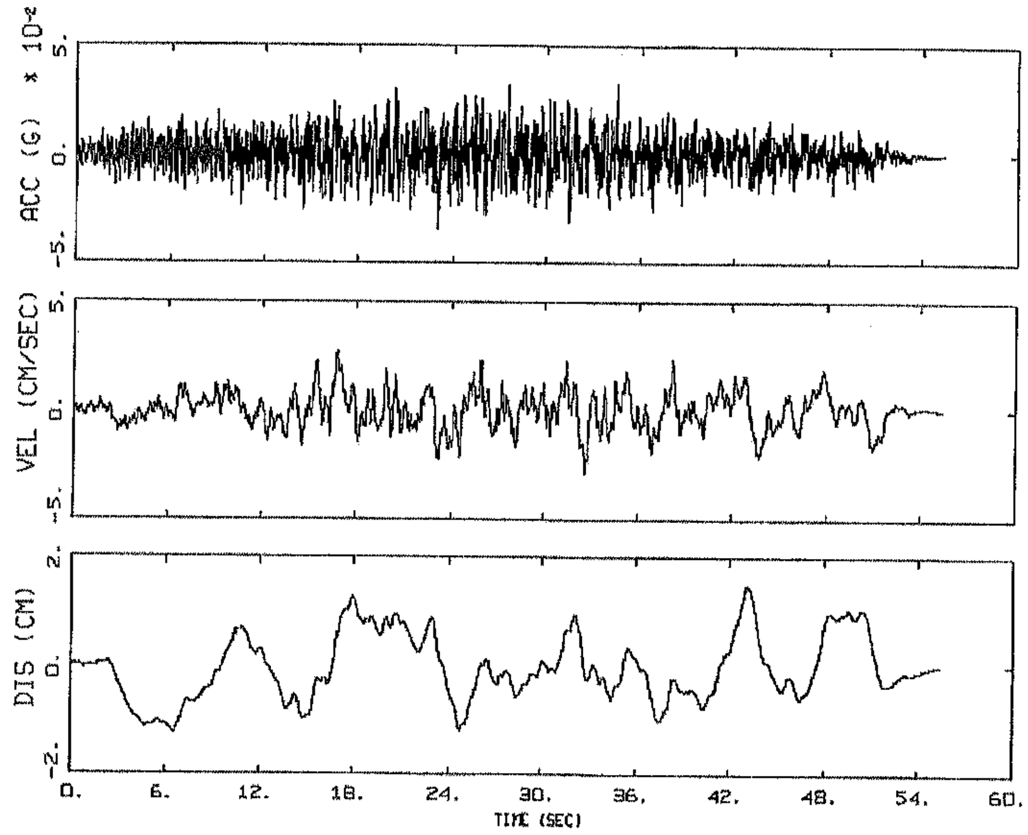

LOWMAN: 2x10-3
BASELINE CORRECTED

Figure Set 15. Spectral match acceleration, velocity, and displacement time histories followed by response spectra (target and spectral match, logarithmic and linear Sa axes) and ratios of time history spectra over target spectra for the horizontal component at the surface for AEF 2 x 10^{-3}.

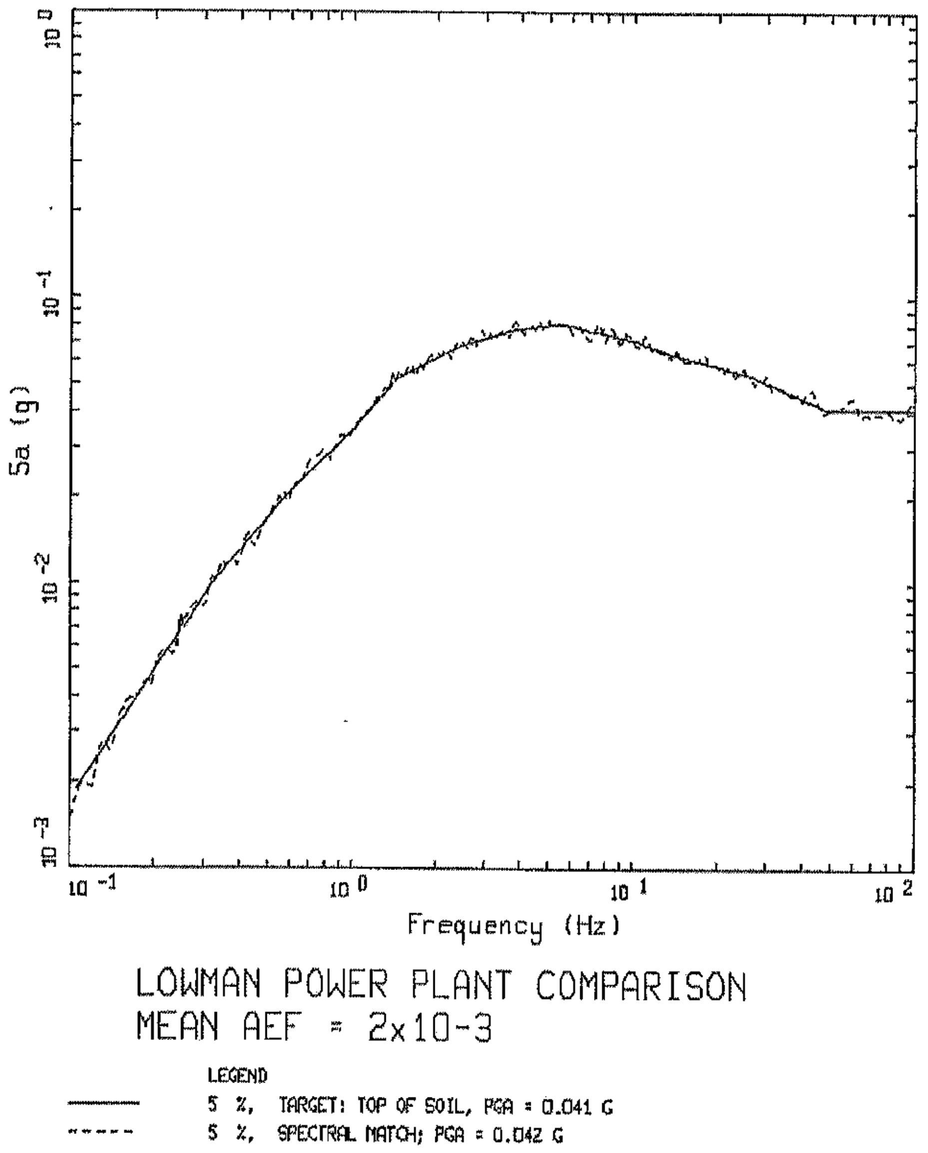

Figure Set 15. (cont.)

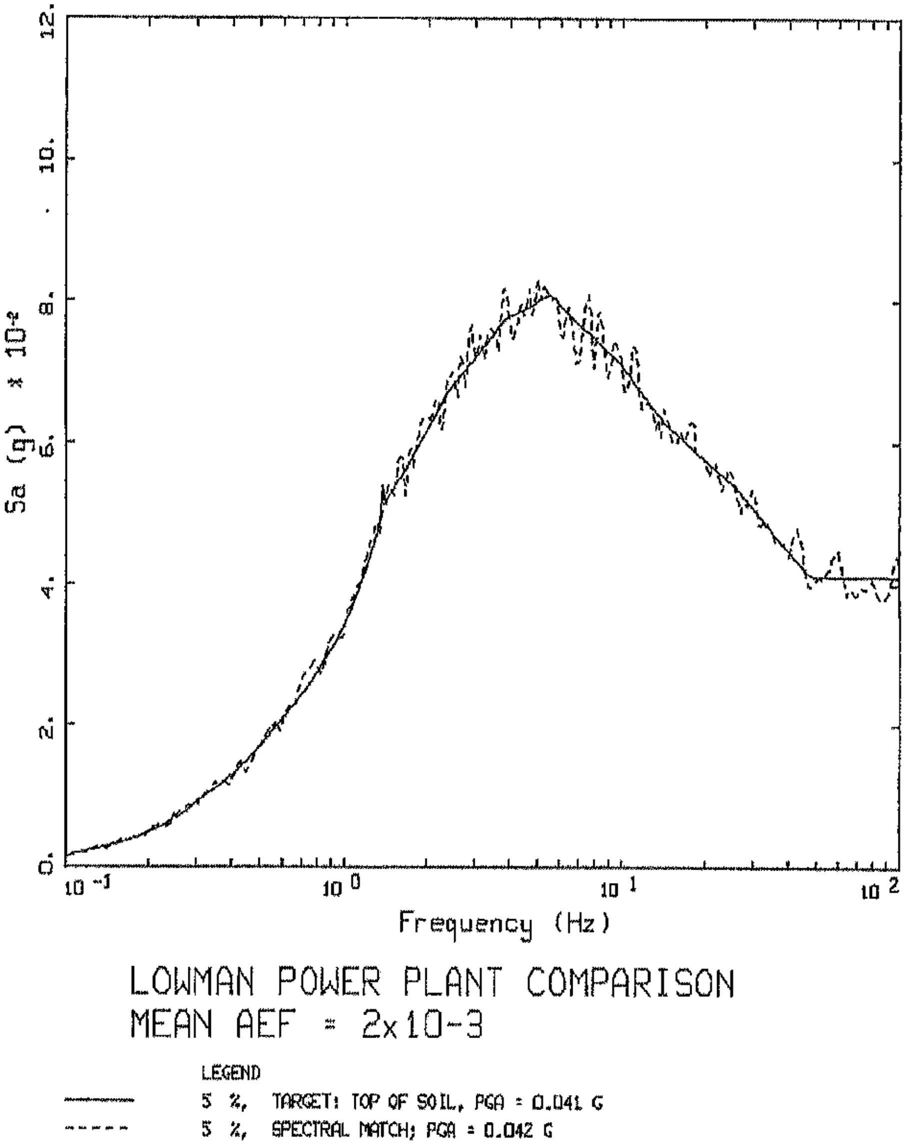

Figure Set 15. (cont.)

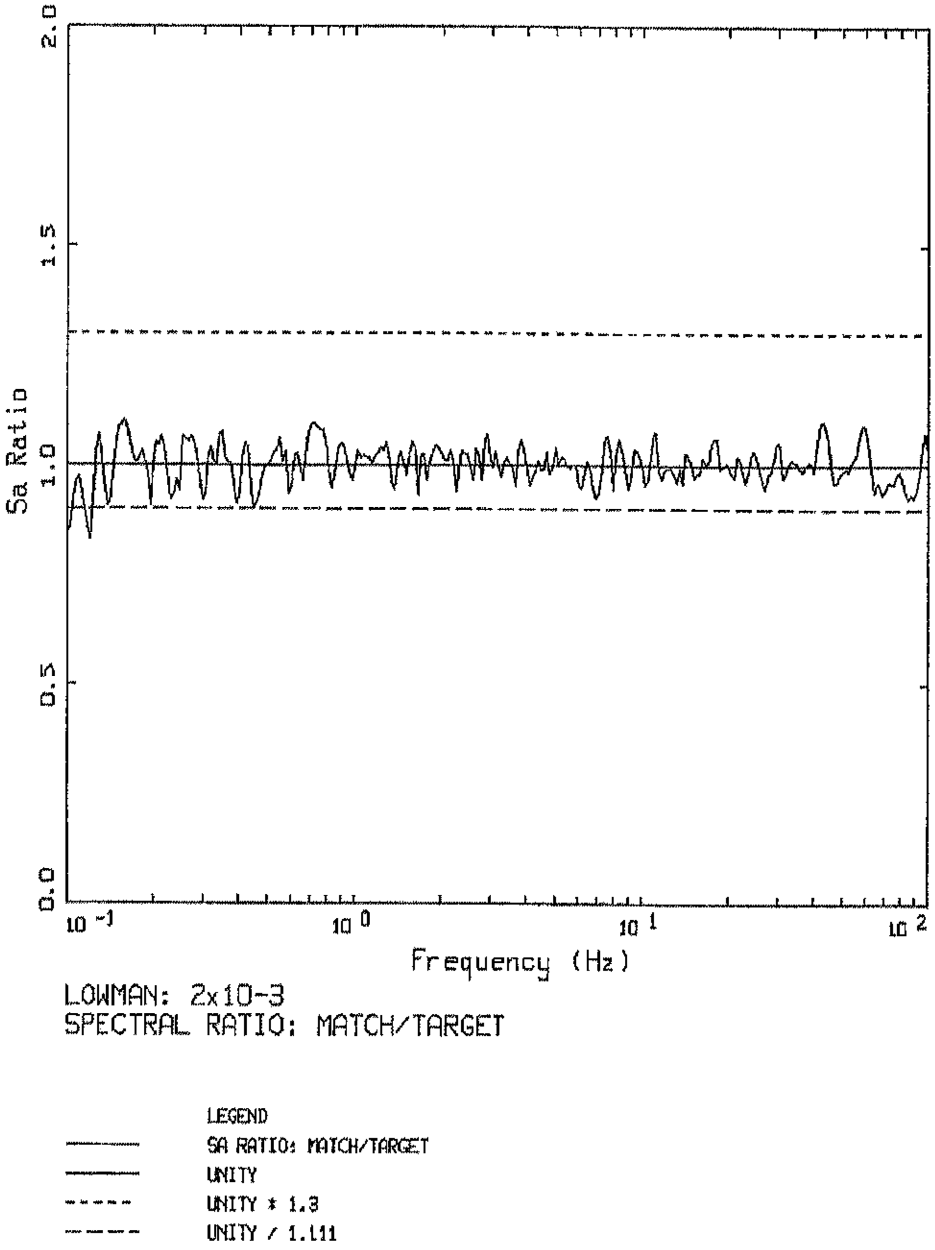

Figure Set 15. (cont.)

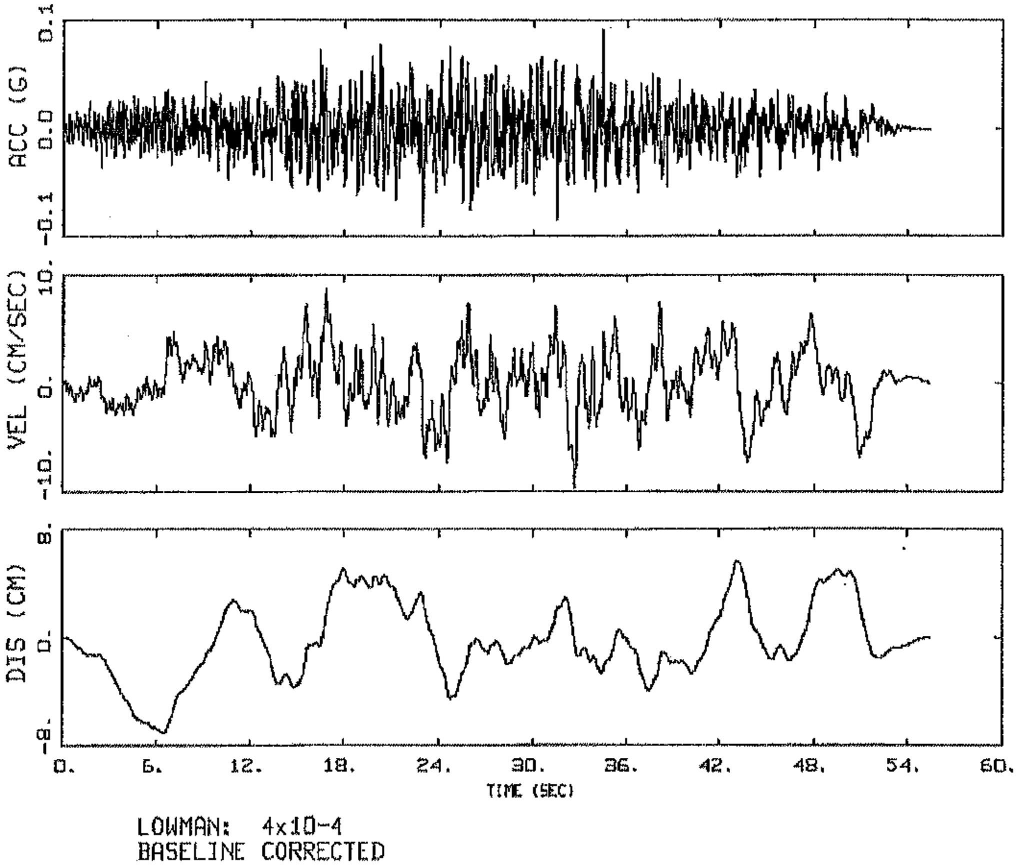

Figure Set 16. Spectral match acceleration, velocity, and displacement time histories followed by response spectra (target and spectral match, logarithmic and linear Sa axes) and ratios of time history spectra over target spectra for the horizontal component at the surface (top-of-soil) for AEF 4 x 10^{-4}.

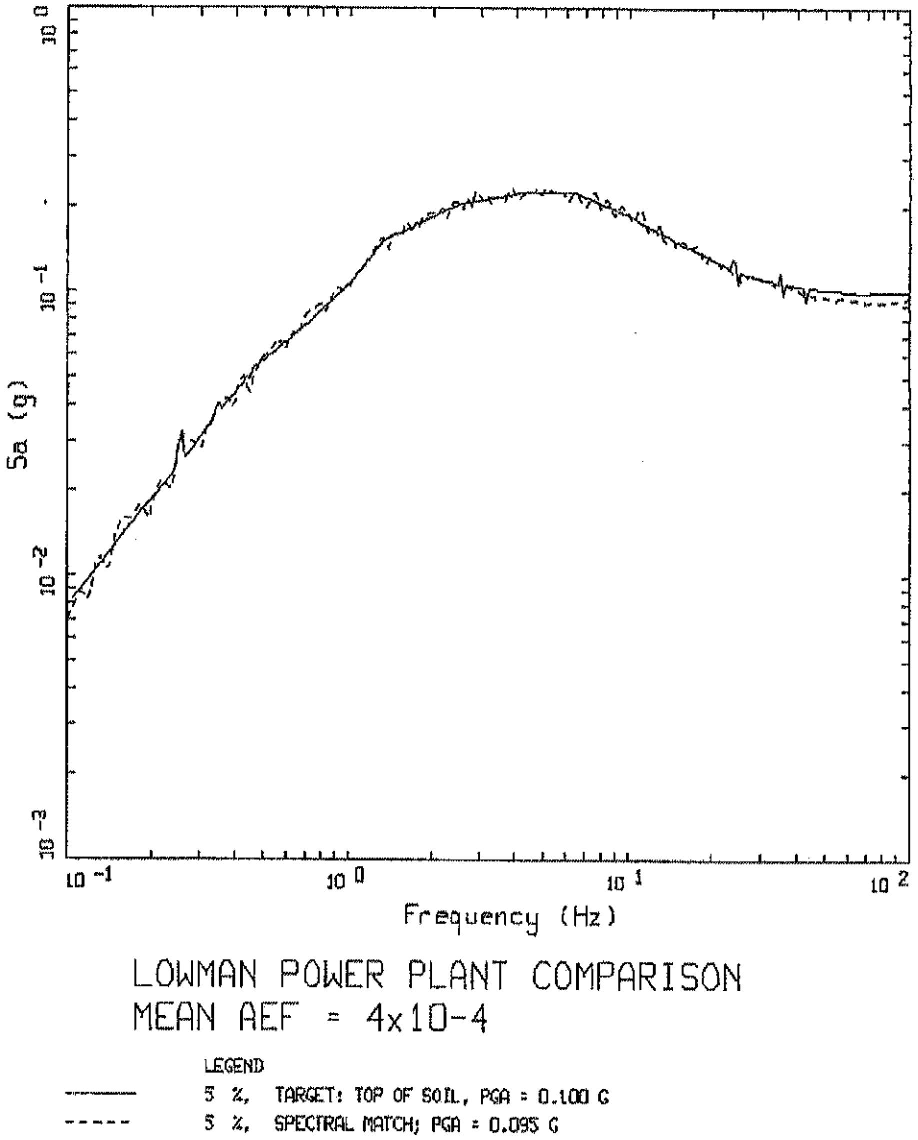

Figure Set 16. (cont.)

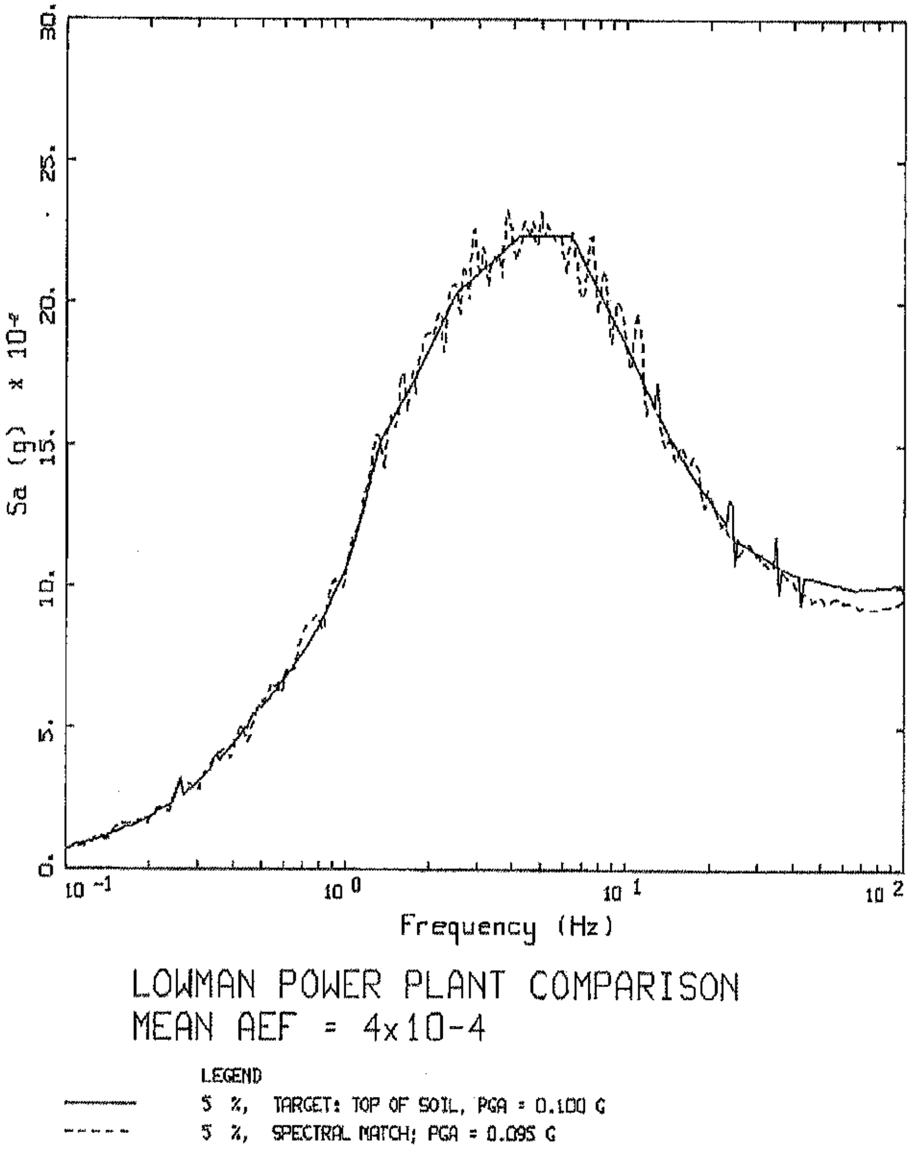

LOWMAN POWER PLANT COMPARISON
MEAN AEF = 4x10-4

Figure Set 16. (cont.)

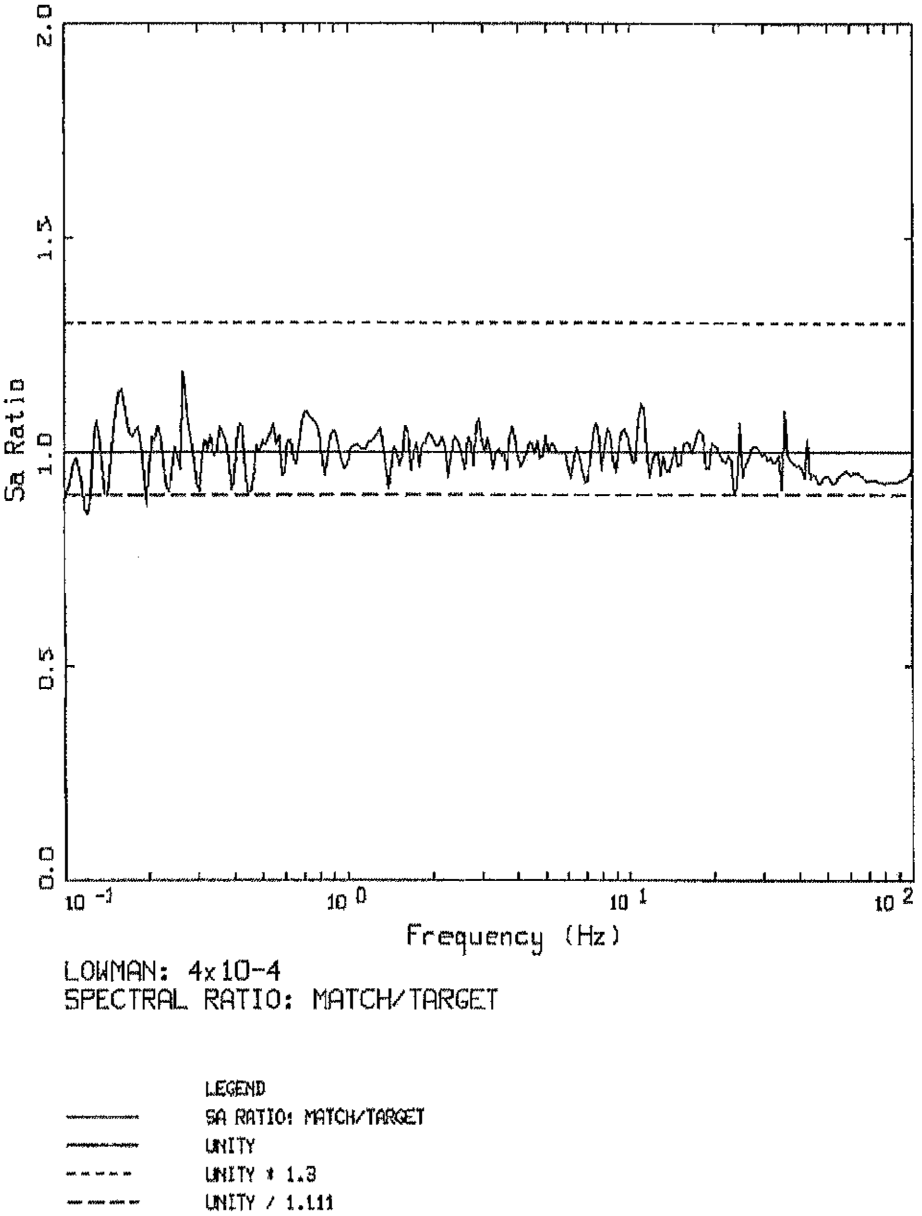

Figure Set 16. (cont.)

Appendix A

August 13, 2003

DEVELOPMENT OF REGIONAL HARD ROCK ATTENUATION RELATIONS FOR CENTRAL AND EASTERN NORTH AMERICA, MID-CONTINENT AND GULF COAST AREAS

Walter Silva[*], Nick Gregor[*], Robert Darragh[*]

Background

Due to the low rates of seismicity, a significant and currently unresolvable issue exists in the estimation of strong ground motions for specified magnitude, distance, and site conditions in central and eastern North America (CENA). The preferred approach to estimating design ground motions is through the use of empirical attenuation relations, perhaps augmented with a model based relation to capture regional influences. For western North America (WNA), particularly California, seismicity rates are such that sufficient strong motion recordings are available for ranges in magnitudes and distances to properly constrain regression analyses. Naturally, not enough recorded data are available at close distances (# 10 km) to large magnitude earthquakes (**M** ∃ 6 3/4) so large uncertainty exists for these design conditions but, in general, ground motions are reasonably well defined. For CENA however, very few data exist and nearly all are for **M** # 5.8 and distances exceeding about 50 km. This is a fortunate circumstance in terms of hazard but, because the potential exists for large, though infrequent, earthquakes in certain areas of CENA, the actual risk to life and structures is comparable to that which exists in seismically active WNA. As a result, the need to characterize strong ground motions is significant and considerable effort has been directed to developing appropriate attenuation relations for CENA conditions (Boore and Atkinson, 1987; Toro and McGuire, 1987; EPRI, 1993; Toro et al., 1997; Atkinson and Boore, 1997). Because the strong motion data set is sparse in the CENA, numerical simulations represent the only available approach and the stochastic point-source model (Appendix C) has generally been the preferred model used to develop attenuation relations. The process involves repeatedly exercising the model for a range in magnitude and distances as well as expected parameter values, adopting a functional form for a regression equation, and finally performing regression analyses to determine coefficients for median predictions as well as variability about the median. Essential elements in this process include: a physically realistic, reasonably robust and well-validated model (Silva et al., 1997; Schneider et al., 1993); appropriate parameter values and their distributions; and a statistically stable estimate of model variability (Appendix C). The model variability is added to the variability resulting from the regression analyses (parametric plus regression variability) to represent the total variability associated with median estimates of ground motions (Appendix C).

---

[*] Pacific Engineering and Analysis, 311 Pomona Ave., El Cerrito, CA 94530
www.pacificengineering.org; e-mail: pacificengineering@juno.com

Model Parameters

For the point-source model implemented here, parameters include stress drop ($\Delta\sigma$), source depth (H), path damping ($Q(f) = Q_o f^{\eta}$), shallow crustal damping (kappa), and crustal amplification. For the regional crust, the Midcontinent and Gulf Coast models from EPRI (1993; also in Toro et al., 1997) were adopted. The crustal models are listed in Table 1 and vertically propagating shear-waves are assumed (Appendices B, C). The Moho is at a depth of about 30 to 40 km. Geometrical attenuation is assumed to be magnitude dependent, using a model based on inversions of the Abrahamson and Silva (1997) empirical attenuation relation with the point-source model. The model for geometrical attenuation is given by

$$R^{-(a + b\,(M - 6.5))},\ R \# 80\ \text{km}; \qquad R^{-(a + b\,(M - 6.5))/2}, \qquad R > 80\ \text{km} \qquad (1)$$

where a = 1.0296, b = -0.0422, and 80 km reflects about twice the crustal thickness (Table 1).

The duration model is taken as the inverse corner frequency plus a smooth distance term of 0.05 times the hypocentral distance (Herrmann, 1985). Monotonic trends in both the geometrical attenuation and distance duration models produced no biases in the validation exercises using WNA and CENA recordings (Appendix C) and are considered appropriate when considerable variability in crustal structure that may exist over a region, as well as variability in source depth. Additionally, extensive modeling exercises have shown that the effects of source finiteness, coupled with variability in source depth and crustal structure, result in smooth attenuation with distance, accompanied by a large variability in ground motions (EPRI, 1993). More recently, regressions for peak acceleration, peak particle velocity, and peak displacement on WNA strong motion data (over 50 earthquakes, **M** ≈ 5.0 to 7.6), including the recent Chi-Chi, Taiwan and Koaceli and Duzce, Turkey earthquakes using a smooth monotonic distance dependency (Equation 3) showed symmetric distributions of residuals about zero (Silva et al., 2002). These results suggest a monotonic distance dependency adequately reflects strong motion distance attenuation when considering multiple earthquakes and variable crustal conditions and is an appropriate assumption for estimating strong ground motions for the next earthquake.

To model shallow crustal damping, a kappa value of 0.006 sec is assumed to apply for the crystalline basement and below (Silva and Darragh, 1995; EPRI, 1993). The Q(f) model is from Silva et al. (1997), based on inversions of CEUS recordings and is given by $Q(f) = 351\ f^{0.84}$ for the Midcontinent region. For the Gulf Coast $Q(f) = 300\ f^{0.81}$ based on inversions of regional LRSM recordings (EPRI 1993). Both magnitude independent and magnitude dependent stress drop models are used. For the magnitude dependent stress drop model, the stress drop varies from 160 bars for **M** 5.5 to 90 bars for **M** 7.5 and 70 bars for **M** 8.5 (the range in magnitudes for the simulations). The magnitude scaling of stress drop is based on point-source inversions of the Abrahamson and Silva (1997) empirical attenuation relation (Silva et al., 1997) and is an empirically driven mechanism to accommodate the observed magnitude saturation due to source finiteness. Similar point-source stress drop scaling has been observed by Atkinson and Silva (1997) using

(WNA) recordings of strong ground motions and from inversions of the Sadigh et al., (1997) attenuation relation (EPRI, 1993). For the CEUS, the stress drop values are constrained by the **M** 5.5 stress drop of 160 bars. This value is from recent work of Gail Atkinson (personal communication, 1998) who determined CENA stress drops based on instrumental and intensity data. Since the majority of her data are from earthquakes below **M** 6 (**M** 4 to 7), it was assumed her average stress drop (. 180 bars adjusted for the regional crustal model to 160 bars) is appropriate for **M** 5.5. Table 2 shows the magnitude dependent as well as magnitude independent stress drops. The magnitude independent stress drop of 120 bars reflects the log average of the **M** 5.5, **M** 6.5, and **M** 7.5 stress drops (Table 2).

The single corner frequency model was also run with a constant stress drop for all magnitudes. A stress drop of 120 bars was applied to all four magnitudes. This is the same constant stress drop used in the Toro et al. (1997; EPRI, 1993) CEUS rock relations. To accommodate uncertainty (epistemic) in median stress drop (parameters) for CEUS earthquakes, both high and low median values were run using a 100% variation on the constant and variable stress drop models (Table 2). The high stress drop model is taken as 2 times the base case values with the low stress drop as the base case values divided by 2.

Source depth is also assumed to be magnitude dependent and is based on the depth distribution of stable continental interiors and margins (EPRI, 1993). The magnitude dependent depth distribution is shown in Table 2.

Another source model considered appropriate for CENA ground motions is the double corner model (Atkinson and Boore, 1997). In this model there is no variation of the stress drop with magnitude. Additionally, stress drop is not explicitly defined for this model and no uncertainties are given for the corner frequencies (which are magnitude dependent). As a result, the parametric uncertainty obtained from the regression analysis will underepresent the total parametric uncertainty. For this reason, the total parametric uncertainty for the two-corner model is taken as the total parametric uncertainty from the single corner model with variable stress drop, which is slightly larger than the parametric uncertainty for the single corner model with constant stress drop scaling (to avoid underestimating the two-corner parametric uncertainty).

To accommodate magnitude saturation in the double-corner and single-corner constant stress drop models, magnitude dependent fictitious depth terms were added to the source depths for simulations at **M** 6.5 and above. The functional form is given by

$$H = H' \, e,^{a + bM} \qquad (2)$$

with

$$a = -1.250, \qquad b = 0.227.$$

H and H' are the fictitious and original source depths respectively and the coefficients are based on the Abrahamson and Silva (1997) empirical attenuation relation. The magnitude saturation built into the constant stress drop single corner and double corner models is then constrained empirically, accommodating source finiteness in a manner consistent with the WUS strong motion database. This approach to limiting unrealistically high ground motions for large magnitude earthquakes at close distances is considered more physically reasonable than limiting the motions directly, which can be rather arbitrary with specific limiting values difficult to defend on a physical basis.

Because of the manner in which the model validations were performed ($\Delta\sigma$, Q(f), and H were optimized), parametric variability for only $\Delta\sigma$, Q(f) and H are required to be reflected in the model simulations (Appendix C; EPRI, 1993; Roblee et. al., 1996). For source depth variability, a lognormal distribution is used with a $\sigma_{\ln} = 0.6$ (EPRI, 1993). Bounds are placed on the distribution to prevent nonphysical realizations (Table 2).

The stress drop variability, $\sigma_{\ln} = 0.5$ is from Silva et al. (1997) and is based on inversions of ground motions for stress drop using WNA earthquakes with **M** ≥ 5. The variability in Q(f) is taken in Q_o alone ($\sigma_{\ln} = 0.4$) and is based on inversions in WNA for Q(f) models (Silva et al., 1997).

Attenuation Relations

To generate data, which consists of 5% damped spectral acceleration, peak acceleration, peak particle velocity, and peak displacements, for the regression analyses, 300 simulations reflecting parametric variability are made at distances of 1, 5, 10, 20, 50, 75, 100, 200, and 400 km. At each distance, five magnitudes are used: **M** 4.5, 5.5, 6.5, 7.5, and 8.5 (Table 2).

The functional form selected for the regressions which provided the best overall fit (from a suite of about 25) to the simulations is given by

$$\ln y = C_1 + C_2 M + (C_6 + C_7 M) * \ln(R + e^{C_4}) + C_{10}(M - 6)^2, \qquad (3)$$

where R is taken as a closest distance to the surface projection of the rupture surface, consistent with the validation exercises (Silva et al., 1997).

Figure 1 shows the simulations for peak accelerations as well as the model fits for the single corner model with variable stress drops for **M** 7.5 and the Midcontinent parameters. In general, the model fits the central trends (medians) of the simulations. Figure 2a summarizes the magnitude dependency of the peak acceleration estimates and saturation is evident, primarily due to the magnitude dependent stress drop. Also evident is the magnitude dependent far-field fall off with a decrease in slope as **M** increases (easily seen beyond 100 km). This feature is especially important in the CEUS where large contributions to the hazard can come from distant sources. The model predicts peak accelerations at a distance of 1 km of about 0.30, 0.70, 1.10, 1.50g for **M** 4.5, 5.5, 6.5, and 7.5, respectively.

For comparison, Figure 2a also shows the results for the Gulf Coast parameters with slightly higher peak accelerations within about 30 km. Beyond about 30 km, the Gulf Coast shows significantly lower motions, particularly at large distance (R $\geq$ 200 km).

The higher close-in Gulf Coast motions are a result of larger crustal amplification while the crossover near 30 km is due to the lower Q(f) model or crustal damping.

Figure 2b illustrates the effect of median stress drop on the peak accelerations, about a factor of 2 (closer to 1.7 overall) at close distances and decreasing with increasing distance (likely due to a decrease in frequency content with increasing distance).

Examples of response spectra at 1 km for **M** 4.5, 5.5, 6.5, 7.5, and 8.5 are shown in Figure 3a for the Midcontinent and Gulf Coast regions. For **M** 7.5, the peak acceleration (Sa at 100 Hz) is about 1.8g with the peak in the spectrum near 0.04 sec. The jagged nature of the Midcontinent spectra is due to unsmoothed coefficients. Figure 3b shows the effect of median stress drop on the spectra for the Midcontinent parameters (effects on the Gulf Coast are quite similar). As expected the maximum effect is at high frequency, decreasing with increasing period, and approaching no effect at the magnitude dependent corner period.

The model regression coefficients are listed in Table 3 along with the parametric and total variability. The modeling variability is taken from Appendix C. The total variability, solid line in Figure Set 4, is large. For the Midcontinent, it ranges from about 2 at short periods to about 4 at a period of 10 sec, where it is dominated by modeling variability. For the Gulf Coast, the high frequency parametric (and total) variability is higher, about 2.5 for the total variability at peak acceleration (100 Hz). This is driven by the effects of the lower Q(f) model. The high frequency large distance motions are lower than the Midcontinent, driven down by the higher crustal damping. This is appropriately accommodated in an increased parametric variability and is a compelling case for a variability model which includes a distance dependency.

The large long period uncertainty is due to the tendency of the point-source model to overpredict low frequency motions at large magnitudes (**M** > 6.5; EPRI, 1993). This trend led Atkinson and Silva (1997, 2000) to introduce a double-corner point-source model for WUS crustal sources, suggesting a similarity in source processes for WUS and CEUS crustal sources, but with CEUS sources being more energetic by about a factor of two (twice WUS stress drops), on average.

The results for the single corner frequency model with constant stress drop scaling are shown in Figure Sets 5 to 8. The same plots are shown as were described for the previous model. These two models estimate similar values with the variable stress drop motions exceeding the constant stress drop motions at the lower magnitudes (**M** ≤ 6.5). The constant stress drop of 120 bars will result in about 30% to 50% higher rock motions at high frequency (> 1 Hz) for **M** 7.5 than the variable stress drop model, with a corresponding stress drop of 95 bars (EPRI, 1993). At small **M**, say **M** 5.5, the variable stress drop motions are higher, reflecting the 160 bar results of Atkinson for CEUS earthquakes with average **M** near 5.5. Also shown are the results for the model with saturation, reducing the large magnitude, close-in motions. The saturation reduces the **M** 7.5 and **M** 8.5 motions by 30 to 50% within about 10 km distance. The parametric variability is also similar to that of the variable stress drop model. The regression coefficients are given in Tables 4 and 5.

The regression results for the double corner frequency model are listed in Tables 6 and 7. The regression model fit to the peak acceleration data as shown in Figure 9 for the Midcontinent. The PGA model is shown in Figure 10, and Figure 12 is a plot of the uncertainty. Figure 11 shows the spectra at a distance of 1 km. At long period (> 1 sec) and large **M** (≥ 6.5) the motions are significantly lower than those of the single-corner models (Figures 3a and 7). The parametric variability was taken as the same as the single corner model with variable stress drop as distributions are not currently available to apply to the two corner frequencies associated with this model (Atkinson and Boore, 1997). Since the two corner frequency source model was not available when the validations were performed (Silva et al., 1997), the model variability for the single corner frequency source model was used. This is considered conservative as the total aleatory variability for the two corner model is likely to be lower than that of the single corner model, as comparisons using WUS data show it provides a better fit to recorded motions at low frequencies (≤ 1 Hz; Atkinson and Silva, 1997, 2000). This is, of course, assuming the aleatory parametric variability associated with the two corner frequencies is not significantly larger than that associated with the single corner frequency stress drop.

At long period (> 1 sec) the total variability is largely empirical, being driven by the modeling component or comparisons to recorded motions. While this variability may be considered large, it includes about 17 earthquakes with magnitudes ranging from **M** 5.3 to **M** 7.4, distances out to 500 km, and both rock and soil sites. The average **M** for the validation earthquakes is about **M** 6.5, near the magnitude where empirical aleatory variability has a significant reduction (Abrahamson and Shedlock, 1997). The magnitude independent point-source variability may then reflect the generally higher variability associated with lower magnitude (**M** ≤ 6.5) earthquakes, being conservative for larger magnitude earthquakes.

Epistemic variability or uncertainty in mean estimates of ground motions is assumed to be accommodated in the use of the three mean stress drop single corner models and the double corner model, all with appropriate weights. This assumption assumes the epistemic uncertainty in the spectral levels of the two corner frequency model are small (indeed zero) and can be neglected. This approach assumes the major contributors to epistemic uncertainty (variability in mean motions) for the CEUS are in single corner mean stress drop and shape of the source spectrum, as well as differences in crustal structure between the Midcontinent and Gulf Coast regions (Table 1). As a guide to estimating appropriate weights for the low, medium, and high median stress drops to accommodate epistemic variability in median CEUS single corner stress drops, the EPRI (1993) value for total variability (epistemic plus aleatory) of 0.7 at large magnitude (**M** ≥ 6.5) may be adopted. Based on the WUS aleatory value of 0.5 (Table 2; Silva et al., 1997), assuming similar aleatory variability in median stress drop for the CEUS, the remaining variability of 0.49 may be attributed to epistemic variability in the median stress drop. For the factors of two above and below the medium stress drop (Table 2), an approximate three point weighting would have weights of 1/6, 2/3, 1/6 (Gabe Toro, personal communication).

REFERENCES

Abrahamson, N.A. and W.J. Silva (1997). "Empirical response spectral attenuation relations for shallow crustal earthquakes." *Seismological Research Let.*, 68(1), 94-127.

Ackerman, H.D (1983). "Seismic refraction study in the area of the Charleston, South Carolina, 1886 earthquake, in studies related to the Charleston, South Carolina, earthquake of 1886 - tectonics and seismicity." G.S. Gohn, ed., *U.S. Geological Survey Professional Paper,* 1313-F, 20p.

Atkinson, G.M and W.J. Silva (2000). AStochastic modeling of California ground motions.@ *Bull. Seism. Soc. Am.* 90(2), 255-274.

Atkinson, G.M. and D.M. Boore (1997). "Some comparisons between recent ground-motion relations." *Seism. Res. Lett.* 68(1), 24-40.

Atkinson, G.M and W.J. Silva (1997). "An empirical study of earthquake source spectra for California earthquakes." *Bull. Seism. Soc. Am.* 87(1), 97-113.

Boore, D.M. and G.M. Atkinson (1987). "Stochastic prediction of ground motion and spectral response parameters at hard-rock sites in eastern North America." *Bull. Seism. Soc. Am.*, 77(2), 440-467.

Campbell, K W. (1997). "Empirical near-source attenuation relationships for horizontal and vertical components of peak ground acceleration, peak ground velocity, and pseudo-absolute acceleration response spectra." *Seismological Research Let.*, 68(1), 154-176.

Electric Power Research Institute (1993). "Guidelines for determining design basis ground motions." Palo Alto, Calif: Electric Power Research Institute, vol. 1-5, EPRI TR-102293.

vol. 1: Methodology and guidelines for estimating earthquake ground motion in eastern North America.
vol. 2: Appendices for ground motion estimation.
vol. 3: Appendices for field investigations.
vol. 4: Appendices for laboratory investigations.
vol. 5: Quantification of seismic source effects.

Herrmann, R.B. (1985). "An extension of random vibration theory estimates of strong ground motion to large distance." *Bull. Seism. Soc. Am.*, 75, 1447-1453.

Rhea, S. (1984). "Q determined from local earthquakes in the South Carolina coastal plain." *Bull. Seism. Soc. Am.*, 74(6), pp. 2257-2268.

Roblee, C.J., W.J. Silva, G.R. Toro, and N. Abrahamson (1996). "Variability in Site-Specific Seismic Ground-Motion Predictions." Uncertainty in the Geologic Environment: From Theory to Practice, Proceedings of "Uncertainty '96" *ASCE* Specialty Conference, Edited by C.D. Shackelford, P.P. Nelson, and M.J.S. Roth, Madison, WI, Aug. 1-3, pp. 1113-1133

Sadigh, K., C.-Y. Chang, J.A. Egan, F. Makdisi, and R.R. Youngs (1997). "Attenuation relationships for shallow crustal earthquakes based on California strong motion data." *Seism. Soc. Am.*, 68(1), 180-189.

Schneider, J.F., W.J. Silva, and C.L. Stark (1993). Ground motion model for the 1989 **M** 6.9 Loma Prieta earthquake including effects of source, path and site. *Earthquake Spectra,* 9(2), 251-287.

Silva, W.J., N. Abrahamson, G. Toro, and C. Costantino (1997). "Description and validation of the stochastic ground motion model." Submitted to Brookhaven National Laboratory, Associated Universities, Inc. Upton, New York.

Silva, W.J. and R. Darragh (1995). "Engineering characterization of earthquake strong ground motion recorded at rock sites." Palo Alto, Calif:Electric Power Research Institute, TR-102261.

Toro, G.R. and R.K. McGuire (1987). "An investigation into earthquake ground motion characteristics in eastern North America." *Bull. Seism. Soc. Am.*, 77(2), 468-489.

Toro, G.R., N.A. Abrahamson, and J.F. Schneider (1997). "A Model of strong ground motions from earthquakes in Central and Eastern North America: Best estimates and uncertainties." *Seismological Research Let.,* 68(1), 41-57.

Table 1
CRUSTAL MODELS*
MID-CONTINENT

Thickness (km)	V_S (km/sec)	Density (cgs)
1.30	2.83	2.52
11.00	3.52	2.71
28.00	3.75	2.78
-----	4.62	3.35
	GULF COAST*	
7.00	2.31	2.37
8.00	3.05	2.58
15.00	3.76	2.78
	4.74	3.40

---

* EPRI mid-continent and Gulf Coast (EPRI, 1993; Toro et al., 1997)

Table 2

PARAMETERS FOR CRYSTALLINE ROCK OUTCROP ATTENUATION SIMULATIONS

M 4.5, 5.5, 6.5, 7.5, 8.5

D (km) 1, 5, 10, 20, 50, 75, 100, 200, 400

300 simulations for each **M**, *R* pair

Randomly vary source depth, $\Delta\sigma$, kappa, Q_o, η, profile

<u>Depth,</u> $\sigma_{\ln H} = 0.6$, Intraplate Seismicity (EPRI, 1993)

M	m_{blg}	Lower Bound (km)	$\overline{H}$ (km)	Upper Bound (km)
4.5	4.9	2	6	15
5.5	6.0	2	6	15
6.5	6.6	4	8	20
7.5	7.1	5	10	20
8.5	7.8	5	10	20

$\Delta\sigma$, $\sigma_{\ln}\Delta\sigma = 0.5$ (Silva et al., 1997)

M	m_{blg}	$\Delta\sigma$ (bars) Base Case Values	
4.5	4.9	160, 120*	AVG. $\Delta\sigma$ (bars) = 123; Assumes **M** 5.5 = 160 bars (Atkinson, 1993) with magnitude scaling taken from WUS (Silva et al., 1997); constant stress drop model has $\Delta\sigma$ (bars) = 120. High and low stress drop models are 100% higher and 100% lower than base case values.
5.5	6.0	160, 120*	
6.5	6.6	120, 120*	
7.5	7.1	90, 120*	
8.5	7.8	70, 120*	

<u>Q(s),</u> = 351, $\eta = 0.84$, $\sigma_{\ln Q_o} = 0.4$, (Mid-Continent; Silva et al., 1997)

<u>Q(s),</u> = 300, $\eta = 0.30$, $\sigma_{\ln Q_o} = 0.4$, (Gulf Coast; EPRI, 1993)

Varying Q_o only sufficient, ± 1 σ covers range of CEUS inversions from 1 to 20 Hz

Kappa, $\overline{\kappa} = 0.006$ sec (EPRI, 1993)

<u>Profile,</u> Crystaline Basement, randomize top 100 ft

Geometrical attenuation $R^{-(a + b\,(M - 6.5))}$, a = 1.0296, b = -0.0422

$R^{-(a + b\,(M - 6.5))/2}$, R > 80 km, approximately twice crustal thickness (Table1)

Based on inversions of the Abrahamson and Silva (1997) relation

---

*Constant Stress Drop Model

Table 3a
MIDCONTINENT
REGRESSION COEFFICIENTS FOR THE SINGLE CORNER MODEL WITH VARIABLE MEDIUM STRESS DROP AS A FUNCTION OF MOMENT MAGNITUDE (**M**)

Freq. Hz	C1	C2	C4	C5	C6	C7	C8	C10	Parametric Sigma	Total Sigma
0.1000	-19.07223	2.57205	2.10000	.00000	-1.41166	.05292	.00000	-.31205	.3559	1.3243
0.2000	-15.15004	2.27308	2.30000	.00000	-1.55609	.06043	.00000	-.38898	.3660	1.1933
0.3333	-11.84462	1.96000	2.40000	.00000	-1.70638	.07232	.00000	-.39806	.3892	1.0462
0.5000	-9.00041	1.66899	2.50000	.00000	-1.86794	.08623	.00000	-.37576	.4160	.9591
0.6250	-7.60788	1.50586	2.50000	.00000	-1.94031	.09384	.00000	-.35415	.4297	.8874
1.0000	-4.51914	1.13220	2.60000	.00000	-2.16445	.11502	.00000	-.29235	.4518	.8021
1.3333	-2.82095	.93101	2.60000	.00000	-2.25774	.12494	.00000	-.24823	.4610	.8050
2.0000	-.84738	.68960	2.60000	.00000	-2.39187	.13949	.00000	-.19435	.4714	.7551
2.5000	.13162	.57890	2.60000	.00000	-2.45001	.14539	.00000	-.16638	.4775	.7396
3.3333	1.12628	.45746	2.60000	.00000	-2.53338	.15420	.00000	-.13930	.4865	.7395
4.1667	1.79388	.38804	2.60000	.00000	-2.58195	.15895	.00000	-.12283	.4950	.7274
5.0000	2.27495	.34400	2.60000	.00000	-2.61448	.16182	.00000	-.11211	.5040	.7247
6.2500	3.13556	.27220	2.70000	.00000	-2.72838	.17012	.00000	-.10222	.5181	.7271
6.6667	3.26041	.25961	2.70000	.00000	-2.74131	.17129	.00000	-.09985	.5249	.7328
8.3333	3.65946	.22693	2.70000	.00000	-2.77660	.17414	.00000	-.09345	.5424	.7503
10.0000	3.92885	.20331	2.70000	.00000	-2.80630	.17658	.00000	-.08961	.5602	.7507
12.5000	4.20238	.17878	2.70000	.00000	-2.84105	.17938	.00000	-.08624	.5731	.7534
14.2857	4.33334	.16542	2.70000	.00000	-2.86188	.18110	.00000	-.08477	.5803	.7585
16.6667	4.89845	.12529	2.80000	.00000	-2.96230	.18763	.00000	-.08349	.5868	.7656
18.1818	4.96669	.11815	2.80000	.00000	-2.97508	.18865	.00000	-.08293	.5907	.7644
20.0000	5.03867	.11102	2.80000	.00000	-2.98849	.18968	.00000	-.08242	.5961	.7711
25.0000	5.20890	.09698	2.80000	.00000	-3.01742	.19172	.00000	-.08150	.6133	.7817
31.0000	5.37895	.08559	2.80000	.00000	-3.04366	.19337	.00000	-.08079	.6227	.7858
40.0000	6.02744	.04417	2.90000	.00000	-3.15877	.20038	.00000	-.08027	.6222	.7823
50.0000	6.07941	.03289	2.90000	.00000	-3.18403	.20265	.00000	-.08044	.6143	.7776
100.000	4.24805	.09552	2.70000	.00000	-2.99165	.19690	.00000	-.08748	.5644	.7392
PGA	4.03930	.10412	2.70000	.00000	-2.97465	.19631	.00000	-.08874	.5592	.7353
PGV	3.22720	.65905	2.40000	.00000	-2.73277	.20009	.00000	-.13903	.4408	--------

Table 3b
MIDCONTINENT
REGRESSION COEFFICIENTS FOR THE SINGLE CORNER MODEL WITH VARIABLE LOW STRESS DROP AS A FUNCTION OF MOMENT MAGNITUDE (M)

Freq. Hz	C1	C2	C4	C5	C6	C7	C8	C10	Parametric Sigma	Total Sigma
0.1000	-18.82818	2.50853	2.10000	.00000	-1.39437	.05155	.00000	-.35284	.3623	1.3261
0.2000	-14.90966	2.17243	2.30000	.00000	-1.51375	.05943	.00000	-.40726	.3774	1.1969
0.3333	-11.55820	1.83734	2.40000	.00000	-1.66484	.07203	.00000	-.39809	.4056	1.0524
0.5000	-8.74448	1.53854	2.50000	.00000	-1.82313	.08612	.00000	-.36309	.4307	.9656
0.6250	-7.14902	1.36498	2.50000	.00000	-1.93736	.09559	.00000	-.33624	.4415	.8932
1.0000	-4.48436	1.01787	2.60000	.00000	-2.10529	.11396	.00000	-.26954	.4580	.8056
1.3333	-2.60545	.81461	2.60000	.00000	-2.24962	.12651	.00000	-.22591	.4650	.8073
2.0000	-.82196	.59874	2.60000	.00000	-2.37729	.14040	.00000	-.17695	.4750	.7574
2.5000	.04301	.50444	2.60000	.00000	-2.43239	.14596	.00000	-.15344	.4816	.7423
3.3333	.91358	.40083	2.60000	.00000	-2.51171	.15434	.00000	-.13143	.4910	.7425
4.1667	1.49580	.34395	2.60000	.00000	-2.55688	.15868	.00000	-.11864	.4995	.7305
5.0000	1.91753	.30871	2.60000	.00000	-2.58706	.16126	.00000	-.11059	.5084	.7278
6.2500	2.71047	.24622	2.70000	.00000	-2.69634	.16908	.00000	-.10327	.5222	.7300
6.6667	2.81889	.23601	2.70000	.00000	-2.70814	.17011	.00000	-.10154	.5289	.7357
8.3333	3.17270	.20990	2.70000	.00000	-2.74034	.17258	.00000	-.09693	.5460	.7529
10.0000	3.41148	.19064	2.70000	.00000	-2.76748	.17469	.00000	-.09418	.5635	.7531
12.5000	3.65547	.17022	2.70000	.00000	-2.79941	.17715	.00000	-.09175	.5760	.7556
14.2857	3.77180	.15884	2.70000	.00000	-2.81861	.17867	.00000	-.09070	.5830	.7605
16.6667	4.31663	.12089	2.80000	.00000	-2.91626	.18495	.00000	-.08978	.5893	.7676
18.1818	4.37793	.11466	2.80000	.00000	-2.92815	.18586	.00000	-.08938	.5931	.7662
20.0000	4.44314	.10840	2.80000	.00000	-2.94065	.18679	.00000	-.08901	.5984	.7729
25.0000	4.60063	.09599	2.80000	.00000	-2.96783	.18862	.00000	-.08835	.6153	.7833
31.0000	4.76103	.08583	2.80000	.00000	-2.99272	.19011	.00000	-.08783	.6246	.7873
40.0000	5.39249	.04598	2.90000	.00000	-3.10501	.19687	.00000	-.08744	.6240	.7837
50.0000	5.43661	.03559	2.90000	.00000	-3.12848	.19893	.00000	-.08760	.6160	.7790
100.000	3.62958	.09547	2.70000	.00000	-2.93410	.19276	.00000	-.09342	.5661	.7405
PGA	3.42714	.10323	2.70000	.00000	-2.91721	.19218	.00000	-.09443	.5610	.7366
PGV	2.77820	.64929	2.40000	.00000	-2.66659	.19477	.00000	-.15404	.4441	--------

Table 3c

MIDCONTINENT

REGRESSION COEFFICIENTS FOR THE SINGLE CORNER MODEL WITH VARIABLE HIGH STRESS DROP AS A FUNCTION OF MOMENT MAGNITUDE (M)

Freq. Hz	C1	C2	C4	C5	C6	C7	C8	C10	Parametric Sigma	Total Sigma
0.1000	-18.80138	2.59958	2.30000	.00000	-1.51629	.05717	.00000	-.25763	.3585	1.3250
0.2000	-15.20886	2.34990	2.40000	.00000	-1.62679	.06230	.00000	-.35359	.3642	1.1928
0.3333	-11.97362	2.06358	2.50000	.00000	-1.77626	.07329	.00000	-.38117	.3821	1.0436
0.5000	-9.12315	1.78482	2.60000	.00000	-1.94059	.08684	.00000	-.37239	.4081	.9557
0.6250	-7.70148	1.62326	2.60000	.00000	-2.01584	.09460	.00000	-.35700	.4242	.8847
1.0000	-4.46472	1.24156	2.70000	.00000	-2.25138	.11635	.00000	-.30377	.4538	.8032
1.3333	-2.67167	1.03112	2.70000	.00000	-2.34731	.12639	.00000	-.26186	.4671	.8085
2.0000	-.51056	.76645	2.70000	.00000	-2.48971	.14173	.00000	-.20549	.4794	.7601
2.5000	.58917	.63923	2.70000	.00000	-2.55190	.14804	.00000	-.17378	.4851	.7445
3.3333	1.72806	.49782	2.70000	.00000	-2.64087	.15740	.00000	-.14160	.4934	.7441
4.1667	2.49641	.41405	2.70000	.00000	-2.69325	.16254	.00000	-.12105	.5013	.7317
5.0000	3.46126	.33544	2.80000	.00000	-2.80186	.16992	.00000	-.10713	.5099	.7289
6.2500	4.02502	.27487	2.80000	.00000	-2.85216	.17467	.00000	-.09403	.5238	.7311
6.6667	4.17095	.25933	2.80000	.00000	-2.86633	.17597	.00000	-.09083	.5305	.7369
8.3333	4.63032	.21818	2.80000	.00000	-2.90541	.17924	.00000	-.08205	.5480	.7543
10.0000	4.94207	.18877	2.80000	.00000	-2.93847	.18204	.00000	-.07672	.5658	.7549
12.5000	5.25826	.15855	2.80000	.00000	-2.97721	.18528	.00000	-.07200	.5789	.7578
14.2857	5.41104	.14236	2.80000	.00000	-3.00040	.18726	.00000	-.06993	.5861	.7629
16.6667	6.03843	.09752	2.90000	.00000	-3.11001	.19437	.00000	-.06812	.5929	.7703
18.1818	6.11753	.08905	2.90000	.00000	-3.12417	.19554	.00000	-.06731	.5968	.7691
20.0000	6.20019	.08062	2.90000	.00000	-3.13898	.19672	.00000	-.06658	.6022	.7758
25.0000	6.39121	.06416	2.90000	.00000	-3.17073	.19905	.00000	-.06525	.6195	.7866
31.0000	6.57730	.05102	2.90000	.00000	-3.19920	.20091	.00000	-.06426	.6289	.7907
40.0000	6.75933	.03739	2.90000	.00000	-3.23117	.20300	.00000	-.06354	.6285	.7873
50.0000	7.35410	-.00721	3.00000	.00000	-3.35245	.21111	.00000	-.06367	.6209	.7829
100.000	5.41652	.06158	2.80000	.00000	-3.15000	.20544	.00000	-.07217	.5713	.7445
PGA	5.19757	.07129	2.80000	.00000	-3.13247	.20485	.00000	-.07375	.5661	.7405
PGV	4.14085	.63457	2.50000	.00000	-2.88388	.20958	.00000	-.11455	.4471	--------

Table 3d
GULF COAST
REGRESSION COEFFICIENTS FOR THE SINGLE CORNER MODEL WITH VARIABLE MEDIUM STRESS DROP AS A FUNCTION OF MOMENT MAGNITUDE (M)

Freq. Hz	C1	C2	C4	C5	C6	C7	C8	C10	Parametric Sigma	Total Sigma
0.1000	-14.54986	2.30998	2.80000	.00000	-2.15716	.09152	.00000	-.34105	.5243	1.3791
0.2000	-9.25169	1.88136	3.10000	.00000	-2.51971	.11010	.00000	-.38752	.5604	1.2665
0.3333	-5.31480	1.49937	3.20000	.00000	-2.79932	.12984	.00000	-.37439	.5958	1.1393
0.5000	-1.92096	1.16422	3.30000	.00000	-3.08551	.15079	.00000	-.33869	.6159	1.0612
0.6250	.25617	.96349	3.40000	.00000	-3.30857	.16627	.00000	-.31189	.6233	.9956
1.0000	4.21778	.55654	3.50000	.00000	-3.70387	.19724	.00000	-.24619	.6483	.9271
1.3333	6.01523	.35576	3.50000	.00000	-3.87179	.21222	.00000	-.20693	.6622	.9349
2.0000	9.10831	.06810	3.60000	.00000	-4.24952	.24024	.00000	-.15976	.6850	.9040
2.5000	10.18655	-.04192	3.60000	.00000	-4.37417	.25066	.00000	-.13932	.6996	.8991
3.3333	2.43075	-.21755	3.70000	.00000	-4.69883	.27269	.00000	-.11900	.7208	.9109
4.1667	13.29372	-.29360	3.70000	.00000	-4.81633	.28167	.00000	-.10754	.7389	.9111
5.0000	13.93331	-.34606	3.70000	.00000	-4.90830	.28841	.00000	-.10055	.7556	.9177
6.2500	15.82366	-.46920	3.80000	.00000	-5.21303	.30744	.00000	-.09434	.7783	.9306
6.6667	16.02650	-.48449	3.80000	.00000	-5.24545	.30976	.00000	-.09294	.7850	.9369
8.3333	16.69027	-.53555	3.80000	.00000	-5.35752	.31804	.00000	-.08918	.8064	.9587
10.0000	17.18425	-.57629	3.80000	.00000	-5.44841	.32521	.00000	-.08711	.8192	.9596
12.5000	17.71756	-.62387	3.80000	.00000	-5.55455	.33408	.00000	-.08558	.8294	.9628
14.2857	17.99875	-.64981	3.80000	.00000	-5.61318	.33907	.00000	-.08507	.8339	.9664
16.6667	18.29779	-.67629	3.80000	.00000	-5.67576	.34425	.00000	-.08473	.8396	.9730
18.1818	18.46167	-.68951	3.80000	.00000	-5.70923	.34685	.00000	-.08461	.8438	.9733
20.0000	18.64419	-.70300	3.80000	.00000	-5.74551	.34952	.00000	-.08451	.8491	.9799
25.0000	20.50874	-.81779	3.90000	.00000	-6.06641	.36944	.00000	-.08430	.8566	.9842
31.0000	20.89870	-.84219	3.90000	.00000	-6.14187	.37424	.00000	-.08421	.8572	.9821
40.0000	19.78142	-.78593	3.80000	.00000	-5.97732	.36646	.00000	-.08469	.8487	.9722
50.0000	19.88182	-.80582	3.80000	.00000	-6.01166	.37073	.00000	-.08525	.8430	.9685
100.000	16.81947	-.70860	3.70000	.00000	-5.55741	.35763	.00000	-.09091	.7733	.9088
PGA	15.27441	-.61726	3.60000	.00000	-5.30301	.34239	.00000	-.09155	.7666	.9031
PGV	11.09786	.03822	3.20000	.00000	-4.40038	.33709	.00000	-.14227	.5888	--------

Table 3e
GULF COAST
REGRESSION COEFFICIENTS FOR THE SINGLE CORNER MODEL WITH VARIABLE LOW STRESS DROP AS A FUNCTION OF MOMENT MAGNITUDE (M)

Freq. Hz	C1	C2	C4	C5	C6	C7	C8	C10	Parametric	Total
									Sigma	Sigma
0.1000	-14.25163	2.23220	2.80000	.00000	-2.13620	.09013	.00000	-.37542	.5238	1.3790
0.2000	-9.24105	1.78174	3.00000	.00000	-2.43210	.10715	.00000	-.39711	.5660	1.2690
0.3333	-4.86624	1.36569	3.20000	.00000	-2.78892	.13082	.00000	-.36709	.6020	1.1426
0.5000	-1.52175	1.02753	3.30000	.00000	-3.07493	.15219	.00000	-.32102	.6191	1.0631
0.6250	.60771	.82916	3.40000	.00000	-3.29808	.16792	.00000	-.29094	.6251	.9968
1.0000	4.38270	.44249	3.50000	.00000	-3.68677	.19846	.00000	-.22467	.6480	.9268
1.3333	6.03088	.26122	3.50000	.00000	-3.84799	.21274	.00000	-.18860	.6618	.9346
2.0000	8.91163	.00198	3.60000	.00000	-4.21624	.23987	.00000	-.14814	.6857	.9045
2.5000	9.88541	-.09326	3.60000	.00000	-4.33601	.24975	.00000	-.13159	.7008	.9001
3.3333	11.99662	-.25104	3.70000	.00000	-4.65152	.27084	.00000	-.11582	.7220	.9119
4.1667	12.77568	-.31521	3.70000	.00000	-4.76255	.27903	.00000	-.10726	.7399	.9119
5.0000	13.35601	-.35932	3.70000	.00000	-4.84920	.28512	.00000	-.10218	.7562	.9182
6.2500	15.16957	-.47298	3.80000	.00000	-5.14508	.30322	.00000	-.09778	.7782	.9305
6.6667	15.35608	-.48604	3.80000	.00000	-5.17562	.30531	.00000	-.09680	.7848	.9367
8.3333	15.96772	-.53011	3.80000	.00000	-5.28098	.31278	.00000	-.09419	.8054	.9578
10.0000	16.42234	-.56572	3.80000	.00000	-5.36596	.31923	.00000	-.09279	.8177	.9583
12.5000	16.90986	-.60751	3.80000	.00000	-5.46428	.32715	.00000	-.09179	.8272	.9609
14.2857	17.16559	-.63027	3.80000	.00000	-5.51821	.33158	.00000	-.09148	.8313	.9642
16.6667	17.43775	-.65344	3.80000	.00000	-5.57562	.33613	.00000	-.09130	.8366	.9704
18.1818	18.95886	-.74635	3.30000	.00000	-5.83325	.35180	.00000	-.09125	.8406	.9705
20.0000	19.13672	-.75882	3.90000	.00000	-5.86837	.35426	.00000	-.09122	.8457	.9770
25.0000	19.56869	-.78618	3.90000	.00000	-5.95141	.35968	.00000	-.09113	.8530	.9811
31.0000	19.93414	-.80760	3.90000	.00000	-6.02190	.36387	.00000	-.09109	.8534	.9788
40.0000	18.81796	-.75053	3.80000	.00000	-5.85612	.35579	.00000	-.09155	.8448	.9688
50.0000	18.89574	-.76779	3.80000	.00000	-5.88521	.35942	.00000	-.09203	.8391	.9651
100.000	15.86483	-.67427	3.70000	.00000	-5.43083	.34620	.00000	-.09664	.7699	.9060
PGA	14.35825	-.58678	3.60000	.00000	-5.18268	.33157	.00000	-.09714	.7633	.9003
PGV	10.31697	.06538	3.20000	.00000	-4.25855	.32343	.00000	-.15899	.5854	---------

Table 3f
GULF COAST
REGRESSION COEFFICIENTS FOR THE SINGLE CORNER MODEL WITH VARIABLE HIGH STRESS DROP AS A FUNCTION OF MOMENT MAGNITUDE (M)

Freq. Hz	C1	C2	C4	C5	C6	C7	C8	C10	Parametric	Total
									Sigma	Sigma
0.1000	-13.91863	2.33294	3.00000	.00000	-2.33817	.09908	.00000	-.29154	.5321	1.3821
0.2000	-9.02136	1.95631	3.20000	.00000	-2.64856	.11437	.00000	-.36070	.5624	1.2674
0.3333	-5.06249	1.59204	3.30000	.00000	-2.93546	.13367	.00000	-.36500	.5952	1.1390
0.5000	-1.56307	1.26035	3.40000	.00000	-3.23534	.15492	.00000	-.34181	.6174	1.0621
0.6250	.72588	1.05610	3.50000	.00000	-3.47121	.17081	.00000	-.32004	.6268	.9978
1.0000	4.94057	.63072	3.60000	.00000	-3.88811	.20282	.00000	-.25891	.6554	.9321
1.3333	6.90409	.41108	3.60000	.00000	-4.06719	.21878	.00000	-.21837	.6699	.9403
2.0000	10.33931	.08773	3.70000	.00000	-4.47467	.24889	.00000	-.16562	.6920	.9093
2.5000	11.55566	-.03985	3.70000	.00000	-4.60821	.26010	.00000	-.14124	.7057	.9039
3.3333	12.94874	-.17886	3.70000	.00000	-4.77368	.27355	.00000	-.11589	.7259	.9150
4.1667	15.04806	-.33259	3.80000	.00000	-5.08734	.29385	.00000	-.10095	.7440	.9152
5.0000	15.77669	-.39607	3.80000	.00000	-5.18780	.30141	.00000	-.09155	.7605	.9217
6.2500	16.59083	-.46325	3.80000	.00000	-5.30738	.31025	.00000	-.08296	.7833	.9348
6.6667	16.81254	-.48116	3.80000	.00000	-5.34165	.31279	.00000	-.08098	.7902	.9412
8.3333	18.86865	-.61723	3.90000	.00000	-5.68075	.33451	.00000	-.07559	.8121	.9635
10.0000	19.43335	-.66605	3.90000	.00000	-5.78203	.34275	.00000	-.07256	.8254	.9649
12.5000	20.04863	-.72294	3.90000	.00000	-5.90140	.35305	.00000	-.07023	.8362	.9687
14.2857	20.37544	-.75402	3.90000	.00000	-5.96788	.35891	.00000	-.06938	.8411	.9726
16.6667	20.72257	-.78585	3.90000	.00000	-6.03900	.36501	.00000	-.06877	.8471	.9795
18.1818	20.91108	-.80174	3.90000	.00000	-6.07691	.36809	.00000	-.06854	.8515	.9800
20.0000	21.11875	-.81789	3.90000	.00000	-6.11772	.37124	.00000	-.06833	.8568	.9866
25.0000	21.61053	-.85260	3.90000	.00000	-6.21225	.37806	.00000	-.06793	.8646	.9912
31.0000	22.02865	-.88044	3.90000	.00000	-6.29329	.38353	.00000	-.06773	.8653	.9892
40.0000	22.40623	-.91637	3.90000	.00000	-6.37768	.39115	.00000	-.06821	.8569	.9794
50.0000	22.54184	-.94055	3.90000	.00000	-6.41953	.39634	.00000	-.06885	.8514	.9758
100.000	17.92864	-.74769	3.70000	.00000	-5.71493	.36837	.00000	-.07577	.7814	.9157
PGA	17.56501	-.73081	3.70000	.00000	-5.65962	.36566	.00000	-.07661	.7747	.9100
PGV	12.88457	-.06337	3.30000	.00000	-4.71837	.36161	.00000	-.11586	.5984	---------

Table 4a
MIDCONTINENT
REGRESSION COEFFICIENTS FOR THE SINGLE CORNER MODEL WITH CONSTANT MEDIUM STRESS DROP

Freq. Hz	C1	C2	C4	C5	C6	C7	C8	C10	Parametric Sigma	Total Sigma
0.1000	-19.48096	2.63369	2.10000	.00000	-1.40816	.05251	.00000	-.27037	.3494	1.3226
0.2000	-15.60343	2.34394	2.30000	.00000	-1.55118	.05960	.00000	-.34570	.3630	1.1924
0.3333	-12.32672	2.03581	2.40000	.00000	-1.70046	.07122	.00000	-.35378	.3863	1.0451
0.5000	-9.51015	1.74832	2.50000	.00000	-1.86136	.08496	.00000	-.33001	.4110	.9570
0.6250	-8.14308	1.58833	2.50000	.00000	-1.93245	.09238	.00000	-.30768	.4231	.8842
1.0000	-5.12369	1.22405	2.60000	.00000	-2.15471	.11324	.00000	-.24573	.4432	.7972
1.3333	-3.47330	1.02939	2.60000	.00000	-2.24741	.12308	.00000	-.20234	.4523	.8000
2.0000	-1.58285	.79993	2.60000	.00000	-2.37885	.13729	.00000	-.15090	.4641	.7506
2.5000	-.65379	.69665	2.60000	.00000	-2.43570	.14303	.00000	-.12494	.4715	.7357
3.3333	.28490	.58358	2.60000	.00000	-2.51730	.15162	.00000	-.10016	.4819	.7365
4.1667	.91433	.51993	2.60000	.00000	-2.56449	.15619	.00000	-.08536	.4912	.7248
5.0000	1.74233	.45792	2.70000	.00000	-2.66338	.16286	.00000	-.07586	.5006	.7224
6.2500	2.19706	.41304	2.70000	.00000	-2.70779	.16694	.00000	-.06715	.5151	.7249
6.6667	2.31425	.40161	2.70000	.00000	-2.72023	.16804	.00000	-.06508	.5220	.7308
8.3333	2.69216	.37212	2.70000	.00000	-2.75418	.17072	.00000	-.05952	.5397	.7483
10.0000	2.94690	.35069	2.70000	.00000	-2.78273	.17300	.00000	-.05619	.5576	.7487
12.5000	3.20588	.32832	2.70000	.00000	-2.81616	.17563	.00000	-.05326	.5706	.7515
14.2857	3.75552	.29046	2.80000	.00000	-2.91238	.18175	.00000	-.05199	.5777	.7565
16.6667	3.88344	.27758	2.80000	.00000	-2.93512	.18355	.00000	-.05087	.5842	.7636
18.1818	3.94814	.27096	2.80000	.00000	-2.94748	.18451	.00000	-.05038	.5881	.7624
20.0000	4.01659	.26433	2.80000	.00000	-2.96045	.18549	.00000	-.04994	.5935	.7691
25.0000	4.18017	.25125	2.80000	.00000	-2.98855	.18741	.00000	-.04913	.6107	.7797
31.0000	4.34502	.24062	2.80000	.00000	-3.01413	.18897	.00000	-.04850	.6201	.7837
40.0000	4.98360	.20066	2.90000	.00000	-3.12766	.19576	.00000	-.04804	.6195	.7802
50.0000	5.03110	.19000	2.90000	.00000	-3.15204	.19790	.00000	-.04818	.6115	.7754
100.000	3.65796	.22258	2.80000	.00000	-3.03868	.19703	.00000	-.05457	.5613	.7369
PGA	3.00730	.25858	2.70000	.00000	-2.94208	.19152	.00000	-.05571	.5561	.7329
PGV	2.34185	.79105	2.40000	.00000	-2.69614	.19476	.00000	-.10359	.4380	--------

Table 4b
MIDCONTINENT
REGRESSION COEFFICIENTS FOR THE SINGLE CORNER MODEL WITH CONSTANT LOW STRESS DROP

Freq. Hz	C1	C2	C4	C5	C6	C7	C8	C10	Parametric Sigma	Total Sigma
0.1000	-19.09237	2.55127	2.10000	.00000	-1.41992	.05359	.00000	-.29994	.3543	1.3239
0.2000	-15.22296	2.22463	2.20000	.00000	-1.53646	.06087	.00000	-.35343	.3702	1.1946
0.3333	-11.90955	1.89523	2.30000	.00000	-1.68527	.07303	.00000	-.34299	.3983	1.0496
0.5000	-9.12644	1.60015	2.40000	.00000	-1.84330	.08701	.00000	-.30641	.4221	.9618
0.6250	-7.79761	1.44039	2.40000	.00000	-1.91307	.09450	.00000	-.27892	.4320	.8885
1.0000	-4.89906	1.08390	2.50000	.00000	-2.13693	.11627	.00000	-.21228	.4482	.8000
1.3333	-3.33687	.89916	2.50000	.00000	-2.23329	.12682	.00000	-.16950	.4562	.8022
2.0000	-1.58102	.68709	2.50000	.00000	-2.36933	.14193	.00000	-.12239	.4684	.7532
2.5000	-.72368	.59402	2.50000	.00000	-2.43076	.14840	.00000	-.10021	.4767	.7391
3.3333	.13269	.49251	2.50000	.00000	-2.51516	.15754	.00000	-.07959	.4879	.7405
4.1667	.71018	.43636	2.50000	.00000	-2.56429	.16246	.00000	-.06770	.4977	.7292
5.0000	1.13055	.40133	2.50000	.00000	-2.59747	.16549	.00000	-.06026	.5075	.7272
6.2500	1.90139	.34023	2.60000	.00000	-2.70593	.17349	.00000	-.05345	.5223	.7301
6.6667	2.00886	.33012	2.60000	.00000	-2.71828	.17461	.00000	-.05184	.5291	.7359
8.3333	2.36108	.30408	2.60000	.00000	-2.75216	.17736	.00000	-.04754	.5470	.7536
10.0000	2.59748	.28497	2.60000	.00000	-2.78005	.17962	.00000	-.04496	.5648	.7541
12.5000	2.83795	.26482	2.60000	.00000	-2.81238	.18218	.00000	-.04266	.5778	.7570
14.2857	2.95159	.25367	2.60000	.00000	-2.83154	.18373	.00000	-.04164	.5848	.7619
16.6667	3.47181	.21711	2.70000	.00000	-2.92538	.18980	.00000	-.04075	.5913	.7691
18.1818	3.53102	.21106	2.70000	.00000	-2.93706	.19071	.00000	-.04035	.5952	.7678
20.0000	3.59389	.20500	2.70000	.00000	-2.94929	.19162	.00000	-.03999	.6005	.7745
25.0000	3.74605	.19303	2.70000	.00000	-2.97578	.19341	.00000	-.03934	.6175	.7850
31.0000	3.90146	.18325	2.70000	.00000	-2.99999	.19487	.00000	-.03882	.6269	.7891
40.0000	4.50286	.14513	2.80000	.00000	-3.10735	.20134	.00000	-.03842	.6263	.7856
50.0000	4.54101	.13536	2.80000	.00000	-3.12969	.20328	.00000	-.03854	.6184	.7809
100.000	2.77858	.19423	2.60000	.00000	-2.94022	.19693	.00000	-.04397	.5680	.7420
PGA	2.57877	.20187	2.60000	.00000	-2.92333	.19630	.00000	-.04493	.5628	.7380
PGV	2.01678	.74196	2.30000	.00000	-2.65712	.19550	.00000	-.10331	.4439	--------

Table 4c
MIDCONTINENT
REGRESSION COEFFICIENTS FOR THE SINGLE CORNER MODEL WITH CONSTANT HIGH STRESS DROP

Freq. Hz	C1	C2	C4	C5	C6	C7	C8	C10	Parametric Sigma	Total Sigma
0.1000	-19.70343	2.68814	2.10000	.00000	-1.41959	.05456	.00000	-.23554	.3441	1.3212
0.2000	-16.02752	2.44418	2.30000	.00000	-1.55334	.06006	.00000	-.32899	.3574	1.1907
0.3333	-12.85572	2.16545	2.40000	.00000	-1.69535	.07035	.00000	-.35582	.3756	1.0412
0.5000	-10.06892	1.89280	2.50000	.00000	-1.85191	.08324	.00000	-.34592	.3980	.9514
0.6250	-8.68001	1.73516	2.50000	.00000	-1.92392	.09060	.00000	-.32977	.4113	.8786
1.0000	-5.55701	1.36536	2.60000	.00000	-2.14802	.11128	.00000	-.27558	.4357	.7931
1.3333	-3.81429	1.16106	2.60000	.00000	-2.24164	.12109	.00000	-.23358	.4473	.7972
2.0000	-1.74607	.90876	2.60000	.00000	-2.37871	.13582	.00000	-.17883	.4603	.7482
2.5000	-.70305	.78942	2.60000	.00000	-2.43840	.14185	.00000	-.14883	.4676	.7332
3.3333	.36441	.65805	2.60000	.00000	-2.52362	.15080	.00000	-.11897	.4780	.7340
4.1667	1.08397	.58122	2.60000	.00000	-2.57366	.15569	.00000	-.10026	.4874	.7223
5.0000	1.97802	.50970	2.70000	.00000	-2.67484	.16259	.00000	-.08779	.4971	.7200
6.2500	2.50153	.45480	2.70000	.00000	-2.72265	.16707	.00000	-.07615	.5121	.7228
6.6667	2.63659	.44078	2.70000	.00000	-2.73607	.16829	.00000	-.07333	.5192	.7288
8.3333	3.06506	.40391	2.70000	.00000	-2.77296	.17133	.00000	-.06565	.5375	.7468
10.0000	3.35414	.37757	2.70000	.00000	-2.80403	.17391	.00000	-.06102	.5558	.7474
12.5000	3.64678	.35047	2.70000	.00000	-2.84039	.17689	.00000	-.05692	.5693	.7505
14.2857	4.21631	.31022	2.80000	.00000	-2.93884	.18324	.00000	-.05514	.5766	.7556
16.6667	4.36033	.29517	2.80000	.00000	-2.96337	.18525	.00000	-.05357	.5834	.7630
18.1818	4.43278	.28752	2.80000	.00000	-2.97664	.18632	.00000	-.05287	.5875	.7619
20.0000	4.50882	.27990	2.80000	.00000	-2.99056	.18741	.00000	-.05224	.5930	.7687
25.0000	4.68655	.26499	2.80000	.00000	-3.02045	.18954	.00000	-.05109	.6105	.7795
31.0000	4.86194	.25301	2.80000	.00000	-3.04739	.19126	.00000	-.05023	.6201	.7837
40.0000	5.51533	.21155	2.90000	.00000	-3.16325	.19826	.00000	-.04959	.6197	.7803
50.0000	5.57118	.19995	2.90000	.00000	-3.18948	.20062	.00000	-.04972	.6119	.7757
100.000	4.18329	.23483	2.80000	.00000	-3.08048	.20033	.00000	-.05744	.5616	.7371
PGA	3.52033	.27213	2.70000	.00000	-2.98288	.19476	.00000	-.05886	.5564	.7140
PGV	2.71517	.80995	2.40000	.00000	-2.74660	.19917	.00000	-.09791	.4373	--------

Table 4d
GULF COAST
REGRESSION COEFFICIENTS FOR THE SINGLE CORNER MODEL WITH CONSTANT MEDIUM STRESS DROP

Freq. Hz	C1	C2	C4	C5	C6	C7	C8	C10	Parametric Sigma	Total Sigma
0.1000	-14.97295	2.37485	2.80000	.00000	-2.14967	.09041	.00000	-.29863	.5217	1.3782
0.2000	-9.72740	1.95572	3.10000	.00000	-2.51098	.10865	.00000	-.34332	.5587	1.2658
0.3333	-5.83777	1.58067	3.20000	.00000	-2.78845	.12797	.00000	-.32881	.5920	1.1373
0.5000	-2.48893	1.25139	3.30000	.00000	-3.07316	.14866	.00000	-.29199	.6097	1.0576
0.6250	-.33936	1.05439	3.40000	.00000	-3.29591	.16405	.00000	-.26496	.6163	.9913
1.0000	3.53746	.65933	3.50000	.00000	-3.68869	.19464	.00000	-.20041	.6409	.9219
1.3333	5.26938	.46791	3.50000	.00000	-3.85384	.20926	.00000	-.16290	.6556	.9302
2.0000	8.26540	.19447	3.60000	.00000	-4.22696	.23667	.00000	-.11889	.6802	.9004
2.5000	9.29703	.09136	3.60000	.00000	-4.34955	.24683	.00000	-.10023	.6958	.8962
3.3333	11.47972	-.07511	3.70000	.00000	-4.66998	.26828	.00000	-.08198	.7177	.9085
4.1667	12.30467	-.14553	3.70000	.00000	-4.78472	.27690	.00000	-.07185	.7363	.9090
5.0000	12.91716	-.19398	3.70000	.00000	-4.87438	.28333	.00000	-.06574	.7531	.9156
6.2500	14.76997	-.31160	3.80000	.00000	-5.17479	.30176	.00000	-.06037	.7758	.9285
6.6667	14.96522	-.32579	3.80000	.00000	-5.20638	.30397	.00000	-.05917	.7825	.9348
8.3333	15.60406	-.37326	3.80000	.00000	-5.31533	.31184	.00000	-.05594	.8038	.9565
10.0000	16.07898	-.41128	3.80000	.00000	-5.40344	.31863	.00000	-.05418	.8166	.9574
12.5000	16.58985	-.45572	3.80000	.00000	-5.50586	.32700	.00000	-.05288	.8266	.9604
14.2857	16.85850	-.47991	3.80000	.00000	-5.56225	.33169	.00000	-.05245	.8310	.9639
16.6667	17.14437	-.50458	3.80000	.00000	-5.62237	.33654	.00000	-.05218	.8365	.9704
18.1818	18.68342	-.59824	3.90000	.00000	-5.88319	.35235	.00000	-.05209	.8407	.9706
20.0000	18.86815	-.61146	3.90000	.00000	-5.91969	.35496	.00000	-.05201	.8459	.9771
25.0000	19.31416	-.64033	3.90000	.00000	-6.00557	.36070	.00000	-.05184	.8533	.9814
31.0000	19.69186	-.66304	3.90000	.00000	-6.07864	.36517	.00000	-.05176	.8538	.9791
40.0000	18.57590	-.60707	3.80000	.00000	-5.91373	.35737	.00000	-.05222	.8453	.9692
50.0000	18.66451	-.62536	3.80000	.00000	-5.94544	.36127	.00000	-.05272	.8395	.9655
100.000	15.61583	-.53024	3.70000	.00000	-5.49076	.34812	.00000	-.05781	.7697	.9057
PGA	14.09083	-.44176	3.60000	.00000	-5.23954	.33332	.00000	-.05839	.7630	.9000
PGV	10.05725	.19114	3.20000	.00000	-4.32766	.32682	.00000	-.10589	.5846	---------

Table 4e
GULF COAST
REGRESSION COEFFICIENTS FOR THE SINGLE CORNER MODEL WITH CONSTANT LOW STRESS DROP

Freq. Hz	C1	C2	C4	C5	C6	C7	C8	C10	Parametric Sigma	Total Sigma
0.1000	-14.51574	2.27743	2.80000	.00000	-2.16004	.09156	.00000	-.32210	.5189	1.3771
0.2000	-9.56051	1.83677	3.00000	.00000	-2.45407	.10808	.00000	-.34227	.5606	1.2666
0.3333	-5.22266	1.42630	3.20000	.00000	-2.81135	.13160	.00000	-.31057	.5946	1.1387
0.5000	-1.89095	1.08997	3.30000	.00000	-3.10319	.15363	.00000	-.26352	.6106	1.0581
0.6250	-.39847	.92377	3.30000	.00000	-3.22226	.16458	.00000	-.23333	.6166	.9915
1.0000	3.27417	.54493	3.40000	.00000	-3.60867	.19579	.00000	-.16807	.6406	.9217
1.3333	5.67074	.32399	3.50000	.00000	-3.90708	.21814	.00000	-.13325	.6561	.9306
2.0000	7.67899	.11381	3.50000	.00000	-4.13972	.23879	.00000	-.09489	.6821	.9018
2.5000	8.63053	.02055	3.50000	.00000	-4.26127	.24915	.00000	-.07940	.6984	.8982
3.3333	10.65378	-.13196	3.60000	.00000	-4.56857	.27022	.00000	-.06472	.7206	.9108
4.1667	11.41205	-.19463	3.60000	.00000	-4.67925	.27864	.00000	-.05678	.7393	.9114
5.0000	13.03902	-.29926	3.70000	.00000	-4.94340	.29508	.00000	-.05208	.7561	.9181
6.2500	13.69482	-.34602	3.70000	.00000	-5.04794	.30235	.00000	-.04799	.7783	.9306
6.6667	13.87411	-.35857	3.70000	.00000	-5.07762	.30440	.00000	-.04708	.7849	.9368
8.3333	14.45860	-.40049	3.70000	.00000	-5.17926	.31164	.00000	-.04464	.8058	.9582
10.0000	16.11475	-.50595	3.80000	.00000	-5.46456	.32967	.00000	-.04331	.8180	.9586
12.5000	16.59372	-.54655	3.80000	.00000	-5.56147	.33740	.00000	-.04233	.8274	.9611
14.2857	16.84332	-.56847	3.80000	.00000	-5.61422	.34167	.00000	-.04202	.8314	.9642
16.6667	17.10860	-.59071	3.80000	.00000	-5.67026	.34603	.00000	-.04182	.8366	.9705
18.1818	17.25532	-.60178	3.80000	.00000	-5.70035	.34821	.00000	-.04176	.8406	.9705
20.0000	17.42110	-.61316	3.80000	.00000	-5.73333	.35047	.00000	-.04171	.8457	.9770
25.0000	17.82567	-.63820	3.80000	.00000	-5.81156	.35548	.00000	-.04159	.8529	.9810
31.0000	18.16727	-.65766	3.80000	.00000	-5.87782	.35931	.00000	-.04152	.8532	.9786
40.0000	18.45810	-.68363	3.80000	.00000	-5.94442	.36483	.00000	-.04192	.8446	.9686
50.0000	17.18549	-.61880	3.70000	.00000	-5.74801	.35480	.00000	-.04232	.8390	.9650
100.000	14.28559	-.52896	3.60000	.00000	-5.31196	.34179	.00000	-.04658	.7693	.9054
PGA	13.95924	-.51587	3.60000	.00000	-5.26211	.33959	.00000	-.04706	.7628	.8999
PGV	9.08776	.19911	3.10000	.00000	-4.16032	.31577	.00000	-.10714	.5825	--------

Table 4f
GULF COAST
REGRESSION COEFFICIENTS FOR THE SINGLE CORNER MODEL WITH CONSTANT HIGH STRESS DROP

Freq. Hz	C1	C2	C4	C5	C6	C7	C8	C10	Parametric Sigma	Total Sigma
0.1000	-14.92343	2.43027	2.90000	.00000	-2.22382	.09485	.00000	-.26850	.5246	1.3793
0.2000	-10.18213	2.06757	3.10000	.00000	-2.51603	.10917	.00000	-.33532	.5581	1.2655
0.3333	-6.35091	1.71518	3.20000	.00000	-2.78676	.12722	.00000	-.33853	.5890	1.1358
0.5000	-2.37232	1.36543	3.40000	.00000	-3.17502	.15221	.00000	-.31410	.6076	1.0564
0.6250	-.80232	1.19788	3.40000	.00000	-3.29152	.16227	.00000	-.29176	.6151	.9905
1.0000	3.21915	.78973	3.50000	.00000	-3.68683	.19276	.00000	-.23069	.6418	.9225
1.3333	5.08922	.58119	3.50000	.00000	-3.85783	.20794	.00000	-.19127	.6568	.9311
2.0000	8.29484	.28003	3.60000	.00000	-4.23968	.23616	.00000	-.14131	.6810	.9010
2.5000	9.43320	.16200	3.60000	.00000	-4.36652	.24675	.00000	-.11874	.6963	.8966
3.3333	11.74743	-.02246	3.70000	.00000	-4.69411	.26892	.00000	-.09568	.7183	.9090
4.1667	12.66006	-.10531	3.70000	.00000	-4.81457	.27820	.00000	-.08232	.7373	.9098
5.0000	13.33561	-.16266	3.70000	.00000	-4.90916	.28523	.00000	-.07402	.7547	.9170
6.2500	15.26405	-.29006	3.80000	.00000	-5.21720	.30448	.00000	-.06652	.7780	.9303
6.6667	15.47703	-.30669	3.80000	.00000	-5.25065	.30691	.00000	-.06481	.7850	.9369
8.3333	16.17236	-.36176	3.80000	.00000	-5.36632	.31558	.00000	-.06017	.8071	.9592
10.0000	16.69021	-.40538	3.80000	.00000	-5.46052	.32310	.00000	-.05758	.8206	.9608
12.5000	17.25027	-.45606	3.80000	.00000	-5.57097	.33242	.00000	-.05561	.8315	.9646
14.2857	18.92158	-.56453	3.90000	.00000	-5.85972	.35100	.00000	-.05491	.8363	.9685
16.6667	19.25288	-.59416	3.90000	.00000	-5.92801	.35673	.00000	-.05441	.8422	.9753
18.1818	19.43335	-.60894	3.90000	.00000	-5.96446	.35961	.00000	-.05422	.8466	.9757
20.0000	19.63311	-.62400	3.90000	.00000	-6.00383	.36256	.00000	-.05406	.8520	.9824
25.0000	20.10895	-.65650	3.90000	.00000	-6.09544	.36898	.00000	-.05373	.8598	.9870
31.0000	20.51285	-.68238	3.90000	.00000	-6.17374	.37408	.00000	-.05357	.8604	.9849
40.0000	19.40352	-.62778	3.80000	.00000	-6.01142	.36670	.00000	-.05403	.8521	.9752
50.0000	19.51657	-.64891	3.80000	.00000	-6.04880	.37128	.00000	-.05461	.8464	.9715
100.000	16.44069	-.55019	3.70000	.00000	-5.59549	.35834	.00000	-.06084	.7761	.9112
PGA	16.08302	-.53416	3.70000	.00000	-5.54089	.35572	.00000	-.06160	.7693	.9054
PGV	10.74525	.17413	3.20000	.00000	-4.45009	.33923	.00000	-.09819	.5915	--------

Table 5a
MIDCONTINENT
REGRESSION COEFFICIENTS FOR THE SINGLE CORNER MODEL WITH CONSTANT MEDIUM STRESS DROP AND SATURATION

Freq. Hz	C1	C2	C4	C5	C6	C7	C8	C10	Parametric Sigma	Total Sigma
0.1000	-17.91423	2.37754	2.30000	.00000	-1.71861	.10433	.00000	-.28182	.3597	1.3253
0.2000	-13.91070	2.07364	2.50000	.00000	-1.88340	.11388	.00000	-.35716	.3757	1.1963
0.3333	-10.54155	1.75532	2.60000	.00000	-2.04882	.12727	.00000	-.36524	.4010	1.0506
0.5000	-7.62375	1.45642	2.70000	.00000	-2.22717	.14299	.00000	-.34147	.4264	.9637
0.6250	-6.23481	1.29417	2.70000	.00000	-2.30231	.15083	.00000	-.31913	.4385	.8917
1.0000	-3.08744	.91539	2.80000	.00000	-2.54658	.17419	.00000	-.25719	.4583	.8057
1.3333	-1.41000	.71797	2.80000	.00000	-2.64410	.18452	.00000	-.21379	.4674	.8087
2.0000	.51857	.48452	2.80000	.00000	-2.78232	.19943	.00000	-.16236	.4790	.7599
2.5000	1.46377	.37971	2.80000	.00000	-2.84201	.20543	.00000	-.13639	.4863	.7453
3.3333	2.42583	.26430	2.80000	.00000	-2.92775	.21443	.00000	-.11161	.4964	.7461
4.1667	3.06862	.19946	2.80000	.00000	-2.97730	.21920	.00000	-.09681	.5054	.7345
5.0000	3.53193	.15880	2.80000	.00000	-3.01048	.22207	.00000	-.08732	.5147	.7322
6.2500	4.46498	.08019	2.90000	.00000	-3.13934	.23200	.00000	-.07861	.5289	.7348
6.6667	4.58602	.06845	2.90000	.00000	-3.15246	.23315	.00000	-.07654	.5356	.7405
8.3333	4.97456	.03821	2.90000	.00000	-3.18830	.23596	.00000	-.07097	.5530	.7580
10.0000	5.23836	.01612	2.90000	.00000	-3.21848	.23835	.00000	-.06764	.5706	.7585
12.5000	5.50813	-.00703	2.90000	.00000	-3.25386	.24112	.00000	-.06471	.5834	.7612
14.2857	5.63835	-.01981	2.90000	.00000	-3.27511	.24282	.00000	-.06344	.5906	.7664
16.6667	6.30181	-.07040	3.00000	.00000	-3.39174	.25111	.00000	-.06233	.5972	.7736
18.1818	6.37083	-.07735	3.00000	.00000	-3.40488	.25213	.00000	-.06184	.6011	.7724
20.0000	6.44374	-.08429	3.00000	.00000	-3.41866	.25316	.00000	-.06139	.6063	.7790
25.0000	6.61705	-.09799	3.00000	.00000	-3.44851	.25520	.00000	-.06059	.6231	.7894
31.0000	6.79091	-.10914	3.00000	.00000	-3.47572	.25685	.00000	-.05996	.6323	.7934
40.0000	6.96175	-.12090	3.00000	.00000	-3.50625	.25870	.00000	-.05949	.6320	.7901
50.0000	7.60902	-.17372	3.10000	.00000	-3.63508	.26806	.00000	-.05964	.6240	.7853
100.000	5.56137	-.09020	2.90000	.00000	-3.40512	.25856	.00000	-.06603	.5741	.7467
PGA	5.35011	-.08193	2.90000	.00000	-3.38707	.25794	.00000	-.06717	.5689	.7427
PGV	4.40490	.47616	2.60000	.00000	-3.09544	.25711	.00000	-.11505	.4493	--------

Table 5b
MIDCONTINENT
REGRESSION COEFFICIENTS FOR THE SINGLE CORNER MODEL WITH CONSTANT LOW STRESS DROP AND SATURATION

Freq. Hz	C1	C2	C4	C5	C6	C7	C8	C10	Parametric Sigma	Total Sigma
0.1000	-17.52612	2.29529	2.30000	.00000	-1.73008	.10536	.00000	-.31139	.3654	1.3269
0.2000	-13.58249	1.96072	2.40000	.00000	-1.85975	.11403	.00000	-.36489	.3842	1.1990
0.3333	-9.90982	1.60565	2.60000	.00000	-2.07280	.13069	.00000	-.35444	.4138	1.0556
0.5000	-7.30278	1.31553	2.60000	.00000	-2.19863	.14381	.00000	-.31786	.4378	.9688
0.6250	-5.63265	1.13348	2.70000	.00000	-2.32961	.15521	.00000	-.29038	.4474	.8961
1.0000	-2.93381	.78321	2.70000	.00000	-2.51701	.17588	.00000	-.22374	.4634	.8086
1.3333	-1.34540	.59571	2.70000	.00000	-2.61803	.18691	.00000	-.18095	.4712	.8109
2.0000	.44711	.37973	2.70000	.00000	-2.76056	.20271	.00000	-.13385	.4831	.7625
2.5000	1.32039	.28510	2.70000	.00000	-2.82477	.20944	.00000	-.11167	.4912	.7485
3.3333	2.19908	.18130	2.70000	.00000	-2.91311	.21897	.00000	-.09104	.5021	.7499
4.1667	2.78943	.12398	2.70000	.00000	-2.96449	.22409	.00000	-.07915	.5117	.7389
5.0000	3.21855	.08824	2.70000	.00000	-2.99921	.22724	.00000	-.07171	.5213	.7369
6.2500	3.64126	.04811	2.70000	.00000	-3.04474	.23151	.00000	-.06490	.5358	.7398
6.6667	3.75047	.03785	2.70000	.00000	-3.05739	.23266	.00000	-.06330	.5426	.7456
8.3333	4.56076	-.02108	2.80000	.00000	-3.17249	.24111	.00000	-.05900	.5601	.7632
10.0000	4.80550	-.04079	2.80000	.00000	-3.20187	.24348	.00000	-.05641	.5777	.7638
12.5000	5.05581	-.06166	2.80000	.00000	-3.23598	.24617	.00000	-.05411	.5906	.7668
14.2857	5.17534	-.07324	2.80000	.00000	-3.25620	.24779	.00000	-.05310	.5976	.7718
16.6667	5.29605	-.08523	2.80000	.00000	-3.27840	.24954	.00000	-.05220	.6042	.7791
18.1818	5.35709	-.09141	2.80000	.00000	-3.29040	.25047	.00000	-.05181	.6081	.7779
20.0000	5.92808	-.13394	2.90000	.00000	-3.39211	.25767	.00000	-.05145	.6133	.7844
25.0000	6.08901	-.14646	2.90000	.00000	-3.42020	.25956	.00000	-.05080	.6300	.7949
31.0000	6.25258	-.15669	2.90000	.00000	-3.44589	.26109	.00000	-.05027	.6391	.7989
40.0000	6.41230	-.16752	2.90000	.00000	-3.47458	.26279	.00000	-.04987	.6388	.7956
50.0000	7.01484	-.21767	3.00000	.00000	-3.59567	.27165	.00000	-.04999	.6309	.7908
100.000	5.03603	-.13680	2.80000	.00000	-3.37101	.26174	.00000	-.05542	.5808	.7518
PGA	4.83071	-.12898	2.80000	.00000	-3.35311	.26108	.00000	-.05639	.5755	.7477
PGV	3.99963	.43627	2.50000	.00000	-3.04259	.25625	.00000	-.11476	.4549	--------

Table 5c
MIDCONTINENT
REGRESSION COEFFICIENTS FOR THE SINGLE CORNER MODEL WITH CONSTANT HIGH STRESS DROP AND SATURATION

Freq. Hz	C1	C2	C4	C5	C6	C7	C8	C10	Parametric Sigma	Total Sigma
0.1000	-17.92122	2.41939	2.40000	.00000	-1.76932	.10861	.00000	-.24700	.3539	1.3238
0.2000	-14.33292	2.17359	2.50000	.00000	-1.88598	.11439	.00000	-.34044	.3691	1.1943
0.3333	-11.07071	1.88506	2.60000	.00000	-2.04376	.12639	.00000	-.36727	.3895	1.0463
0.5000	-8.18384	1.60124	2.70000	.00000	-2.21757	.14122	.00000	-.35737	.4130	.9578
0.6250	-6.43297	1.42055	2.80000	.00000	-2.35414	.15261	.00000	-.34123	.4266	.8859
1.0000	-3.52171	1.05720	2.80000	.00000	-2.53979	.17215	.00000	-.28704	.4510	.8016
1.3333	-1.75176	.85016	2.80000	.00000	-2.63826	.18244	.00000	-.24504	.4627	.8060
2.0000	.35595	.59376	2.80000	.00000	-2.78233	.19789	.00000	-.19028	.4757	.7578
2.5000	1.41567	.47284	2.80000	.00000	-2.84495	.20419	.00000	-.16028	.4829	.7431
3.3333	2.50733	.33905	2.80000	.00000	-2.93443	.21356	.00000	-.13042	.4931	.7439
4.1667	3.24100	.26094	2.80000	.00000	-2.98696	.21867	.00000	-.11171	.5023	.7324
5.0000	3.76921	.21066	2.80000	.00000	-3.02221	.22178	.00000	-.09924	.5118	.7302
6.2500	4.77362	.12203	2.90000	.00000	-3.15491	.23211	.00000	-.08761	.5265	.7331
6.6667	4.91274	.10766	2.90000	.00000	-3.16905	.23338	.00000	-.08479	.5334	.7389
8.3333	5.35255	.06996	2.90000	.00000	-3.20795	.23656	.00000	-.07711	.5513	.7567
10.0000	5.65135	.04288	2.90000	.00000	-3.24075	.23928	.00000	-.07247	.5693	.7575
12.5000	5.95548	.01492	2.90000	.00000	-3.27916	.24241	.00000	-.06838	.5826	.7606
14.2857	6.10266	-.00018	2.90000	.00000	-3.30216	.24432	.00000	-.06659	.5900	.7659
16.6667	6.25069	-.01554	2.90000	.00000	-3.32741	.24639	.00000	-.06502	.5969	.7734
18.1818	6.86357	-.06114	3.00000	.00000	-3.43540	.25399	.00000	-.06433	.6009	.7723
20.0000	6.94435	-.06911	3.00000	.00000	-3.45017	.25514	.00000	-.06369	.6063	.7790
25.0000	7.13246	-.08472	3.00000	.00000	-3.48193	.25740	.00000	-.06255	.6234	.7897
31.0000	7.31723	-.09725	3.00000	.00000	-3.51057	.25921	.00000	-.06168	.6328	.7938
40.0000	7.49863	-.11031	3.00000	.00000	-3.54270	.26124	.00000	-.06105	.6326	.7906
50.0000	8.16024	-.16443	3.10000	.00000	-3.67439	.27088	.00000	-.06117	.6248	.7859
100.000	6.09264	-.07836	2.90000	.00000	-3.44793	.26192	.00000	-.06890	.5749	.7473
PGA	5.87466	-.06918	2.90000	.00000	-3.42987	.26131	.00000	-.07032	.5697	.7433
PGV	4.79171	.49399	2.60000	.00000	-3.14834	.26171	.00000	-.10937	.4492	-------

Table 5d
GULF COAST
REGRESSION COEFFICIENTS FOR THE SINGLE CORNER MODEL WITH CONSTANT MEDIUM STRESS DROP AND SATURATION

Freq. Hz	C1	C2	C4	C5	C6	C7	C8	C10	Parametric Sigma	Total Sigma
0.1000	-12.36761	2.03153	3.10000	.00000	-2.63877	.15707	.00000	-.31008	.5339	1.3828
0.2000	-7.18334	1.59845	3.30000	.00000	-2.98527	.17746	.00000	-.35477	.5716	1.2715
0.3333	-3.08593	1.20331	3.40000	.00000	-3.29709	.20010	.00000	-.34026	.6050	1.1441
0.5000	1.25366	.80656	3.60000	.00000	-3.74757	.23195	.00000	-.30344	.6221	1.0648
0.6250	2.84583	.63403	3.60000	.00000	-3.87433	.24315	.00000	-.27642	.6282	.9987
1.0000	7.02300	.20984	3.70000	.00000	-4.31520	.27841	.00000	-.21186	.6525	.9300
1.3333	8.82898	.01214	3.70000	.00000	-4.49285	.29408	.00000	-.17435	.6669	.9382
2.0000	12.13819	-.29103	3.80000	.00000	-4.91519	.32617	.00000	-.13035	.6911	.9086
2.5000	13.22694	-.39862	3.80000	.00000	-5.04733	.33707	.00000	-.11168	.7063	.9044
3.3333	14.47052	-.51361	3.80000	.00000	-5.20994	.34992	.00000	-.09344	.7278	.9165
4.1667	16.60473	-.66904	3.90000	.00000	-5.54036	.37238	.00000	-.08331	.7461	.9169
5.0000	17.26232	-.72060	3.90000	.00000	-5.63758	.37933	.00000	-.07720	.7626	.9235
6.2500	18.00368	-.77536	3.90000	.00000	-5.75279	.38735	.00000	-.07183	.7850	.9362
6.6667	18.20699	-.79010	3.90000	.00000	-5.78572	.38965	.00000	-.07062	.7917	.9425
8.3333	20.35514	-.93590	4.00000	.00000	-6.14146	.41343	.00000	-.06740	.8126	.9639
10.0000	20.87722	-.97756	4.00000	.00000	-6.23744	.42083	.00000	-.06563	.8251	.9646
12.5000	21.44261	-1.02649	4.00000	.00000	-6.34895	.42994	.00000	-.06434	.8350	.9676
14.2857	21.74098	-1.05317	4.00000	.00000	-6.41027	.43505	.00000	-.06391	.8394	.9711
16.6667	22.05839	-1.08042	4.00000	.00000	-6.47563	.44033	.00000	-.06363	.8448	.9775
18.1818	22.23245	-1.09401	4.00000	.00000	-6.51064	.44297	.00000	-.06354	.8489	.9777
20.0000	22.42674	-1.10792	4.00000	.00000	-6.54872	.44569	.00000	-.06346	.8540	.9841
25.0000	22.89529	-1.13831	4.00000	.00000	-6.63833	.45168	.00000	-.06330	.8613	.9883
31.0000	23.29188	-1.16219	4.00000	.00000	-6.71452	.45635	.00000	-.06322	.8618	.9861
40.0000	23.64102	-1.19389	4.00000	.00000	-6.79201	.46299	.00000	-.06368	.8532	.9761
50.0000	23.74361	-1.21411	4.00000	.00000	-6.82593	.46721	.00000	-.06417	.8477	.9726
100.000	18.80216	-.98785	3.80000	.00000	-6.06348	.43296	.00000	-.06926	.7782	.9130
PGA	18.44350	-.97271	3.80000	.00000	-6.00839	.43044	.00000	-.06984	.7716	.9073
PGV	13.42744	-.26637	3.40000	.00000	-4.94368	.41289	.00000	-.11734	.5929	--------

Table 5e
GULF COAST
REGRESSION COEFFICIENTS FOR THE SINGLE CORNER MODEL WITH CONSTANT LOW STRESS DROP AND SATURATION

Freq. Hz	C1	C2	C4	C5	C6	C7	C8	C10	Parametric Sigma	Total Sigma
0.1000	-12.34486	1.95845	3.00000	.00000	-2.57317	.15404	.00000	-.33355	.5320	1.3821
0.2000	-7.12762	1.49148	3.20000	.00000	-2.91057	.17493	.00000	-.35373	.5744	1.2728
0.3333	-2.46635	1.04807	3.40000	.00000	-3.32053	.20386	.00000	-.32203	.6080	1.1457
0.5000	1.09160	.68925	3.50000	.00000	-3.64922	.22956	.00000	-.27498	.6233	1.0655
0.6250	2.63452	.51855	3.50000	.00000	-3.77700	.24128	.00000	-.24479	.6289	.9992
1.0000	6.58784	.11210	3.60000	.00000	-4.20864	.27695	.00000	-.17953	.6525	.9300
1.3333	9.24442	-.13451	3.70000	.00000	-4.54798	.30336	.00000	-.14471	.6676	.9387
2.0000	11.35480	-.35323	3.70000	.00000	-4.79775	.32541	.00000	-.10635	.6930	.9101
2.5000	12.35996	-.45077	3.70000	.00000	-4.92830	.33648	.00000	-.09086	.7090	.9065
3.3333	14.67303	-.63086	3.80000	.00000	-5.28067	.36186	.00000	-.07617	.7309	.9190
4.1667	15.48361	-.69729	3.80000	.00000	-5.40014	.37090	.00000	-.06824	.7493	.9195
5.0000	16.08791	-.74305	3.80000	.00000	-5.49275	.37755	.00000	-.06353	.7658	.9261
6.2500	18.11166	-.87999	3.90000	.00000	-5.82243	.39947	.00000	-.05945	.7878	.9385
6.6667	18.30605	-.89356	3.90000	.00000	-5.85465	.40170	.00000	-.05854	.7942	.9446
8.3333	18.94247	-.93912	3.90000	.00000	-5.96502	.40954	.00000	-.05610	.8148	.9657
10.0000	19.41416	-.97570	3.90000	.00000	-6.05319	.41621	.00000	-.05476	.8269	.9662
12.5000	19.91774	-1.01826	3.90000	.00000	-6.15421	.42427	.00000	-.05379	.8362	.9687
14.2857	20.18058	-1.04126	3.90000	.00000	-6.20917	.42872	.00000	-.05347	.8403	.9719
16.6667	20.45986	-1.06460	3.90000	.00000	-6.26753	.43327	.00000	-.05328	.8454	.9780
18.1818	20.61413	-1.07622	3.90000	.00000	-6.29889	.43554	.00000	-.05322	.8493	.9781
20.0000	20.78819	-1.08818	3.90000	.00000	-6.33324	.43789	.00000	-.05317	.8543	.9844
25.0000	21.21243	-1.11449	3.90000	.00000	-6.41476	.44311	.00000	-.05305	.8614	.9884
31.0000	21.57041	-1.13489	3.90000	.00000	-6.48374	.44710	.00000	-.05297	.8618	.9861
40.0000	21.87723	-1.16223	3.90000	.00000	-6.55296	.45285	.00000	-.05337	.8530	.9759
50.0000	21.95228	-1.17915	3.90000	.00000	-6.58099	.45634	.00000	-.05377	.8474	.9723
100.000	17.30516	-.96734	3.70000	.00000	-5.85881	.42361	.00000	-.05803	.7783	.9131
PGA	16.96725	-.95374	3.70000	.00000	-5.80700	.42132	.00000	-.05852	.7718	.9075
PGV	12.26101	-.23705	3.30000	.00000	-4.74443	.39834	.00000	-.11859	.5911	--------

Table 5f
GULF COAST
REGRESSION COEFFICIENTS FOR THE SINGLE CORNER MODEL WITH CONSTANT HIGH STRESS DROP AND SATURATION

Freq. Hz	C1	C2	C4	C5	C6	C7	C8	C10	Parametric Sigma	Total Sigma
0.1000	-12.65135	2.09962	3.10000	.00000	-2.65372	.15931	.00000	-.27995	.5362	1.3837
0.2000	-7.63385	1.70983	3.30000	.00000	-2.99118	.17807	.00000	-.34677	.5704	1.2710
0.3333	-2.92833	1.29933	3.50000	.00000	-3.40943	.20580	.00000	-.34999	.6013	1.1422
0.5000	.76119	.94998	3.60000	.00000	-3.74466	.23048	.00000	-.32555	.6196	1.0634
0.6250	2.38331	.77804	3.60000	.00000	-3.87013	.24129	.00000	-.30322	.6270	.9980
1.0000	6.70599	.34088	3.70000	.00000	-4.31367	.27643	.00000	-.24215	.6534	.9306
1.3333	8.65230	.12586	3.70000	.00000	-4.49751	.29269	.00000	-.20273	.6683	.9392
2.0000	12.17467	-.20531	3.80000	.00000	-4.92914	.32564	.00000	-.15276	.6921	.9094
2.5000	13.37181	-.32798	3.80000	.00000	-5.06579	.33699	.00000	-.13019	.7071	.9050
3.3333	14.74399	-.46111	3.80000	.00000	-5.23503	.35058	.00000	-.10713	.7288	.9173
4.1667	16.97448	-.62936	3.90000	.00000	-5.57259	.37377	.00000	-.09378	.7475	.9181
5.0000	17.69717	-.69006	3.90000	.00000	-5.67505	.38135	.00000	-.08547	.7645	.9250
6.2500	18.50771	-.75440	3.90000	.00000	-5.79682	.39016	.00000	-.07798	.7875	.9383
6.6667	20.19141	-.86646	4.00000	.00000	-6.07056	.40801	.00000	-.07627	.7944	.9448
8.3333	20.94827	-.92609	4.00000	.00000	-6.19648	.41744	.00000	-.07162	.8162	.9669
10.0000	21.51625	-.97369	4.00000	.00000	-6.29904	.42562	.00000	-.06904	.8294	.9683
12.5000	22.13508	-1.02936	4.00000	.00000	-6.41929	.43578	.00000	-.06706	.8401	.9721
14.2857	22.46355	-1.05978	4.00000	.00000	-6.48596	.44153	.00000	-.06636	.8449	.9760
16.6667	22.81270	-1.09092	4.00000	.00000	-6.55721	.44750	.00000	-.06586	.8508	.9827
18.1818	23.00275	-1.10647	4.00000	.00000	-6.59524	.45051	.00000	-.06568	.8551	.9831
20.0000	23.21284	-1.12231	4.00000	.00000	-6.63632	.45359	.00000	-.06551	.8603	.9896
25.0000	23.71273	-1.15652	4.00000	.00000	-6.73191	.46030	.00000	-.06519	.8679	.9941
31.0000	24.13701	-1.18374	4.00000	.00000	-6.81358	.46562	.00000	-.06503	.8687	.9922
40.0000	24.51845	-1.21926	4.00000	.00000	-6.89791	.47308	.00000	-.06549	.8601	.9822
50.0000	24.64848	-1.24267	4.00000	.00000	-6.93799	.47804	.00000	-.06606	.8546	.9786
100.000	19.65149	-1.01014	3.80000	.00000	-6.17228	.44358	.00000	-.07230	.7848	.9186
PGA	19.28060	-.99348	3.80000	.00000	-6.11546	.44085	.00000	-.07305	.7781	.9129
PGV	14.16517	-.28835	3.40000	.00000	-5.07478	.42615	.00000	-.10965	.6001	--------

Table 6a
MIDCONTINENT
REGRESSION COEFFICIENTS FOR THE DOUBLE CORNER MODEL

Freq. Hz	C1	C2	C4	C5	C6	C7	C8	C10	Parametric Sigma	Total Sigma
0.1000	-17.74463	2.22485	2.10000	.00000	-1.40084	.05305	.00000	-.31641	.3559	1.3243
0.2000	-13.88893	1.89859	2.30000	.00000	-1.54772	.06068	.00000	-.28960	.3660	1.1933
0.3333	-11.04809	1.64665	2.40000	.00000	-1.70010	.07272	.00000	-.22943	.3892	1.0462
0.5000	-8.76880	1.45200	2.50000	.00000	-1.86494	.08722	.00000	-.18125	.4160	.9591
0.6250	-7.68301	1.34978	2.50000	.00000	-1.94573	.09603	.00000	-.16127	.4297	.8874
1.0000	-5.47019	1.12590	2.50000	.00000	-2.13473	.11710	.00000	-.13830	.4518	.8021
1.3333	-3.77355	.98718	2.60000	.00000	-2.28113	.13007	.00000	-.13323	.4610	.8050
2.0000	-1.95968	.80810	2.60000	.00000	-2.41132	.14449	.00000	-.12529	.4714	.7551
2.5000	-.96872	.71370	2.60000	.00000	-2.46500	.15003	.00000	-.11749	.4775	.7396
3.3333	.10920	.59537	2.60000	.00000	-2.54120	.15808	.00000	-.10506	.4865	.7395
4.1667	.86777	.52085	2.60000	.00000	-2.58506	.16235	.00000	-.09484	.4950	.7274
5.0000	1.42831	.46988	2.60000	.00000	-2.61380	.16486	.00000	-.08671	.5040	.7247
6.2500	1.99361	.41219	2.60000	.00000	-2.65510	.16868	.00000	-.07801	.5181	.7271
6.6667	2.14018	.39715	2.60000	.00000	-2.66676	.16973	.00000	-.07573	.5249	.7328
8.3333	2.60454	.35667	2.60000	.00000	-2.69927	.17238	.00000	-.06929	.5424	.7503
10.0000	3.30684	.30373	2.70000	.00000	-2.79751	.17893	.00000	-.06512	.5602	.7507
12.5000	3.62400	.27369	2.70000	.00000	-2.83163	.18170	.00000	-.06128	.5731	.7534
14.2857	3.77510	.25773	2.70000	.00000	-2.85226	.18339	.00000	-.05952	.5803	.7585
16.6667	3.92454	.24169	2.70000	.00000	-2.87495	.18521	.00000	-.05791	.5868	.7656
18.1818	3.99907	.23357	2.70000	.00000	-2.88734	.18619	.00000	-.05717	.5907	.7644
20.0000	4.07670	.22547	2.70000	.00000	-2.90040	.18720	.00000	-.05647	.5961	.7711
25.0000	4.69293	.18262	2.80000	.00000	-3.00672	.19396	.00000	-.05520	.6133	.7817
31.0000	4.86717	.17018	2.80000	.00000	-3.03252	.19560	.00000	-.05434	.6227	.7858
40.0000	5.03119	.15779	2.80000	.00000	-3.06134	.19746	.00000	-.05377	.6222	.7823
50.0000	5.06834	.14806	2.80000	.00000	-3.08409	.19935	.00000	-.05361	.6143	.7776
100.000	3.74623	.18152	2.70000	.00000	-2.98867	.19854	.00000	-.05734	.5644	.7392
PGA	3.54103	.18904	2.70000	.00000	-2.97418	.19819	.00000	-.05814	.5592	.7353
PGV	4.06989	.46794	2.50000	.00000	-2.77481	.19743	.00000	-.07606	.4408	--------

NOTE: PARAMETRIC SIGMA VALUES ARE FROM THE 1 CORNER VARIABLE STRESS DROP MODEL

Table 6b
GULF COAST
REGRESSION COEFFICIENTS FOR THE DOUBLE CORNER MODEL

Freq. Hz	C1	C2	C4	C5	C6	C7	C8	C10	Parametric Sigma	Total Sigma
0.1000	-16.41379	2.20767	2.50000	.00000	-1.74567	.06829	.00000	-.33131	.5243	1.3791
0.2000	-12.20468	1.83553	2.70000	.00000	-1.95111	.07737	.00000	-.29415	.5604	1.2665
0.3333	-8.83853	1.54958	2.90000	.00000	-2.21747	.09356	.00000	-.23217	.5958	1.1393
0.5000	-6.28665	1.33826	3.00000	.00000	-2.43987	.10973	.00000	-.18303	.6159	1.0612
0.6250	-5.10947	1.24004	3.00000	.00000	-2.53021	.11775	.00000	-.16323	.6233	.9956
1.0000	-2.15831	.99778	3.10000	.00000	-2.82918	.14191	.00000	-.13999	.6483	.9271
1.3333	-.12511	.83880	3.20000	.00000	-3.05030	.15823	.00000	-.13454	.6622	.9349
2.0000	1.93674	.64984	3.20000	.00000	-3.22152	.17312	.00000	-.12608	.6850	.9040
2.5000	2.99580	.55002	3.20000	.00000	-3.30621	.17993	.00000	-.11838	.6996	.8991
3.3333	4.87830	.39924	3.30000	.00000	-3.51506	.19281	.00000	-.10565	.7208	.9109
4.1667	5.74732	.31977	3.30000	.00000	-3.58708	.19746	.00000	-.09504	.7389	.9111
5.0000	7.09082	.22710	3.40000	.00000	-3.76365	.20689	.00000	-.08680	.7556	.9177
6.2500	7.79199	.16914	3.40000	.00000	-3.83080	.21046	.00000	-.07794	.7783	.9306
6.6667	7.97786	.15425	3.40000	.00000	-3.85005	.21146	.00000	-.07567	.7850	.9369
8.3333	9.36118	.06628	3.50000	.00000	-4.05250	.22188	.00000	-.06891	.8064	.9587
10.0000	9.79610	.03112	3.50000	.00000	-4.11197	.22526	.00000	-.06459	.8192	.9596
12.5000	10.26367	-.00857	3.50000	.00000	-4.18673	.22992	.00000	-.06062	.8294	.9628
14.2857	10.51625	-.03055	3.50000	.00000	-4.23161	.23289	.00000	-.05885	.8339	.9664
16.6667	11.69837	-.10103	3.60000	.00000	-4.43516	.24410	.00000	-.05724	.8396	.9730
18.1818	11.85646	-.11325	3.60000	.00000	-4.46406	.24596	.00000	-.05650	.8438	.9733
20.0000	12.02874	-.12544	3.60000	.00000	-4.49489	.24783	.00000	-.05578	.8491	.9799
25.0000	12.42738	-.15043	3.60000	.00000	-4.56505	.25176	.00000	-.05445	.8566	.9842
31.0000	13.81046	-.22653	3.70000	.00000	-4.80279	.26447	.00000	-.05370	.8572	.9821
40.0000	14.14384	-.25488	3.70000	.00000	-4.87587	.26995	.00000	-.05318	.8487	.9722
50.0000	14.33926	-.28175	3.70000	.00000	-4.93249	.27571	.00000	-.05331	.8430	.9685
100.000	11.07839	-.18783	3.50000	.00000	-4.49420	.26735	.00000	-.05801	.7733	.9088
PGA	9.90148	-.12757	3.40000	.00000	-4.30771	.25806	.00000	-.05882	.7666	.9031
PGV	8.13980	.18271	3.00000	.00000	-3.72218	.26644	.00000	-.08657	.5888	-------

NOTE: PARAMETRIC SIGMA VALUES ARE FROM THE 1 CORNER VARIABLE STRESS DROP MODEL
(MEDIUM STRESS DROP)

Table 7a
MIDCONTINENT
REGRESSION COEFFICIENTS FOR THE DOUBLE CORNER MODEL WITH SATURATION

Freq. Hz	C1	C2	C4	C5	C6	C7	C8	C10	Parametric	Total
									Sigma	Sigma
0.1000	-16.16329	1.96535	2.30000	.00000	-1.71374	.10547	.00000	-.32832	.3559	1.3243
0.2000	-12.17910	1.62451	2.50000	.00000	-1.88291	.11564	.00000	-.30150	.3660	1.1933
0.3333	-9.24347	1.36201	2.60000	.00000	-2.05193	.12954	.00000	-.24133	.3892	1.0462
0.5000	-6.86049	1.15548	2.70000	.00000	-2.23472	.14610	.00000	-.19315	.4160	.9591
0.6250	-5.75016	1.05061	2.70000	.00000	-2.32003	.15540	.00000	-.17317	.4297	.8874
1.0000	-3.10841	.79561	2.80000	.00000	-2.58562	.18195	.00000	-.15020	.4518	.8021
1.3333	-1.68010	.66971	2.80000	.00000	-2.68318	.19261	.00000	-.14513	.4610	.8050
2.0000	.17104	.48663	2.80000	.00000	-2.81997	.20773	.00000	-.13719	.4714	.7551
2.5000	1.17695	.39078	2.80000	.00000	-2.87626	.21352	.00000	-.12940	.4775	.7396
3.3333	2.27626	.27031	2.80000	.00000	-2.95623	.22193	.00000	-.11697	.4865	.7395
4.1667	3.04705	.19471	2.80000	.00000	-3.00223	.22639	.00000	-.10675	.4950	.7274
5.0000	3.61568	.14311	2.80000	.00000	-3.03239	.22900	.00000	-.09861	.5040	.7247
6.2500	4.19281	.08441	2.80000	.00000	-3.07579	.23300	.00000	-.08991	.5181	.7271
6.6667	4.34277	.06911	2.80000	.00000	-3.08805	.23409	.00000	-.08764	.5249	.7328
8.3333	4.81663	.02793	2.80000	.00000	-3.12224	.23686	.00000	-.08119	.5424	.7503
10.0000	5.13706	-.00173	2.80000	.00000	-3.15185	.23929	.00000	-.07703	.5602	.7507
12.5000	5.94942	-.06741	2.90000	.00000	-3.27328	.24822	.00000	-.07318	.5731	.7534
14.2857	6.10708	-.08387	2.90000	.00000	-3.29509	.25000	.00000	-.07142	.5803	.7585
16.6667	6.26384	-.10044	2.90000	.00000	-3.31911	.25192	.00000	-.06982	.5868	.7656
18.1818	6.34238	-.10886	2.90000	.00000	-3.33222	.25295	.00000	-.06908	.5907	.7644
20.0000	6.42423	-.11726	2.90000	.00000	-3.34604	.25401	.00000	-.06838	.5961	.7711
25.0000	6.61204	-.13370	2.90000	.00000	-3.37593	.25613	.00000	-.06711	6133	.7817
31.0000	7.33736	-.18563	3.00000	.00000	-3.49824	.26456	.00000	-.06625	.6227	7858
40.0000	7.51145	-.19862	3.00000	.00000	-3.52888	.26652	.00000	-.06568	.6222	.7823
50.0000	7.55648	-.20898	3.00000	.00000	-3.55306	.26853	.00000	-.06551	.6143	.7776
100.000	6.12213	-.16489	2.90000	.00000	-3.43941	.26601	.00000	-.06925	.5644	.7392
PGA	5.91196	-.15727	2.90000	.00000	-3.42401	.26564	.00000	-.07004	.5592	.7353
PGV	5.79531	.17529	2.60000	.00000	-3.11215	.25573	.00000	-.08796	.4408	------

NOTE: PARAMETRIC SIGMA VALUES ARE FROM THE 1 CORNER VARIABLE STRESS DROP MODEL

Table 7b
GULF COAST
REGRESSION COEFFICIENTS FOR THE DOUBLE CORNER MODEL WITH SATURATION

Freq. Hz	C1	C2	C4	C5	C6	C7	C8	C10	Parametric Sigma	Total Sigma
0.1000	-14.54243	1.91703	2.70000	.00000	-2.10859	.12608	.00000	-.34322	.5243	1.3791
0.2000	-9.76826	1.50496	3.00000	.00000	-2.41187	.14194	.00000	-.30605	.5604	1.2665
0.3333	-6.54516	1.21492	3.10000	.00000	-2.65122	.15876	.00000	-.24408	.5958	1.1393
0.5000	-3.83140	.98710	3.20000	.00000	-2.90058	.17769	.00000	-.19493	.6159	1.0612
0.6250	-2.06630	.85356	3.30000	.00000	-3.09220	.19167	.00000	-.17514	.6233	.9956
1.0000	.53026	.62351	3.30000	.00000	-3.32873	.21370	.00000	-.15190	.6483	.9271
1.3333	2.74561	.44592	3.40000	.00000	-3.57911	.23302	.00000	-.14644	.6622	.9349
2.0000	4.87153	.25189	3.40000	.00000	-3.76122	.24875	.00000	-.13799	.6850	.9040
2.5000	5.96206	.14984	3.40000	.00000	-3.85124	.25592	.00000	-.13028	.6996	.8991
3.3333	8.03762	-.01963	3.50000	.00000	-4.09059	.27175	.00000	-.11756	.7208	.9109
4.1667	8.93501	-.10061	3.50000	.00000	-4.16740	.27663	.00000	-.10695	.7389	.9111
5.0000	9.59190	-.15735	3.50000	.00000	-4.22645	.28002	.00000	-.09871	.7556	.9177
6.2500	11.20299	-.27131	3.60000	.00000	-4.44627	.29278	.00000	-.08984	.7783	.9306
6.6667	11.39716	-.28656	3.60000	.00000	-4.46693	.29383	.00000	-.08758	.7850	.9369
8.3333	12.01553	-.33472	3.60000	.00000	-4.53955	.29762	.00000	-.08082	.8064	.9587
10.0000	13.46434	-.43179	3.70000	.00000	-4.76782	.31108	.00000	-.07649	.8192	.9596
12.5000	13.96635	-.47347	3.70000	.00000	-4.84844	.31607	.00000	-.07252	.8294	.9628
14.2857	14.23988	-.49678	3.70000	.00000	-4.89689	.31927	.00000	-.07075	.8339	.9664
16.6667	14.53975	-.52162	3.70000	.00000	-4.95186	.32294	.00000	-.06914	.8396	.9730
18.1818	15.83611	-.60342	3.80000	.00000	-5.16886	.33606	.00000	-.06840	.8438	.9733
20.0000	16.02362	-.61652	3.80000	.00000	-5.20228	.33809	.00000	-.06769	.8491	.9799
25.0000	16.45698	-.64342	3.80000	.00000	-5.27833	.34234	.00000	-.06636	.8566	.9842
31.0000	16.84962	-.66794	3.80000	.00000	-5.35052	.34658	.00000	-.06561	.8572	.9821
40.0000	17.20090	-.69766	3.80000	.00000	-5.42663	.35229	.00000	-.06508	.8487	.9722
50.0000	17.40998	-.72596	3.80000	.00000	-5.48554	.35830	.00000	-.06521	.8430	.9685
100.000	13.83032	-.59892	3.60000	.00000	-4.99790	.34481	.00000	-.06992	.7733	.9088
PGA	13.52127	-.58872	3.60000	.00000	-4.95888	.34391	.00000	-.07073	.7666	.9031
PGV	10.31841	-.16678	3.10000	.00000	-4.13550	.33428	.00000	-.09848	.5888	--------

NOTE: PARAMETRIC SIGMA VALUES ARE FROM THE 1 CORNER VARIABLE STRESS DROP MODEL-MEDIUM STRESS DROP

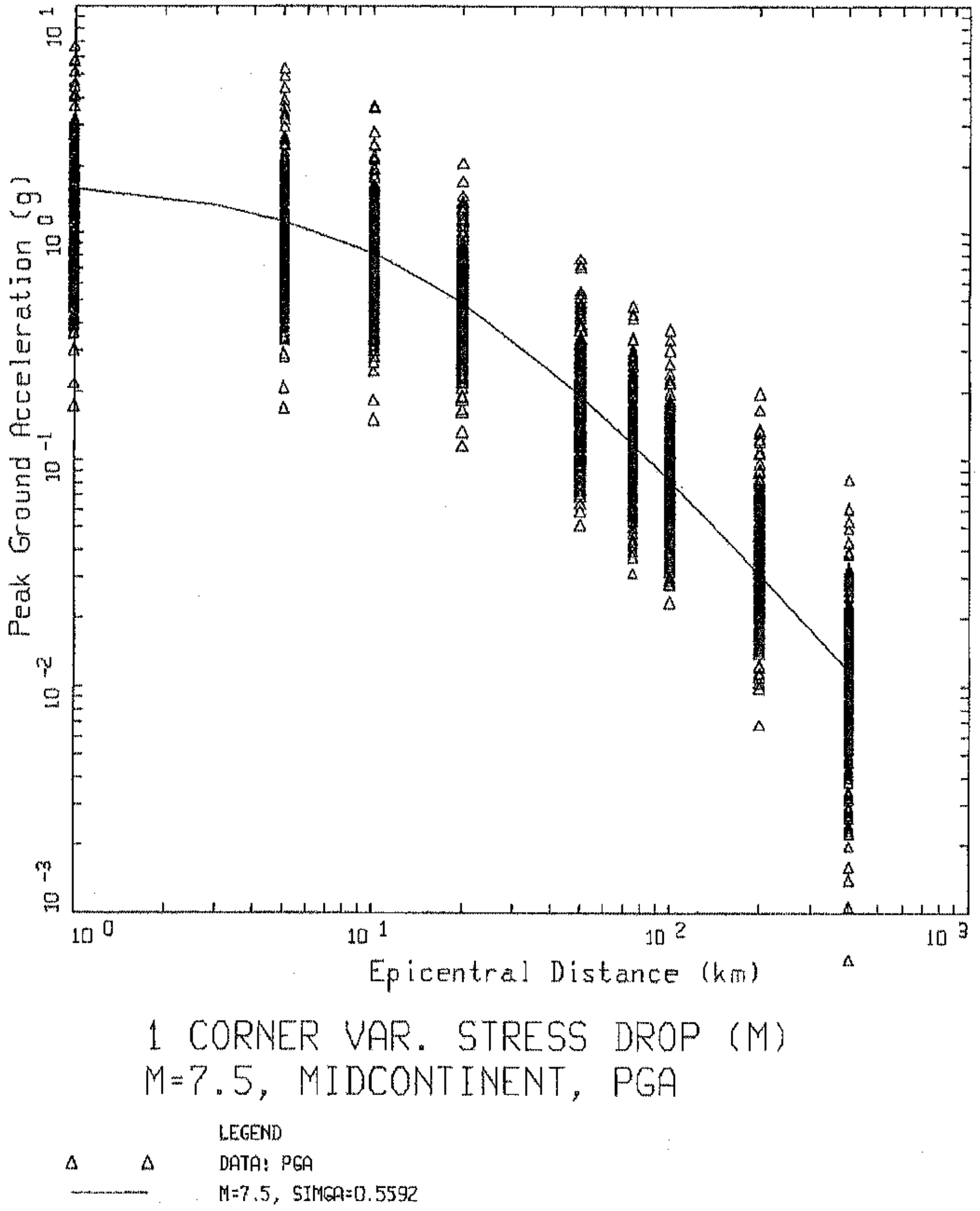

Figure 1. Peak acceleration estimates and regression fit at **M** 7.5 for the single corner model with variable (medium) stress drop, Midcontinent.

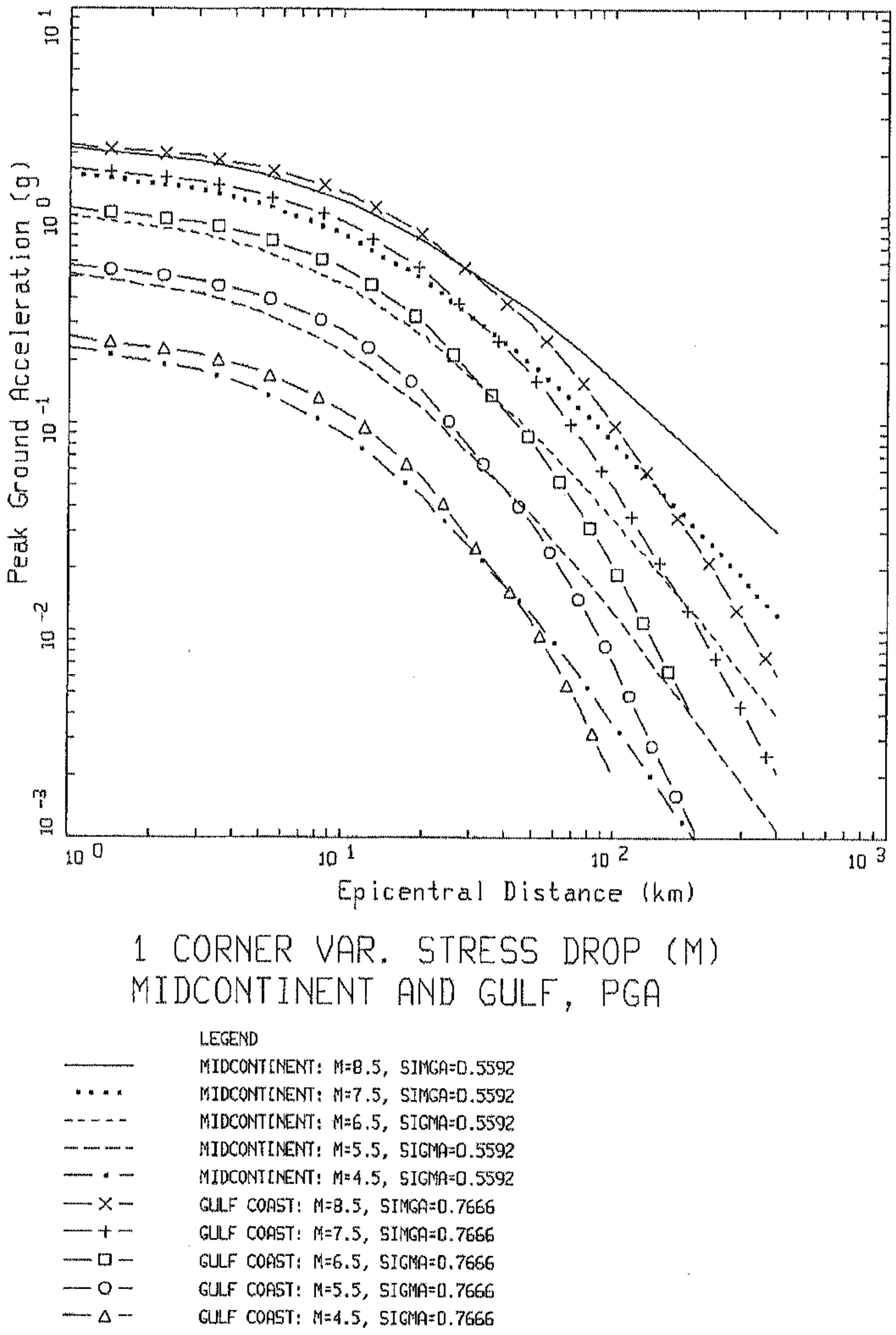

Figure 2a. Attenuation of median peak horizontal accelerations at **M** 4.5, 5.5, 6.5, 7.5 and 8.5 for the single corner model with variable (medium) stress drop, Midcontinent and Gulf Coast.

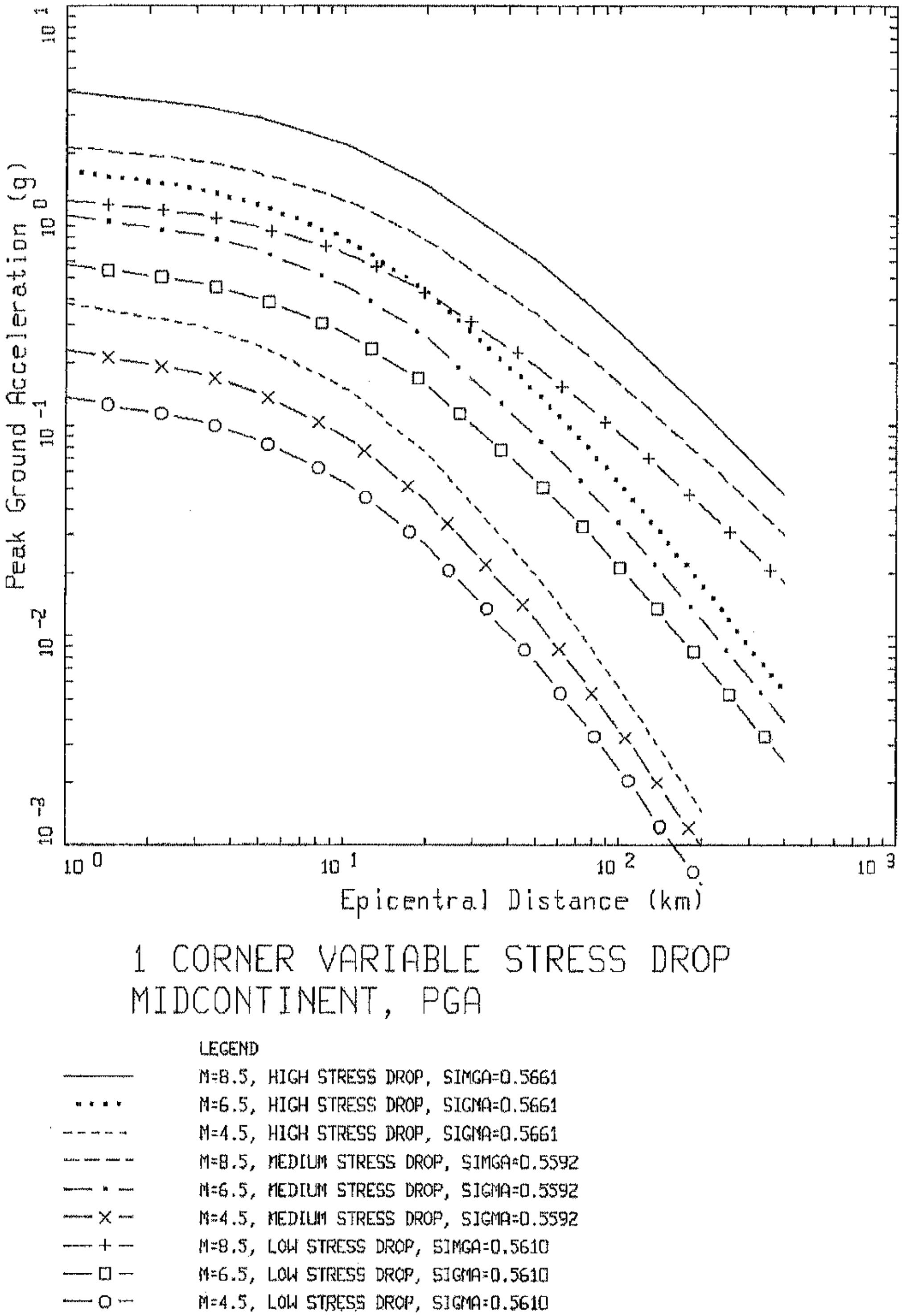

Figure 2b. Attenuation of median peak horizontal accelerations at **M** 4.5, 5.5, 6.5, 7.5 and 8.5 for the single corner model with variable (medium) stress drop, Midcontinent, effect of stress drop.

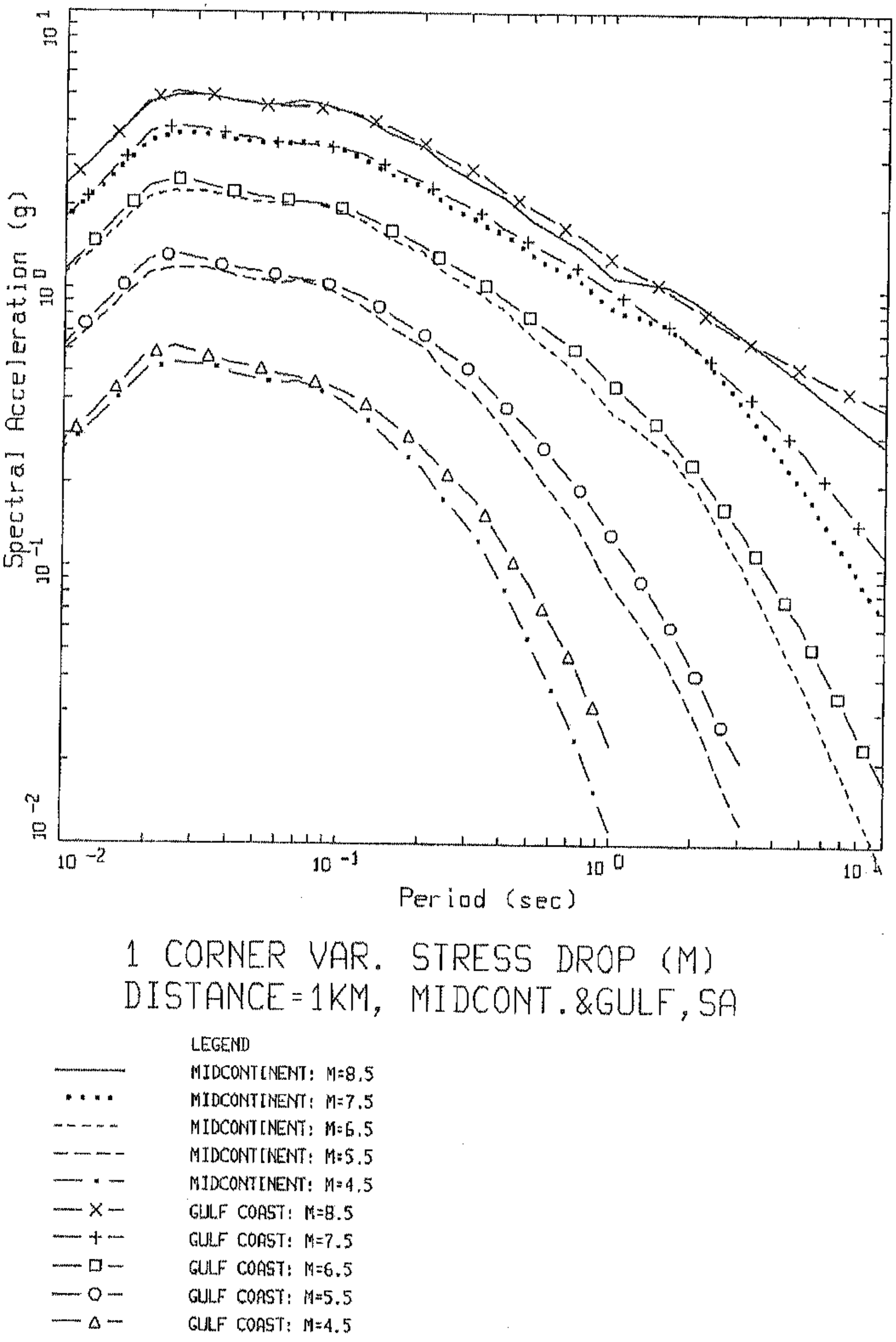

Figure 3a. Median response spectra (5% damping) at a distance of 1 km for magnitudes **M** 4.5, 5.5, 6.5, 7.5, and 8.5 for the single corner model with variable (medium) stress drop, Midcontinent and Gulf Coast.

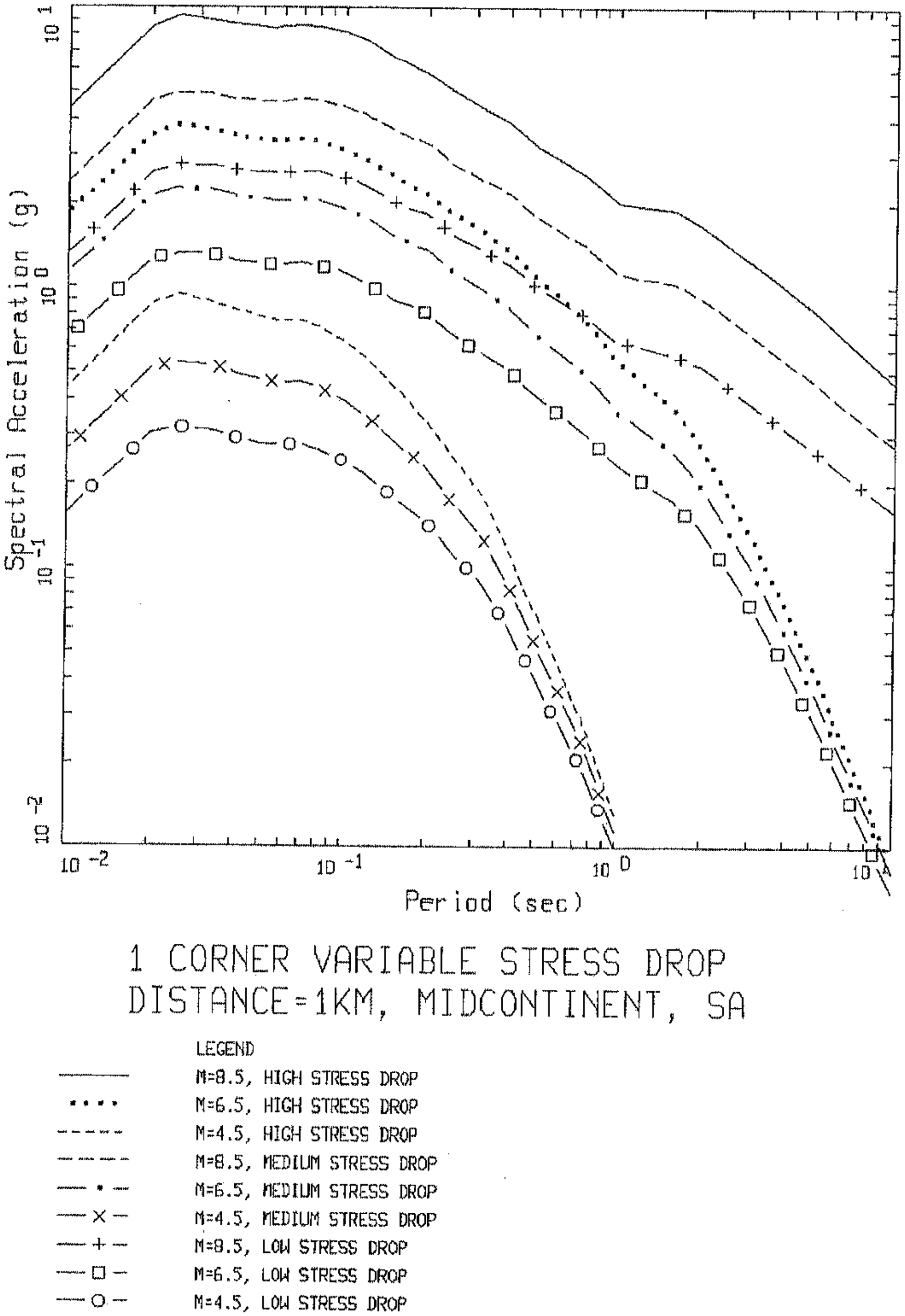

Figure 3b. Median response spectra (5% damping) at a distance of 1 km for magnitudes **M** 4.5, 5.5, 6.5, 7.5, and 8.5 for the single corner model with variable (medium) stress drop, Midcontinent, effect of stress drop.

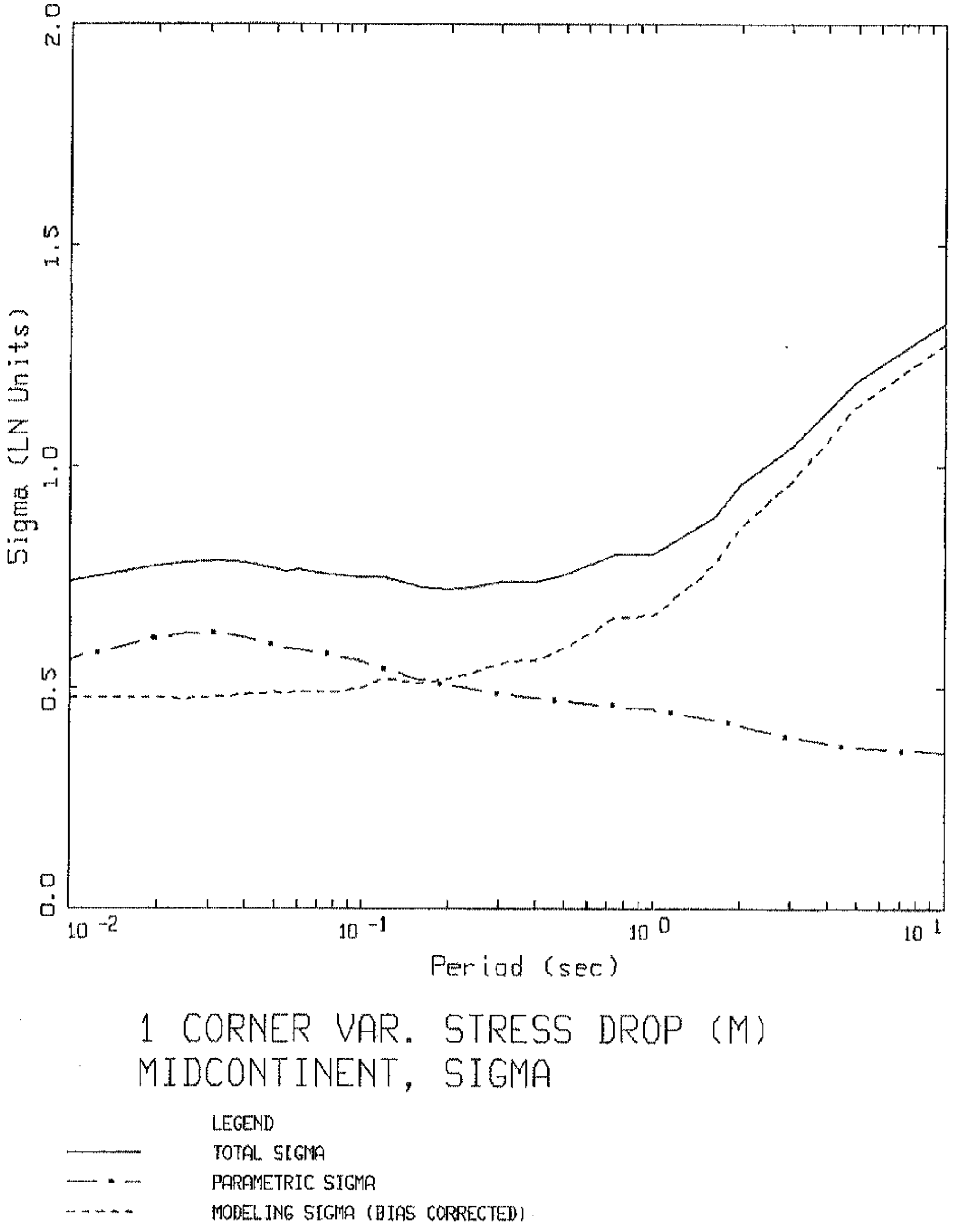

Figure 4a. Estimates of total variability (uncertainty) for the Midcontinent attenuation model. Parametric variability is due to variation of variable (medium) stress drop, single corner frequency point-source parameters (Table 2), and fit of regression model (Table 3a). Model variability is from validation exercises with 16 earthquakes (**M** 5.3 to 7.4) at 500 sites over the fault distance range of 1 to 460 km (Appendix C).

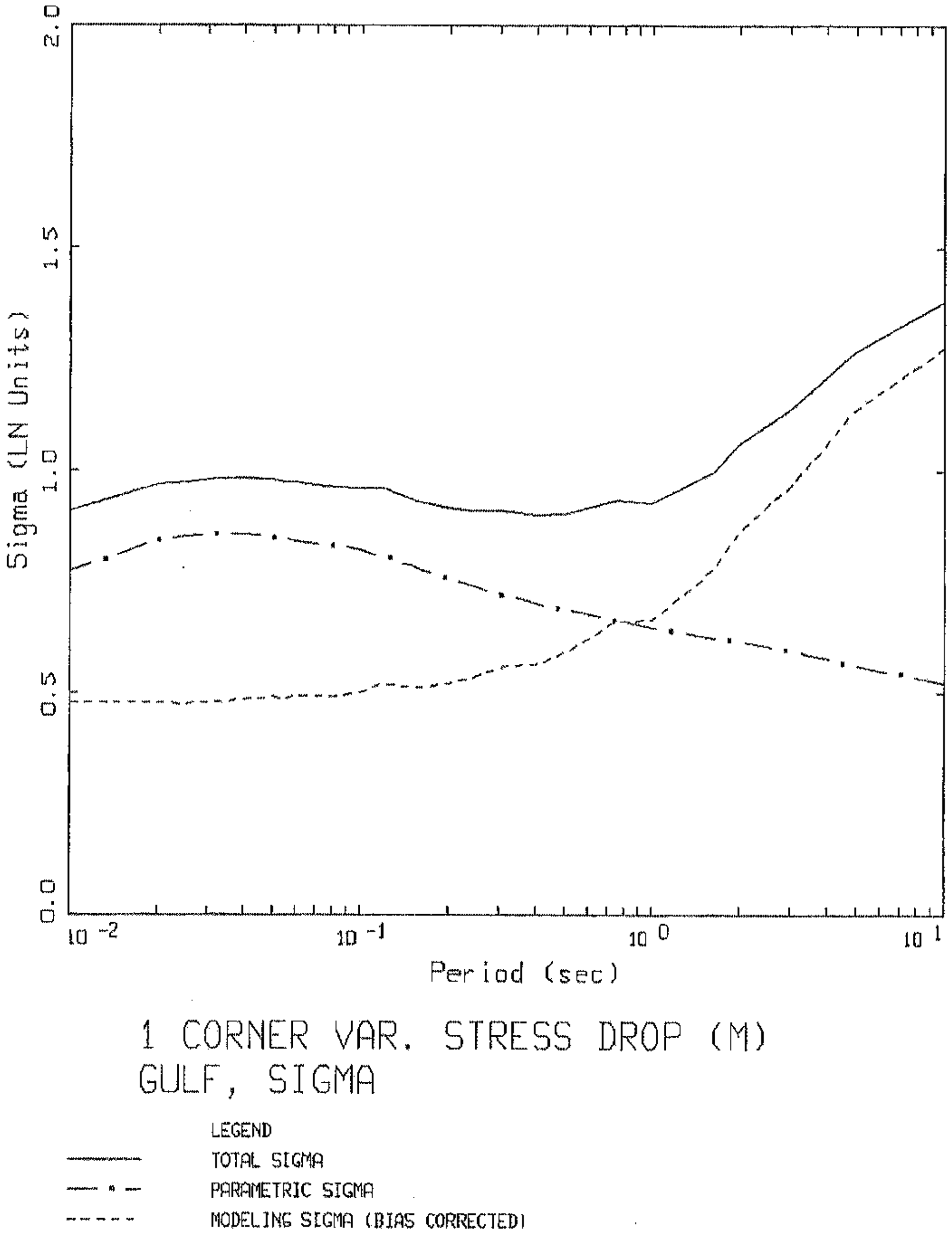

Figure 4b. Estimates of total variability (uncertainty) for the Gulf Coast attenuation model. Parametric variability is due to variation of variable (medium) stress drop, single corner frequency point-source parameters (Table 2), and fit of regression model (Table 3d). Model variability is from validation exercises with 16 earthquakes (**M** 5.3 to 7.4) at 500 sites over the fault distance range of 1 to 460 km (Appendix C).

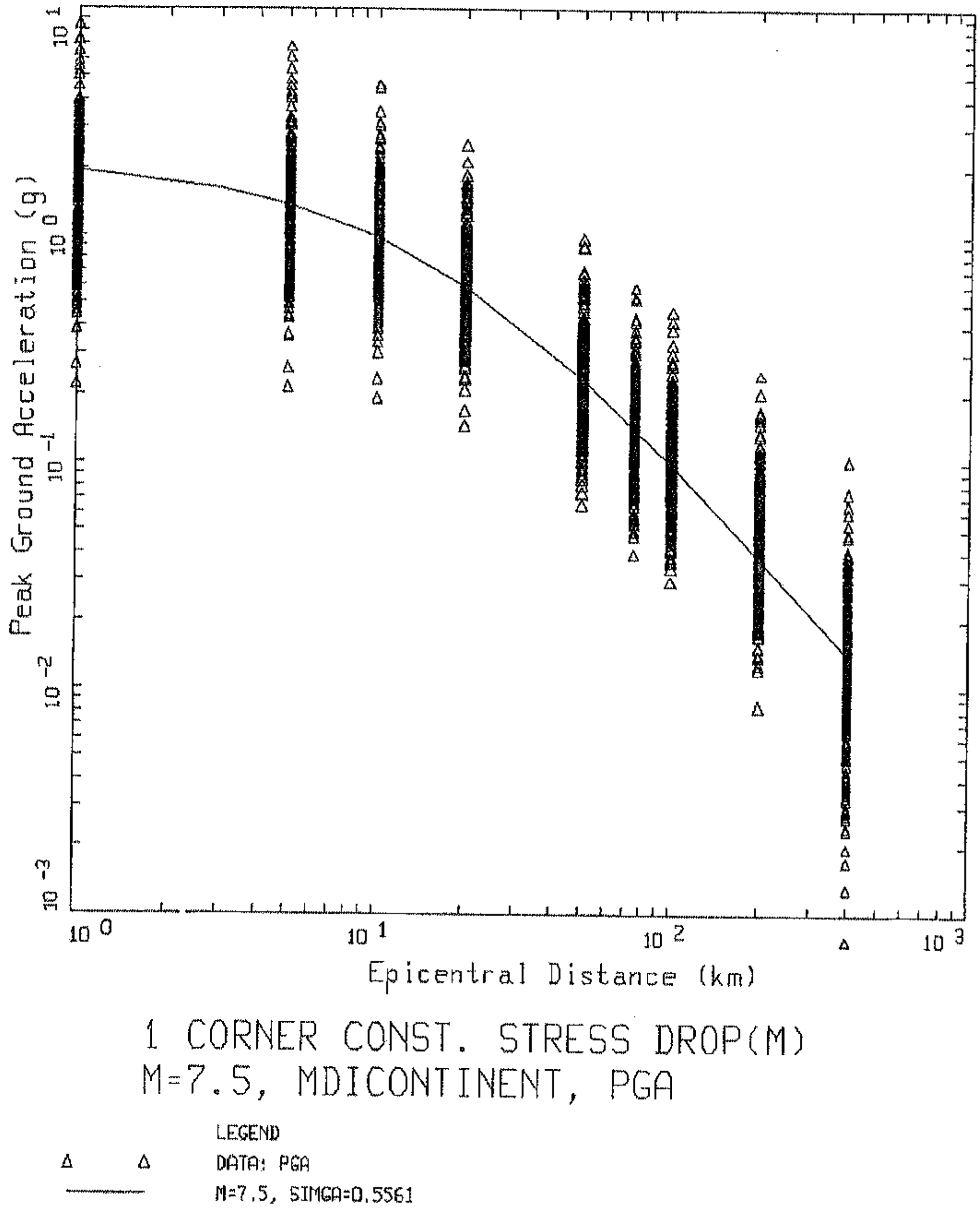

Figure 5. Peak acceleration estimates and regression fit at M 7.5 for the single corner model with constant (medium) stress drop, Midcontinent.

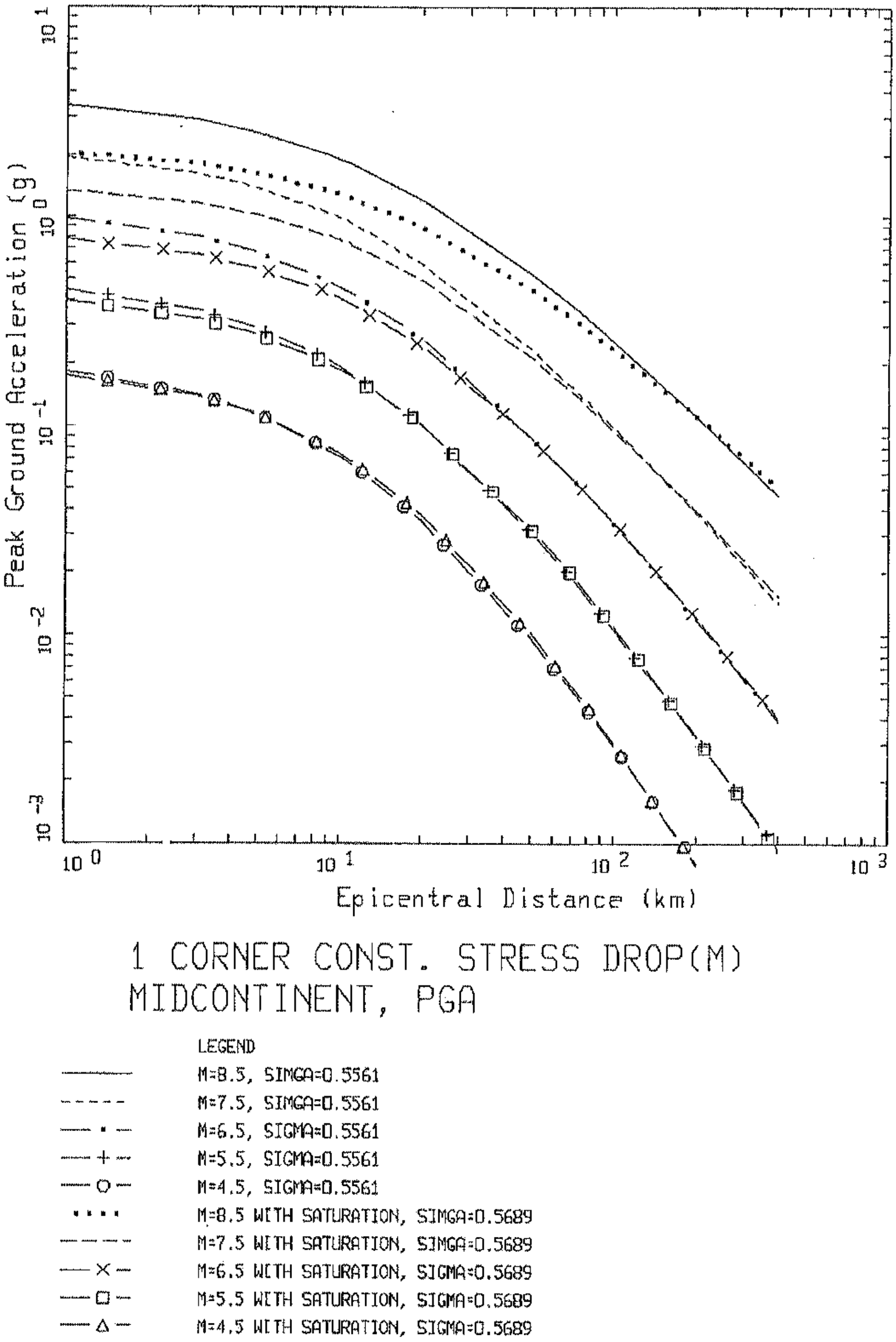

Figure 6. Attenuation of median peak horizontal accelerations at **M** 4.5, 5.5, 6.5, 7.5, and 8.5 for the single corner model with constant (medium) stress drop, with and without saturation, Midcontinent.

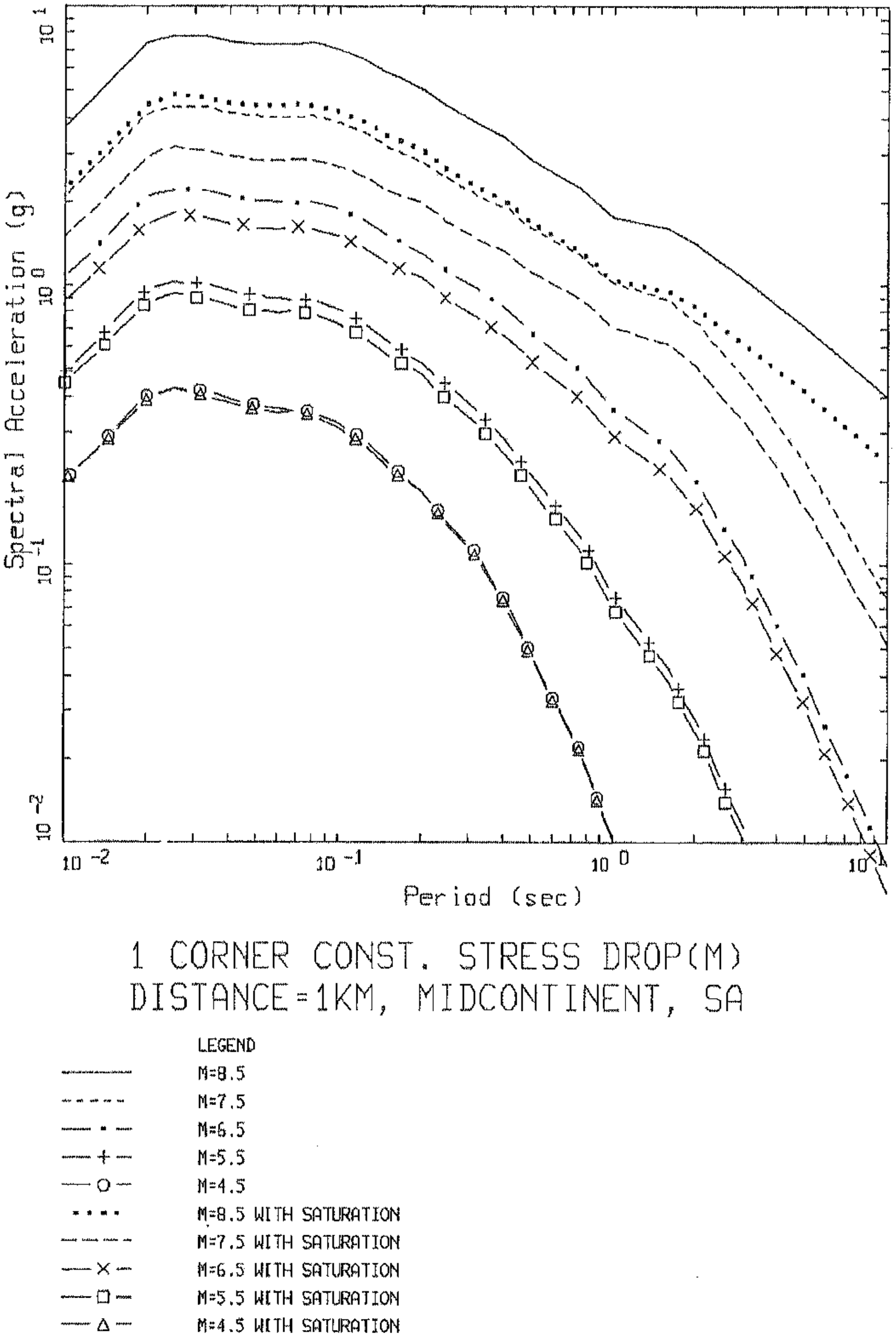

Figure 7. Median response spectra (5% damping) at a distance of 1 km for magnitudes **M** 4.5, 5.5, 6.5, 7.5, and 8.5 for the single corner model with constant (medium) stress drop, with and without saturation.

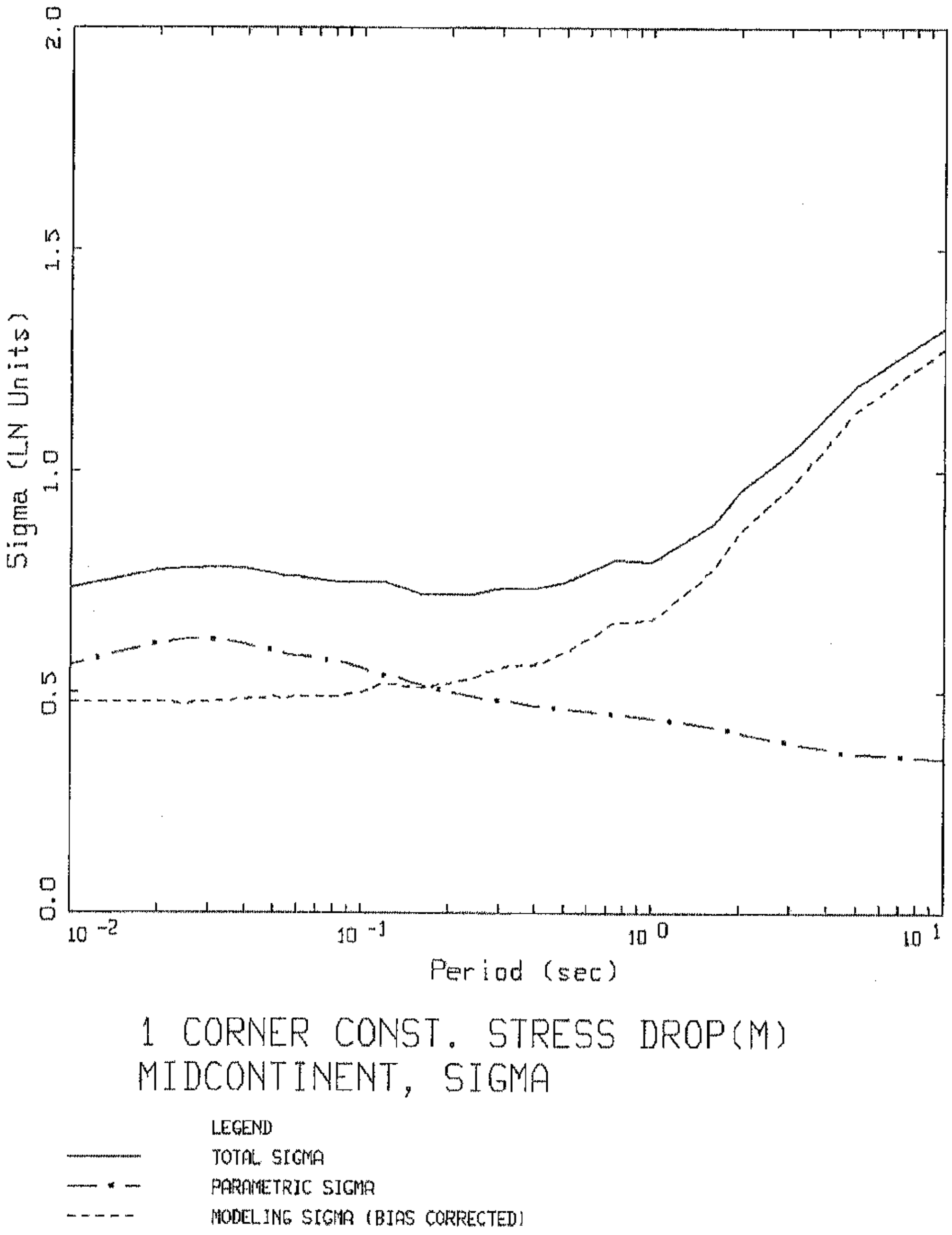

Figure 8a. Estimates of total variability (uncertainty) for the Midcontinent attenuation model. Parametric variability is due to variation of constant (medium) stress drop, single corner frequency point-source parameters (Table 2), and fit of regression model (Table 4a). Model variability is from validation exercises with 16 earthquakes (**M** 5.3 to 7.4) at 500 sites over the fault distance range of 1 to 460 km (Appendix C).

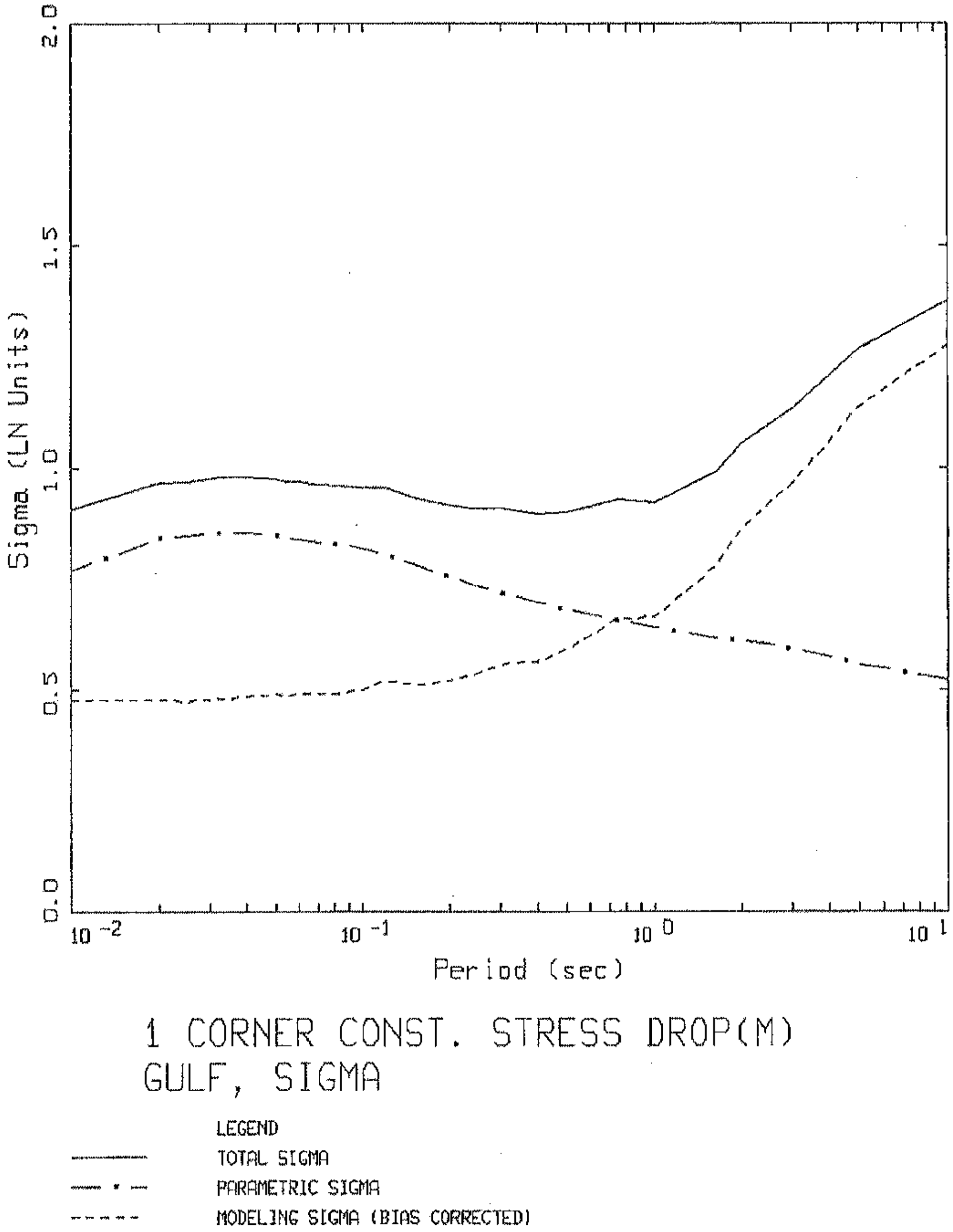

Figure 8b. Estimates of total variability (uncertainty) for the Gulf Coast attenuation model. Parametric variability is due to variation of constant (medium) stress drop, single corner frequency point-source parameters (Table 2), and fit of regression model (Table 4d). Model variability is from validation exercises with 16 earthquakes (**M** 5.3 to 7.4) at 500 sites over the fault distance range of 1 to 460 km (Appendix C).

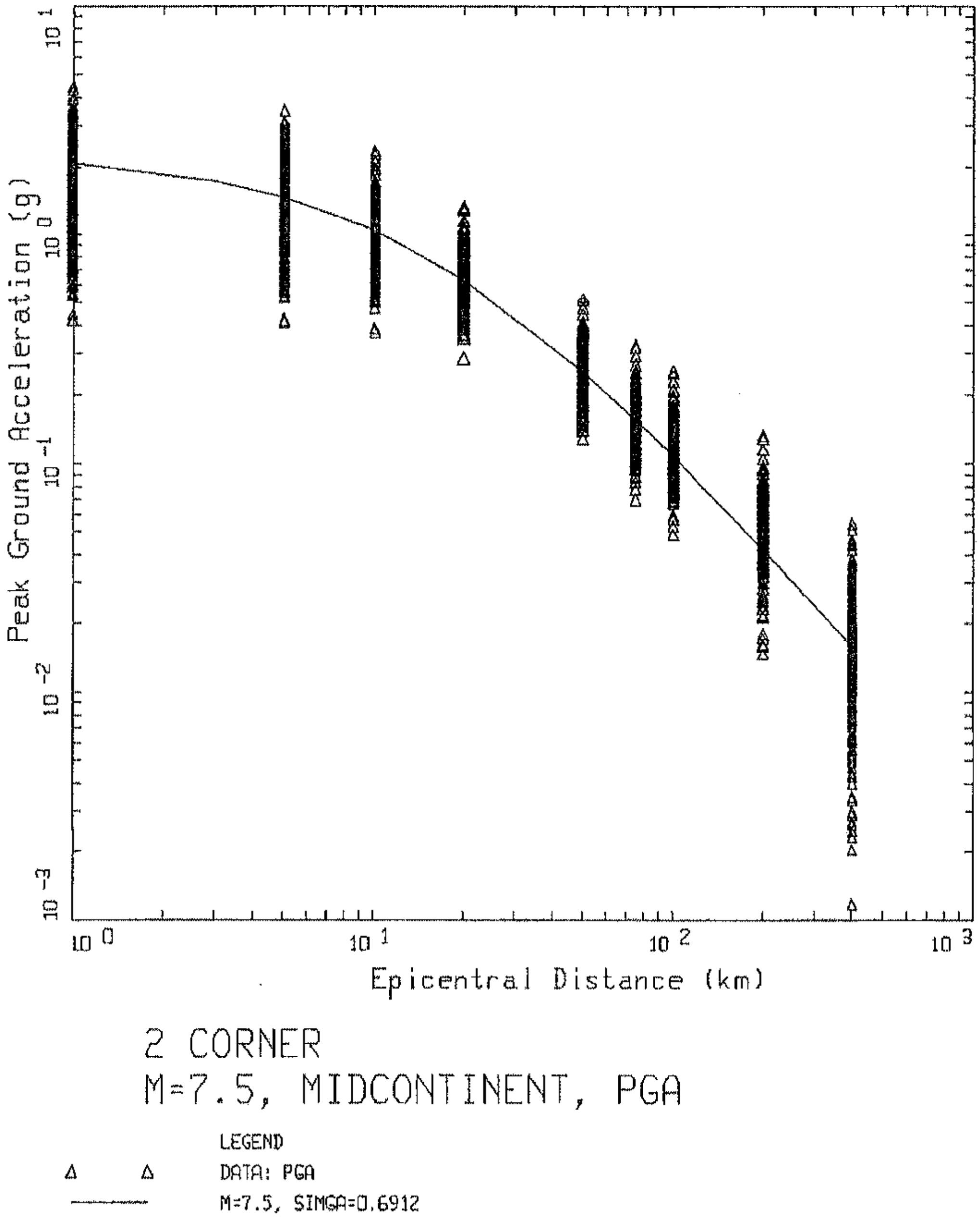

Figure 9. Peak acceleration estimates and regression fit at **M** 7.5 for the double corner model, Midcontinent.

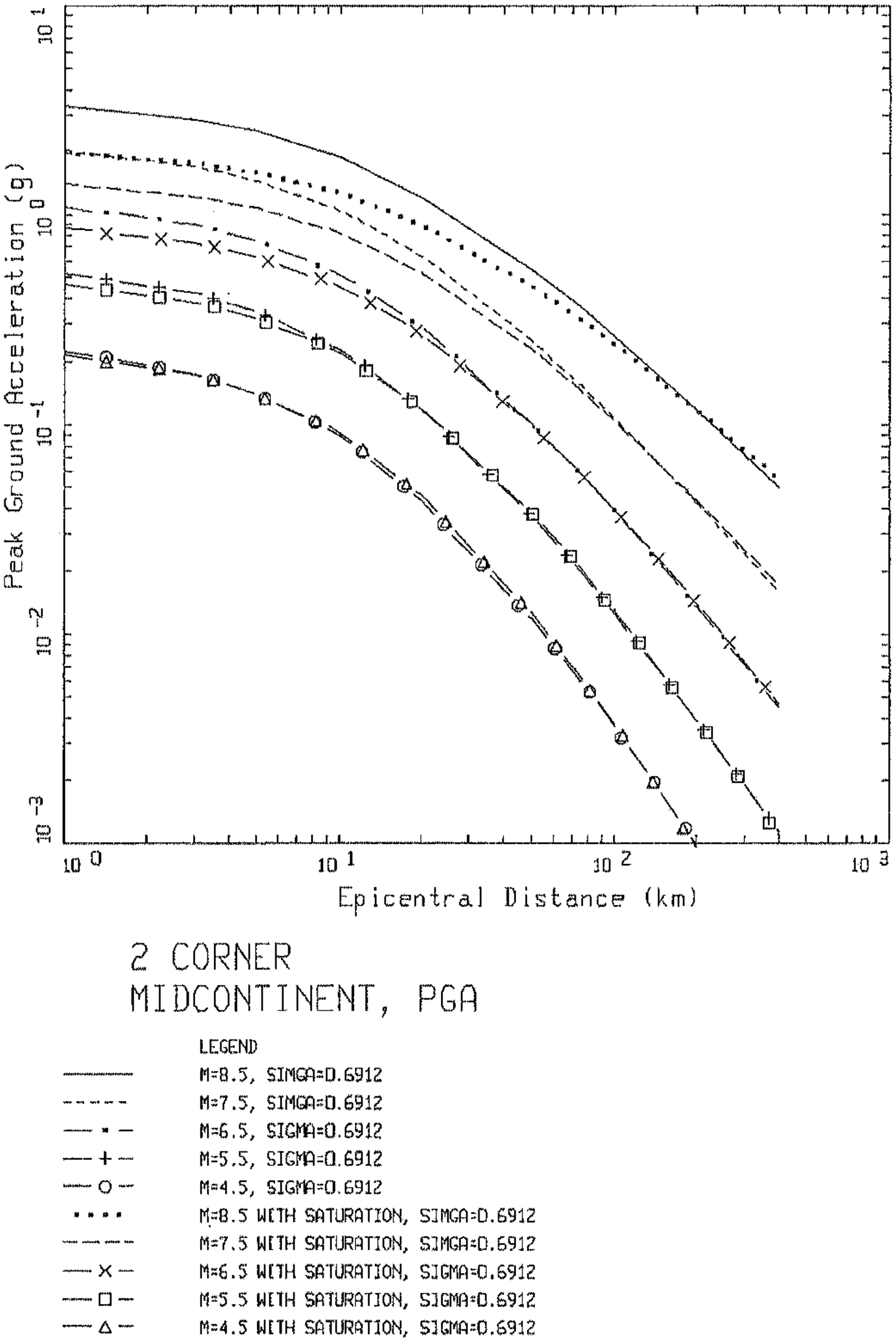

Figure 10. Attenuation of median peak horizontal accelerations at **M** 4.5, 5.5, 6.5, 7.5, and 8.5 for the double corner model, with and without saturation, Midcontinent.

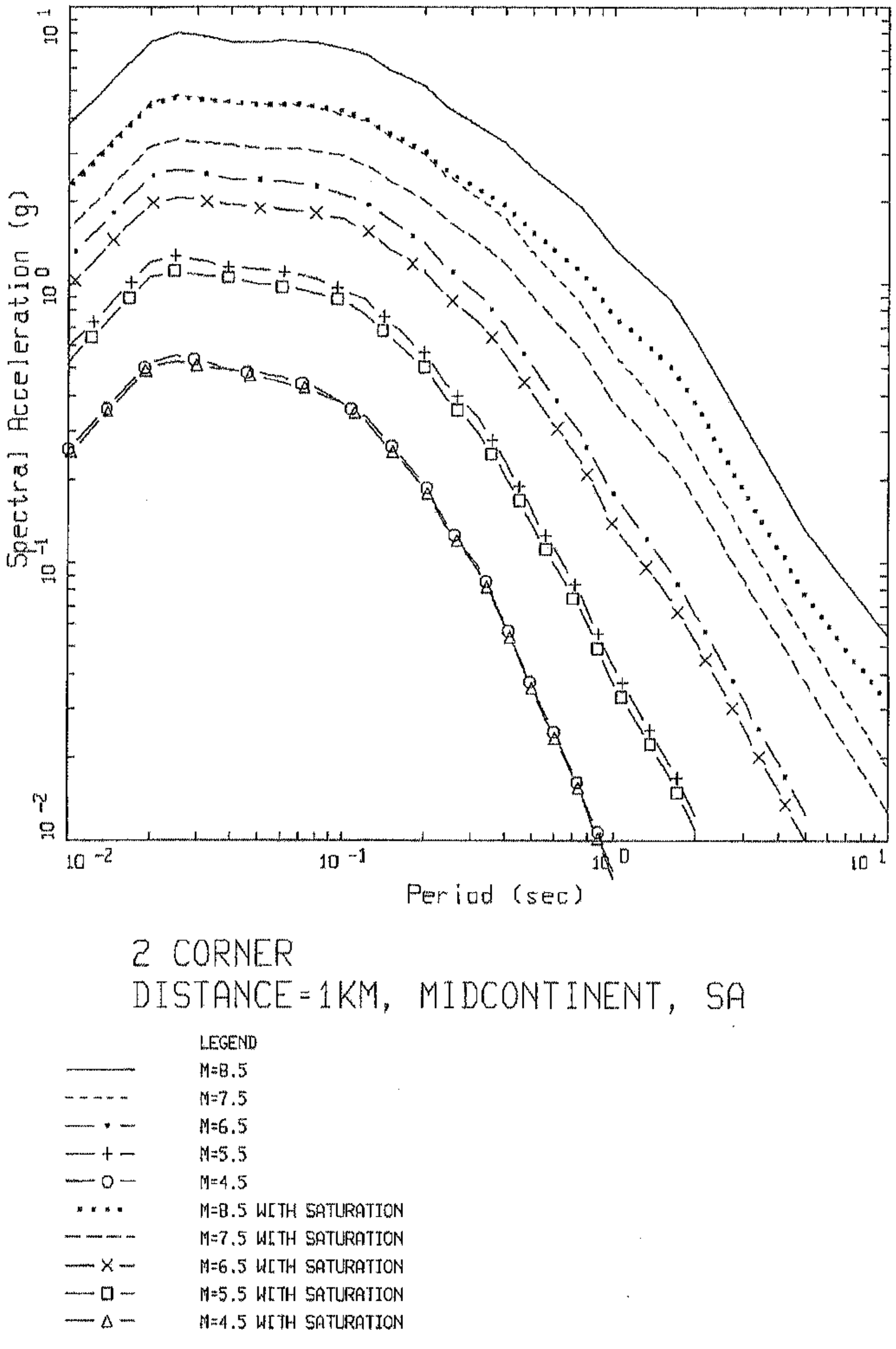

Figure 11. Median response spectra (5% damping) at a distance of 1 km for magnitudes **M** 4.5, 5.5, 6.5, 7.5, and 8.5 for the double corner model, Micontinent.

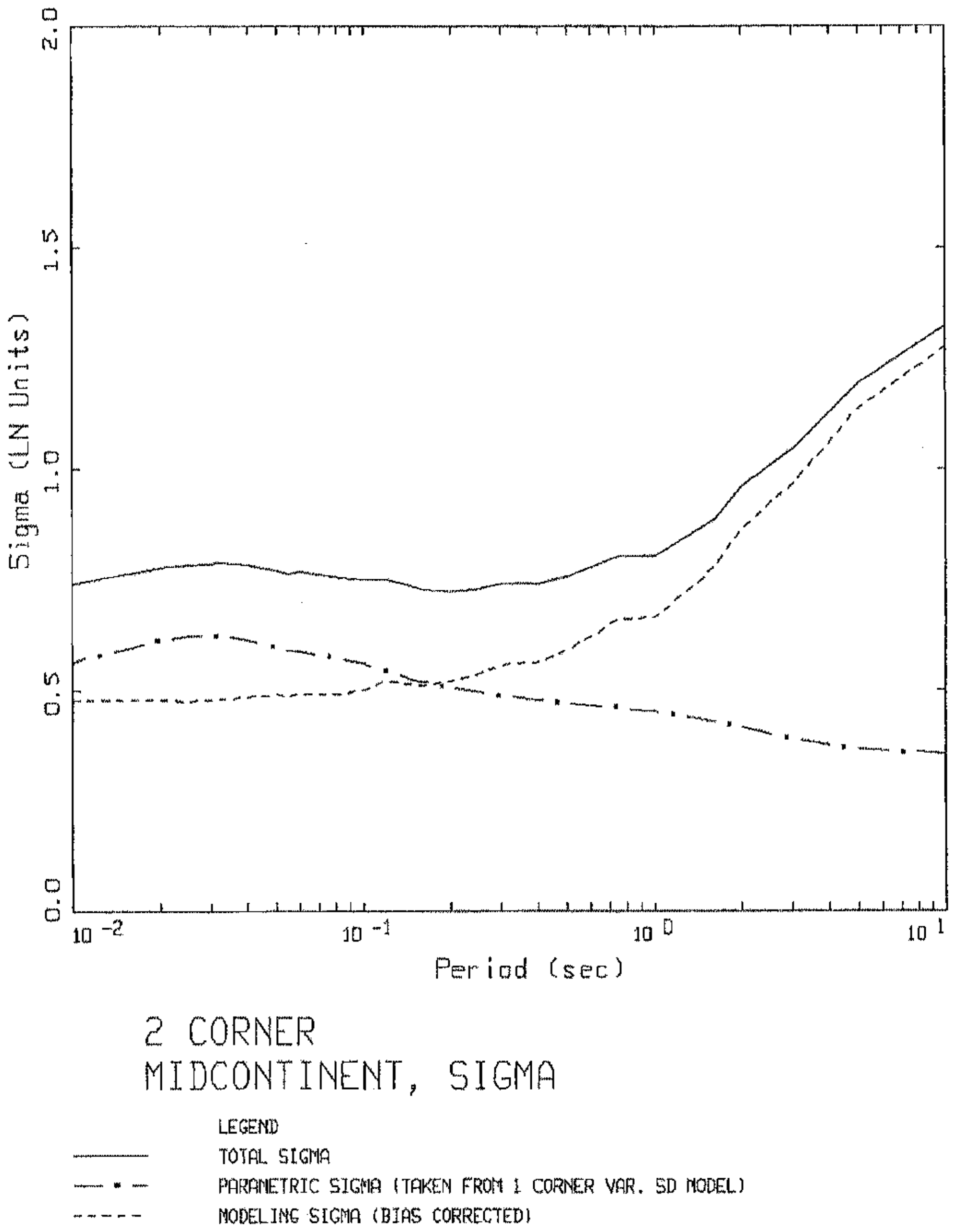

Figure 12a. Estimates of total variability (uncertainty) for the Midcontinent attenuation model. Parametric variability is due to variation of variable stress drop, single corner frequency point-source parameters (Table 2) and fit of regression model (Table 6a). Model variability is from validation exercises with 16 earthquakes (M 5.3 to 7.4) at 500 sites over the fault distance range of 1 to 460 km using the single corner frequency model (Appendix C).

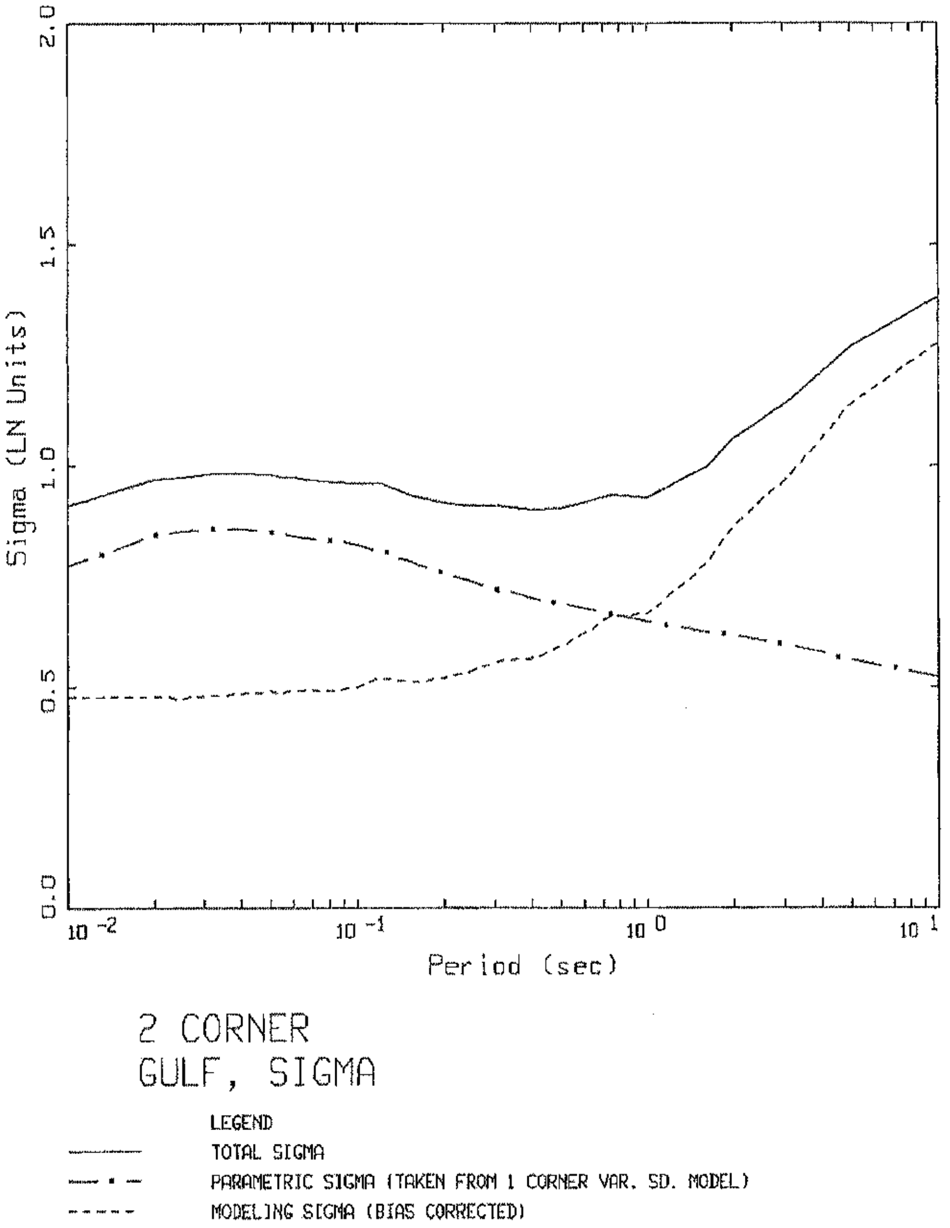

Figure 12b. Estimates of total variability (uncertainty) for the Gulf Coast attenuation model. Parametric variability is due to variation of variable stress drop, single corner frequency point-source parameters (Table 2) and fit of regression model (Table 6b). Model variability is from validation exercises with 16 earthquakes (**M** 5.3 to 7.4) at 500 sites over the fault distance range of 1 to 460 km using the single corner frequency model (Appendix C).

APPENDIX B

SITE RESPONSE ANALYSIS METHOD

Development of Site Specific Soil Motions

The conventional approach to estimating the effects of site-specific site conditions on strong ground motions involves development of a set (1, 2, or 3 component) of time histories compatible with the specified outcrop response spectra to serve as control (or input) motions. The control motions are then used to drive a nonlinear computational formulation to transmit the motions through the profile. Simplified analyses generally assume vertically propagating shear-waves for horizontal components and vertically propagating compression-waves for vertical motions. These are termed one-dimensional site response analyses.

Equivalent-Linear Computational Scheme

The computational scheme which has been most widely employed to evaluate one-dimensional site response assumes vertically-propagating plane shear-waves. Departures of soil response from a linear constitutive relation are treated in an approximate manner through the use of the equivalent-linear approach.

The equivalent-linear approach, in its present form, was introduced by Seed and Idriss (1970). This scheme is a particular application of the general equivalent-linear theory developed by Iwan (1967). Basically, the approach is to approximate a second order nonlinear equation, over a limited range of its variables, by a linear equation. Formally this is done in such a way that the average of the difference between the two systems is minimized. This was done in an ad-hoc manner for ground response modeling by defining an effective strain which is assumed to exist for the duration of the excitation. This value is usually taken as 65% of the peak time-domain strain calculated at the midpoint of each layer, using a linear analysis. Modulus reduction and hysteretic damping curves are then used to define new parameters for each layer based on the effective strain computations. The linear response calculation is repeated, new effective strains evaluated, and iterations performed until the changes in parameters are below some tolerance level. Generally a few iterations are sufficient to achieve a strain-compatible linear solution.

This stepwise analysis procedure was formalized into a one-dimensional, vertically propagating shear-wave code called SHAKE (Schnabel et al., 1972). Subsequently, this code has easily become the most widely used analysis package for one-dimensional site response calculations.

The advantages of the equivalent-linear approach are that parameterization of complex nonlinear soil models is avoided and the mathematical simplicity of a linear analysis is preserved. A truly nonlinear approach requires the specification of the shapes of hysteresis curves and their cyclic dependencies through an increased number of material parameters. In the equivalent-linear methodology the soil data are utilized directly and, because at each iteration the problem is linear and the material properties are frequency independent, the damping is rate independent and hysteresis loops close.

Careful validation exercises between equivalent-linear and fully nonlinear formulations using recorded motions from 0.05 to 0.50g showed little difference in results (EPRI, 1993). Both formulations compared very favorably to recorded motions suggesting both the adequacy of the vertically propagating shear-wave model and the approximate equivalent-linear formulation. While the assumptions of vertically propagating shear-waves and equivalent-linear soil response certainly represent approximations to actual conditions, their combination has achieved demonstrated success in modeling observations of site effects and represent a stable, mature, and reliable means of estimating the effects of site conditions on strong ground motions (Schnabel et al., 1972; Silva et al., 1988; Schneider et al., 1993; EPRI, 1993).

To accommodate both uncertainty and randomness in dynamic material properties, analyses are typically done for the best estimate shear-wave velocity profile as well as upper- and lower-range profiles. The upper- and lower-ranges are usually specified as twice and one-half the best estimate shear-wave moduli. Depending upon the nature of the structure, the final design spectrum is then based upon an envelope or average of the three spectra.

For vertical motions, the SHAKE code is also used with compression-wave velocities and damping substituted for the shear-wave values. To accommodate possible nonlinear response on the vertical component, since modulus reduction and hysteretic damping curves are not generally available for the constrained modulus, the low-strain Poisson's ratio is usually fixed and strain compatible compression-wave velocities calculated using the strain compatible shear moduli from the horizontal component analyses combined with the low-strain Poisson's ratios. In a similar manner, strain compatible compression-wave damping values are estimated by combining the strain compatible shear-wave damping values with the low-strain damping in bulk or pure volume change. This process assumes the loss in bulk (volume change) is constant or strain independent. Alternatively, zero loss in bulk is assumed and the equation relating shear- and compression-wave damping (η_S and η_P) and velocities (V_S and V_P)

$$\eta_P \approx \frac{4}{3} \frac{V_S}{V_P} \eta_S, \qquad \text{(B-1)}$$

is used.

RVT Based Computational Scheme

The computational scheme employed to compute the site response for this project uses an alternative approach employing random vibration theory (RVT). In this approach the control motion power spectrum is propagated through the one-dimensional soil profile using the plane-wave propagators of Silva (1976). In this formulation only SH waves are considered. Arbitrary angles of incidence may be specified but normal incidence is used throughout the present analyses.

In order to treat possible material nonlinearities, an RVT based equivalent-linear formulation is employed. Random process theory is used to predict peak time domain values of shear-strain based upon the shear-strain power spectrum. In this sense the procedure is analogous to the program SHAKE except that peak shear-strains in SHAKE are measured in the time domain. The purely frequency domain approach obviates a time domain control motion and, perhaps just as significant, eliminates the need for a suite of analyses based on different input motions. This arises because each time domain analysis may be viewed as one realization of a random process. Different control motion time histories reflecting different time domain characteristics but with nearly identical response spectra can result in different nonlinear and equivalent-linear response.

In this case, several realizations of the random process must be sampled to have a statistically stable estimate of site response. The realizations are usually performed by employing different control motions with approximately the same level of peak accelerations and response spectra.

In the case of the frequency domain approach, the estimates of peak shear-strain as well as oscillator response are, as a result of the random process theory, fundamentally probabilistic in nature. For fixed material properties, stable estimates of site response can then be obtained with a single run.

In the context of the RVT equivalent-linear approach, a more robust method of incorporating uncertainty and randomness of dynamic material properties into the computed response has been developed. Because analyses with multiple time histories are not required, parametric variability can be accurately assessed through a Monte Carlo approach by randomly varying dynamic material properties. This results in median as well as other fractile levels (e.g. 16th, mean, 84th) of smooth response spectra at the surface of the site. The availability of fractile levels reflecting randomness and uncertainty in dynamic material properties then permits a more rational basis for selecting levels of risk.

In order to randomly vary the shear-wave velocity profile, a profile randomization scheme has been developed which varies both layer velocity and thickness. The randomization is based on a correlation model developed from an analysis of variance on about 500 measured shear-wave velocity profiles (EPRI, 1993; Silva et al., 1997). Profile depth (depth to competent material) is also varied on a site specific basis using a uniform distribution. The depth range is generally selected to reflect expected variability over the structural foundation as well as uncertainty in the estimation of depth to competent material.

APPENDIX B

To model parametric variability for compression-waves, the base-case Poisson's ratio is generally fixed. Suites of compatible random compression- and shear-wave velocities are then generated based on the random shear-wave velocities profiles.

To accommodate variability in modulus reduction and hysteretic damping curves on a generic basis, the curves are independently randomized about the base case values. A log normal distribution is assumed with a $\sigma_{\ln}$ of 0.35 at a cyclic shear strain of $3 \times 10^{-2}\%$. These values are based on an analysis of variance on a suite of laboratory test results. An upper and lower bound truncation of 2σ is used to prevent modulus reduction or damping models that are not physically possible. The random curves are generated by sampling the transformed normal distribution with a $\sigma_{\ln}$ of 0.35, computing the change in normalized modulus reduction or percent damping at $3 \times 10^{-2}\%$ shear strain, and applying this factor at all strains. The random perturbation factor is reduced or tapered near the ends of the strain range to preserve the general shape of the median curves (Silva, 1992).

To model vertical motions, incident inclined compression- and shear (SV)-waves are assumed. Raytracing is done from the source location to the site to obtain appropriate angles of incidence. In the P-SV site response analyses, linear response is assumed in both compression and shear with the low-strain shear-wave damping used for the compression-wave damping (Johnson and Silva, 1981). The vertical and horizontal motions are treated independently in separate analyses. Validation exercises with a fully 3-D soil model using recorded motions up to 0.50%g showed these approximations to be validate (EPRI, 1993).

In addition, the site response model for the vertical motions has been validated at over 100 rock and soil sites for three large earthquakes: 1989 **M** 6.9 Loma Prieta, 1992 **M** 7.2 Landers, and the 1994 Northridge earthquakes. In general, the model performs well and captures the site and distance dependency of vertical motions over the frequency range of about 0.3 to 50.0 Hz and the fault distance range of about 1 to 100 km.

APPENDIX B

REFERENCES

Electric Power Research Institute (1993). "Guidelines for determining design basis ground motions." Palo Alto, Calif: Electric Power Research Institute, vol. 1-5, EPRI TR-102293.

- vol. 1: Methodology and guidelines for estimating earthquake ground motion in eastern North America.
- vol. 2: Appendices for ground motion estimation.
- vol. 3: Appendices for field investigations.
- vol. 4: Appendices for laboratory investigations.
- vol. 5: Quantification of seismic source effects.

Iwan, W.D. (1967). "On a class of models for the yielding behavior of continuous and composite systems." *J. Appl. Mech.*, 34, 612-617.

Johnson, L.R. and W.J. Silva (1981). "The effects of unconsolidated sediments upon the ground motion during local earthquakes." *Bull. Seism. Soc. Am.*, 71, 127-142.

Schnabel, P.B., J. Lysmer, and H.B. Seed (1972). *SHAKE: a Computer Program for Earthquake Response Analysis of Horizontally Layered Sites.* Earthq. Engin. Res. Center, Univ. of Calif. at Berkeley, EERC 72-12.

Schneider, J.F., W.J. Silva, and C.L. Stark (1993). Ground motion model for the 1989 **M** 6.9 Loma Prieta earthquake including effects of source, path and site. *Earthquake Spectra,* 9(2), 251-287.

Seed, H.B. and I.M. Idriss (1970). *"Soil Moduli and Damping Factors for Dynamic Response Analyses,"* Earthq. Eng. Res. Center, Univ. of Calif. at Berkeley, Report No. UCB/EERC-70/10.

Silva, W.J., N. Abrahamson, G. Toro, and C. Costantino (1997). "Description and validation of the stochastic ground motion model." Submitted to Brookhaven National Laboratory, Associated Universities, Inc. Upton, New York.

Silva, W.J. (1992). "Factors controlling strong ground motions and their associated uncertainties." *Dynamic Analysis and Design Considerations for High Level Nuclear Waste Repositories, ASCE* 132-161.

Silva, W. J., T. Turcotte, and Y. Moriwaki, (1988). "Soil Response to Earthquake Ground Motion," Electric Power Research Institute, Walnut Creek, California, Report No. NP-5747.

Silva, W.J. (1976). "Body Waves in a Layered Anelastic soilid." *Bull. Seis. Soc. Am.*, vol.66(5), 1539-1554.

APPENDIX C

STOCHASTIC GROUND MOTION MODEL DESCRIPTION

BACKGROUND

In the context of strong ground motion, the term "stochastic" can be a fearful concept to some and may be interpreted to represent a fundamentally incorrect or inappropriate model (albeit the many examples demonstrating that it works well; Boore, 1983, 1986). To allay any initial misgivings, a brief discussion seems prudent to explain the term stochastic in the stochastic ground motion model.

The stochastic point-source model may be termed a spectral model in that it fundamentally describes the Fourier amplitude spectral density at the surface of a half-space (Hanks and McGuire, 1981). The model uses a Brune (1970, 1971) omega-square description of the earthquake source Fourier amplitude spectral density. This model is easily the most widely used and qualitatively validated source description available. Seismic sources ranging from **M** = -6 (hydrofracture) to **M** = 8 have been interpreted in terms of the Brune omega-square model in dozens of papers over the last 30 years. The general conclusion is that it provides a reasonable and consistent representation of crustal sources, particularly for tectonically active regions such as plate margins. A unique phase spectrum can be associated with the Brune source amplitude spectrum to produce a complex spectrum which can be propagated using either exact or approximate (1-2- or 3-D) wave propagation algorithms to produce single or multiple component time histories. In this context the model is not stochastic, it is decidedly deterministic and as exact and rigorous as one chooses. A two-dimensional array of such point-sources may be appropriately located on a fault surface (area) and fired with suitable delays to simulate rupture propagation on an extended rupture plane (Section 2.2). As with the single point-source, any degree of rigor may be used in the wave propagation algorithm to produce multiple component or average horizontal component time histories. The result is a kinematic[1] finite-source model which has as its basis a source time history defined as a Brune pulse whose Fourier amplitude spectrum follows an omega-square model. This finite-fault model would be very similar to that used in published inversions for slip models (Chapter 4) if the 1-D propagation were treated using a reflectivity algorithm (Aki and Richards, 1980). This algorithm is a complete solution to the wave equation from static offsets (near-field terms) to an arbitrarily selected high frequency cutoff (generally 1-2 Hz).

Alternatively, to model the wave propagation more accurately, recordings of small earthquakes at the site of interest and with source locations distributed along the fault of interest may be used as empirical Green functions (Hartzell, 1978). To model the design earthquake, the empirical Green functions are delayed and summed in a manner to simulate rupture propagation (Hartzell,

---

[1] Kinematic source model is one whose slip (displacement) is defined (imposed) while in a dynamic source model forces (stress) are defined (see Aki and Richards 1980 for a complete description).

1978). Provided a sufficient number of small earthquakes are recorded at the site of interest, the source locations adequately cover the expected rupture surface, and sufficient low frequency energy is present in the Green functions, this would be the most appropriate procedure to use if nonlinear site response is not an issue. With this approach the wave propagation is, in principle, exactly represented from each Green function source to the site. However, nonlinear site response is not treated unless Green function motions are recorded at a nearby rock outcrop with dynamic material properties similar to the rock underlying the soils at the site or recordings are made at depth within the site soil column. These motions may then be used as input to either total or effective stress site response codes to model nonlinear effects. Important issues associated with this approach include the availability of an appropriate nearby (1 to 2 km) rock outcrop and, for the downhole recordings, the necessity to remove all downgoing energy from the at-depth soil recordings. The downgoing energy must be removed from the downhole Green functions (recordings) prior to generating the control motions (summing) as only the upgoing wavefields are used as input to the nonlinear site response analyses. Removal of the downgoing energy from each recording requires multiple site response analyses which introduce uncertainty into the Green functions due to uncertainty in dynamic material properties and the numerical site response model used to separate the upgoing and downgoing wavefields.

To alleviate these difficulties one can use recordings well distributed in azimuth at close distances to a small earthquake and correct the recordings back to the source by removing wave propagation effects using a simple approximation (say 1/R plus a constant for crustal amplification and radiation pattern), to obtain an empirical source function. This source function can be used to replace the Brune pulse to introduce some natural (although source, path, and site specific) variation into the dislocation time history. If this is coupled to an approximate wave propagation algorithm (asymptotic ray theory) which includes the direct rays and those which have undergone a single reflection, the result is the empirical source function method (EPRI, 1993). Combining the reflectivity propagation (which is generally limited to frequencies □ 1-2 Hz due to computational demands) with the empirical source function approach (appropriate for frequencies ≥ 1 Hz; EPRI, 1993) results in a broad band simulation procedure which is strictly deterministic at low frequencies (where an analytical source function is used) and incorporates some natural variation at high frequencies through the use of an empirical source function (Somerville et al., 1995).

All of these techniques are fundamentally similar, well founded in seismic source and wave propagation physics, and importantly, they are <u>all</u> approximate. Simply put, all models are wrong (approximate) and the single essential element in selecting a model is to incorporate the appropriate degree of rigor, commensurate with uncertainties and variabilities in crustal structure and site effects, through extensive validation exercises. It is generally felt that more complicated models produce more accurate results, however, the implications of more sophisticated models with the increased number of parameters which must be specified is often overlooked. This is not too serious a consequence in modeling past earthquakes since a reasonable range in parameter space can be explored to give the "best" results. However for future predictions, this increased rigor may carry undesirable baggage in increased parametric variability (Roblee et al., 1996). The effects of lack of knowledge (epistemic uncertainty; EPRI, 1993) regarding parameter values for future occurrences results in uncertainty or variability in ground motion predictions. It may easily be the case that a very simple model, such as the point-source model, can have comparable, or even smaller, total variability (modeling plus parametric) than a much more rigorous model with an increased number of parameters (EPRI, 1993). What is desired in a model is sufficient sophistication such that it captures the dominant and stable features of source, distance, and site dependencies observed in strong ground motions. It is these considerations which led to the development of the stochastic point- and finite-source models and, in part, lead to the stochastic element of the models.

The stochastic nature of the point- and finite-source RVT models is simply the assumption made about the character of ground motion time histories that permits stable estimates of peak parameters (e.g. acceleration, velocity, strain, stress, oscillator response) to be made without computing detailed time histories (Hanks and McGuire, 1981; Boore, 1983). This process uses random vibration theory to relate a time domain peak value to the time history root-mean-square (RMS) value (Boore, 1983). The assumption of the character of the time history for this process to strictly apply is that it be normally distributed random noise and stationary (its statistics do not change with time) over its duration. A visual examination of any time history quickly reveals that this is clearly not the case: time histories (acceleration, velocity, stress, strain, oscillator) start, build up, and then diminish with time. However poor the assumption of stationary Gaussian noise may appear, the net result is that the assumption is weak enough to permit the approach to work surprisingly well, as numerous comparisons with recorded motions and both qualitative and quantative validations have shown (Hanks and McGuire, 1981; Boore, 1983, 1986; McGuire et al., 1984; Boore and Atkinson, 1987; Silva and Lee, 1987; Toro and McGuire, 1987; Silva et al., 1990; EPRI, 1993; Schneider et al., 1993; Silva and Darragh, 1995; Silva et al., 1997). Corrections to RVT are available to accommodate different distributions as well as non-stationarity and are usually applied to the estimation of peak oscillator response in the calculated response spectra (Boore and Joyner, 1984; Toro, 1985).

Point-source Model

The conventional stochastic ground motion model uses an ω-square source model (Brune, 1970, 1971) with a single corner frequency and a constant stress drop (Boore, 1983; Atkinson, 1984). Random vibration theory is used to relate RMS (root-mean-square) values to peak values of acceleration (Boore, 1983), and oscillator response (Boore and Joyner, 1984; Toro, 1985; Silva and Lee, 1987) computed from the power spectra to expected peak time domain values (Boore, 1983).

The shape of the acceleration spectral density, a(f), is given by

$$a(f) = C \frac{f^2}{1+\left(\frac{f}{f_0}\right)^2} \frac{M_0}{R} P(f)\, A(f)\, e^{-\frac{\pi f R}{\beta_0 Q(f)}} \qquad \text{(C-1)}$$

where

C $= (\frac{1}{\rho_0 \beta_0^3}) \bullet (2) \bullet (0.55) \bullet (\frac{1}{\sqrt{2}}) \bullet \pi.$
M_0 = seismic moment,
R = hypocentral distance,
β_0 = shear-wave velocity at the source,
ρ_0 = density at the source
Q(f) = frequency dependent quality factor (crustal damping),
A(f) = crustal amplification,

P(f) = high-frequency truncation filter,
f_0 = source corner frequency.

C is a constant which contains source region density (ρ_0) and shear-wave velocity terms and accounts for the free-surface effect (factor of 2), the source radiation pattern averaged over a sphere (0.55) (Boore, 1986), and the partition of energy into two horizontal components $(1/\sqrt{2})$.

Source scaling is provided by specifying two independent parameters, the seismic moment (M_0) and the high-frequency stress parameter or stress drop ($\Delta\sigma$). The seismic moment is related to magnitude through the definition of moment magnitude **M** by the relation

$$\log M_0 = 1.5\,\mathbf{M} + 16.05 \qquad \text{(Hanks and Kanamori, 1979)} \qquad \text{(C-2).}$$

The stress drop ($\Delta\sigma$) relates the corner frequency f_0 to M_0 through the relation

$$f_0 = \beta_0\,(\Delta\sigma/8.44\,M_0)^{1/3} \qquad \text{(Brune; 1970, 1971)} \qquad \text{(C-3).}$$

The stress drop is sometimes referred to as the high frequency stress parameter (Boore, 1983) (or simply the stress parameter) since it directly scales the Fourier amplitude spectrum for frequencies above the corner frequency (Silva, 1991; Silva and Darragh 1995). High (> 1 Hz) frequency model predictions are then very sensitive to this parameter (Silva, 1991; EPRI, 1993) and the interpretation of it being a stress drop or simply a scaling parameter depends upon how well real earthquake sources (on average) obey the omega-square scaling (Equation C-3) and how well they are fit by the single-corner-frequency model. If earthquakes truly have single-corner-frequency omega-square sources, the stress drop in Equation C-3 is a physical parameter and its values have a physical interpretation of the forces (stresses) accelerating the relative slip across the rupture surface. High stress drop sources are due to a smaller source (fault) area (for the same **M**) than low stress drop sources (Brune, 1970). Otherwise, it simply a high frequency scaling or fitting parameter.

APPENDIX C

The spectral shape of the single-corner-frequency ω-square source model is then described by the two free parameters M_0 and $\Delta\sigma$. The corner frequency increases with the shear-wave velocity and with increasing stress drop, both of which may be region dependent.

The crustal amplification accounts for the increase in wave amplitude as seismic energy travels through lower- velocity crustal materials from the source to the surface. The amplification depends on average crustal and near surface shear-wave velocity and density (Boore, 1986).

The P(f) filter is used in an attempt to model the observation that acceleration spectral density appears to fall off rapidly beyond some region- or site-dependent maximum frequency (Hanks, 1982; Silva and Darragh, 1995). This observed phenomenon truncates the high frequency portion of the spectrum and is responsible for the band-limited nature of the stochastic model. The band limits are the source corner frequency at low frequency and the high frequency spectral attenuation. This spectral fall-off at high frequency has been attributed to near-site attenuation (Hanks, 1982; Anderson and Hough, 1984) or to source processes (Papageorgiou and Aki, 1983) or perhaps to both effects. In the Anderson and Hough (1984) attenuation model, adopted here, the form of the P(f) filter is taken as

$$P(f, r) = e^{-\pi\kappa(r)f} \qquad \text{(C-4).}$$

Kappa (r) (κ(r) in Equation C-4) is a site and distance dependent parameter that represents the effect of intrinsic attenuation upon the wavefield as it propagates through the crust from source to receiver. Kappa (r) depends on epicentral distance (r) and on both the shear-wave velocity (β) and quality factor (Q_S) averaged over a depth of H beneath the site (Hough et al., 1988). At zero epicentral distance kappa (κ) is given by

$$\kappa(0) = \frac{H}{\overline{\beta}\,\overline{Q_S}} \qquad \text{(C-5),}$$

and is referred to as κ.

The bar in Equation C-5 represents an average of these quantities over a depth H. The value of kappa at zero epicentral distance is attributed to attenuation in the very shallow crust directly below the site (Hough and Anderson, 1988; Silva and Darragh, 1995). The intrinsic attenuation along this part of the path is not thought to be frequency dependent and is modeled as a frequency independent, but site and crustal region dependent, constant value of kappa (Hough et al., 1988; Rovelli et al., 1988). This zero epicentral distance kappa is the model implemented in this study.

The crustal path attenuation from the source to just below the site is modeled with the frequency-dependent quality factor Q(f). Thus the distance component of the original κ(r) (Equation C-4) is accommodated by Q(f) and R in the last term of Equation C-1:

$$\kappa(r) = \frac{H}{\overline{\beta}\,\overline{Q}_S} + \frac{R}{\beta_0 Q(f)} \qquad \text{(C-6).}$$

The Fourier amplitude spectrum, a(f), given by Equation C-1 represents the stochastic ground motion model employing a Brune source spectrum that is characterized by a single corner frequency. It is a point source and models direct shear-waves in a homogeneous half-space (with effects of a velocity gradient captured by the A(f) filter, Equation C-1). For horizontal motions, vertically propagating shear-waves are assumed. Validations using incident inclined SH-waves accompanied with raytracing to find appropriate incidence angles leaving the source showed little reduction in uncertainty compared to results using vertically propagating shear-waves. For vertical motions, P/SV propagators are used coupled with raytracing to model incident inclined plane waves (EPRI, 1993). This approach has been validated with recordings from the 1989 **M** 6.9 Loma Prieta earthquake (EPRI, 1993).

Equation C-1 represents an elegant ground motion model that accommodates source and wave propagation physics as well as propagation path and site effects with an attractive simplicity. The model is appropriate for an engineering characterization of ground motion since it captures the general features of strong ground motion in terms of peak acceleration and spectral composition with a minimum of free parameters (Boore, 1983; McGuire et al., 1984; Boore, 1986; Silva and Green, 1988; Silva et al., 1988; Schneider et al., 1993; Silva and Darragh, 1995). An additional important aspect of the stochastic model employing a simple source description is that the region-dependent parameters may be evaluated by observations of small local or regional earthquakes. Region-specific seismic hazard evaluations can then be made for areas with sparse strong motion data with relatively simple spectral analyses of weak motion (Silva, 1992).

In order to compute peak time-domain values, i.e. peak acceleration and oscillator response, RVT is used to relate RMS computations to peak value estimates. Boore (1983) and Boore and Joyner (1984) present an excellent development of the RVT methodology as applied to the stochastic ground motion model. The procedure involves computing the RMS value by integrating the power spectrum from zero frequency to the Nyquist frequency and applying Parsevall's relation. Extreme value theory is then used to estimate the expected ratio of the peak value to the RMS value of a specified duration of the stochastic time history. The duration is taken as the inverse of the source corner frequency (Boore, 1983).

Factors that affect strong ground motions such as surface topography, finite and propagating seismic sources, laterally varying near-surface velocity and Q gradients, and random inhomogeneities along the propagation path are not included in the model. While some or all of these factors are generally present in any observation of ground motion and may exert controlling influences in some cases, the simple stochastic point-source model appears to be robust in predicting median or average properties of ground motion (Boore 1983, 1986;

Schneider et al., 1993; Silva and Stark, 1993). For this reason it represents a powerful predictive and interpretative tool for engineering characterization of strong ground motion.

Finite-source Model Ground Motion Model

In the near-source region of large earthquakes, aspects of a finite-source including rupture propagation, directivity, and source-receiver geometry can be significant and may be incorporated into strong ground motion predictions. To accommodate these effects, a methodology that combines the aspects of finite-earthquake-source modeling techniques (Hartzell, 1978; Irikura 1983) with the stochastic point-source ground motion model has been developed to produce response spectra as well as time histories appropriate for engineering design (Silva et al., 1990; Silva and Stark, 1993; Schneider et al., 1993). The approach is very similar to the empirical Green function methodology introduced by Hartzell (1978) and Irikura (1983). In this case however, the stochastic point-source is substituted for the empirical Green function and peak amplitudes; PGA, PGV, and response spectra (when time histories are not produced) are estimated using random process theory.

Use of the stochastic point-source as a Green function is motivated by its demonstrated success in modeling ground motions in general and strong ground motions in particular (Boore, 1983, 1986; Silva and Stark, 1993; Schneider et al., 1993; Silva and Darragh, 1995) and the desire to have a model that is truly site- and region-specific. The model can accommodate a region specific Q(f), Green function sources of arbitrary moment or stress drop, and site specific kappa values. The necessity for having available regional and site specific recordings or modifying possibly inappropriate empirical Green functions is eliminated.

For the finite-source characterization, a rectangular fault is discretized into NS subfaults of moment M_0^S. The empirical relationship

$$\log (A) = \mathbf{M} - 4.0, \quad A \text{ in km}^2 \qquad \text{(C-7).}$$

is used to assign areas to both the target earthquake (if its rupture surface is not fixed) as well as to the subfaults. This relation results from regressing log area on **M** using the data of Wells and Coppersmith (1994). In the regression, the coefficient on **M** is set to unity which implies a constant static stress drop of about 30 bars (Equation C-9). This is consistent with the general observation of a constant static stress drop for earthquakes based on aftershock locations (Wells and Coppersmith 1994). The static stress drop, defined by Equation C-10, is related to the average slip over the rupture surface as well as rupture area. It is theoretically identical to the stress drop in Equation C-3 which defines the omega-square source corner frequency assuming the rupture surface is a circular crack model (Brune, 1970; 1971). The stress drop determined by the source corner frequency (or source duration) is usually estimated through the Fourier amplitude spectral density while the static stress drop uses the moment magnitude and an estimate of the rupture area. The two estimates for the same earthquake seldom yield the same values with the static generally being the smaller. In a recent study (Silva et al., 1997), the average stress drop based on Fourier amplitude spectra determined from an empirical attenuation relation (Abrahamson and Silva, 1997) is about 70 bars while the average static stress drop for the crustal earthquakes studied by Wells and Coppersmith (1994) is about 30 bars. These results reflect a general factor of about 2 on average between the two values. These large differences may simply be the result of using an inappropriate estimate of rupture area as the zone of actual slip is difficult to determine unambiguously. In general however, even for individual earthquakes, the two stress drops scale similarly with high static stress drops (> 30 bars) resulting in large high frequency (> 1 Hz for **M** □ 5) ground motions which translates to high corner frequencies (Equation C-3).

The subevent magnitude M_S is generally taken in the range of 5.0-6.5 depending upon the size of the target event. M_S 5.0 is used for crustal earthquakes with **M** in the range of 5.5 to 8.0 and M_S 6.4 is used for large subduction earthquakes with **M** > 7.5. The value of NS is determined as the ratio of the target event area to the subfault area. To constrain the proper moment, the total number of events summed (N) is given by the ratio of the target event moment to the subevent moment. The subevent and target event rise times (duration of slip at a point) are determined by the equation

$$\log \tau = 0.33 \log M_0 - 8.54 \qquad \text{(C-8)}$$

which results from a fit to the rise times used in the finite-fault modeling exercises, (Silva et al., 1997). Slip on each subfault is assumed to continue for a time τ. The ratio of target-to-subevent rise times is given by

$$\frac{\tau}{\tau^s} = 10^{0.5(\mathrm{M}-\mathrm{M}^s)} \qquad \text{(C-9)}$$

and determines the number of subevents to sum in each subfault. This approach is generally referred to as the constant-rise-time model and results in variable slip velocity for nonuniform slip distributions. Alternatively, one can assume a constant slip velocity resulting in a variable-rise-time model for heterogenous slip distributions.

Recent modeling of the Landers (Wald and Heaton, 1994), Kobe (Wald, 1996) and Northridge (Hartzell et al. 1996) earthquakes suggests that a mixture of both constant rise time and constant slip velocity may be present. Longer rise times seem to be associated with areas of larger slip with the ratio of slip-to-rise time (slip velocity) being depth dependent. Lower slip velocities (longer rise times) are associated with shallow slip resulting in relatively less short period seismic radiation. This result may explain the general observation that shallow slip is largely aseismic. The significant contributions to strong ground motions appear to originate at depths exceeding about 4 km (Campbell, 1993; Boore et al., 1994) as the fictitious depth term in empirical attenuation relation (Abrahamson and Silva, 1997; Boore et al., 1997). Finite-fault models generally predict unrealistically large strong ground motions for large shallow (near surface) slip using rise times or slip velocities associated with deeper (> 4 km) zones of slip. This is an important and unresolved issue in finite-fault modeling and the general approach is to constrain the slip to relatively small values in the top 2 to 4 km. A more thorough analysis is necessary, ideally using several well validated models, before this issue can be satisfactorily resolved.

To introduce heterogeneity of the earthquake source process into the stochastic finite-fault model, the location of the sub-events within each subfault (Hartzell, 1978) are randomized as is the subevent rise time. The stress drop of the stochastic point-source Green function is taken as 30 bars, consistent with the static value based on the **M** 5.0 subevent area using the equation

$$\Delta\sigma = \frac{7}{16}\left(\frac{M_e}{R_e^3}\right) \qquad \text{(Brune, 1970, 1971)} \qquad \text{(C-10)}$$

where R_e is the equivalent circular radius of the rectangular sub-event.

Different values of slip are assigned to each subfault as relative weights so that asperities or non-uniform slip can be incorporated into the methodology. For validation exercises, slip models are taken from the literature and are based on inversions of strong motion as well as regional or teleseismic recordings. To produce slip distributions for future earthquakes, random slip models are generated based on a statistical asperity model with parameters calibrated to the published slip distributions. This approach has been validated by comparing the modeling uncertainty and bias estimates for the Loma Prieta and Whittier Narrows earthquakes using motion at each site averaged over several (30) random slip models to the bias and uncertainty estimates using the published slip model. The results show nearly identical bias and uncertainty estimates suggesting that averaging the motions over random slip models produces as accurate a prediction at a site as a single motion computed using the "true" slip model which is determined from inverting actual recordings.

The rupture velocity is taken as depth independent at a value of 0.8 times the shear-wave velocity, generally at the depth of the dominant slip. This value is based on a number of studies of source rupture processes which also suggest that rupture velocity is non-uniform. To capture the effects of non-uniform rupture velocity, a random component (20%) is added. The radiation pattern is computed for each subfault, a random component added, and the RMS applied to the motions computed at the site.

The ground-motion time history at the receiver is computed by summing the contributions from each subfault associated with the closest Green function, transforming to the frequency domain, and convolving with the Green function spectrum (Equation C-1). The locations of the Green functions are generally taken at center of each subfault for small subfaults or at a maximum separation of about 5 to 10 km for large subfaults. As a final step, the individual contributions associated with each Green function are summed in the frequency domain, multiplied by the RMS radiation pattern, and the resultant power spectrum at the site is computed. The appropriate duration used in the RVT computations for PGA, PGV, and oscillator response is computed by transforming the summed Fourier spectrum into the time domain and computing the 5 to 75% Arias intensity (Ou and Herrmann, 1990).

As with the point-source model, crustal response effects are accommodated through the amplification factor (A(f)) or by using vertically propagating shear waves through a vertically heterogenous crustal structure. Propagation path damping, through the Q(f) model, is incorporated from each fault element to the site. Near-surface crustal damping is incorporated through the kappa operator (Equation C-1). To model crustal propagation path effects, the raytracing method of Ou and Herrmann (1990) is applied from each subfault to the site.

Time histories may be computed in the process as well by simply adding a phase spectrum appropriate to the subevent earthquake. The phase spectrum can be extracted from a recording made at close distance to an earthquake of a size comparable to that of the subevent (generally **M** 5.0 to 6.5). Interestingly, the phase spectrum need not be from a recording in the region of interest (Silva et al., 1989). A recording in WNA (Western North America) can effectively be used to simulate motions appropriate to ENA (Eastern North America). Transforming the Fourier spectrum computed at the site into the time domain results in a computed time history which then includes all of the aspects of rupture propagation and source finiteness, as well as region specific propagation path and site effects.

For fixed fault size, mechanism, and moment, the specific source parameters for the finite-fault are slip distribution, location of nucleation point, and site azimuth. The propagation path and site parameters remain identical for both the point- and finite-source models.

Partition and assessment of ground motion variability

An essential requirement of any numerical modeling approach, particularly one which is implemented in the process of defining design ground motions, is a quantative assessment of prediction accuracy. A desirable approach to achieving this goal is in a manner which lends itself to characterizing the variability associated with model predictions. For a ground motion model, prediction variability is comprised of two components: modeling variability and parametric variability. Modeling variability is a measure of how well the model works (how accurately it predicts ground motions) when specific parameter values are known. Modeling variability is measured by misfits of model predictions to recorded motions through validation exercises and is due to unaccounted for components in the source, path, and site models (i.e. a point-source cannot model the effects of directivity and linear site response cannot accommodate nonlinear effects). Results from a viable range of values for model parameters (i.e., slip distribution, soil profile, G/G_{max} and hysteretic damping curves, etc). Parametric variability is the sensitivity of a model to a viable range of values for model parameters. The total variability, modeling plus parametric, represents the variance associated with the ground motion prediction and, because it is a necessary component in estimating fractile levels, may be regarded as important as median predictions.

Both the modeling and parametric variabilities may have components of randomness and uncertainty. Table C.1 summarizes the four components of total variability in the context of ground motion predictions. Uncertainty is that portion of both modeling and parametric variability which, in principle, can be reduced as additional information becomes available, whereas randomness represents the intrinsic or irreducible component of variability for a given model or parameter. Randomness is that component of variability which is intrinsic or irreducible <u>for a given model.</u> The uncertainty component reflects a lack of knowledge and may be reduced as more data are analyzed. For example, in the point-source model, stress drop is generally taken to be independent of source mechanism as well as tectonic region and is found to have a standard error of about 0.7 (natural log) for the CEUS (EPRI, 1993). This variation or uncertainty plus randomness in $\Delta\sigma$ results in a variability in ground motion predictions for future earthquakes. If, for example, it is found that normal faulting earthquakes have generally lower stress drops than strike-slip which are, in turn, lower than reverse mechanism earthquakes, perhaps much of the variability in $\Delta\sigma$ may be reduced. In extensional regimes, where normal faulting earthquakes are most likely to occur, this new information may provide a reduction in variability (uncertainty component) for stress drop, say to 0.3 or 0.4 resulting in less ground motion variation due to a lack of knowledge of the mean or median stress drop. There is, however, a component of this stress drop variability which can <u>never</u> be reduced in the context of the Brune model. This is simply due to the heterogeneity of the earthquake dynamics which is not accounted for in the model and results in the randomness component of parametric variability in stress drop. A more sophisticated model may be able to accommodate or model more accurately source dynamics but, perhaps, at the expense of a larger number of parameters and increased parametric uncertainty (i.e. the finite-fault with slip model and nucleation point as unknown parameters for future earthquakes). That is, more complex models typically seek to reduce modeling randomness by more closely modeling physical phenomena. However, such models often require more comprehensive sets of observed data to constrain additional model parameters, which generally leads to increased parametric variability. If the increased parametric variability is primarily in the form of uncertainty, it is possible to reduce total variability, but only at the additional expense of constraining the additional parameters. Therefore, existing knowledge and/or available resources may limit the ability of more complex models to reduce total variability.

The distinction of randomness and uncertainty is model driven and somewhat arbitrary. The allocation is only important in the context of probabilistic seismic hazard analyses as uncertainty is treated as alternative hypotheses in logic trees while randomness is integrated over in the hazard calculation (Cornell, 1968). For example, the uncertainty component in stress drop may be treated by using an N-point approximation to the stress drop distribution and assigning a branch in a logic tree for each stress drop and associated weight. A reasonable three point approximation to a normal distribution is given by weights of 0.2, 0.6, 0.2 for expected 5%, mean, and 95% values of stress drop respectively. If the distribution of uncertainty in stress drop was such that the 5%, mean, and 95% values were 50, 100, and 200 bars respectively, the stress drop branch on a logic tree would have 50, and 200 bars with weights of 0.2 and 100 bars with a weight of 0.6. The randomness component in stress drop variability would then be formally integrated over in the hazard calculation.

Assessment of Modeling Variability

Modeling variability (uncertainty plus randomness) is usually evaluated by comparing response spectra computed from recordings to predicted spectra and is a direct assessment of model accuracy. The modeling variability is defined as the standard error of the residuals of the log of the average horizontal component (or vertical component) response spectra. The residual is defined as the difference of the logarithms of the observed average 5% damped acceleration response spectra and the predicted response spectra. At each period, the residuals are squared, and summed over the total number of sites for one or all earthquakes modeled. Dividing the resultant sum by the number of sites results in an estimate of the model variance. Any model bias (average offset) that exists may be estimated in the process (Abrahamson et al., 1990; EPRI, 1993) and used to correct (lower) the variance (and to adjust the median as well). In this approach, the modeling variability can be separated into randomness and uncertainty where the bias corrected variability represents randomness and the total variability represents randomness plus uncertainty. The uncertainty is captured in the model bias as this may be reduced in the future by refining the model. The remaining variability (randomness) remains irreducible for this model. In computing the variance and bias estimates only the frequency range between processing filters at each site (minimum of the 2 components) should be used.

Assessment of Parametric Variability

Parametric variability, or the variation in ground motion predictions due to uncertainty and randomness in model parameters is difficult to assess. Formally, it is straight-forward in that a Monte Carlo approach may be used with each parameter randomly sampled about its mean (median) value either individually for sensitivity analyses (Silva, 1992; Roblee et al., 1996) or in combination to estimate the total parametric variability (Silva, 1992; EPRI, 1993). In reality, however, there are two complicating factors.

The first factor involves the specific parameters kept fixed with all earthquakes, paths, and sites when computing the modeling variability. These parameters are then implicitly included in modeling variability provided the data sample a sufficiently wide range in source, path, and site conditions. The parameters which are varied during the assessment of modeling variation should have a degree of uncertainty and randomness associated with them for the next earthquake. Any ground motion prediction should then have a variation reflecting this lack of knowledge and randomness in the free parameters.

An important adjunct to fixed and free parameters is the issue of parameters which may vary but by fixed rules. For example, source rise time (Equation C-8) is magnitude dependent and in the stochastic finite-source model is specified by an empirical relation. In evaluating the modeling variability with different magnitude earthquakes, rise time is varied, but because it follows a strict rule, any variability associated with rise time variation is counted in modeling variability. This is strictly true only if the sample of earthquakes has adequately spanned the space of magnitude, source mechanism, and other factors which may affect rise time. Also, the earthquake to be modeled must be within that validation space. As a result, the validation or assessment of model variation should be done on as large a number of earthquakes of varying sizes and mechanisms as possible.

The second, more obvious factor in assessing parametric variability is a knowledge of the appropriate distributions for the parameters (assuming correct values for median or mean estimates are known). In general, for the stochastic models, median parameter values and uncertainties are based, to the extent possible, on evaluating the parameters derived from previous earthquakes (Silva, 1992; EPRI, 1993).

The parametric variability is site, path, and source dependent and must be evaluated for each modeling application (Roblee et al., 1996). For example, at large source-to-site distances, crustal path damping may control short-period motions. At close distances to a large fault, both the site and finite-source (asperity location and nucleation point) may dominate, and, depending upon site characteristics, the source or site may control different frequency ranges (Silva, 1992; Roblee et al., 1996). Additionally, level of control motion may affect the relative importance of G/G_{max} and hysteretic damping curves.

In combining modeling and parametric variations, independence is assumed (covariance is zero) and the variances are simply added to give the total variability.

$${}_{\ln}\sigma^2{}_T = {}_{\ln}\sigma^2{}_M + {}_{\ln}\sigma^2{}_P \qquad \text{(C-11),}$$[2]

where

${}_{\ln}\sigma^2{}_M$ = modeling variation,

${}_{\ln}\sigma^2{}_P$ = parametric variation.

Validation Of The Point- and Finite-Source Models

In a recent Department of Energy sponsored project (Silva et al., 1997), both the point- and finite-source stochastic models were validated in a systematic and comprehensive manner. In this project, 16 well recorded earthquakes were modeled at about 500 sites. Magnitudes ranged from **M** 5.3 to **M** 7.4 with fault distances from about 1 km out to 218 km for WUS earthquakes and 460 km for CEUS earthquakes. This range in magnitude and distance as well as number of

---

[2] Strong ground motions are generally considered to be log normally distributed.

earthquakes and sites results in the most comprehensively validated model currently available to simulate strong ground motions.

A unique aspect of this validation is that rock and soil sites were modeled using generic rock and soil profiles and equivalent-linear site response. Validations done with other simulation procedures typically neglect site conditions as well as nonlinearity resulting in ambiguity in interpretation of the simulated motions.

Point-Source Model

Final model bias and variability estimates for the point-source model are shown in Figure C1. Over all the sites (Figure C1) the bias is slightly positive for frequencies greater than about 10 Hz and is near zero from about 10 Hz to 1 Hz. Below 1 Hz, a stable point-source overprediction is reflected in the negative bias. The analyses are considered reliable down to about 0.3 Hz (3.3 sec) where the point-source shows about a 40% overprediction.

The model variability is low, about 0.5 above about 3 to 4 Hz and increases with decreasing frequency to near 1 at 0.3 Hz. Above 1 Hz, there is little difference between the total variability (uncertainty plus randomness) and randomness (bias corrected variability) reflecting the near zero bias estimates. Below 1 Hz there is considerable uncertainty contributing to the total variability suggesting that the model can be measurably improved as its predictions tend to be consistently high at very low frequencies (□ 1 Hz). This stable misfit may be interpreted as the presence of a second corner frequency for WNA sources (Atkinson and Silva, 1997).

Finite-Source Model

For the finite-fault, Figure C2 shows the corresponding bias and variability estimates. For all the sites, the finite-source model provides slightly smaller bias estimates and, surprisingly, slightly higher variability for frequencies exceeding about 5 Hz. The low frequency (□≤ 1 Hz) point-source overprediction is not present in the finite-source results, indicating that it is giving more accurate predictions than the point-source model over a broad frequency range, from about 0.3 Hz (the lowest frequency of reliable analyses) to the highest frequency of the analyses.

In general, for frequencies of about 1 Hz and above the point-source and finite-source give comparable results: the bias estimates are small (near zero) and the variabilities range from about 0.5 to 0.6. These estimates are low considering the analyses are based on a data set comprised of earthquakes with **M** less than **M** 6.5 (288 of 513 sites) and high frequency ground motion variance decreases with increasing magnitude, particularly above **M** 6.5 (Youngs et al., 1995) Additionally, for the vast majority of sites, generic site conditions were used (inversion kappa values were used for only the Saguenay and Nahanni earthquake analyses, 25 rock sites). As a result, the model variability (mean = 0) contains the total uncertainty and randomness contribution for the site. The parametric variability due to uncertainty and randomness in site parameters: shear-wave velocity, profile depth, G/G_{max} and hysteretic damping curves need not be added to the model variability estimates. It is useful to perform parametric variations to assess site parameter sensitivities on the ground motions, but only source and path damping Q(f) parametric variabilities require assessment on a site specific basis and added to the model variability. The source uncertainty and randomness components include point-source stress drop and finite-source slip model and nucleation point variations (Silva, 1992).

Empirical Attenuation Model

As an additional assessment of the stochastic models, bias and variability estimates were made over the same earthquakes (except Saguenay since it was not used in the regressions) and sites using a recently develop empirical attenuation relation (Abrahamson and Silva, 1997). For all the sites, the estimates are shown in Figure C3. Interestingly, the point-source overprediction below about 1 Hz is present in the empirical relation perhaps suggesting that this suite of earthquakes possess lower than expected motions in this frequency range as the empirical model does not show this bias over all earthquake (≈ 50) used in its development. Comparing these results to the point- and finite-source results (Figures C1 and C2) show comparable bias and variability estimates. For future predictions, source and path damping parametric variability must be added to the numerical simulations which will contribute a σ_{ln} of about 0.2 to 0.4, depending upon frequency, source and path conditions, and site location. This will raise the modeling variability from about 0.50 to the range of 0.54 to 0.64, about 10 to 30%. These values are still comparable to the variability of the empirical relation indicating that the point- and finite-source numerical models perform about as well as a recently developed empirical attenuation relation for the validation earthquakes and sites.

These results are very encouraging and provide an additional qualitative validation of the point- and finite-source models. Paranthetically this approach provides a rational basis for evaluating empirical attenuation models.

APPENDIX C

REFERENCES

Abrahamson, N.A. and W.J. Silva (1997). "Empirical response spectral attenuation relations for shallow crustal earthquakes." *Seismological Research Let.,* 68(1), 94-127.

Abrahamson, N.A., P.G. Somerville, and C.A. Cornell (1990). "Uncertainty in numerical strong motion predictions" *Proc. Fourth U.S. Nat. Conf. Earth. Engin.*, Palm Springs, CA., 1, 407-416.

Aki, K. and P.G. Richards. (1980). *"Quantitative siesmology."* W. H. Freeman and Co., San Francisco, California.

Atkinson, G.M and W.J. Silva (1997). "An empirical study of earthquake source spectra for California earthquakes." *Bull. Seism. Soc. Am.* 87(1), 97-113.

Anderson, J.G. and S.E. Hough (1984). "A Model for the Shape of the Fourier Amplitude Spectrum of Acceleration at High Frequencies." *Bulletin of the Seismological Society of America,* 74(5), 1969-1993.

Atkinson, G.M. (1984). "Attenuation of strong ground motion in Canada from a random vibrations approach." *Bull. Seism. Soc. Am.*, 74(5), 2629-2653.

Boore, D.M., W.B. Joyner, and T.E. Fumal (1997). "Equations for estimating horizontal response spectra and peak acceleration from Western North American earthquakes: A summary of recent work." *Seism. Res. Lett.* 68(1), 128-153.

Boore, D.M., W.B. Joyner, and T.E. Fumal (1994). "Estimation of response spectra and peak accelerations from western North American earthquakes: and interim report. Part 2. *U.S. Geological Survey Open-File Rept.* 94-127.

Boore, D.M., and G.M. Atkinson (1987). "Stochastic prediction of ground motion and spectral response parameters at hard-rock sites in eastern North America." *Bull. Seism. Soc. Am.*, 77(2), 440-467.

Boore, D.M. (1986). "Short-period P- and S-wave radiation from large earthquakes: implications for spectral scaling relations." *Bull. Seism. Soc. Am.*, 76(1) 43-64.

Boore, D.M. and W.B. Joyner (1984). "A note on the use of random vibration theory to predict peak amplitudes of transient signals." *Bull. Seism. Soc. Am.*, 74, 2035-2039.

Boore, D.M. (1983). "Stochastic simulation of high-frequency ground motions based on seismological models of the radiated spectra." *Bull. Seism. Soc. Am.*, 73(6), 1865-1894.

Brune, J.N. (1971). "Correction." *J. Geophys. Res.* 76, 5002.

Brune, J.N. (1970). "Tectonic stress and the spectra of seismic shear waves from earthquakes." *J. Geophys. Res.* 75, 4997-5009.

Campbell, K.W. (1993) "Empirical prediction of near-source ground motion from large earthquakes." in V.K. Gaur, ed., *Proceedings, Intern'l Workshop on Earthquake Hazard and Large Dams in the Himalya.* INTACH, New Delhi, p. 93-103.

Cornell, C.A. (1968). "Engineering seismic risk analysis." *Bull. Seism. Soc. Am.*, 58, 1583-1606.

Electric Power Research Institute (1993). "Guidelines for determining design basis ground motions." Palo Alto, Calif: Electric Power Research Institute, vol. 1-5, EPRI TR-102293.

vol. 1: Methodology and guidelines for estimating earthquake ground motion in eastern North America.
vol. 2: Appendices for ground motion estimation.
vol. 3: Appendices for field investigations.
vol. 4: Appendices for laboratory investigations.
vol. 5: Quantification of seismic source effects.

Hanks, T.C. (1982). "f_{max}." *Bull. Seism. Soc. Am.*, 72, 1867-1879.

Hanks, T.C. and R.K. McGuire (1981). "The character of high-frequency strong ground motion." *Bull. Seism. Soc. Am.*, 71(6), 2071-2095.

Hanks, T.C. and H. Kanamori (1979). "A moment magnitude scale." *J. Geophys. Res.*, 84, 2348-2350.

Hartzell, S., A. Leeds, A. Frankel, and J. Michael (1996). "Site response for urban Los Angeles using aftershocks of the Northridge earthquake." *Bull. Seism. Soc. Am.*, 86(1B), S168-S192.

Hartzell, S.H. (1978). "Earthquake aftershocks as Green's functions." *Geophys. Res. Letters*, 5, 1-4.

Hough, S.E., J.G. Anderson, J. Brune, F. Vernon III, J. Berger, J. Fletcher, L. Haar, T. Hanks, and L. Baker (1988). "Attenuation near Anza, California." *Bull. Seism. Soc. Am.*, 78(2), 672-691.

Hough, S.E. and J.G. Anderson (1988). "High-Frequency Spectra Observed at Anza, California: Implications for Q Structure." *Bull. Seism. Soc. Am.*, 78(2), 692-707.

Irikura, K. (1983). "Semi-empirical estimation of strong ground motions during large earthquakes." *Bull. Disaster Prevention Res. Inst.*, Kyoto Univ., 33, 63-104.

McGuire, R. K., A.M. Becker, and N.C. Donovan (1984). "Spectral Estimates of Seismic Shear Waves." *Bull. Seism. Soc. Am.*, 74(4), 1427-1440.

Ou, G.B. and R.B. Herrmann (1990). "Estimation theory for strong ground motion." *Seism Res. Letters.* 61.

Papageorgiou, A.S. and K. Aki (1983). "A specific barrier model for the quantitative description of inhomogeneous faulting and the prediction of strong ground motion, part I, Description of the model." *Bull. Seism. Soc. Am.*, 73(4), 693-722.

Roblee, C.J., W.J. Silva, G.R. Toro and N. Abrahamson (1996). "Variability in site-specific seismic ground-motion design predictions." Uncertainty in the Geologic Environment: From Theory to Practice, Proceedings of "Uncertainty '96" ASCE Specialty Conference, Edited by C.D. Shackelford, P.P. Nelson, and M.J.S. Roth, Madison, WI, Aug. 1-3, pp. 1113-1133.

Rovelli, A., O. Bonamassa, M. Cocco, M. Di Bona, and S. Mazza (1988). "Scaling laws and spectral parameters of the ground motion in active extensional areas in Italy." *Bull. Seism. Soc. Am.*, 78(2), 530-560.

Schneider, J.F., W.J. Silva, and C.L. Stark (1993). "Ground motion model for the 1989 **M** 6.9 Loma Prieta earthquake including effects of source, path and site." *Earthquake Spectra*, 9(2), 251-287.

Silva, W.J., N. Abrahamson, G. Toro, and C. Costantino (1997). "Description and validation of the stochastic ground motion model." Submitted to Brookhaven National Laboratory, Associated Universities, Inc. Upton, New York.

Silva, W.J. and R. Darragh (1995). "Engineering characterization of earthquake strong ground motion recorded at rock sites." Palo Alto, Calif:Electric Power Research Institute, TR-102261.

Silva, W.J. and C.L. Stark (1993) "Source, path, and site ground motion model for the 1989 **M** 6.9 Loma Prieta earthquake." CDMG draft final report.

Silva, W.J. (1992). "Factors controlling strong ground motions and their associated uncertainties." *Dynamic Analysis and Design Considerations for High Level Nuclear Waste Repositories, ASCE* 132-161.

Silva, W.J. (1991). "Global characteristics and site geometry." Chapter 6 in *Proceedings: NSF/EPRI Workshop on Dynamic Soil Properties and Site Characterization.* Palo Alto, Calif.: Electric Power Research Institute, NP-7337.

Silva, W. J., R. Darragh, C. Stark, I. Wong, J. C. Stepp, J. Schneider, and S-J. Chiou (1990). "A Methodology to Estimate Design Response Spectra in the Near-Source Region of Large Earthquakes Using the Band-Limited-White-Noise Ground Motion Model". *Procee. of the Fourth U.S. Conf. on Earthquake Engineering,* Palm Springs, California. 1, 487-494.

Silva, W.J., R.B. Darragh, R.K. Green and F.T. Turcotte (1989). *Estimated Ground Motions for a New Madrid Event.* U.S. Army Engineer Waterways Experiment Station, Wash., DC, Misc. Paper GL-89-17.

Silva, W. J. and R. K. Green (1988). "Magnitude and Distance Scaling of Response Spectral Shapes for Rock Sites with Applications to North American Environments." In *Proceedings: Workshop on Estimation of Ground Motion in the Eastern United States*, EPRI NP-5875, Electric Power Research Institute.

Silva, W. J., T. Turcotte, and Y. Moriwaki (1988). "Soil Response to Earthquake Ground Motion," Electric Power Research Institute, Walnut Creek, California, Report No. NP-5747.

Silva, W.J. and K. Lee (1987). "*WES RASCAL code for synthesizing earthquake ground motions.*" State-of-the-Art for Assessing Earthquake Hazards in the United States, Report 24, U.S. Army Engineers Waterways Experiment Station, Miscellaneous Paper S-73-1.

Somerville, P.G., R. Graves and C. Saikia (1995). "TECHNICAL REPORT: Characterization of ground motions during the Northridge earthquake of January 17, 1994." *Structural Engineers Association of California (SEAOC).* Report No. SAC-95-03.

Toro, G. R. and R. K. McGuire (1987). "An Investigation into Earthquake Ground Motion Characteristics in Eastern North America." *Bull. Seism. Soc. Am.*, 77(2), 468-489.

Toro, G. R. (1985). "Stochastic Model Estimates of Strong Ground Motion." In *Seismic Hazard Methodology for Nuclear Facilities in the Eastern United States*, Appendix B, R. K. McGuire, ed., Electric Power Research Institute, Project P101-29.

Wald, D.J. (1996). "Slip history of the 1995 Kobe, Japan, earthquake determined from strong motion, teleseismic, and geodetic data." *J. of Physics of the Earth,* 44(5), 489-504.

Wald, D.J. and T.H. Heaton (1994). "Spatial and temporal distribution of slip for the 1992 Landers, California, earthquake." *Bull. Seism. Soc. Amer.*, 84(3), 668-691.

APPENDIX C

Wells, D.L. and K.J. Coppersmith (1994). "New empirical relationships among magnitude, rupture length, rupture width, rupture area, and surface displacement." *Bull. Seism. Soc. Am.* 84(4), 974-1002.

Youngs, R.R., N.A. Abrahamson, F. Makdisi, and K. Sadigh (1995). "Magnitude dependent dispersion in peak ground acceleration." *Bull. Seism. Soc. Amer.*, 85(1), 161-1, 176.

Table C.1

CONTRIBUTIONS TO TOTAL VARIABILITY IN GROUND MOTION MODELS

	Modeling Variability	Parametric Variability
Uncertainty *(also Epistemic Uncertainty)*	Modeling Uncertainty: Variability in predicted motions resulting from particular model assumptions, simplifications and/or fixed parameter values. *Can be reduced by adjusting or "calibrating" model to better fit observed earthquake response.*	Parametric Uncertainty: Variability in predicted motions resulting from incomplete data needed to characterize parameters. *Can be reduced by collection of additional information which better constrains parameters*
Randomness *(also Aleatory Uncertainty)*	Modeling Randomness: Variability in predicted motions resulting from discrepancies between model and actual complex physical processes. *Cannot be reduced for a given model form.*	Parametric Randomness: Variability in predicted motions resulting from inherent randomness of parameter values. *Cannot be reduced a priori*[***] *by collection of additional information.*

[***] Some parameters (e.g. source characteristics) may be well defined after an earthquake.

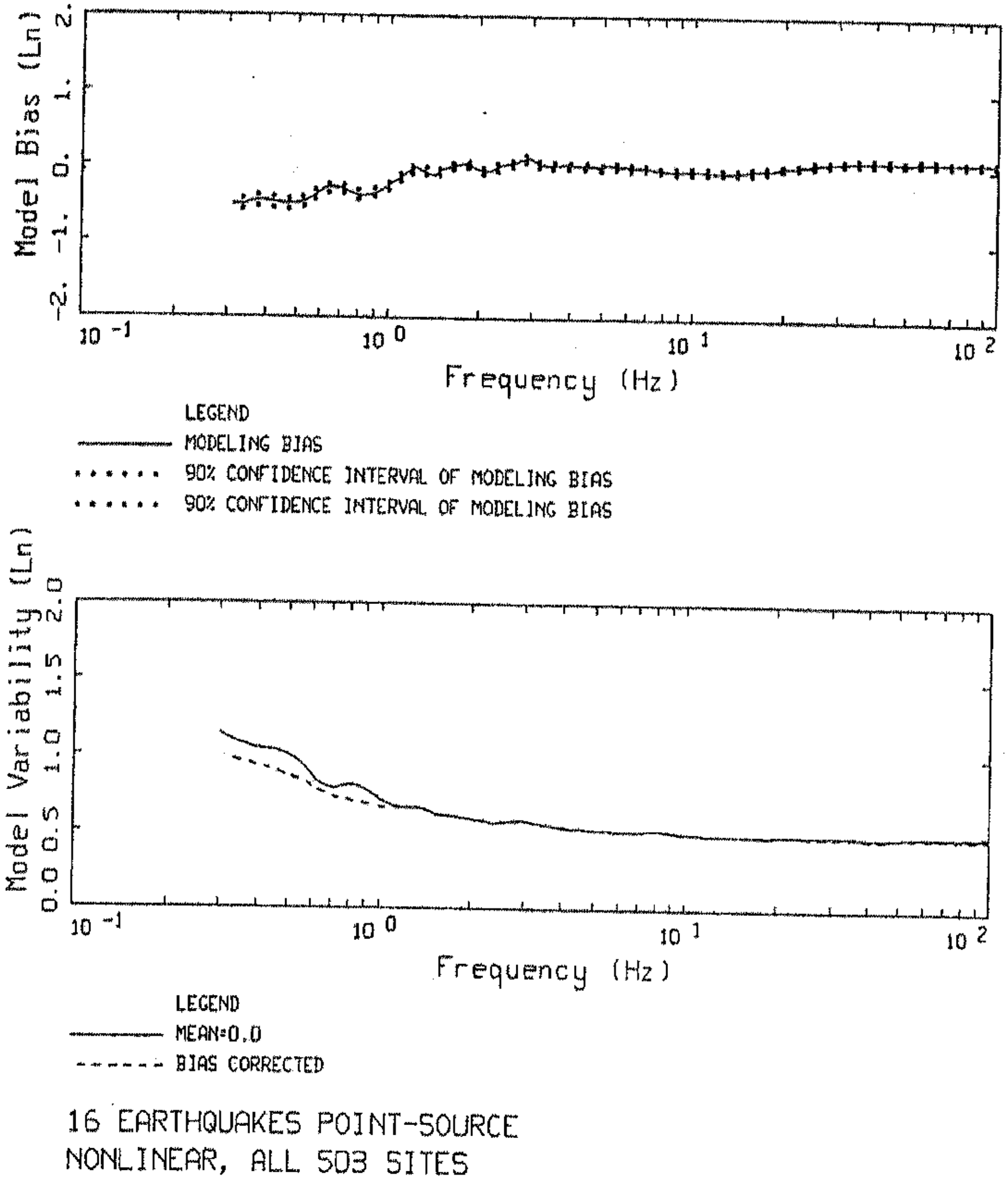

Figure C1. Model bias and variability estimates for all earthquakes computed over all 503 sites for the point-source model.

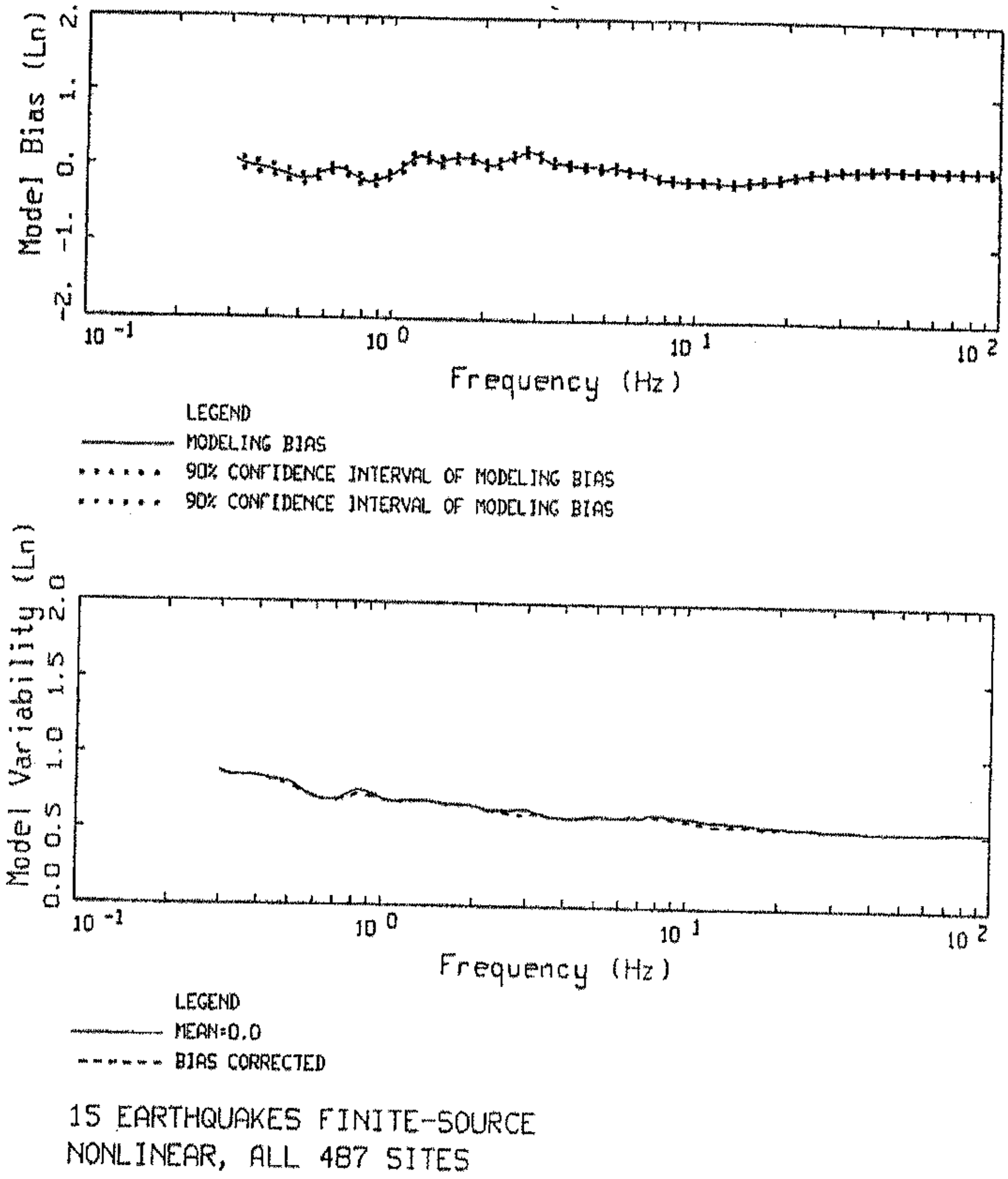

Figure C2. Model bias and variability estimates for all earthquakes computed over all 487 sites for the finite-source model.

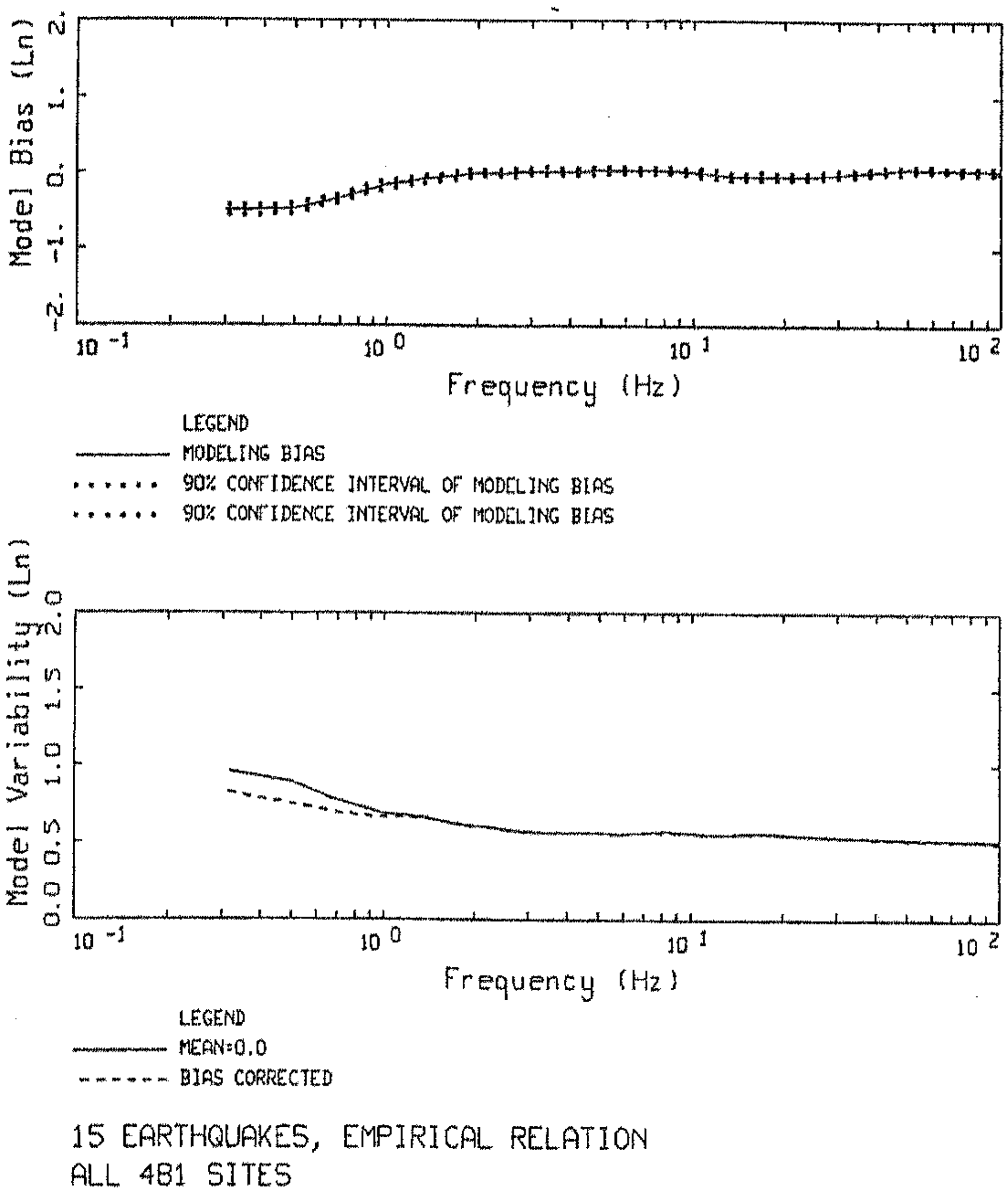

Figure C-3. Model bias and variability estimates for all earthquakes computed over all 481 sites for the empirical model.

APPENDIX D

APPROACHES TO DEVELOP SITE-SPECIFIC HAZARD

In developing site-specific UHRS's or hazard there are two goals which must be met to achieve desired risk levels:

1) Preserve the hazard level (AEF) of the reference site PSHA across structural frequency (hazard consistent),

2) Incorporate site-specific aleatory (randomness) and epistemic (uncertainty) variabilities of dynamic material properties in the hazard.

Description of Approaches

In general there are four fairly distinct approaches intended to accomplish the stated goals. The approaches range from the simplest and least accurate (Approach 1), which scales the reference site UHRS on the basis of a site-response analysis using a broad-band control motion to the most complex and most accurate, a PSHA computed using attenuation relations, median estimates and standard deviations, developed for the specific-site (Approach 4).

Approach 1: This approach is fundamentally deterministic and involves, for a rock references site, use of the outcrop UHS to drive the site-specific column(s). By definition it assumes a rock outcrop hazard (UHS) has similar characteristics as rock beneath soil, not generally a valid assumption for soft rock (NUREG/CR-6728), and has no mechanism to conserve the outcrop AEF. For cases where the hazard is dominated by earthquakes with significantly different **M** at low (e.g. ≤ 1 Hz to 2.5 Hz) and high (e.g. ≥ 5 Hz to 10 Hz) structural frequencies, the outcrop UHS may be quite broad, unlike any single earthquake, resulting in unconservative high-frequency motions (too nonlinear in site response). Even if only a single earthquake is the major contributor at all structural frequencies, variabilities incorporated in the hazard analysis may result in a broad spectrum, again unlike any single earthquake. For these reasons, this approach is discouraged and Approach 2, an alternative semi-deterministic method may be used.

Approach 2: This approach is also fundamentally deterministic and is intended to avoid the broad-band control motion of Approach 1. For a rock reference site, Approach 2 uses low-and high-frequency (and intermediate if necessary) deterministic spectra computed from the attenuation relations used in the PSHA, or suitable spectral shapes (NUREG/CR-6728), reflecting expected rock conditions beneath the local soils, scaled to the UHRS at the appropriate frequencies (e.g., RG 1.165). These scaled motions, computed for the modal deaggregation **M** and *D* are then used as control motions to develop multiple (typically 2 to 3) mean transfer functions based on randomized soil columns. If the control motions are developed from the attenuation relations used in the reference PSHA, the generic site condition they reflect must be appropriate for the rock beneath the local soils. Additionally, separate control motions should be developed for each attenuation relation to include the effects of spectral shape uncertainty (epistemic) on soil response. The resulting mean transfer functions would then be combined using the same relative weights as in the reference PSHA. The mean transfer functions are then enveloped with the resulting transfer function applied to the outcrop (rock or soil) UHS. This method was termed Approach 2A in NUREG/CR-6728. The use of mean (rather than median) transfer functions followed by enveloping is an empirical procedure to conservatively maintain the outcrop exceedence probability (NUREG/CR-6728 and –6769), as this fundamentally deterministic approach does not include the contributions to soil spectra from the entire range in rock or reference site hazard (Bazzurro and Cornell, 2004). The motivation for this "empirical" procedure is discussed in Approach 3 – Approximate Method.

For cases where there may be a wide magnitude range contributing to the hazard at low- or high-frequency and/or the site has highly nonlinear dynamic material properties, low, medium, and high **M** control motion spectra may be developed at each frequency of interest. A weighted mean transfer function (e.g., with weight of 0.2, 0.6, 0.2 reflecting 5%, mean, 95% **M** contributions) is then developed at each structural frequency of interest. Following Approach 2A, the weighted mean transfer functions for each frequency of interest are then enveloped with the resultant applied to the outcrop UHS. This more detailed analysis procedure was termed Approach 2B.

Approach 3: This approach is a fully probabilistic analysis procedure which moves the site response, in an approximate way, into the hazard integral. The approach is described by Bazzurro and Cornell (2004) and NUREG/CR-6769. In this approach, the hazard at the soil surface is computed by integrating the site-specific hazard curve at the bedrock level with the probability distribution of the amplification factors (Lee *et al.*, 1998; 1999). The site-specific amplification, relative to CENA rock is characterized by a suite of frequency-dependent amplification factors that can account for nonlinearity in soil response. Approach 3 involves approximations to the hazard integration using suites of transfer functions, which result in complete hazard curves at the ground surface, or any other location, for specific ground motion parameters (e.g., spectral accelerations) and a range of frequencies.

The basis for Approach 3 is a modification of the standard PSHA integration:

$$P[A_S>z] = \int\int\int P\left[AF > \frac{z}{a} \middle| m, r, a\right] f_{M,R|A}\ (m,r;a) f_A(a) dmdrda \qquad (1)$$

where A_S is the random ground motion amplitude on soil at a certain natural frequency, z is a specific level of A_S, m is earthquake magnitude, r is distance, a is an amplitude level of the random reference site (e.g. hard rock) ground motion, A, at the same frequency as A_S, $f_A(a)$ is derived from the rock hazard curve for this frequency (namely it is the absolute value of its derivative), and $f_{M,R|A}$ is the deaggregated hazard (i.e., the joint distribution of M and R, given that the rock amplitude is level a). AF is an amplification factor defined as:

$$AF = A_S/a$$

(2)

where AF is a random variable with a distribution that can be a function of m, r, and a. To accommodate epistemic uncertainties in site dynamic material properties, multiple suites of AF may be used and the resulting hazard curves combined with weights to properly reflect mean hazard and fractiles.

Soil response, in terms of site amplification (Sa (site)/Sa (reference)), is controlled primarily by the level of rock motion and m, so Equation 1 can be approximated by:

$$P[A_S>z] = \int\int P[AF > \frac{z}{a}(m,a)f_{M|A}(m;a)f_A(a)dmda \quad (3)$$

where r is dropped because it has an insignificant effect in most applications. To implement Equation 3, only the conditional magnitude distribution for relevant amplitudes of a is needed. $f_{M|A}(m;a)$ can be represented (with successively less accuracy) by a continuous function, with three discrete values or with a single point, (e.g., $m^1(a)$, the model magnitude given a). With the latter, Equation 3 can be simplified to:

$$P[A>z] = \int\int P[AF > \frac{z}{a}|a,m^1(a)]f_A(a)da$$

(4)

where, $f_{M|A}(m;a)$ has been replaced with m^1 derived from deaggregation. With this equation, one can integrate over the rock acceleration, a, to calculate $P[A_S>z]$ for a range of soil amplitudes, z.

It is important to note there are two ways to implement Approach 3. The full integration method described below or simply modifying the attenuation relation ground motion value during the hazard analysis with a suite of transfer functions (Cramer, 2003). Both implementation result in very similar site-specific hazard (Cramer, 2003) and both will tend to double count site aleatory variability, once in the suite of transfer function realizations and again in the aleatory variability about each median attenuation relation. The full integration method tends to lessen any potential impacts of the large total site aleatory variability (Bazzuro and Cornell, 2004). Approximate corrections, for the site component of aleatory variability, may be made by implementing the approximate technique (Equation 7) with C = 0, AF =1, and a negative exponential, where a_{rp} = the soil amplitude and σ the component of variability that is removed. For the typical aleatory variability of the amplification factors ($\sigma_{ln} \approx 0.1\text{-}0.3$) and typical hazard curve slopes in the CENA ($\kappa \approx 2\text{-}3$) the reduction in motion is about 5% to 10%.

Approach 4: Approach 4 entails the development and use of site-specific attenuation relationships, median estimates and aleatory variabilities, developed specifically for the site of interest which incorporate the site response characteristics of the site. The PSHA is performed using these site-specific relationships for the specified AEF. This approach is considered the most accurate as it is intended to accommodate the appropriate amounts of a aleatory variability into site and region specific attenuation relations. Epistemic variability is appropriately captured through the use of multiple attenuation relations. Approach 3 is considered as a fully probabilistic approximation to Approach 4.

Approach 3 – Full Integration Method

The site-specific hazard curve can be calculated using the discretized form of Equation 3 from Bazzurro and Cornell (2004).

$$G_Z(z) = \sum_{all\ x_j} P\left[Y \geq \frac{z}{x}\middle| x_j\right] px(x_j) = \sum_{all\ x_j} G_{Y|X}\left(\frac{z}{x}\middle| x_j\right) p_X(x_j). \qquad (5)$$

where $G_Z(z)$ is the sought hazard curve for $S^s{}_a(f)$, that is, the annual probability of exceeding level z.

$$G_{Y|X}\left(\frac{z}{x}\middle| x\right) = \hat{\Phi}\left(\frac{ln\left[\frac{z}{x}\right] - ln\left[\hat{m}_{Y|X}(x)\right]}{\sigma_{\ln Y|X}}\right)$$

(6)

where $G_{Y|X}$ is the complementary cumulative distribution function of (CCDF) Y = AF(f), conditional on a rock amplitude x. This is simply the CCDF of the site amplification factors as a function of control motion (e.g. rock or reference site) loading level.

$\hat{\Phi} = 1 - \Phi$ - the widely tabulated complementary standard Gaussian cumulative distribution function.

$\hat{m}_{Y|X}$ - the conditional median of Y (the amplification factor).

$\sigma_{\ln Y|X}$ - the conditional standard deviation of the natural logarithm of Y (aleatory variability of the amplification factor).

$p_X(x_j)$ - the probability that the rock or reference site control motion level is equal to (or better, in the neighborhood of) x_j.

Equation 5 is the essence of Approach 3 and simply states that the soil hazard curve is computed as the product of the soil amplification (specifically its CCDF), conditional on a reference (rock) amplitude x, times the probability of obtaining that reference amplitude, summed over all reference amplitudes.

The soil amplifications, median and $\sigma_{\ln}$ estimates are all that is required and are generated by driving the soil column at a suite of reference site motions. At each reference motion, multiple realizations of randomized dynamic material properties are developed followed by site response analyses to generate a suite, typically 30 to 100, of amplification factors. From that suite, a median and $\sigma_{\ln}$ is computed, generally assuming a log-normal distribution.

The probability of obtaining a reference motion is simply the derivative of the reference (e.g. rock) hazard curve obtained from the PSHA. This is done numerically and is a stable process as the hazard curves are quite smooth. Equation 5 can quite easily be put into an EXCEL spread sheet. It forms the entire basis of our FORTRAN code. Approach 3 is indeed, one simple equation. This approach is implemented in the computer program SOILUHSI

Approach 3 – Approximate Method

An alternative solution to Equation 4 can also be calculated using Equation (7) from Bazzuro and Cornell (2004). This is a closed form approximation of the integration of the amplification factor over a range of rock amplitudes.

$$z_{rp} = a_{rp}\ \overline{AF_{rp}}\ \exp\left(\frac{\sigma_{\delta}^{2}}{2}\frac{\kappa}{1-C}\right) \qquad (7)$$

where z_{rp} is soil amplitude z associated with return period r_p; a_{rp} is the reference spectral acceleration a associated with return period r_p; $\overline{AF_{rp}}$ is the geometric mean (mean log) amplification factor for the reference (e.g. rock) motions with return period r_p; k is the log-log slope of the reference hazard curve that is calculated at each point from the reference hazard curve and typically ranges from about 2 to 3 for CENA and possibly as large as 6 for WNA. C is the log-log slope (absolute value) of the amplification factor with respect to the reference motion that is calculated at each point from the amplification factors, AF and is a measure of the degree of soil nonlinearity. If $C = 0$, the response is linear and highly nonlinear for C approaching 1, where the approximation breaks down (Bazzurro and Cornell, 2004). As previously mentioned, C typically ranges from about 0.1 to about 0.8 (Bazzurro and Cornell, 2004). σ_{δ} is the log standard deviation of the AF and is typically around 0.3 ($\sigma_{\ln}$) or less. In other words, at a given AEF or point on the reference site hazard curve, the corresponding soil amplitude is given as the median soil amplification times the rock or reference site amplitude plus an exponential factor.
The exponential factor is necessary to maintain the reference AEF and accommodates both the aleatory variability as well as the degree of nonlinearity of the site amplification. The slope of the reference hazard curve is a weighting factor that includes the contributions to the soil amplitude for all reference hazard levels. Equation 7 clearly demonstrates the additional factors needed over median amplification to preserve the hazard level (AEF) of the reference motion. This Equation shows that in order to preserve the reference site (e.g. rock) hazard level, multiplying the reference motion by the median soil amplification requires an additional exponential term. This additional term includes the aleatory variability of the soil or amplification factor, the slope of the

reference site hazard curve, as well as the slope of the amplification factors (e.g. with varying reference motion). This exponential factor accommodates the potential contributions to a given soil motion by the entire range in reference site motions due to soil nonlinearity. That is, a given soil motion may have the same value at low levels of reference loading (relatively linear response) and at high loading levels (relatively nonlinear response). To preserve the reference site exceedence frequency, all the contributions to a given soil motions over the entire range in reference loading levels must be included in the soil hazard. These contributions are not explicitly considered in the deterministic Approach 2 method. Additionally, the effects of aleatory variability in the soil amplification due to lateral variability in velocities and depth to basement as well as randomness in G/G_{max} and hysteretic damping curves are included in the exponential term. For a linear site, C is zero so it is easy to see the exponential term then accommodates the effects of profile variability in the soil hazard. The reference hazard curve slope (κ in Equation 7) is present to accommodate the impacts of the soil variability and nonlinear amplification over the entire reference site motion or hazard curve. In the case $C = 0$ and for a reference hazard slope near 1, the median amplification times the exponential term simply reflects the mean, for a lognormal distribution. This was the motivation for using mean, rather than median amplification factors in Approach 2. However, for more realistic reference site hazard curve slopes, use of the mean amplification alone will result in motions that are too low for the assumed AEF. The difference or underestimate increases as soil nonlinearity, characterized through C, becomes larger for a given aleatory variability in the amplification factors. This was the motivation for the "empirical" correction in Approach 2 of enveloping the low- and high-frequency transfer functions. The high-frequency transfer function will typically have lower high-frequency amplification than the low-frequency amplification factor as it reflects higher loading levels, resulting in a higher degree of nonlinearity, and a greater value of C. Use of mean amplification alone may then depart significantly from Equation 7 resulting in higher probability motions than would be consistent with the reference hazard level, depending on the value of C and the slope of the reference hazard curve. Using an envelop of the low-frequency amplification, which typically does not reflect nearly as high loading levels at high-frequency, and the high-frequency amplification was an ad-hoc manner of conservatively achieving the desired AEF using deterministic analyses.

It is important to point out that a similar issue, though less significant, can occur at low-frequency. In this case the high-frequency amplification has larger low-frequency amplification than the low-frequency amplification. The envelope at low-frequency is then controlled by the high-frequency amplification, compensating for the neglect of the complete exponential in the low-frequency mean amplification (NUREG/CR-6728). This approach is implemented in the computer program SOILUHS.

Implementation of Approach 3

Approach 3 is implemented using the full integration method which consists simply of coding Equation 5. The soil (or rock) amplification distributions relative to the reference site condition are developed by driving the site-specific column at a suite of distances generated on a grid of expected reference site peak accelerations, to accommodate nonlinear soil response. At each distance, or reference site expected peak acceleration, random suites of dynamic material properties are generated resulting in a distribution of structural frequency dependent amplification factors (Sa (site)/Sa (reference)). For a given structural frequency, say 1 Hz, this process results in median and sigma estimates, for each loading level, from which a CCDF is produced using standard asymptotic expressions, accurate typically to the fourth decimal place. For each loading level, reference Sa at 1 Hz, the amplification CCDF is then available to integrate over the entire reference 1 Hz hazard curve. This is precisely the motivation for the wide range in reference peak accelerations, 0.01g to 1.50g , to cover the entire reference hazard curve for <u>each</u> structural frequency. For reference site motion outside the range, the closest values are used. To minimize any error in interpolation (log) for reference site motions between grid points, a dense sampling of typically 11 (e.g. 0.01, 0.05, 0.10, 0.20, 0.30, 0.40, 0.50, 0.75, 1.00, 1.25, 1.50g) values of expected (median) reference site peak accelerations are used. The array of peak accelerations is sampled more densely over the range in values contributing most to the hazard, typically 0.2g to 0.5g. Since the amplification factors are smooth (Bazzurro and Cornell, 2004; Silva et al., 1999), interpolation is not a significant issue and an 11 point grid is adequate to capture site nonlinearity.

To compute the probability of reference motions (P(x) in Equation 5), the reference motion hazard curve is numerically differentiated using central differences. Although hazard curves are smooth so differencing is a stable process, the curves are interpolated to 300 points to maximize the integration accuracy of Equation 5. The use of 300 points was established by increasing the number of points until stability (no change in derived soil hazard) was achieved. This typically occurred between 100 to 200 points so 300 points has been adopted as a conservative value for integration.

It is important to point out, because multiple levels of reference motions contribute to the soil or site-specific hazard, a wider range in reference hazard than soil hazard is necessary to achieve accuracy in the soil hazard. Extensive tests have shown that a conservative range over which to integrate the reference hazard is a factor of 10 in AEF beyond that desired for the soil or site-specific AEF. In other words, if site-specific hazard is desired to 10^{-6} AEF, reference hazard is required to an AEF of 10^{-7}. Additionally, same consideration applies at high exceedence frequencies as well. In this case, if site-specific hazard is desired at 10^{-2} AEF, reference hazard is conservatively required to an AEF of 10^{-1}.

Approach 3 is also appropriate for computing site-specific vertical hazard from horizontal site-specific hazard curves, producing vertical UHRS at the same AEF as the horizontal UHRS. Resulting horizontal and vertical UHRS's then both achieve the same target performance goals. As with the horizontal site-specific hazard, regarding the range in the reference site hazard, accuracy in the vertical hazard requires a wide integration range over the site-specific horizontal hazard. As a result to achieve an AEF of 10^{-6} for the vertical site-specific hazard requires the reference site hazard to an AEF of 10^{-8}.

APPENDIX D

REFERENCES:

Bazzurro, Paolo and C.A. Cornell (2004). "Nonlinear soil-site effects in probabilistic seismic-hazard analysis." *Bulletin of Seismological Society of America*, 94(6), 2110-2123.

Cramer, C. H. (2003) "Site-specific seismic hazard analysis that is completely probabilistic." *Bulletin of Seismological Society of America*, 93, 1841-1846.

Lee, R., M. E. Maryak, and J. Kimball (1999). "A methodology to estimate site-specific seismic hazard for critical facilities on soil or soft-rock sites." *Seismological Research Letters,* 70, 230.

Lee, R., W.J. Silva, and C. A. Cornell (1998). " Alternatives in evaluating soil- and rock-site seismic hazard." *Seismological Research Letters, 69, 81.*

McGuire, R.K.,W.J. Silva and C.J. Costantino (2001). "Technical basis for revision of regulatory guidance on design ground motions: hazard- and risk-consistent ground motions spectra guidelines." Prepared for Division of Engineering Technology, Washington, DC, *NUREG/CR-6728 and 6769.*

Silva, W. J.,S. Li, B. Darragh, and N. Gregor (1999). "Surface geology based strong motion amplification factors for the San Francisco Bay and Los Angeles Areas."A PEARL report to PG&E/CEC/Caltrans, Award No. SA2120-59652.

Appendix H

Makdisi and Seed Seismic Deformation Analysis Charts

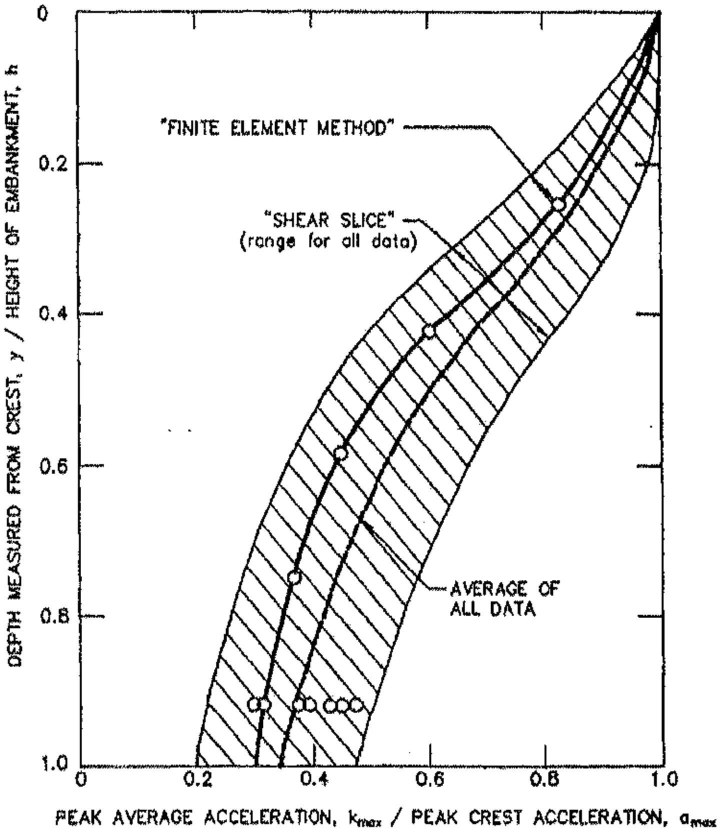

Figure 48. Variation of peak average acceleration ratio with depth of sliding mass (Makdisi and Seed, 1978, reprinted by permission of ASCE).

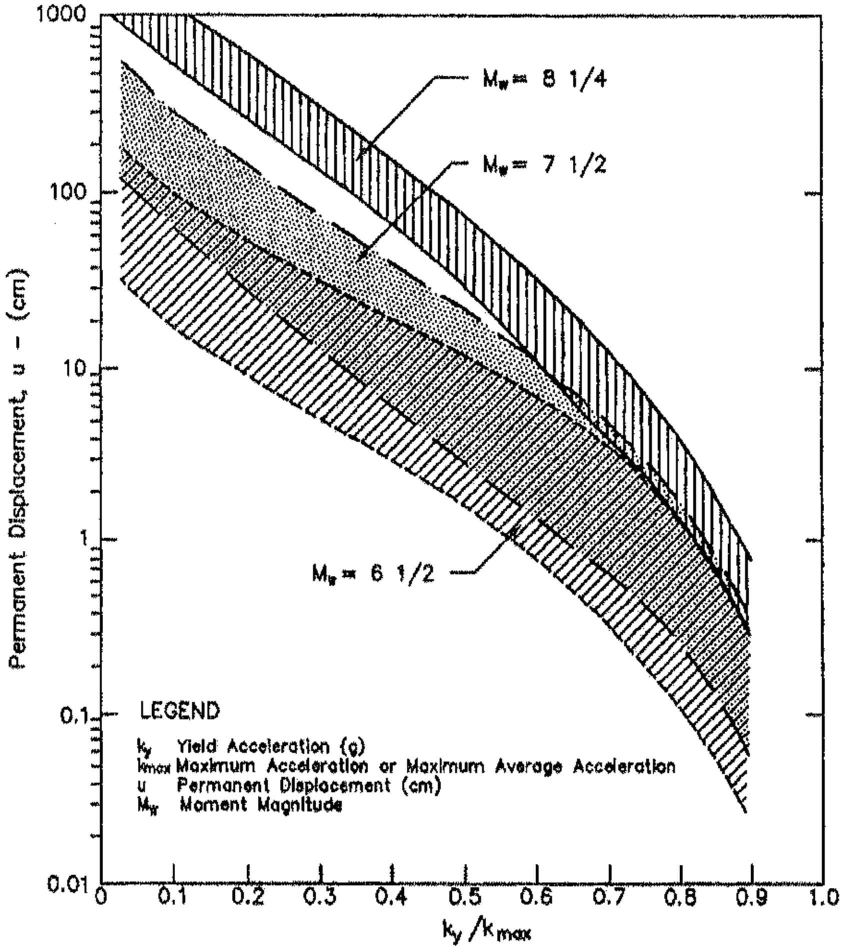

Figure 53. Permanent displacement versus normalized yield acceleration for embankments (after Makdisi and Seed, 1978, reprinted by permission of ASCE).

Appendix I

Seismic Stability and Deformation Analysis

DAN BROWN AND ASSOCIATES

Project Lowman PP Section D
Project No. 16-099
Sheet 1 **of** 2
Date 9 / 29 / 2016
Engineer BJT
Checked by TCS

Design Calculations for Permanent Seismic Displacement of Berm Charles R. Lowman Power Plant

The following calculations are for seismic displacement of berm Section D-D' at the Charles R. Lowman Power Plant with the berm height reduced by approximately 2.5 ft.

Makdisi, F.I. and Seed, H.B. (1978). "Simplified procedure for estimating dam and embankment earthquake-induced deformations" Journal of the Geotechnical Engineering Division, 104(GT7), 849-868.

Maximum expected ground acceleration $a_{max} := 0.1g$ (Uniform Hazard Spectral Acceleration 2% Probability of Exceedence in 50 years)

Embankment height $H := 11ft$

Unit weight of embankment material $\gamma_s := 112pcf$

Mass density of embankment material $\rho := \frac{\gamma_s}{g} = 3.481 \cdot \frac{slug}{ft^3}$

Shear wave velocity of embankment material $v_s := 650 \frac{ft}{sec}$

Maximum shear modulus of embankment material $G_{max} := \rho \cdot v_s^{\,2} = 1.471 \times 10^6 \cdot psf$

Step 1. Assume the average shear strain (γ) within the embankment. Makdisi and Seed report a range of measured maximum shear strain values generally between 0.1 and 0.5 percent.

Assumed average shear strain $\gamma_{assumed} := 0.0025\%$ $\log(\gamma_{assumed} \cdot 100) = -2.6$

Step 2. For the assumed average shear strain, compute a reduced shear modulus (G), damping ratio (λ) and equivalent shear wave velocity (v).

Reduced shear modulus $G := 0.94 \cdot G_{max} = 1.383 \times 10^6 \cdot psf$

Damping ratio $\lambda := 3.0\%$

Reduced shear wave velocity $v := \sqrt{\frac{G}{\rho}} = 630.198 \cdot \frac{ft}{sec}$

Step 3. Calculate the three modal periods.

$T_1 := 2.618 \cdot \frac{H}{v} = 0.046\,s$ $T_2 := 1.138 \cdot \frac{H}{v} = 0.02\,s$ $T_3 := 0.726 \cdot \frac{H}{v} = 0.013\,s$

Step 4. Determine the spectral accelerations that correspond to the modal periods and damping ratio.

$S_{a1} := .14g$ $S_{a2} := .10g$ $S_{a3} := .10g$

Step 5. Estimate the maximum acceleration occurs at the crest of the embankment.

Maximum acceleration at the crest of the embankment $uu_{max} := \sqrt{0.256 \cdot S_{a1}{}^2 + 1.12 \cdot S_{a2}{}^2 + 0.74 \cdot S_{a3}{}^2} = 0.154 \cdot g$

Step 6. Calculate the average shear strain based on the computed spectral acceleration.

Average shear strain $\gamma_{ave} := 0.195 \cdot \left(\frac{H}{v^2}\right) \cdot S_{a1} = 0.0024 \cdot \%$

Step 7. Compare the computed average shear strain to the assumed shear strain in Step 1. If they do not agree to an acceptable level, the return to Step 1 and assume a different shear strain.

Ratio of γ_{ave} to $\gamma_{assumed}$ $\frac{\gamma_{ave}}{\gamma_{assumed}} = 0.97$

Step 8. Determine the yield acceleration of the critical failure surface and the depth of the critical failure surface.

Yield acceleration of critical failure surface $k_y := 0.051g$

Depth of critical failure surface $y := 29ft$

Step 9. Determine the value of maximum average acceleration (k_{max}) for the computed value of y/H.

Ratio y to H $\frac{y}{H} = 2.636$

Determine k_{max} from Makdisi and Seed chart $k_{max} := uu_{max} \cdot 0.32 = 0.049 \cdot g$

Step 10. Calculate ratio of k_y to k_{max} and use Makdisi and See chart to estimate permanent seismic displacement.

Ratio of k_y to k_{max} $\frac{k_y}{k_{max}} = 1.037$

Moment magnitude of design earthquake $M_w := 7.5$

The yield acceleration is the minimum acceleration that triggers permanent seismic displacement. The maximum average acceleration is less than the yield acceleration which indicates that yielding does not occur and that there is zero permanent seismic displacement

Additional Reference:

Abramson, L.W., Lee, T.S., Sharma, S. and Boyce, G.M. (1996). Slope stability and stabilization methods, John Wiley & Sons, 629 p.

Method: Spencer

Calculated Factor of Safety: 1.007

Yield Acceleration (ky): 0.051g

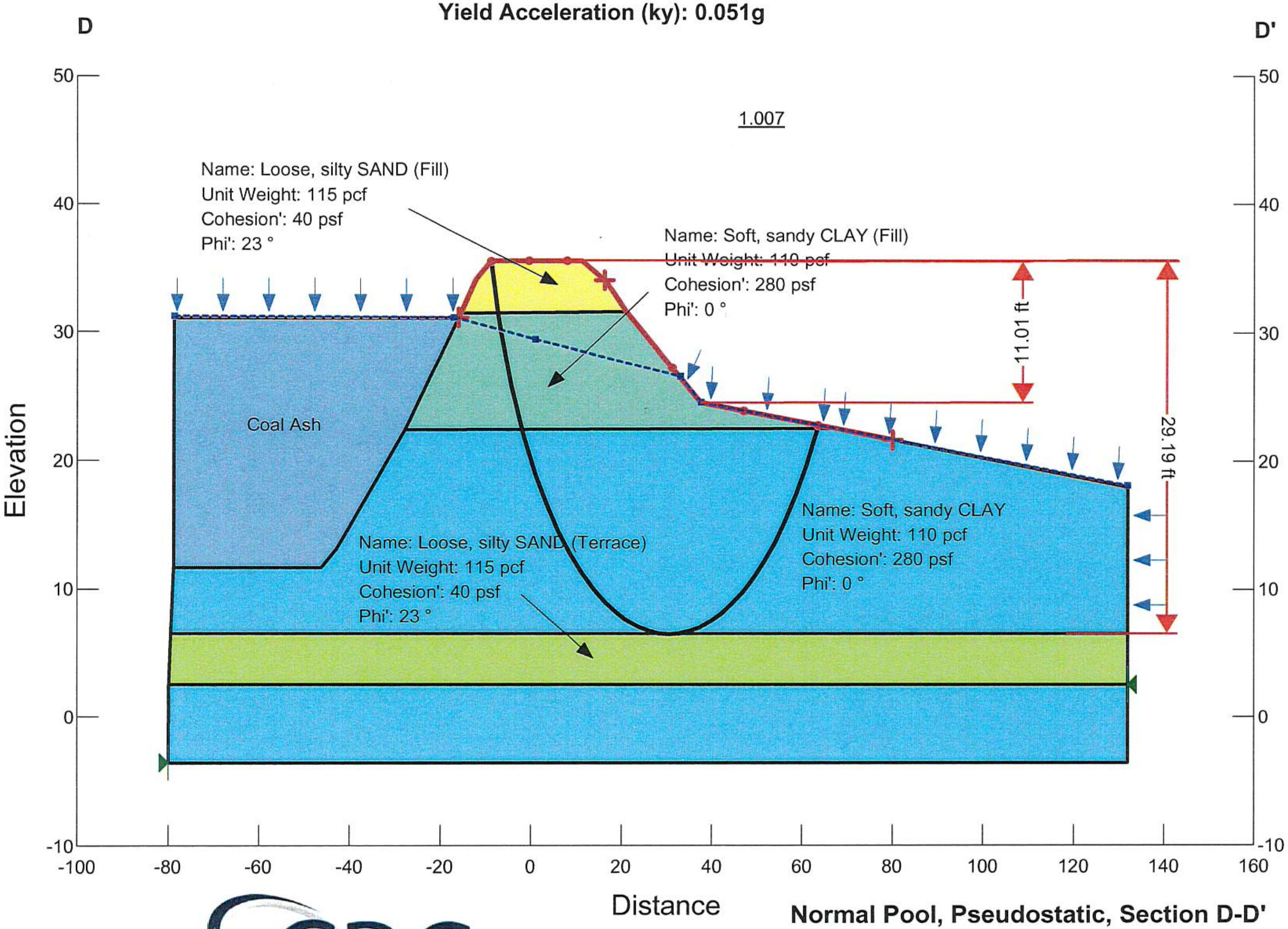

Engineering. Environmental. Answers.

Normal Pool, Pseudostatic, Section D-D'

Unit 1 Impoundment

Charles R. Lowman Power Plant

CDG Project No. 061521207

Scale: As Shown

Project <u>Lowman PP Section E</u>
Project No. <u>16-099</u>
Sheet <u>1</u> **of** <u>2</u>
Date <u>9/1/2016</u>
Engineer <u>BJT</u>
Checked by <u>TCS</u>

Design Calculations for Permanent Seismic Displacement of Berm Charles R. Lowman Power Plant

The following calculations are for seismic displacement of berm Section E-E' at the Charles R. Lowman Power Plant.

Makdisi, F.I. and Seed, H.B. (1978). "Simplified procedure for estimating dam and embankment earthquake-induced deformations" Journal of the Geotechnical Engineering Division, 104(GT7), 849-868.

Maximum expected ground acceleration $a_{max} := 0.1g$ (Uniform Hazard Spectral Acceleration 2% Probability of Exceedence in 50 years)

Embankment height $H := 3ft$

Unit weight of embankment material $\gamma_s := 120pcf$

Mass density of embankment material $\rho := \frac{\gamma_s}{g} = 3.73 \cdot \frac{slug}{ft^3}$

Shear wave velocity of embankment material $v_s := 650 \frac{ft}{sec}$

Maximum shear modulus of embankment material $G_{max} := \rho \cdot v_s^2 = 1.576 \times 10^6 \cdot psf$

Step 1. Assume the average shear strain (γ) within the embankment. Makdisi and Seed report a range of measured maximum shear strain values generally between 0.1 and 0.5 percent.

Assumed average shear strain $\gamma_{assumed} := 0.0004\ \%$ $\log(\gamma_{assumed} \cdot 100) = -3.398$

Step 2. For the assumed average shear strain, compute a reduced shear modulus (G), damping ratio (λ) and equivalent shear wave velocity (v).

Reduced shear modulus $G := 0.99 \cdot G_{max} = 1.56 \times 10^6 \cdot psf$

Damping ratio $\lambda := 2.0\%$

Reduced shear wave velocity $v := \sqrt{\frac{G}{\rho}} = 647 \cdot \frac{ft}{sec}$

Step 3. Calculate the three modal periods.

$T_1 := 2.618 \cdot \frac{H}{v} = 0.012\,s$ $T_2 := 1.138 \cdot \frac{H}{v} = 0.005\,s$ $T_3 := 0.726 \cdot \frac{H}{v} = 0.003\,s$

Step 4. Determine the spectral accelerations that correspond to the modal periods and damping ratio.

$S_{a1} := .10g$ $S_{a2} := .10g$ $S_{a3} := .10g$

Project _Lowman PP Section E_
Project No.__16-099____
Sheet ___2__ of _2__
Date ___9/1/2016____
Engineer__BJT________
Checked by___TCS______

Step 5. Estimate the maximum acceleration occurs at the crest of the embankment.

Maximum acceleration at the crest of the embankment $uu_{max} := \sqrt{0.256 \cdot S_{a1}^{2} + 1.12 \cdot S_{a2}^{2} + 0.74 \cdot S_{a3}^{2}} = 0.145 \cdot g$

Step 6. Calculate the average shear strain based on the computed spectral acceleration.

Average shear strain $\gamma_{ave} := 0.195 \cdot \left(\frac{H}{v^{2}}\right) \cdot S_{a1} = 0.0004 \cdot \%$

Step 7. Compare the computed average shear strain to the assumed shear strain in Step 1. If they do not agree to an acceptable level, the return to Step 1 and assume a different shear strain.

Ratio of γ_{ave} to $\gamma_{assumed}$ $\frac{\gamma_{ave}}{\gamma_{assumed}} = 1.12$

Step 8. Determine the yield acceleration of the critical failure surface and the depth of the critical failure surface.

Yield acceleration of critical failure surface $k_y := 0.57g$ (provided by CDG)

Depth of critical failure surface $y := 5ft$

Step 9. Determine the value of maximum average acceleration (k_{max}) for the computed value of y/H.

Ratio y to H $\frac{y}{H} = 1.667$

Determine k_{max} from Makdisi and Seed chart $k_{max} := uu_{max} \cdot 0.32 = 0.047 \cdot g$ (0.32 applies for y/h > 1)

Step 10. Calculate ratio of k_y to k_{max} and use Makdisi and See chart to estimate permanent seismic displacement.

Ratio of k_y to k_{max} $\frac{k_y}{k_{max}} = 12.245$

Moment magnitude of design earthquake $M_w := 7.5$

The yield acceleration is the minimum acceleration that triggers permanent seismic displacement. The maximum average acceleration is less than the yield acceleration which indicates that yielding does not occur and that there is zero permanent seismic displacement

Additional Reference:

Abramson, L.W., Lee, T.S., Sharma, S. and Boyce, G.M. (1996). Slope stability and stabilization methods, John Wiley & Sons, 629 p.

Methoc pencer

Calculated Factor of Safety: 0.998

Yield Acceleration (ky): 0.57g

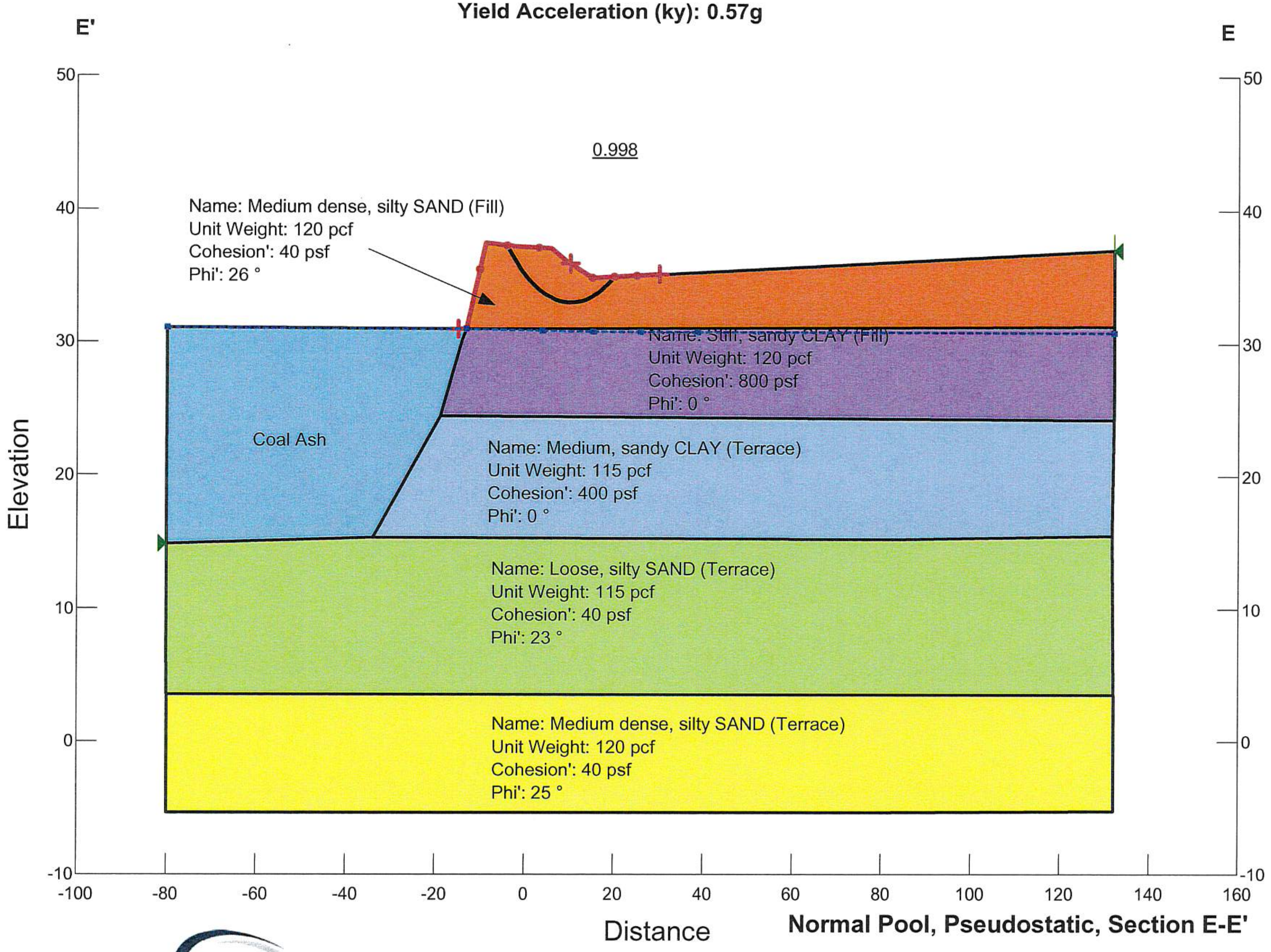

CDG

Engineering. Environmental. Answers.

Normal Pool, Pseudostatic, Section E-E'

Unit 1 Impoundment
Charles R. Lowman Power Plant
CDG Project No. 061521207
Scale: As Shown

Project Lowman PP Section G
Project No. 16-099
Sheet 1 **of** 2
Date 9 / 1 / 2016
Engineer BJT
Checked by TCS

Design Calculations for Permanent Seismic Displacement of Berm
Charles R. Lowman Power Plant

The following calculations are for seismic displacement of berm Section F-F' at the Charles R. Lowman Power Plant.

Makdisi, F.I. and Seed, H.B. (1978). "Simplified procedure for estimating dam and embankment earthquake-induced deformations" Journal of the Geotechnical Engineering Division, 104(GT7), 849-868.

Maximum expected ground acceleration $a_{max} := 0.1g$ (Uniform Hazard Spectral Acceleration 2% Probability of Exceedence in 50 years)

Embankment height $H := 5.3ft$

Unit weight of embankment material $\gamma_s := 115pcf$

Mass density of embankment material $\rho := \frac{\gamma_s}{g} = 3.574 \cdot \frac{slug}{ft^3}$

Shear wave velocity of embankment material $v_s := 650 \frac{ft}{sec}$

Maximum shear modulus of embankment material $G_{max} := \rho \cdot v_s^2 = 1.51 \times 10^6 \cdot psf$

Step 1. Assume the average shear strain (γ) within the embankment. Makdisi and Seed report a range of measured maximum shear strain values generally between 0.1 and 0.5 percent.

Assumed average shear strain $\gamma_{assumed} := 0.00088\%$ $\log(\gamma_{assumed} \cdot 100) = -3.056$

Step 2. For the assumed average shear strain, compute a reduced shear modulus (G), damping ratio (λ) and equivalent shear wave velocity (v).

Reduced shear modulus $G := 0.98 \cdot G_{max} = 1.48 \times 10^6 \cdot psf$

Damping ratio $\lambda := 2.0\%$

Reduced shear wave velocity $v := \sqrt{\frac{G}{\rho}} = 643.467 \cdot \frac{ft}{sec}$

Step 3. Calculate the three modal periods.

$T_1 := 2.618 \cdot \frac{H}{v} = 0.022\,s$ $T_2 := 1.138 \cdot \frac{H}{v} = 0.009\,s$ $T_3 := 0.726 \cdot \frac{H}{v} = 0.006\,s$

Step 4. Determine the spectral accelerations that correspond to the modal periods and damping ratio.

$S_{a1} := .11g$ $S_{a2} := .1g$ $S_{a3} := .1g$

Step 5. Estimate the maximum acceleration occurs at the crest of the embankment.

Maximum acceleration at the crest of the embankment $uu_{max} := \sqrt{0.256 \cdot S_{a1}^2 + 1.12 \cdot S_{a2}^2 + 0.74 \cdot S_{a3}^2} = 0.147 \cdot g$

Step 6. Calculate the average shear strain based on the computed spectral acceleration.

Average shear strain $\gamma_{ave} := 0.195 \cdot \left(\frac{H}{v^2}\right) \cdot S_{a1} = 0.00088 \cdot \%$

Step 7. Compare the computed average shear strain to the assumed shear strain in Step 1. If they do not agree to an acceptable level, the return to Step 1 and assume a different shear strain.

Ratio of γ_{ave} to $\gamma_{assumed}$ $\frac{\gamma_{ave}}{\gamma_{assumed}} = 1$

Step 8. Determine the yield acceleration of the critical failure surface and the depth of the critical failure surface.

Yield acceleration of critical failure surface $k_y := 0.20g$

Depth of critical failure surface $y := 26ft$

Step 9. Determine the value of maximum average acceleration (k_{max}) for the computed value of y/H.

Ratio y to H $\frac{y}{H} = 4.906$

Determine k_{max} from Makdisi and Seed chart $k_{max} := uu_{max} \cdot 0.32 = 0.047 \cdot g$ (0.32 applies for y/h > 1)

Step 10. Calculate ratio of k_y to k_{max} and use Makdisi and See chart to estimate permanent seismic displacement.

Ratio of k_y to k_{max} $\frac{k_y}{k_{max}} = 4.243$

Moment magnitude of design earthquake $M_w := 7.5$

The yield acceleration is the minimum acceleration that triggers permanent seismic displacement. The maximum average acceleration is less than the yield acceleration which indicates that yielding does not occur and that there is zero permanent seismic displacement

Additional Reference:

Abramson, L.W., Lee, T.S., Sharma, S. and Boyce, G.M. (1996). Slope stability and stabilization methods, John Wiley & Sons, 629 p.

Metł . Spencer

Calculated Factor of Safety: 0.999

Yield Acceleration (ky): 0.20g

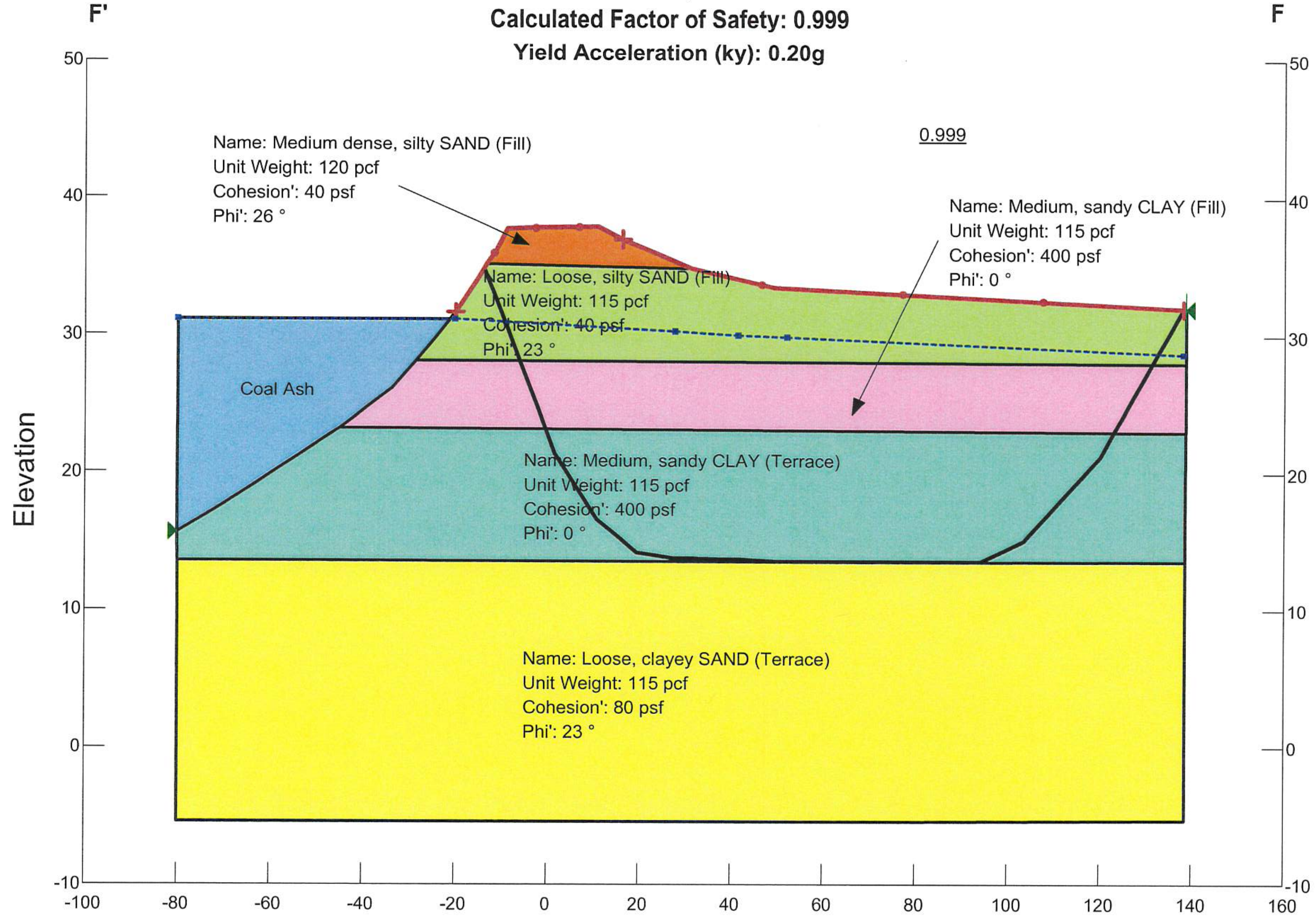

Normal Pool, Pseudostatic, Section F-F'

Unit 1 Impoundment
Charles R. Lowman Power Plant
CDG Project No. 061521207
Scale: As Shown

CDG
Engineering. Environmental. Answers.

Project Lowman PP Section G
Project No. 16-099
Sheet 1 **of** 2
Date 9 / 1 / 2016
Engineer BJT
Checked by TCS

Design Calculations for Permanent Seismic Displacement of Berm
Charles R. Lowman Power Plant

The following calculations are for seismic displacement of berm Section G-G' at the Charles R. Lowman Power Plant.

Makdisi, F.I. and Seed, H.B. (1978). "Simplified procedure for estimating dam and embankment earthquake-induced deformations" Journal of the Geotechnical Engineering Division, 104(GT7), 849-868.

Maximum expected ground acceleration $a_{max} := 0.1g$ (Uniform Hazard Spectral Acceleration 2% Probability of Exceedence in 50 years)

Embankment height $H := 13ft$

Unit weight of embankment material $\gamma_s := 125pcf$

Mass density of embankment material $\rho := \frac{\gamma_s}{g} = 3.885 \cdot \frac{slug}{ft^3}$

Shear wave velocity of embankment material $v_s := 650 \frac{ft}{sec}$

Maximum shear modulus of embankment material $G_{max} := \rho \cdot v_s^2 = 1.641 \times 10^6 \cdot psf$

Step 1. Assume the average shear strain (γ) within the embankment. Makdisi and Seed report a range of measured maximum shear strain values generally between 0.1 and 0.5 percent.

Assumed average shear strain $\gamma_{assumed} := 0.0031\%$ $\log(\gamma_{assumed} \cdot 100) = -2.509$

Step 2. For the assumed average shear strain, compute a reduced shear modulus (G), damping ratio (λ) and equivalent shear wave velocity (v).

Reduced shear modulus $G := 0.90 \cdot G_{max} = 1.477 \times 10^6 \cdot psf$

Damping ratio $\lambda := 3\%$

Reduced shear wave velocity $v := \sqrt{\frac{G}{\rho}} = 616.644 \cdot \frac{ft}{sec}$

Step 3. Calculate the three modal periods.

$T_1 := 2.618 \cdot \frac{H}{v} = 0.055\,s$ $T_2 := 1.138 \cdot \frac{H}{v} = 0.024\,s$ $T_3 := 0.726 \cdot \frac{H}{v} = 0.015\,s$

Step 4. Determine the spectral accelerations that correspond to the modal periods and damping ratio.

$S_{a1} := .15g$ $S_{a2} := .11g$ $S_{a3} := .1g$

Project Lowman PP Section G
Project No. 16-099
Sheet 2 **of** 2
Date 9 / 1 / 2016
Engineer BJT
Checked by TCS

Step 5. Estimate the maximum acceleration occurs at the crest of the embankment.

Maximum acceleration at the crest of the embankment $uu_{max} := \sqrt{0.256 \cdot S_{a1}^{2} + 1.12 \cdot S_{a2}^{2} + 0.74 \cdot S_{a3}^{2}} = 0.163 \cdot g$

Step 6. Calculate the average shear strain based on the computed spectral acceleration.

Average shear strain $\gamma_{ave} := 0.195 \cdot \left(\frac{H}{v^2} \right) \cdot S_{a1} = 0.0032 \cdot \%$

Step 7. Compare the computed average shear strain to the assumed shear strain in Step 1. If they do not agree to an acceptable level, the return to Step 1 and assume a different shear strain.

Ratio of γ_{ave} to $\gamma_{assumed}$ $\frac{\gamma_{ave}}{\gamma_{assumed}} = 1.04$

Step 8. Determine the yield acceleration of the critical failure surface and the depth of the critical failure surface.

Yield acceleration of critical failure surface $k_y := 0.22g$

Depth of critical failure surface $y := 21ft$

Step 9. Determine the value of maximum average acceleration (k_{max}) for the computed value of y/H.

Ratio y to H $\frac{y}{H} = 1.615$

Determine k_{max} from Makdisi and Seed chart $k_{max} := uu_{max} \cdot 0.32 = 0.052 \cdot g$

Step 10. Calculate ratio of k_y to k_{max} and use Makdisi and See chart to estimate permanent seismic displacement.

Ratio of k_y to k_{max} $\frac{k_y}{k_{max}} = 4.206$

Moment magnitude of design earthquake $M_w := 7.5$

The yield acceleration is the minimum acceleration that triggers permanent seismic displacement. The maximum average acceleration is less than the yield acceleration which indicates that yielding does not occur and that there is zero permanent seismic displacement

Additional Reference:

Abramson, L.W., Lee, T.S., Sharma, S. and Boyce, G.M. (1996). Slope stability and stabilization methods, John Wiley & Sons, 629 p.

Method: Spencer

Calculated Factor of Safety: 0.993

Yield Acceleration (ky): 0.22g

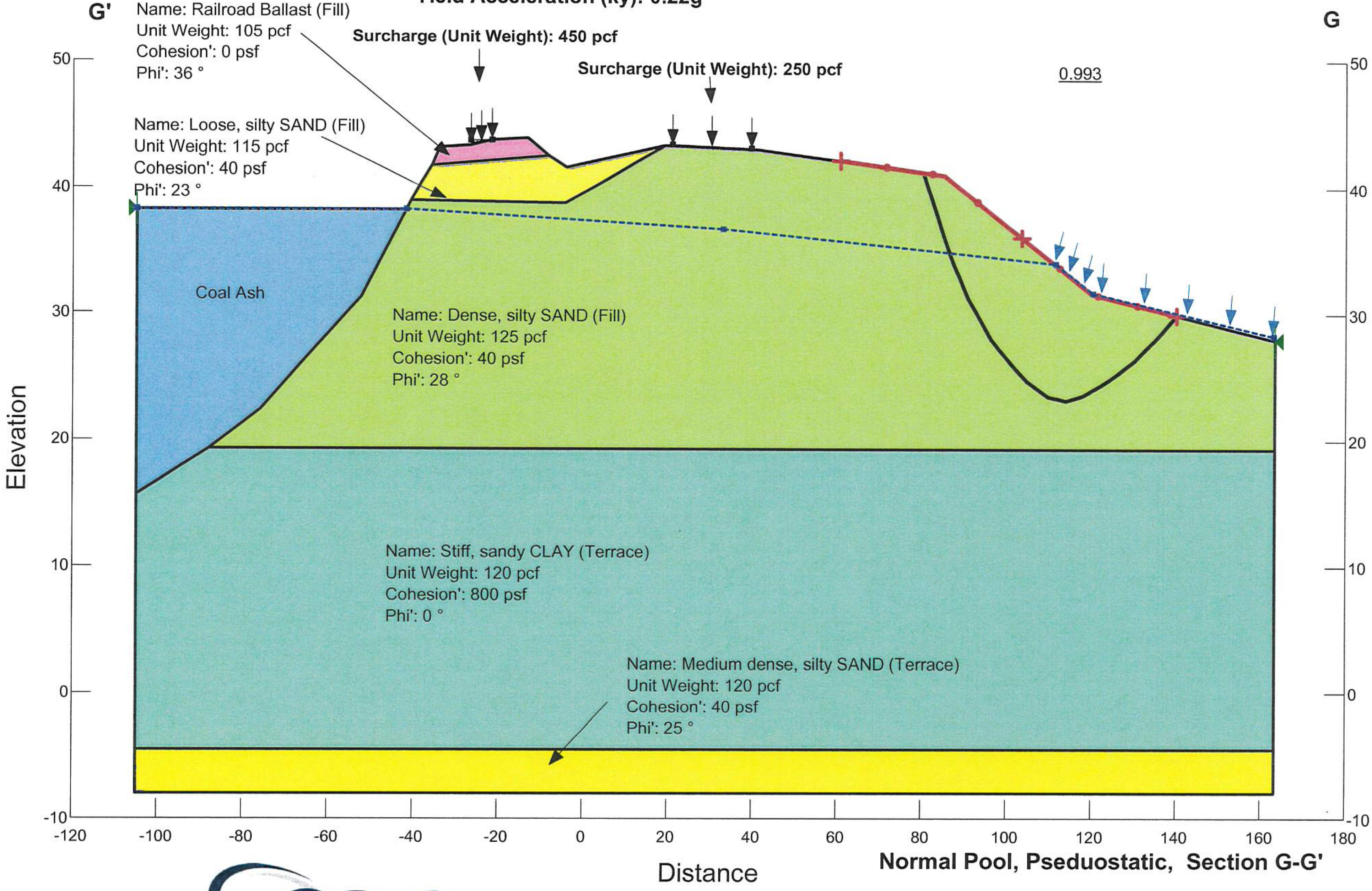

Normal Pool, Pseduostatic, Section G-G'

Unit 2/3 Impoundment
Charles R. Lowman Power Plant
CDG Project No. 061521207
Scale: As Shown

Engineering. Environmental. Answers.

Project Lowman PP Section H
Project No. 16-099
Sheet 1 **of** 2
Date 9 / 1 / 2016[
Engineer BJT
Checked by TCS

Design Calculations for Permanent Seismic Displacement of Berm
Charles R. Lowman Power Plant

The following calculations are for seismic displacement of berm Section H-H' at the Charles R. Lowman Power Plant.

Makdisi, F.I. and Seed, H.B. (1978). "Simplified procedure for estimating dam and embankment earthquake-induced deformations" Journal of the Geotechnical Engineering Division, 104(GT7), 849-868.

Maximum expected ground acceleration $a_{max} := 0.1g$ (Uniform Hazard Spectral Acceleration 2% Probability of Exceedence in 50 years)

Embankment height $H := 13ft$

Unit weight of embankment material $\gamma_s := 120pcf$

Mass density of embankment material $\rho := \frac{\gamma_s}{g} = 3.73 \cdot \frac{slug}{ft^3}$

Shear wave velocity of embankment material $v_s := 650 \frac{ft}{sec}$

Maximum shear modulus of embankment material $G_{max} := \rho \cdot v_s^{\,2} = 1.576 \times 10^6 \cdot psf$

Step 1. Assume the average shear strain (γ) within the embankment. Makdisi and Seed report a range of measured maximum shear strain values generally between 0.1 and 0.5 percent.

Assumed average shear strain $\gamma_{assumed} := 0.0032\%$ $\log(\gamma_{assumed} \cdot 100) = -2.495$

Step 2. For the assumed average shear strain, compute a reduced shear modulus (G), damping ratio (λ) and equivalent shear wave velocity (v).

Reduced shear modulus $G := 0.9 \cdot G_{max} = 1.418 \times 10^6 \cdot psf$

Damping ratio $\lambda := 3\%$

Reduced shear wave velocity $v := \sqrt{\frac{G}{\rho}} = 616.644 \cdot \frac{ft}{sec}$

Step 3. Calculate the three modal periods.

$T_1 := 2.618 \cdot \frac{H}{v} = 0.055\,s$ $T_2 := 1.138 \cdot \frac{H}{v} = 0.024\,s$ $T_3 := 0.726 \cdot \frac{H}{v} = 0.015\,s$

Step 4. Determine the spectral accelerations that correspond to the modal periods and damping ratio.

$S_{a1} := .15g$ $S_{a2} := .11g$ $S_{a3} := .1g$

Project Lowman PP Section H
Project No. 16-099
Sheet 2 of 2
Date 9 / 1 / 2016
Engineer BJT
Checked by TCS

Step 5. Estimate the maximum acceleration occurs at the crest of the embankment.

Maximum acceleration at the crest of the embankment $uu_{max} := \sqrt{0.256 \cdot S_{a1}^{\ 2} + 1.12 \cdot S_{a2}^{\ 2} + 0.74 \cdot S_{a3}^{\ 2}} = 0.163 \cdot g$

Step 6. Calculate the average shear strain based on the computed spectral acceleration.

Average shear strain $\gamma_{ave} := 0.195 \cdot \left(\frac{H}{v^2}\right) \cdot S_{a1} = 0.0032 \cdot \%$

Step 7. Compare the computed average shear strain to the assumed shear strain in Step 1. If they do not agree to an acceptable level, the return to Step 1 and assume a different shear strain.

Ratio of γ_{ave} to $\gamma_{assumed}$ $\frac{\gamma_{ave}}{\gamma_{assumed}} = 1.01$

Step 8. Determine the yield acceleration of the critical failure surface and the depth of the critical failure surface.

Yield acceleration of critical failure surface $k_y := 0.18g$

Depth of critical failure surface $y := 23ft$

Step 9. Determine the value of maximum average acceleration (k_{max}) for the computed value of y/H.

Ratio y to H $\frac{y}{H} = 1.769$

Determine k_{max} from Makdisi and Seed chart $k_{max} := uu_{max} \cdot 0.32 = 0.052 \cdot g$

Step 10. Calculate ratio of k_y to k_{max} and use Makdisi and See chart to estimate permanent seismic displacement.

Ratio of k_y to k_{max} $\frac{k_y}{k_{max}} = 3.442$

Moment magnitude of design earthquake $M_w := 7.5$

The yield acceleration is the minimum acceleration that triggers permanent seismic displacement. The maximum average acceleration is less than the yield acceleration which indicates that yielding does not occur and that there is zero permanent seismic displacement

Additional Reference:

Abramson, L.W., Lee, T.S., Sharma, S. and Boyce, G.M. (1996). Slope stability and stabilization methods, John Wiley & Sons, 629 p.

Method: Spc er

Calculated Factor of Safety: 1.003

Yield Acceleration (ky): 0.18g

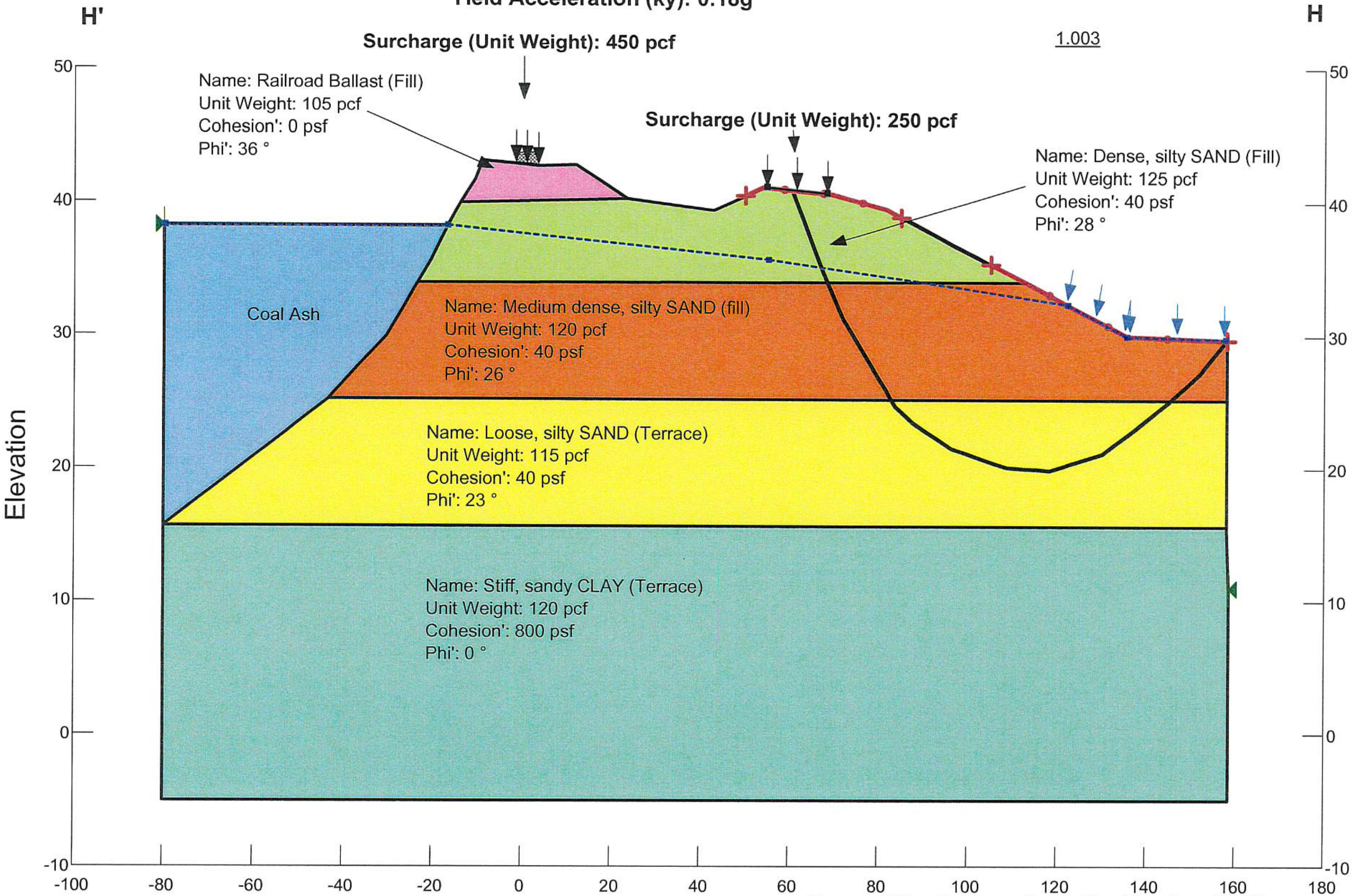

Normal Pool, Pseudostatic, Section H-H'

Unit 2/3 Impoundment
Charles R. Lowman Power Plant
CDG Project No. 061521207
Scale: As Shown

CDG
Engineering. Environmental. Answers.

Project Lowman PP Section J
Project No. 16-099
Sheet 1 **of** 2
Date 9 / 1 / 2016
Engineer BJT
Checked by TCS

Design Calculations for Permanent Seismic Displacement of Berm Charles R. Lowman Power Plant

The following calculations are for seismic displacement of berm Section J-J' at the Charles R. Lowman Power Plant.

Makdisi, F.I. and Seed, H.B. (1978). "Simplified procedure for estimating dam and embankment earthquake-induced deformations" Journal of the Geotechnical Engineering Division, 104(GT7), 849-868.

Maximum expected ground acceleration $a_{max} := 0.1g$ (Uniform Hazard Spectral Acceleration 2% Probability of Exceedence in 50 years)

Embankment height $H := 15ft$

Unit weight of embankment material $\gamma_s := 125pcf$

Mass density of embankment material $\rho := \frac{\gamma_s}{g} = 3.885 \cdot \frac{slug}{ft^3}$

Shear wave velocity of embankment material $v_s := 650 \frac{ft}{sec}$

Maximum shear modulus of embankment material $G_{max} := \rho \cdot v_s^2 = 1.641 \times 10^6 \cdot psf$

Step 1. Assume the average shear strain (γ) within the embankment. Makdisi and Seed report a range of measured maximum shear strain values generally between 0.1 and 0.5 percent.

Assumed average shear strain $\gamma_{assumed} := 0.004\%$ $\log(\gamma_{assumed} \cdot 100) = -2.398$

Step 2. For the assumed average shear strain, compute a reduced shear modulus (G), damping ratio (λ) and equivalent shear wave velocity (v).

Reduced shear modulus $G := 0.88 \cdot G_{max} = 1.444 \times 10^6 \cdot psf$

Damping ratio $\lambda := 3.5\%$

Reduced shear wave velocity $v := \sqrt{\frac{G}{\rho}} = 609.754 \cdot \frac{ft}{sec}$

Step 3. Calculate the three modal periods.

$T_1 := 2.618 \cdot \frac{H}{v} = 0.064\,s$ $T_2 := 1.138 \cdot \frac{H}{v} = 0.028\,s$ $T_3 := 0.726 \cdot \frac{H}{v} = 0.018\,s$

Step 4. Determine the spectral accelerations that correspond to the modal periods and damping ratio.

$S_{a1} := .16g$ $S_{a2} := .11g$ $S_{a3} := .1g$

Step 5. Estimate the maximum acceleration occurs at the crest of the embankment.

Maximum acceleration at the crest of the embankment $uu_{max} := \sqrt{0.256 \cdot S_{a1}^{\ 2} + 1.12 \cdot S_{a2}^{\ 2} + 0.74 \cdot S_{a3}^{\ 2}} = 0.166 \cdot g$

Step 6. Calculate the average shear strain based on the computed spectral acceleration.

Average shear strain $\gamma_{ave} := 0.195 \cdot \left(\frac{H}{v^2}\right) \cdot S_{a1} = 0.004 \cdot \%$

Step 7. Compare the computed average shear strain to the assumed shear strain in Step 1. If they do not agree to an acceptable level, the return to Step 1 and assume a different shear strain.

Ratio of γ_{ave} to $\gamma_{assumed}$ $\frac{\gamma_{ave}}{\gamma_{assumed}} = 1.01$

Step 8. Determine the yield acceleration of the critical failure surface and the depth of the critical failure surface.

Yield acceleration of critical failure surface $k_y := 0.20g$

Depth of critical failure surface $y := 14ft$

Step 9. Determine the value of maximum average acceleration (k_{max}) for the computed value of y/H.

Ratio y to H $\frac{y}{H} = 0.93$

Determine k_{max} from Makdisi and Seed chart $k_{max} := uu_{max} \cdot 0.35 = 0.058 \cdot g$

Step 10. Calculate ratio of k_y to k_{max} and use Makdisi and See chart to estimate permanent seismic displacement.

Ratio of k_y to k_{max} $\frac{k_y}{k_{max}} = 3.445$

Moment magnitude of design earthquake $M_w := 7.5$

The yield acceleration is the minimum acceleration that triggers permanent seismic displacement. The maximum average acceleration is less than the yield acceleration which indicates that yielding does not occur and that there is zero permanent seismic displacement

Additional Reference:

Abramson, L.W., Lee, T.S., Sharma, S. and Boyce, G.M. (1996). Slope stability and stabilization methods, John Wiley & Sons, 629 p.

Method: Spencer

Calculated Factor of Safety: 0.986

Yield Acceleration (ky): 0.20g

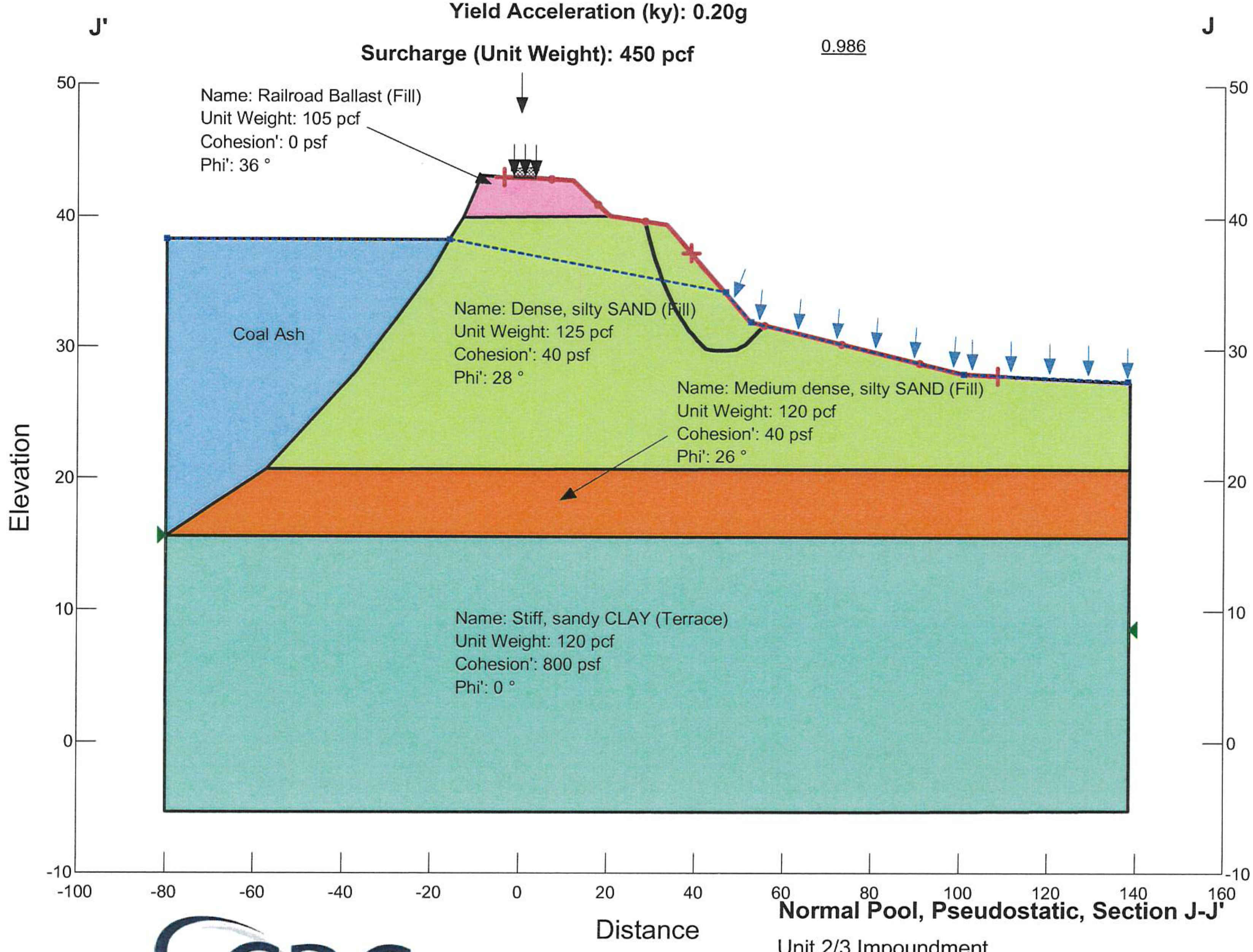

Normal Pool, Pseudostatic, Section J-J'

Unit 2/3 Impoundment
Charles R. Lowman Power Plant
CDG Project No. 061521207
Scale: As Shown

CDG
Engineering. Environmental. Answers.

Project Lowman PP Section K
Project No. 16-099
Sheet 1 of 2
Date 9 / 1 / 2016
Engineer BJT
Checked by TCS

Design Calculations for Permanent Seismic Displacement of Berm
Charles R. Lowman Power Plant

The following calculations are for seismic displacement of berm Section K-K' at the Charles R. Lowman Power Plant.

Makdisi, F.I. and Seed, H.B. (1978). "Simplified procedure for estimating dam and embankment earthquake-induced deformations" Journal of the Geotechnical Engineering Division, 104(GT7), 849-868.

Maximum expected ground acceleration $a_{max} := 0.1g$ (Uniform Hazard Spectral Acceleration 2% Probability of Exceedence in 50 years)

Embankment height $H := 16ft$

Unit weight of embankment material $\gamma_s := 125pcf$

Mass density of embankment material $\rho := \frac{\gamma_s}{g} = 3.885\frac{slug}{ft^3}$

Shear wave velocity of embankment material $v_s := 650\frac{ft}{sec}$

Maximum shear modulus of embankment material $G_{max} := \rho \cdot v_s^{\,2} = 1.641\times 10^6 \cdot psf$

Step 1. Assume the average shear strain (γ) within the embankment. Makdisi and Seed report a range of measured maximum shear strain values generally between 0.1 and 0.5 percent.

Assumed average shear strain $\gamma_{assumed} := 0.0049\%$ $\log(\gamma_{assumed} \cdot 100) = -2.31$

Step 2. For the assumed average shear strain, compute a reduced shear modulus (G), damping ratio (λ) and equivalent shear wave velocity (v).

Reduced shear modulus $G := 0.83 \cdot G_{max} = 1.362\times 10^6 \cdot psf$

Damping ratio $\lambda := 3.5\%$

Reduced shear wave velocity $v := \sqrt{\frac{G}{\rho}} = 592.178 \cdot \frac{ft}{sec}$

Step 3. Calculate the three modal periods.

$T_1 := 2.618 \cdot \frac{H}{v} = 0.071\,s$ $T_2 := 1.138 \cdot \frac{H}{v} = 0.031\,s$ $T_3 := 0.726 \cdot \frac{H}{v} = 0.02\,s$

Step 4. Determine the spectral accelerations that correspond to the modal periods and damping ratio.

$S_{a1} := .17g$ $S_{a2} := .12g$ $S_{a3} := .11g$

Project Lowman PP Section K
Project No. 16-099
Sheet 2 **of** 2
Date 9 / 1 / 2016
Engineer BJT
Checked by TCS

Step 5. Estimate the maximum acceleration occurs at the crest of the embankment.

Maximum acceleration at the crest of the embankment $uu_{max} := \sqrt{0.256 \cdot S_{a1}^{2} + 1.12 \cdot S_{a2}^{2} + 0.74 \cdot S_{a3}^{2}} = 0.18 \cdot g$

Step 6. Calculate the average shear strain based on the computed spectral acceleration.

Average shear strain $\gamma_{ave} := 0.195 \cdot \left(\frac{H}{v^{2}}\right) \cdot S_{a1} = 0.0049 \cdot \%$

Step 7. Compare the computed average shear strain to the assumed shear strain in Step 1. If they do not agree to an acceptable level, the return to Step 1 and assume a different shear strain.

Ratio of γ_{ave} to $\gamma_{assumed}$ $\frac{\gamma_{ave}}{\gamma_{assumed}} = 0.99$

Step 8. Determine the yield acceleration of the critical failure surface and the depth of the critical failure surface.

Yield acceleration of critical failure surface $k_y := 0.14g$

Depth of critical failure surface $y := 16ft$

Step 9. Determine the value of maximum average acceleration (k_{max}) for the computed value of y/H.

Ratio y to H $\frac{y}{H} = 1$

Determine k_{max} from Makdisi and Seed chart $k_{max} := uu_{max} \cdot 0.32 = 0.058 \cdot g$

Step 10. Calculate ratio of k_y to k_{max} and use Makdisi and See chart to estimate permanent seismic displacement.

Ratio of k_y to k_{max} $\frac{k_y}{k_{max}} = 2.428$

Moment magnitude of design earthquake $M_w := 7.5$

The yield acceleration is the minimum acceleration that triggers permanent seismic displacement. The maximum average acceleration is less than the yield acceleration which indicates that yielding does not occur and that there is zero permanent seismic displacement

Additional Reference:

Abramson, L.W., Lee, T.S., Sharma, S. and Boyce, G.M. (1996). Slope stability and stabilization methods, John Wiley & Sons, 629 p.

Method: Spencer

Calculated Factor of Safety: 0.984

Yield Acceleration (ky): 0.14g

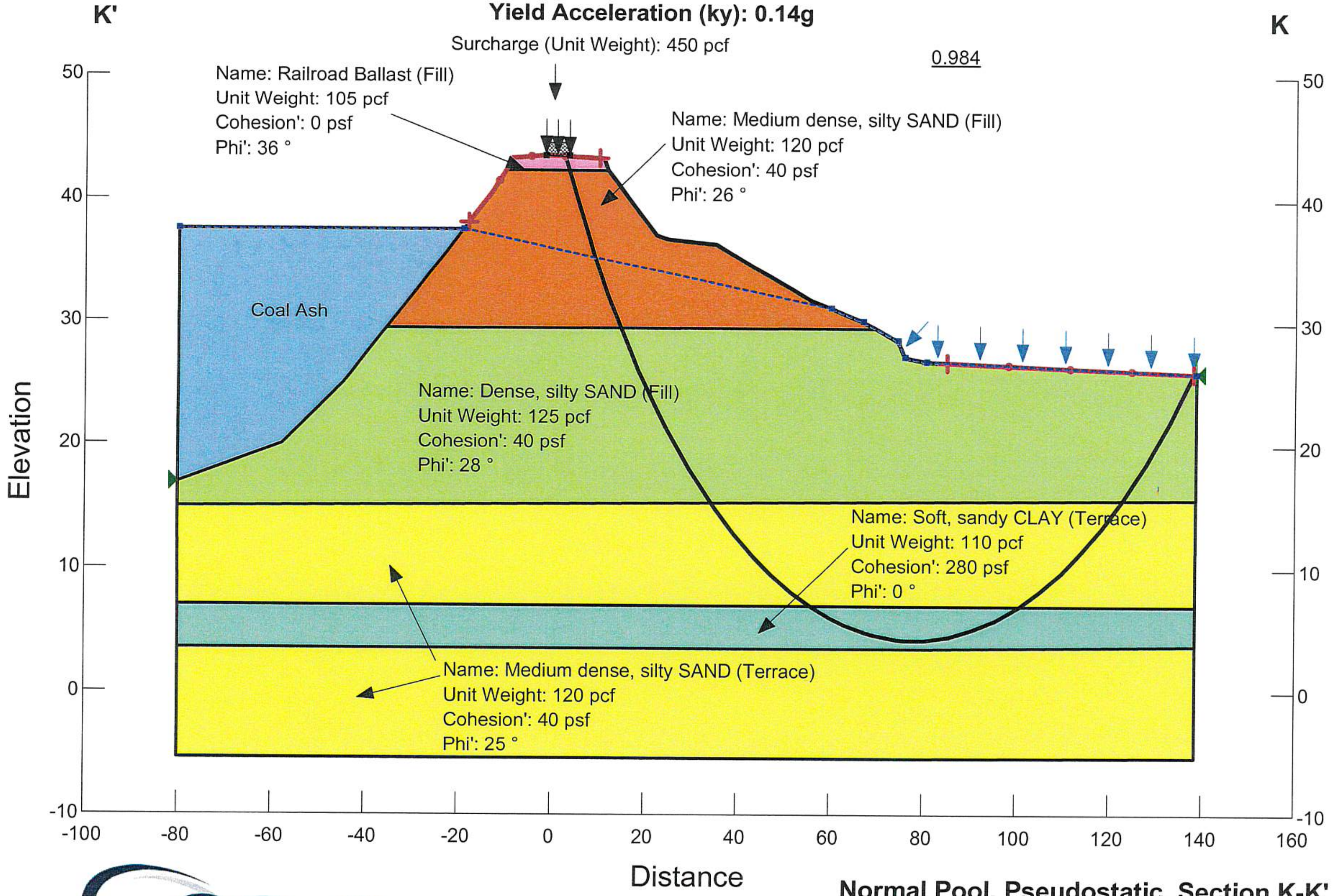

Engineering. Environmental. Answers.

Normal Pool, Pseudostatic, Section K-K'
FGD Impoundment
Charles R. Lowman Power Plant
CDG Project No. 061521207
Scale: As Shown

Project Lowman PP Section L
Project No. 16-099
Sheet 1 **of** 2
Date 9 / 1 / 2016
Engineer BJT
Checked by TCS

Design Calculations for Permanent Seismic Displacement of Berm Charles R. Lowman Power Plant

The following calculations are for seismic displacement of berm Section L-L' at the Charles R. Lowman Power Plant.

Makdisi, F.I. and Seed, H.B. (1978). "Simplified procedure for estimating dam and embankment earthquake-induced deformations" Journal of the Geotechnical Engineering Division, 104(GT7), 849-868.

Maximum expected ground acceleration	$a_{max} := 0.1g$	(Uniform Hazard Spectral Acceleration 2% Probability of Exceedence in 50 years)
Embankment height	$H := 22ft$	
Unit weight of embankment material	$\gamma_s := 125pcf$	
Mass density of embankment material	$\rho := \frac{\gamma_s}{g} = 3.885 \frac{slug}{ft^3}$	
Shear wave velocity of embankment material	$v_s := 650 \frac{ft}{sec}$	
Maximum shear modulus of embankment material	$G_{max} := \rho \cdot {v_s}^2 = 1.641 \times 10^6 \cdot psf$	

Step 1. Assume the average shear strain (γ) within the embankment. Makdisi and Seed report a range of measured maximum shear strain values generally between 0.1 and 0.5 percent.

Assumed average shear strain $\gamma_{assumed} := 0.0088\%$ $\log(\gamma_{assumed} \cdot 100) = -2.056$

Step 2. For the assumed average shear strain, compute a reduced shear modulus (G), damping ratio (λ) and equivalent shear wave velocity (v).

Reduced shear modulus	$G := 0.78 G_{max} = 1.28 \times 10^6 \cdot psf$
Damping ratio	$\lambda := 4.5\%$
Reduced shear wave velocity	$v := \sqrt{\frac{G}{\rho}} = 574.064 \cdot \frac{ft}{sec}$

Step 3. Calculate the three modal periods.

$T_1 := 2.618 \cdot \frac{H}{v} = 0.1\,s$ $T_2 := 1.138 \cdot \frac{H}{v} = 0.044\,s$ $T_3 := 0.726 \cdot \frac{H}{v} = 0.028\,s$

Step 4. Determine the spectral accelerations that correspond to the modal periods and damping ratio.

$S_{a1} := .21g$ $S_{a2} := .12g$ $S_{a3} := .11g$

Step 5. Estimate the maximum acceleration occurs at the crest of the embankment.

Maximum acceleration at the crest of the embankment $uu_{max} := \sqrt{0.256 \cdot S_{a1}^{2} + 1.12 \cdot S_{a2}^{2} + 0.74 \cdot S_{a3}^{2}} = 0.191 \cdot g$

Step 6. Calculate the average shear strain based on the computed spectral acceleration.

Average shear strain $\gamma_{ave} := 0.195 \cdot \left(\frac{H}{v^{2}}\right) \cdot S_{a1} = 0.0088 \cdot \%$

Step 7. Compare the computed average shear strain to the assumed shear strain in Step 1. If they do not agree to an acceptable level, the return to Step 1 and assume a different shear strain.

Ratio of γ_{ave} to $\gamma_{assumed}$ $\frac{\gamma_{ave}}{\gamma_{assumed}} = 1$

Step 8. Determine the yield acceleration of the critical failure surface and the depth of the critical failure surface.

Yield acceleration of critical failure surface $k_y := 0.13g$

Depth of critical failure surface $y := 22ft$

Step 9. Determine the value of maximum average acceleration (k_{max}) for the computed value of y/H.

Ratio y to H $\frac{y}{H} = 1$

Determine k_{max} from Makdisi and Seed chart $k_{max} := uu_{max} \cdot 0.32 = 0.061 \cdot g$

Step 10. Calculate ratio of k_y to k_{max} and use Makdisi and See chart to estimate permanent seismic displacement.

Ratio of k_y to k_{max} $\frac{k_y}{k_{max}} = 2.13$

Moment magnitude of design earthquake $M_w := 7.5$

The yield acceleration is the minimum acceleration that triggers permanent seismic displacement. The maximum average acceleration is less than the yield acceleration which indicates that yielding does not occur and that there is zero permanent seismic displacement

Additional Reference:

Abramson, L.W., Lee, T.S., Sharma, S. and Boyce, G.M. (1996). Slope stability and stabilization methods, John Wiley & Sons, 629 p.

Method pencer

Calculated Factor of Safety: 0.987

Yield Acceleration (ky): 0.13g

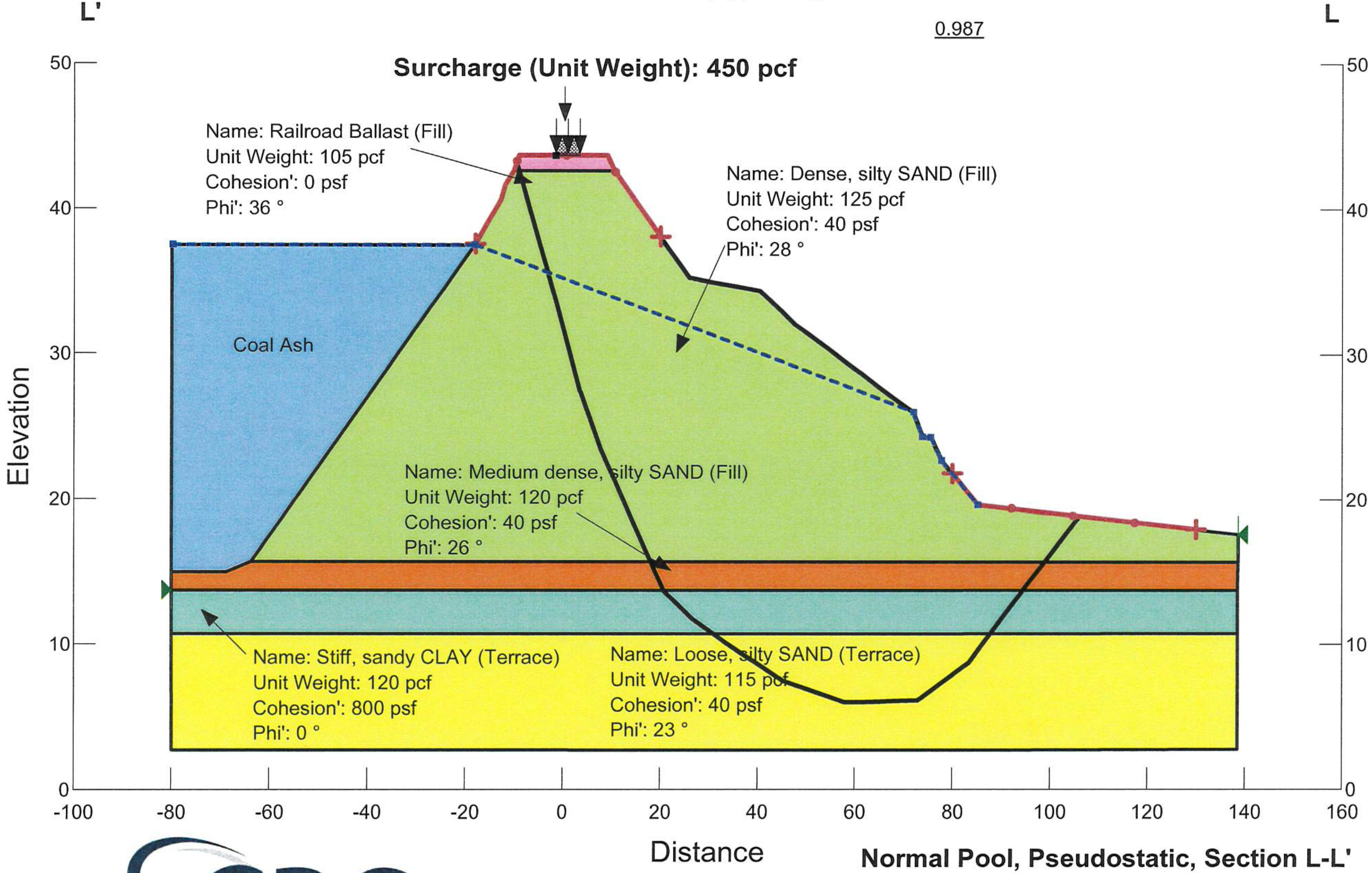

Engineering. Environmental. Answers.

Normal Pool, Pseudostatic, Section L-L'
FGD Impoundment
Charles R. Lowman Power Plant
CDG Project No. 061521207
Scale: As Shown

Lowman I'I' Section D
4 of 7

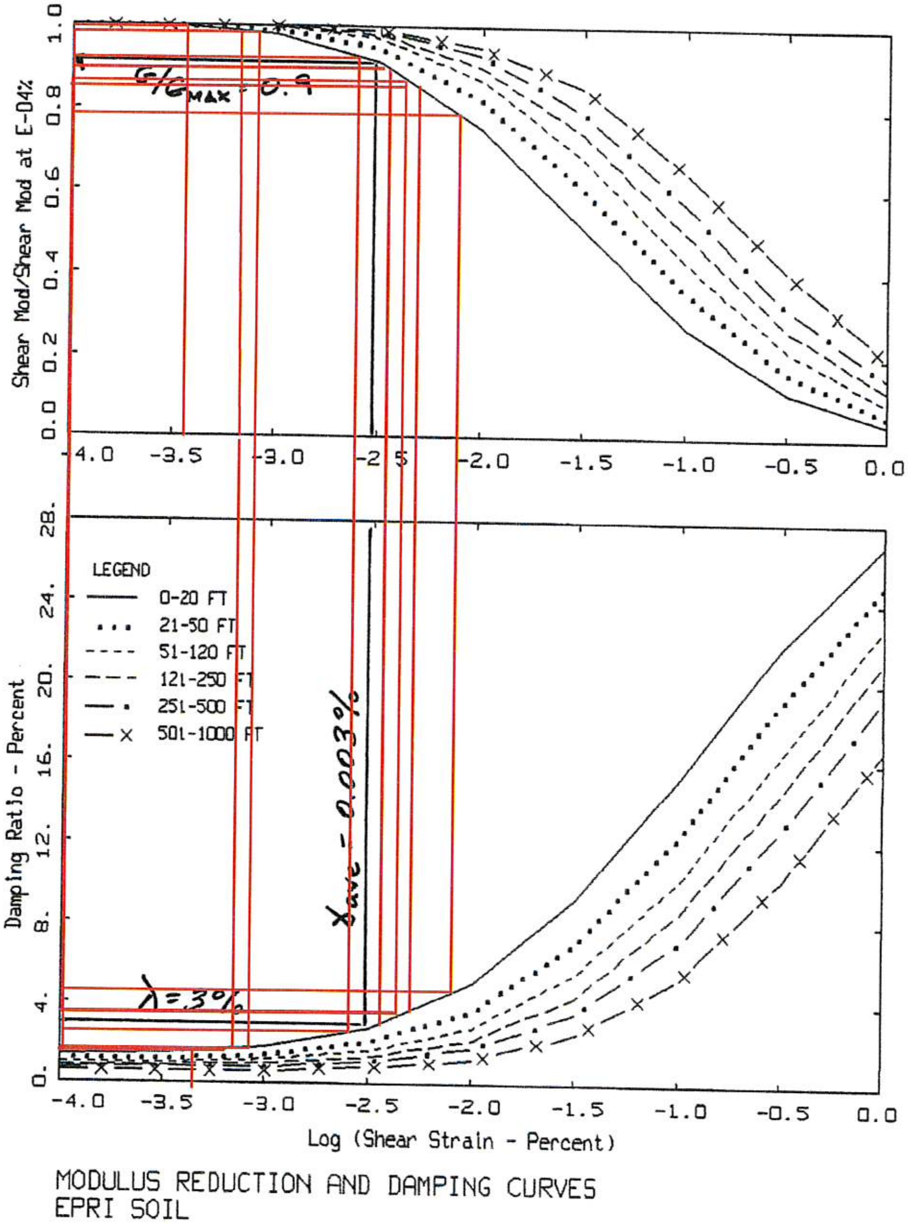

Figure 10. Generic G/Gmax and hysteretic damping curves for cohesionless soil (EPRI, 1993).

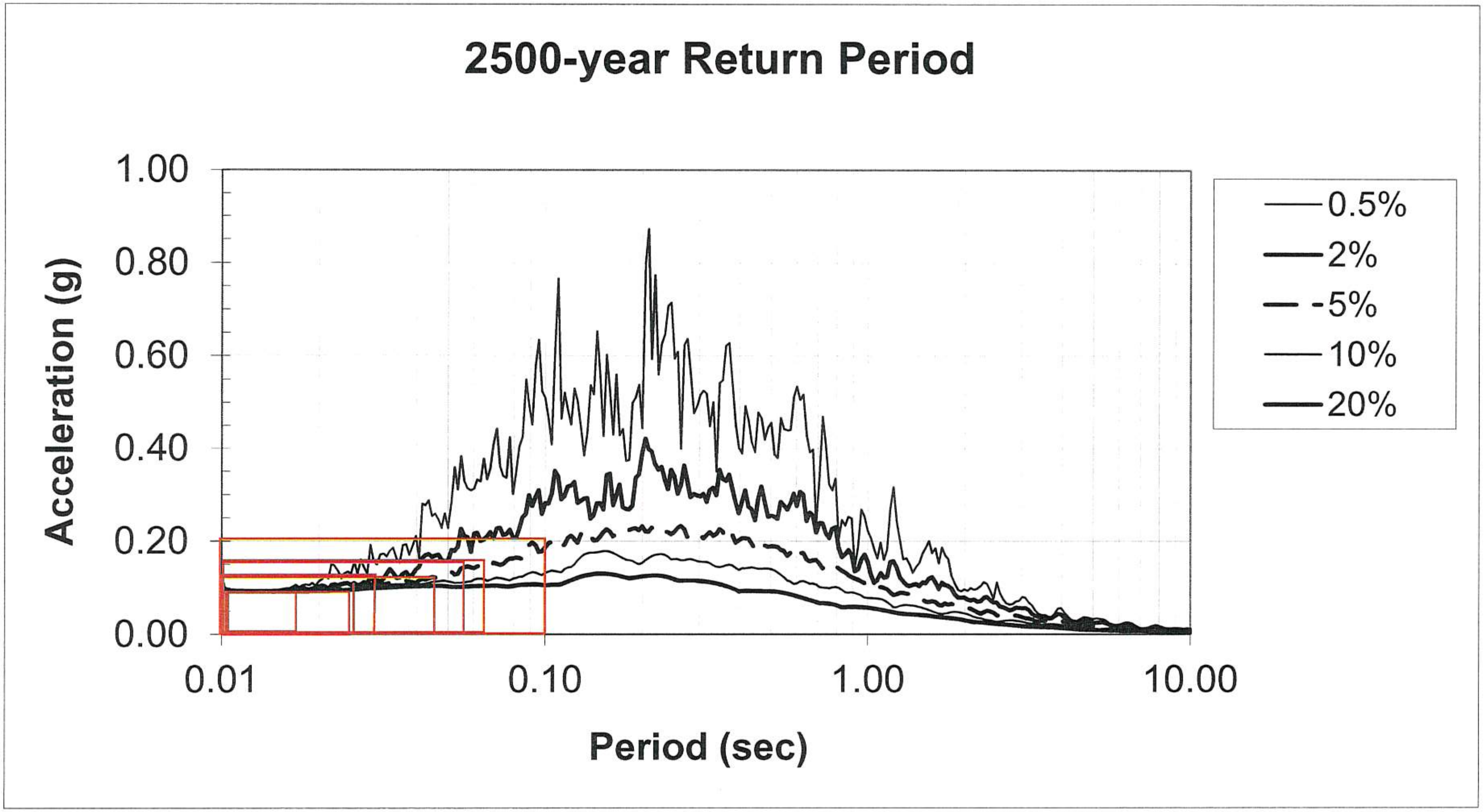
2500-year Return Period
Acceleration (g)
1.00
0.80
0.60
0.40
0.20
0.00
0.01
0.10
1.00
10.00
Period (sec)
0.5%
2%
-5%
10%
20%

Appendix J
Liquefaction Potential Analysis

Project Lowman PP Sec D EL 25
Project No. 16-099
Sheet 1 of 4
Date 9 / 6 / 2016
Engineer TCS
Checked by DD

The following calculations for liquefaction of soils with sand-like behavior are based on Soil Liquefactior During Earthquakes - Monograph MNO-12 by I.M. Idriss and R.W. Boulanger (2008) published by the Earthquake Engineering Research Institute.

Soil Stress Conditions -

average total unit weight of soil $\gamma_{total} := 115pcf$

unit weight of water $\gamma_{water} := 62.4pcf$

water table depth below ground surface $d_w := 12ft$

sample depth Boring T-1 Depth 15 $z := 15ft$

total vertical stress $\sigma tot_v := \gamma_{total} \cdot z$ $\sigma tot_v = 1725 \cdot psf$

static water pressure $u_o := (z - d_w) \cdot \gamma_{water}$ $u_o = 187 \cdot psf$

effective vertical stress $\sigma eff_v := \sigma tot_v - u_o$ $\sigma eff_v = 1538 \cdot psf$

Standard Penetration N-value Correction -

Standard Penetration Test N-value $N_m := 4$

fines content $FC := 72.3$

energy correction $C_E := 1.46$

borehole diameter correction $C_B := 1.00$

rod length correction $C_R := 0.85$

sampler correction $C_S := 1$

Hammer	CE
Doughnut	0.5-1.0
Safety	0.7-1.2
Automatic	0.8-1.3

(Skempton, 1986)

Borehole dia.	CB
65-115mm	1.0
150mm	1.05
200mm	1.15

(Skempton, 1986)

Rod length	CR
<3m	0.75
3-4m	0.80
4-6m	0.85
6-10m	0.95
10-30m	1.00

SPT N-value for an energy ratio of 60% $N_{60} := C_E \cdot C_B \cdot C_R \cdot C_S \cdot N_m$

$N_{60} = 5$

overburden correction factor
(based on overburden stress only)

$$C_{N\_a} := \left(\frac{P_a}{\sigma eff_v}\right)^{0.5}$$

$C_{N\_a} = 1.173$

normalized SPT N-value
(based on overburden stress only) $N_{1\_60} := C_{N\_a} \cdot N_{60}$ $N_{1\_60} = 5.8$

Project Lowman PP Sec D EL 25
Project No. 16-099
Sheet 2 of 4
Date 9 / 6 / 2016
Engineer TCS
Checked by DD

---

overburden correction factor (based on overburden stress and relative density)

$$C_{N\_b} := \left(\frac{P_a}{\sigma eff_v}\right)^{0.784-0.078\cdot\left(N_{1\_60}\right)^{0.5}}$$

$$C_{N\_b} = 1.209$$

overburden correction factor used in liquefaction analysis (max CN = 1.7)

$$C_N := 1.2$$

recalculated normalized SPT N-value

$$N_{1\_60} := C_N \cdot N_{60}$$

$$N_{1\_60} = 6$$

overburden correction factor used in liquefaction analysis

$$C_{N\_check} := \left(\frac{P_a}{\sigma eff_v}\right)^{0.784-0.078\cdot\left(N_{1\_60}\right)^{0.5}}$$

$$C_{N\_check} = 1.209$$

fines content adjustment to SPT N-value

$$\Delta N_{1\_60} := \exp\left[1.63 + \frac{9.7}{FC + 0.01} - \left(\frac{15.7}{FC + 0.01}\right)^2\right]$$

$$\Delta N_{1\_60} = 5.6$$

normalized SPT N-value (clean sands)

$$N_{1\_60\_cs} := N_{1\_60} + \Delta N_{1\_60}$$

$$N_{1\_60\_cs} = 11.5$$

Earthquake Conditions -

peak ground accelerationl

$$a_{max} := 0.1\,g$$

earthquake moment magnitude

$$M_w := 7.5$$

variable α for stress reduction factor

$$\alpha := -1.012 - 1.126\cdot\sin\left(\frac{\frac{z}{3.28ft}}{11.73} + 5.133\right)$$

variable β for stress reduction factor

$$\beta := 0.106 + 0.118\,\sin\left(\frac{\frac{z}{3.28ft}}{11.28} + 5.142\right)$$

Project Lowman PP Sec D EL 25
Project No. 16-099
Sheet 3 **of** 4
Date 9 / 6 / 2016
Engineer TCS
Checked by DD

---

stress reduction factor $r_d := \exp(\alpha + \beta \cdot M_w)$ $r_d = 0.966$

Liquefaction Calculations -

cyclic stress ratio $CSR := 0.65 \cdot \frac{\sigma tot_v}{\sigma eff_v} \cdot \frac{a_{max}}{g} \cdot r_d$ $CSR = 0.07$

cyclic resistance ratio

$$CRR_{M7.5\_\sigma eff1} := \exp\left[\frac{N_{1\_60\_cs}}{14.1} + \left(\frac{N_{1\_60\_cs}}{126}\right)^2 - \left(\frac{N_{1\_60\_cs}}{23.6}\right)^3 + \left(\frac{N_{1\_60\_cs}}{25.4}\right)^4 - 2.8\right]$$

magnitude scaling factor
(maximum MSF = 1.8) $MSF := 6.9 \exp\left(\frac{-M_w}{4}\right) - 0.058$ $MSF = 1$

coefficient for overburden correction factor
(maximum Cσ=0.3) $C_\sigma := \frac{1}{18.9 - 2.55 \cdot (N_{1\_60})^{0.5}}$ $C_\sigma = 0.079$

overburden correction factor
(maximum Kσ=1.1) $K_\sigma := 1 - C_\sigma \cdot \ln\left(\frac{\sigma eff_v}{P_a}\right)$ $K_\sigma = 1.025$

estimated static shear stress on horizontal plane $\tau ho := 35psf$

effective friction angle $\phi_{eff} := \text{atan}\left(\frac{N_{60}}{12.2 + 20.3 \cdot \frac{\sigma eff_v}{P_a}}\right)^{0.34}$ $\phi_{eff} = 32.111 \cdot deg$

Ko for NC soil $K_o := (1 - \sin(\phi_{eff}))$ $K_o = 0.468$

empirical constant for dilatancy $Q := 10$

Grain type.	Q
quartz and feldspar	10
limestone	8
anthracite	7
chalk	5.5

Project _Lowman PP Sec D EL 25_
Project No._16-099_
Sheet _4_ of _4_
Date _9 / 6 / 2016_
Engineer_TCS_
Checked by_DD_

---

relative state parameter
(-0.61<ξR<0.11)

$$\zeta_R := \frac{1}{Q - \ln\left[\frac{100\cdot\left(1 + 2K_o\right)\sigma eff_v}{3\cdot P_a}\right]} - \left(\frac{N_{1\_60}}{46}\right)^{0.5} \qquad \zeta_R = -0.197$$

alpha factor
(maximum α=0.35)

$$\alpha\_factor := \frac{\tau_{ho}}{\sigma eff_v} \qquad \alpha\_factor = 0.023$$

$$a := 1267 + 636\alpha\_factor^2 - 634\cdot\exp(\alpha\_factor) - 632\cdot\exp(-\alpha\_factor)$$

$$b := \exp\left(-1.11 + 12.3\alpha\_factor^2 + 1.31\cdot\ln(\alpha\_factor + 0.0001)\right)$$

$$c := 0.138 + 0.126\cdot\alpha\_factor + 2.52\cdot\alpha\_factor^3$$

static shear stress correction factor

$$K_\alpha := a + b\cdot\exp\left(\frac{-\zeta_R}{c}\right) \qquad K_\alpha = 0.966$$

corrected cyclic stress ratio

$$CRR_{M\_\sigma effv} := CRR_{M7.5\_\sigma eff1}\cdot MSF\cdot K_\sigma\cdot K_\alpha$$

factor of safety for liquefaction

$$FS_{liq} := \frac{CRR_{M\_\sigma effv}}{CSR} \qquad FS_{liq} = 1.81$$

ALL=29 and PI=11 classify this material as "clay-like" behavior according to Idriss and Boulanger.

Project Lowman PP Sec G EL 29
Project No. 16-099
Sheet 1 of 4
Date 9 / 6 / 2016
Engineer TCS
Checked by DD

The following calculations for liquefaction of soils with sand-like behavior are based on Soil Liquefactior During Earthquakes - Monograph MNO-12 by I.M. Idriss and R.W. Boulanger (2008) published by the Earthquake Engineering Research Institute.

Soil Stress Conditions -

average total unit weight of soil $\gamma_{total} := 115pcf$

unit weight of water $\gamma_{water} := 62.4pcf$

water table depth below ground surface $d_w := 8ft$

sample depth Boring S-6 Depth 14 $z := 14ft$

total vertical stress $\sigma tot_v := \gamma_{total} \cdot z$ $\sigma tot_v = 1610 \cdot psf$

static water pressure $u_o := (z - d_w) \cdot \gamma_{water}$ $u_o = 374 \cdot psf$

effective vertical stress $\sigma eff_v := \sigma tot_v - u_o$ $\sigma eff_v = 1236 \cdot psf$

Standard Penetration N-value Correction -

Standard Penetration Test N-value $N_m := 48$

fines content $FC := 25$

energy correction $C_E := 1.46$

borehole diameter correction $C_B := 1.05$

rod length correction $C_R := 0.85$

sampler correction $C_S := 1$

Hammer	CE
Doughnut	0.5-1.0
Safety	0.7-1.2
Automatic	0.8-1.3
(Skempton, 1986)	

Borehole dia.	CB
65-115mm	1.0
150mm	1.05
200mm	1.15
(Skempton, 1986)	

Rod length	CR
<3m	0.75
3-4m	0.80
4-6m	0.85
6-10m	0.95
10-30m	1.00

SPT N-value for an energy ratio of 60% $N_{60} := C_E \cdot C_B \cdot C_R \cdot C_S \cdot N_m$

$N_{60} = 62.5$

overburden correction factor
(based on overburden stress only)

$$C_{N\_a} := \left(\frac{P_a}{\sigma eff_v} \right)^{0.5}$$

$C_{N\_a} = 1.309$

normalized SPT N-value
(based on overburden stress only) $N_{1\_60} := C_{N\_a} \cdot N_{60}$ $N_{1\_60} = 81.9$

Project Lowman PP Sec G EL 29
Project No. 16-099
Sheet 2 **of** 4
Date 9 / 6 / 2016
Engineer TCS
Checked by DD

---

overburden correction factor (based on overburden stress and relative density)

$$C_{N\_b} := \left(\frac{P_a}{\sigma eff_v}\right)^{0.784-0.078\cdot\left(N_{1\_60}\right)^{0.5}}$$

$$C_{N\_b} = 1.043$$

overburden correction factor used in liquefaction analysis (max CN = 1.7)

$$C_N := 1.08$$

recalculated normalized SPT N-value

$$N_{1\_60} := C_N \cdot N_{60}$$

$$N_{1\_60} = 67.6$$

overburden correction factor used in liquefaction analysis

$$C_{N\_check} := \left(\frac{P_a}{\sigma eff_v}\right)^{0.784-0.078\cdot\left(N_{1\_60}\right)^{0.5}}$$

$$C_{N\_check} = 1.08$$

fines content adjustment to SPT N-value

$$\Delta N_{1\_60} := \exp\left[1.63 + \frac{9.7}{FC + 0.01} - \left(\frac{15.7}{FC + 0.01}\right)^2\right]$$

$$\Delta N_{1\_60} = 5.1$$

normalized SPT N-value (clean sands)

$$N_{1\_60\_cs} := N_{1\_60} + \Delta N_{1\_60}$$

$$N_{1\_60\_cs} = 72.6$$

Earthquake Conditions -

peak ground accelerationl $a_{max} := 0.1\cdot g$

earthquake moment magnitude $M_w := 7.5$

variable α for stress reduction factor

$$\alpha := -1.012 - 1.126\cdot\sin\left(\frac{\frac{z}{3.28ft}}{11.73} + 5.133\right)$$

variable β for stress reduction factor

$$\beta := 0.106 + 0.118\sin\left(\frac{\frac{z}{3.28ft}}{11.28} + 5.142\right)$$

Project Lowman PP Sec G EL 29
Project No. 16-099
Sheet 3 of 4
Date 9 / 6 / 2016
Engineer TCS
Checked by DD

---

stress reduction factor $r_d := \exp\left(\alpha + \beta \cdot M_w\right)$ $r_d = 0.969$

Liquefaction Calculations -

cyclic stress ratio $CSR := 0.65 \cdot \frac{\sigma tot_v}{\sigma eff_v} \cdot \frac{a_{max}}{g} \cdot r_d$ $CSR = 0.082$

cyclic resistance ratio

$$CRR_{M7.5\_\sigma eff1} := \exp\left[\frac{N_{1\_60\_cs}}{14.1} + \left(\frac{N_{1\_60\_cs}}{126}\right)^2 - \left(\frac{N_{1\_60\_cs}}{23.6}\right)^3 + \left(\frac{N_{1\_60\_cs}}{25.4}\right)^4 - 2.8\right]$$

magnitude scaling factor
(maximum MSF = 1.8) $MSF := 6.9 \exp\left(\frac{-M_w}{4}\right) - 0.058$ $MSF = 1$

coefficient for overburden correction factor
(maximum Cσ=0.3) $C_\sigma := \frac{1}{18.9 - 2.55 \cdot \left(N_{1\_60}\right)^{0.5}}$ $C_\sigma = -0.486$

overburden correction factor
(maximum Kσ=1.1) $K_\sigma := 1 - C_\sigma \cdot \ln\left(\frac{\sigma eff_v}{P_a}\right)$ $K_\sigma = 0.739$

estimated static shear stress on horizontal plane $\tau_{ho} := 35psf$

effective friction angle $\phi_{eff} := \operatorname{atan}\left(\frac{N_{60}}{12.2 + 20.3 \cdot \frac{\sigma eff_v}{P_a}}\right)^{0.34}$ $\phi_{eff} = 61.023 \cdot deg$

Ko for NC soil $K_o := \left(1 - \sin\left(\phi_{eff}\right)\right)$ $K_o = 0.125$

empirical constant for dilatancy $Q := 10$

Grain type.	Q
quartz and feldspar	10
limestone	8
anthracite	7
chalk	5.5

Project Lowman PP Sec G EL 29
Project No. 16-099
Sheet 4 **of** 4
Date 9 / 6 / 2016
Engineer TCS
Checked by DD

---

relative state parameter
(-0.61<ξR<0.11)

$$\zeta_R := \frac{1}{Q - \ln\left[\frac{100\cdot\left(1 + 2K_o\right)\sigma eff_v}{3\cdot P_a}\right]} - \left(\frac{N_{1\_60}}{46}\right)^{0.5} \qquad \zeta_R = -1.065$$

alpha factor
(maximum α=0.35)

$$\alpha\_factor := \frac{\tau_{ho}}{\sigma eff_v} \qquad \alpha\_factor = 0.028$$

$$a := 1267 + 636\alpha\_factor^2 - 634\cdot\exp(\alpha\_factor) - 632\cdot\exp(-\alpha\_factor)$$

$$b := \exp\left(-1.11 + 12.3\alpha\_factor^2 + 1.31\cdot\ln(\alpha\_factor + 0.0001)\right)$$

$$c := 0.138 + 0.126\cdot\alpha\_factor + 2.52\cdot\alpha\_factor^3$$

static shear stress correction factor

$$K_\alpha := a + b\cdot\exp\left(\frac{-\zeta_R}{c}\right) \qquad K_\alpha = 6.729$$

corrected cyclic stress ratio

$$CRR_{M\_\sigma effv} := CRR_{M7.5\_\sigma eff1}\cdot MSF\cdot K_\sigma\cdot K_\alpha$$

factor of safety for liquefaction

$$FS_{liq} := \frac{CRR_{M\_\sigma effv}}{CSR} \qquad FS_{liq} = 2.06\times 10^{19}$$

This sample is classified as non-plastic.

Project <u>Lowman PP Sec H EL 31</u>
Project No. <u>16-099</u>
Sheet <u>1</u> **of** <u>4</u>
Date <u>9 / 6 / 2016</u>
Engineer <u>TCS</u>
Checked by <u>DD</u>

The following calculations for liquefaction of soils with sand-like behavior are based on Soil Liquefactior During Earthquakes - Monograph MNO-12 by I.M. Idriss and R.W. Boulanger (2008) published by the Earthquake Engineering Research Institute.

Soil Stress Conditions -

average total unit weight of soil $\gamma_{total} := 115pcf$

unit weight of water $\gamma_{water} := 62.4pcf$

water table depth below ground surface $d_w := 5ft$

sample depth Boring T-2 Depth 11 $z := 11ft$

total vertical stress $\sigma tot_v := \gamma_{total} \cdot z$ $\sigma tot_v = 1265 \cdot psf$

static water pressure $u_o := (z - d_w) \cdot \gamma_{water}$ $u_o = 374 \cdot psf$

effective vertical stress $\sigma eff_v := \sigma tot_v - u_o$ $\sigma eff_v = 891 \cdot psf$

Standard Penetration N-value Correction -

Standard Penetration Test N-value $N_m := 15$

fines content $FC := 20$

energy correction $C_E := 1.46$

borehole diameter correction $C_B := 1.00$

rod length correction $C_R := 0.80$

sampler correction $C_S := 1$

<u>Hammer</u>	<u>CE</u>
Doughnut	0.5-1.0
Safety	0.7-1.2
Automatic	0.8-1.3

(Skempton, 1986)

<u>Borehole dia.</u>	<u>CB</u>
65-115mm	1.0
150mm	1.05
200mm	1.15

(Skempton, 1986)

<u>Rod length</u>	<u>CR</u>
<3m	0.75
3-4m	0.80
4-6m	0.85
6-10m	0.95
10-30m	1.00

SPT N-value for an energy ratio of 60% $N_{60} := C_E \cdot C_B \cdot C_R \cdot C_S \cdot N_m$

$N_{60} = 17.5$

overburden correction factor
(based on overburden stress only)

$$C_{N\_a} := \left(\frac{P_a}{\sigma eff_v}\right)^{0.5}$$

$C_{N\_a} = 1.541$

normalized SPT N-value
(based on overburden stress only) $N_{1\_60} := C_{N\_a} \cdot N_{60}$ $N_{1\_60} = 27$

Project **Lowman PP Sec H EL 31**
Project No. **16-099**
Sheet **2** **of** **4**
Date **9 / 6 / 2016**
Engineer **TCS**
Checked by **DD**

---

overburden correction factor
(based on overburden stress and
relative density)

$$C_{N\_b} := \left(\frac{P_a}{\sigma eff_v}\right)^{0.784-0.078\cdot\left(N_{1\_60}\right)^{0.5}}$$

$$C_{N\_b} = 1.388$$

overburden correction factor
used in liquefaction analysis
(max CN = 1.7)

$$C_N = 1.4$$

recalculated normalized SPT N-value

$$N_{1\_60} := C_N \cdot N_{60}$$

$$N_{1\_60} = 24.5$$

overburden correction factor
used in liquefaction analysis

$$C_{N\_check} := \left(\frac{P_a}{\sigma eff_v}\right)^{0.784-0.078\cdot\left(N_{1\_60}\right)^{0.5}}$$

$$C_{N\_check} = 1.411$$

fines content adjustment to SPT N-value

$$\Delta N_{1\_60} := \exp\left[1.63 + \frac{9.7}{FC + 0.01} - \left(\frac{15.7}{FC + 0.01}\right)^2\right]$$

$$\Delta N_{1\_60} = 4.5$$

normalized SPT N-value (clean sands)

$$N_{1\_60\_cs} := N_{1\_60} + \Delta N_{1\_60}$$

$$N_{1\_60\_cs} = 29$$

Earthquake Conditions -

peak ground accelerationl

$$a_{max} = 0.1g$$

earthquake moment magnitude

$$M_w = 7.5$$

variable α for stress reduction factor

$$\alpha := -1.012 - 1.126\cdot\sin\left(\frac{\frac{z}{3.28ft}}{11.73} + 5.133\right)$$

variable β for stress reduction factor

$$\beta := 0.106 + 0.118\,\sin\left(\frac{\frac{z}{3.28ft}}{11.28} + 5.142\right)$$

stress reduction factor $r_d := \exp(\alpha + \beta \cdot M_w)$ $r_d = 0.978$

Liquefaction Calculations -

cyclic stress ratio $CSR := 0.65 \cdot \frac{\sigma tot_v}{\sigma eff_v} \cdot \frac{a_{max}}{g} \cdot r_d$ $CSR = 0.09$

cyclic resistance ratio

$$CRR_{M7.5\_\sigma eff1} := \exp\left[\frac{N_{1\_60\_cs}}{14.1} + \left(\frac{N_{1\_60\_cs}}{126}\right)^2 - \left(\frac{N_{1\_60\_cs}}{23.6}\right)^3 + \left(\frac{N_{1\_60\_cs}}{25.4}\right)^4 - 2.8\right]$$

magnitude scaling factor
(maximum MSF = 1.8) $MSF := 6.9 \exp\left(\frac{-M_w}{4}\right) - 0.058$ $MSF = 1$

coefficient for overburden correction factor
(maximum Cσ=0.3) $C_\sigma := \frac{1}{18.9 - 2.55 \cdot (N_{1\_60})^{0.5}}$ $C_\sigma = 0.159$

overburden correction factor
(maximum Kσ=1.1) $K_\sigma := 1 - C_\sigma \cdot \ln\left(\frac{\sigma eff_v}{P_a}\right)$ $K_\sigma = 1.138$

estimated static shear stress on horizontal plane $Tho := 35psf$

effective friction angle $\phi_{eff} := \operatorname{atan}\left(\frac{N_{60}}{12.2 + 20.3 \cdot \frac{\sigma eff_v}{P_a}}\right)^{0.34}$ $\phi_{eff} = 50.785 \cdot deg$

Ko for NC soil $K_o := (1 - \sin(\phi_{eff}))$ $K_o = 0.225$

empirical constant for dilatancy $Q := 10$

Grain type.	Q
quartz and feldspar	10
limestone	8
anthracite	7
chalk	5.5

Project Lowman PP Sec H EL 31
Project No. 16-099
Sheet 4 **of** 4
Date 9 / 6 / 2016
Engineer TCS
Checked by DD

---

relative state parameter
($-0.61<\xi R<0.11$)

$$\zeta_R := \frac{1}{Q - \ln\left[\frac{100\cdot\left(1 + 2K_o\right)\sigma eff_v}{3\cdot P_a}\right]} - \left(\frac{N_{1\_60}}{46}\right)^{0.5} \qquad \zeta_R = -0.587$$

alpha factor
(maximum α=0.35)

$$\alpha\_factor := \frac{\tau_{ho}}{\sigma eff_v} \qquad \alpha\_factor = 0.039$$

$$a := 1267 + 636\alpha\_factor^2 - 634\cdot\exp(\alpha\_factor) - 632\cdot\exp(-\alpha\_factor)$$

$$b := \exp\left(-1.11 + 12.3\alpha\_factor^2 + 1.31\cdot\ln(\alpha\_factor + 0.0001)\right)$$

$$c := 0.138 + 0.126\cdot\alpha\_factor + 2.52\cdot\alpha\_factor^3$$

static shear stress correction factor

$$K_\alpha := a + b\cdot\exp\left(\frac{-\zeta_R}{c}\right) \qquad K_\alpha = 1.22$$

corrected cyclic stress ratio

$$CRR_{M\_\sigma effv} := CRR_{M7.5\_\sigma eff1}\cdot MSF\cdot K_\sigma\cdot K_\alpha$$

factor of safety for liquefaction

$$FS_{liq} := \frac{CRR_{M\_\sigma effv}}{CSR} \qquad FS_{liq} = 6.61$$

This sample is classified as non-plastic.

Project Lowman PP Sec J EL 19
Project No. 16-099
Sheet 1 **of** 4
Date 9 / 6 / 2016
Engineer TCS
Checked by DD

The following calculations for liquefaction of soils with sand-like behavior are based on Soil Liquefactio During Earthquakes - Monograph MNO-12 by I.M. Idriss and R.W. Boulanger (2008) published by the Earthquake Engineering Research Institute.

Soil Stress Conditions -

average total unit weight of soil $\gamma_{total} := 115pcf$

unit weight of water $\gamma_{water} := 62.4pcf$

water table depth below ground surface $d_w := 5ft$

sample depth Boring S-10 Depth 24' $z := 24ft$

total vertical stress $\sigma tot_v := \gamma_{total} \cdot z$ $\sigma tot_v = 2760 \cdot psf$

static water pressure $u_o := (z - d_w) \cdot \gamma_{water}$ $u_o = 1186 \cdot psf$

effective vertical stress $\sigma eff_v := \sigma tot_v - u_o$ $\sigma eff_v = 1574 \cdot psf$

Standard Penetration N-value Correction -

Standard Penetration Test N-value $N_m := 17$

fines content $FC := 13$

energy correction $C_E := 1.46$

borehole diameter correction $C_B := 1.05$

rod length correction $C_R := 0.95$

sampler correction $C_S := 1$

Hammer	CE
Doughnut	0.5-1.0
Safety	0.7-1.2
Automatic	0.8-1.3

(Skempton, 1986)

Borehole dia.	CB
65-115mm	1.0
150mm	1.05
200mm	1.15

(Skempton, 1986)

Rod length	CR
<3m	0.75
3-4m	0.80
4-6m	0.85
6-10m	0.95
10-30m	1.00

SPT N-value for an energy ratio of 60% $N_{60} := C_E \cdot C_B \cdot C_R \cdot C_S \cdot N_m$

$N_{60} = 24.8$

overburden correction factor
(based on overburden stress only)

$$C_{N\_a} := \left(\frac{P_a}{\sigma eff_v}\right)^{0.5}$$

$C_{N\_a} = 1.159$

normalized SPT N-value
(based on overburden stress only) $N_{1\_60} := C_{N\_a} \cdot N_{60}$ $N_{1\_60} = 28.7$

Project **Lowman PP Sec J EL 19**
Project No. **16-099**
Sheet **2** **of** **4**
Date **9 / 6 / 2016**
Engineer **TCS**
Checked by **DD**

---

overburden correction factor
(based on overburden stress and
relative density)

$$C_{N\_b} := \left(\frac{P_a}{\sigma eff_v}\right)^{0.784-0.078\cdot\left(N_{1\_60}\right)^{0.5}}$$

$$C_{N\_b} = 1.114$$

overburden correction factor
used in liquefaction analysis
(max CN = 1.7)

$$C_N := 1.11$$

recalculated normalized SPT N-value

$$N_{1\_60} := C_N \cdot N_{60}$$

$$N_{1\_60} = 27.5$$

overburden correction factor
used in liquefaction analysis

$$C_{N\_check} := \left(\frac{P_a}{\sigma eff_v}\right)^{0.784-0.078\cdot\left(N_{1\_60}\right)^{0.5}}$$

$$C_{N\_check} = 1.117$$

fines content adjustment to SPT N-value

$$\Delta N_{1\_60} := \exp\left[1.63 + \frac{9.7}{FC + 0.01} - \left(\frac{15.7}{FC + 0.01}\right)^2\right]$$

$$\Delta N_{1\_60} = 2.5$$

normalized SPT N-value (clean sands)

$$N_{1\_60\_cs} := N_{1\_60} + \Delta N_{1\_60}$$

$$N_{1\_60\_cs} = 30$$

Earthquake Conditions -

peak ground accelerationl

$$a_{max} := 0.1\,g$$

earthquake moment magnitude

$$M_w := 7.5$$

variable α for stress reduction factor

$$\alpha := -1.012 - 1.126\cdot\sin\left(\frac{\frac{z}{3.28ft}}{11.73} + 5.133\right)$$

variable β for stress reduction factor

$$\beta := 0.106 + 0.118\sin\left(\frac{\frac{z}{3.28ft}}{11.28} + 5.142\right)$$

Project Lowman PP Sec J EL 19
Project No. 16-099
Sheet 3 of 4
Date 9 / 6 / 2016
Engineer TCS
Checked by DD

---

stress reduction factor $r_d := \exp(\alpha + \beta \cdot M_w)$ $r_d = 0.933$

Liquefaction Calculations -

cyclic stress ratio $CSR := 0.65 \cdot \frac{\sigma tot_v}{\sigma eff_v} \cdot \frac{a_{max}}{g} \cdot r_d$ $CSR = 0.106$

cyclic resistance ratio

$$CRR_{M7.5\_\sigma eff1} := \exp\left[\frac{N_{1\_60\_cs}}{14.1} + \left(\frac{N_{1\_60\_cs}}{126}\right)^2 - \left(\frac{N_{1\_60\_cs}}{23.6}\right)^3 + \left(\frac{N_{1\_60\_cs}}{25.4}\right)^4 - 2.8\right]$$

magnitude scaling factor
(maximum MSF = 1.8)

$MSF := 6.9 \exp\left(\frac{-M_w}{4}\right) - 0.058$ $MSF = 1$

coefficient for overburden correction factor
(maximum Cσ=0.3)

$C_\sigma := \frac{1}{18.9 - 2.55 \cdot \left(N_{1\_60}\right)^{0.5}}$ $C_\sigma = 0.181$

overburden correction factor
(maximum Kσ=1.1)

$K_\sigma := 1 - C_\sigma \cdot \ln\left(\frac{\sigma eff_v}{P_a}\right)$ $K_\sigma = 1.053$

estimated static shear stress on horizontal plane $Tho := 35psf$

effective friction angle $\phi_{eff} := \operatorname{atan}\left(\frac{N_{60}}{12.2 + 20.3 \cdot \frac{\sigma eff_v}{P_a}}\right)^{0.34}$ $\phi_{eff} = 51.638 \cdot deg$

Ko for NC soil $K_o := \left(1 - \sin\left(\phi_{eff}\right)\right)$ $K_o = 0.216$

empirical constant for dilatancy $Q := 10$

Grain type.	Q
quartz and feldspar	10
limestone	8
anthracite	7
chalk	5.5

Project Lowman PP Sec J EL 19
Project No. 16-099
Sheet 4 **of** 4
Date 9 / 6 / 2016
Engineer TCS
Checked by DD

---

relative state parameter
(-0.61<ξR<0.11)

$$\zeta_R := \frac{1}{Q - \ln\left[\frac{100\cdot\left(1 + 2K_o\right)\sigma eff_v}{3\cdot P_a}\right]} - \left(\frac{N_{1\_60}}{46}\right)^{0.5} \qquad \zeta_R = -0.617$$

alpha factor
(maximum α=0.35)

$$\alpha\_factor := \frac{\tau_{ho}}{\sigma eff_v} \qquad \alpha\_factor = 0.022$$

$$a := 1267 + 636\alpha\_factor^2 - 634\cdot \exp(\alpha\_factor) - 632\cdot \exp(-\alpha\_factor)$$

$$b := \exp\left(-1.11 + 12.3\alpha\_factor^2 + 1.31\cdot \ln(\alpha\_factor + 0.0001)\right)$$

$$c := 0.138 + 0.126\cdot\alpha\_factor + 2.52\cdot\alpha\_factor^3$$

static shear stress correction factor

$$K_\alpha := a + b\cdot \exp\left(\frac{-\zeta_R}{c}\right) \qquad K_\alpha = 1.14$$

corrected cyclic stress ratio

$$CRR_{M\_\sigma effv} := CRR_{M7.5\_\sigma eff1}\cdot MSF\cdot K_\sigma\cdot K_\alpha$$

factor of safety for liquefaction

$$FS_{liq} := \frac{CRR_{M\_\sigma effv}}{CSR} \qquad FS_{liq} = 5.47$$

Project Lowman PP Sec K EL 12
Project No. 16-099
Sheet 1 of 4
Date 9 / 6 / 2016
Engineer TCS
Checked by DD

The following calculations for liquefaction of soils with sand-like behavior are based on Soil Liquefaction During Earthquakes - Monograph MNO-12 by I.M. Idriss and R.W. Boulanger (2008) published by the Earthquake Engineering Research Institute.

Soil Stress Conditions -

average total unit weight of soil $\gamma_{total} := 115pcf$

unit weight of water $\gamma_{water} := 62.4pcf$

water table depth below ground surface $d_w := 7ft$

sample depth Boring T-3 Depth 30 $z := 30ft$

total vertical stress $\sigma tot_v := \gamma_{total} \cdot z$ $\sigma tot_v = 3450 \cdot psf$

static water pressure $u_o := \left(z - d_w\right) \cdot \gamma_{water}$ $u_o = 1435 \cdot psf$

effective vertical stress $\sigma eff_v := \sigma tot_v - u_o$ $\sigma eff_v = 2015 \cdot psf$

Standard Penetration N-value Correction -

Standard Penetration Test N-value $N_m := 16$

fines content $FC := 10.3$

energy correction $C_E := 1.46$

borehole diameter correction $C_B := 1.00$

rod length correction $C_R := 0.95$

sampler correction $C_S := 1$

Hammer	CE
Doughnut	0.5-1.0
Safety	0.7-1.2
Automatic	0.8-1.3

(Skempton, 1986)

Borehole dia.	CB
65-115mm	1.0
150mm	1.05
200mm	1.15

(Skempton, 1986)

Rod length	CR
<3m	0.75
3-4m	0.80
4-6m	0.85
6-10m	0.95
10-30m	1.00

SPT N-value for an energy ratio of 60% $N_{60} := C_E \cdot C_B \cdot C_R \cdot C_S \cdot N_m$

$N_{60} = 22.2$

overburden correction factor
(based on overburden stress only)

$$C_{N\_a} := \left(\frac{P_a}{\sigma eff_v}\right)^{0.5}$$

$C_{N\_a} = 1.025$

normalized SPT N-value
(based on overburden stress only) $N_{1\_60} := C_{N\_a} \cdot N_{60}$ $N_{1\_60} = 22.7$

Project <u>Lowman PP Sec K EL 12</u>
Project No. <u>16-099</u>
Sheet <u>2</u> **of** <u>4</u>
Date <u>9 / 6 / 2016</u>
Engineer <u>TCS</u>
Checked by <u>DD</u>

---

overburden correction factor (based on overburden stress and relative density)

$$C_{N\_b} := \left(\frac{P_a}{\sigma eff_v}\right)^{0.784-0.078\cdot\left(N_{1\_60}\right)^{0.5}}$$

$$C_{N\_b} = 1.02$$

overburden correction factor used in liquefaction analysis (max CN = 1.7)

$$C_N = 1$$

recalculated normalized SPT N-value

$$N_{1\_60} := C_N \cdot N_{60}$$

$$N_{1\_60} = 22.2$$

overburden correction factor used in liquefaction analysis

$$C_{N\_check} := \left(\frac{P_a}{\sigma eff_v}\right)^{0.784-0.078\cdot\left(N_{1\_60}\right)^{0.5}}$$

$$C_{N\_check} = 1.021$$

fines content adjustment to SPT N-value

$$\Delta N_{1\_60} := \exp\left[1.63 + \frac{9.7}{FC + 0.01} - \left(\frac{15.7}{FC + 0.01}\right)^2\right]$$

$$\Delta N_{1\_60} = 1.3$$

normalized SPT N-value (clean sands)

$$N_{1\_60\_cs} := N_{1\_60} + \Delta N_{1\_60}$$

$$N_{1\_60\_cs} = 23.5$$

Earthquake Conditions -

peak ground accelerationl $a_{max} = 0.1 g$

earthquake moment magnitude $M_w = 7.5$

variable α for stress reduction factor

$$\alpha := -1.012 - 1.126\cdot\sin\left(\frac{\frac{z}{3.28ft}}{11.73} + 5.133\right)$$

variable β for stress reduction factor

$$\beta := 0.106 + 0.118\sin\left(\frac{\frac{z}{3.28ft}}{11.28} + 5.142\right)$$

Project Lowman PP Sec K EL 12
Project No. 16-099
Sheet 3 of 4
Date 9 / 6 / 2016
Engineer TCS
Checked by DD

---

stress reduction factor $r_d := \exp(\alpha + \beta \cdot M_w)$ $r_d = 0.908$

Liquefaction Calculations -

cyclic stress ratio $CSR := 0.65 \cdot \frac{\sigma tot_v}{\sigma eff_v} \cdot \frac{a_{max}}{g} \cdot r_d$ $CSR = 0.101$

cyclic resistance ratio

$$CRR_{M7.5\_\sigma eff1} := \exp\left[\frac{N_{1\_60\_cs}}{14.1} + \left(\frac{N_{1\_60\_cs}}{126}\right)^2 - \left(\frac{N_{1\_60\_cs}}{23.6}\right)^3 + \left(\frac{N_{1\_60\_cs}}{25.4}\right)^4 - 2.8\right]$$

magnitude scaling factor
(maximum MSF = 1.8) $MSF := 6.9\exp\left(\frac{-M_w}{4}\right) - 0.058$ $MSF = 1$

coefficient for overburden correction factor
(maximum Cσ=0.3) $C_\sigma := \frac{1}{18.9 - 2.55 \cdot (N_{1\_60})^{0.5}}$ $C_\sigma = 0.145$

overburden correction factor
(maximum Kσ=1.1) $K_\sigma := 1 - C_\sigma \cdot \ln\left(\frac{\sigma eff_v}{P_a}\right)$ $K_\sigma = 1.007$

estimated static shear stress on horizontal plane $Tho := 35psf$

effective friction angle $\phi_{eff} := \operatorname{atan}\left(\frac{N_{60}}{12.2 + 20.3 \cdot \frac{\sigma eff_v}{P_a}}\right)^{0.34}$ $\phi_{eff} = 48.521 \cdot deg$

Ko for NC soil $K_o := (1 - \sin(\phi_{eff}))$ $K_o = 0.251$

empirical constant for dilatancy $Q := 10$

Grain type.	Q
quartz and feldspar	10
limestone	8
anthracite	7
chalk	5.5

Project Lowman PP Sec K EL 12
Project No. 16-099
Sheet 4 **of** 4
Date 9 / 6 / 2016
Engineer TCS
Checked by DD

---

relative state parameter
(-0.61<ξR<0.11)

$$\zeta_R := \frac{1}{Q - \ln\left[\frac{100\cdot(1 + 2K_o)\sigma eff_v}{3\cdot P_a}\right]} - \left(\frac{N_{1\_60}}{46}\right)^{0.5} \qquad \zeta_R = -0.532$$

alpha factor
(maximum α=0.35)

$$\alpha\_factor := \frac{\tau_{ho}}{\sigma eff_v} \qquad \alpha\_factor = 0.017$$

$$a := 1267 + 636\alpha\_factor^2 - 634\cdot\exp(\alpha\_factor) - 632\cdot\exp(-\alpha\_factor)$$

$$b := \exp\left(-1.11 + 12.3\alpha\_factor^2 + 1.31\cdot\ln(\alpha\_factor + 0.0001)\right)$$

$$c := 0.138 + 0.126\cdot\alpha\_factor + 2.52\cdot\alpha\_factor^3$$

static shear stress correction factor

$$K_\alpha := a + b\cdot\exp\left(\frac{-\zeta_R}{c}\right) \qquad K_\alpha = 1.039$$

corrected cyclic stress ratio

$$CRR_{M\_\sigma effv} := CRR_{M7.5\_\sigma eff1}\cdot MSF\cdot K_\sigma\cdot K_\alpha$$

factor of safety for liquefaction

$$FS_{liq} := \frac{CRR_{M\_\sigma effv}}{CSR} \qquad FS_{liq} = 2.67$$

This sample is classified as non-plastic.

Project Lowman PP Sec L EL 29
Project No. 16-099
Sheet 1 of 4
Date 9 / 6 / 2016
Engineer TCS
Checked by DD

The following calculations for liquefaction of soils with sand-like behavior are based on Soil Liquefactio
During Earthquakes - Monograph MNO-12 by I.M. Idriss and R.W. Boulanger (2008) published by the Earthquake Engineering Research Institute.

Soil Stress Conditions -

average total unit weight of soil $\gamma_{total} := 115pcf$

unit weight of water $\gamma_{water} := 62.4pcf$

water table depth below ground surface $d_w := 8ft$

sample depth Boring S-12 Depth 14' $z := 14ft$

total vertical stress $\sigma tot_v := \gamma_{total} \cdot z$ $\sigma tot_v = 1610 \cdot psf$

static water pressure $u_o := (z - d_w) \cdot \gamma_{water}$ $u_o = 374 \cdot psf$

effective vertical stress $\sigma eff_v := \sigma tot_v - u_o$ $\sigma eff_v = 1236 \cdot psf$

Standard Penetration N-value Correction -

Standard Penetration Test N-value $N_m := 36$

fines content $FC := 8.4$

energy correction $C_E := 1.46$

borehole diameter correction $C_B := 1.05$

rod length correction $C_R := 0.85$

sampler correction $C_S := 1$

<u>Hammer</u>	<u>CE</u>
Doughnut	0.5-1.0
Safety	0.7-1.2
Automatic	0.8-1.3
(Skempton, 1986)	

<u>Borehole dia.</u>	<u>CB</u>
65-115mm	1.0
150mm	1.05
200mm	1.15
(Skempton, 1986)	

SPT N-value for an energy ratio of 60% $N_{60} := C_E \cdot C_B \cdot C_R \cdot C_S \cdot N_m$

$N_{60} = 46.9$

<u>Rod length</u>	<u>CR</u>
<3m	0.75
3-4m	0.80
4-6m	0.85
6-10m	0.95
10-30m	1.00

overburden correction factor
(based on overburden stress only)

$$C_{N\_a} := \left(\frac{P_a}{\sigma eff_v}\right)^{0.5}$$

$C_{N\_a} = 1.309$

normalized SPT N-value
(based on overburden stress only) $N_{1\_60} := C_{N\_a} \cdot N_{60}$ $N_{1\_60} = 61.4$

Project _Lowman PP Sec L EL 29_
Project No._16-099_
Sheet _2_ of _4_
Date _9 / 6 / 2016_
Engineer_TCS_
Checked by_DD_

---

overburden correction factor
(based on overburden stress and
relative density)

$$C_{N\_b} := \left(\frac{P_a}{\sigma eff_v}\right)^{0.784-0.078\cdot\left(N_{1\_60}\right)^{0.5}}$$

$$C_{N\_b} = 1.097$$

overburden correction factor
used in liquefaction analysis
(max CN = 1.7)

$$C_N := 1.1$$

recalculated normalized SPT N-value

$$N_{1\_60} := C_N \cdot N_{60}$$

$$N_{1\_60} = 51.6$$

overburden correction factor
used in liquefaction analysis

$$C_{N\_check} := \left(\frac{P_a}{\sigma eff_v}\right)^{0.784-0.078\cdot\left(N_{1\_60}\right)^{0.5}}$$

$$C_{N\_check} = 1.128$$

fines content adjustment to SPT N-value

$$\Delta N_{1\_60} := \exp\left[1.63 + \frac{9.7}{FC + 0.01} - \left(\frac{15.7}{FC + 0.01}\right)^2\right]$$

$$\Delta N_{1\_60} = 0.5$$

normalized SPT N-value (clean sands)

$$N_{1\_60\_cs} := N_{1\_60} + \Delta N_{1\_60}$$

$$N_{1\_60\_cs} = 52.1$$

Earthquake Conditions -

peak ground accelerationl $a_{max} := 0.1\,g$

earthquake moment magnitude $M_w := 7.5$

variable α for stress reduction factor

$$\alpha := -1.012 - 1.126\cdot\sin\left(\frac{\frac{z}{3.28ft}}{11.73} + 5.133\right)$$

variable β for stress reduction factor

$$\beta := 0.106 + 0.118\,\sin\left(\frac{\frac{z}{3.28ft}}{11.28} + 5.142\right)$$

Project Lowman PP Sec L EL 29
Project No. 16-099
Sheet 3 of 4
Date 9 / 6 / 2016
Engineer TCS
Checked by DD

---

stress reduction factor $r_d := \exp\left(\alpha + \beta \cdot M_w\right)$ $r_d = 0.969$

Liquefaction Calculations -

cyclic stress ratio $CSR := 0.65 \cdot \frac{\sigma tot_v}{\sigma eff_v} \cdot \frac{a_{max}}{g} \cdot r_d$ $CSR = 0.082$

cyclic resistance ratio

$$CRR_{M7.5\_\sigma eff1} := \exp\left[\frac{N_{1\_60\_cs}}{14.1} + \left(\frac{N_{1\_60\_cs}}{126}\right)^2 - \left(\frac{N_{1\_60\_cs}}{23.6}\right)^3 + \left(\frac{N_{1\_60\_cs}}{25.4}\right)^4 - 2.8\right]$$

magnitude scaling factor
(maximum MSF = 1.8)
$MSF := 6.9\exp\left(\frac{-M_w}{4}\right) - 0.058$ $MSF = 1$

coefficient for overburden correction factor
(maximum Cσ=0.3)
$C_\sigma := \frac{1}{18.9 - 2.55 \cdot \left(N_{1\_60}\right)^{0.5}}$ $C_\sigma = 1.717$

overburden correction factor
(maximum Kσ=1.1)
$K_\sigma := 1 - C_\sigma \cdot \ln\left(\frac{\sigma eff_v}{P_a}\right)$ $K_\sigma = 1.924$

estimated static shear stress on horizontal plane $\tau_{ho} := 35psf$

effective friction angle $\phi_{eff} := \operatorname{atan}\left(\frac{N_{60}}{12.2 + 20.3 \cdot \frac{\sigma eff_v}{P_a}}\right)^{0.34}$ $\phi_{eff} = 59.128 \cdot deg$

Ko for NC soil $K_o := \left(1 - \sin\left(\phi_{eff}\right)\right)$ $K_o = 0.142$

empirical constant for dilatancy $Q := 10$

Grain type.	Q
quartz and feldspar	10
limestone	8
anthracite	7
chalk	5.5

Project Lowman PP Sec L EL 29
Project No. 16-099
Sheet 4 of 4
Date 9 / 6 / 2016
Engineer TCS
Checked by DD

---

relative state parameter
(-0.61<ξR<0.11)

$$\zeta_R := \frac{1}{Q - \ln\left[\frac{100\cdot\left(1 + 2K_o\right)\sigma eff_v}{3\cdot P_a}\right]} - \left(\frac{N_{1\_60}}{46}\right)^{0.5} \qquad \zeta_R = -0.912$$

alpha factor
(maximum α=0.35)

$$\alpha\_factor := \frac{\tau_{ho}}{\sigma eff_v} \qquad \alpha\_factor = 0.028$$

$$a := 1267 + 636\alpha\_factor^2 - 634\cdot\exp(\alpha\_factor) - 632\cdot\exp(-\alpha\_factor)$$

$$b := \exp\left(-1.11 + 12.3\alpha\_factor^2 + 1.31\cdot\ln(\alpha\_factor + 0.0001)\right)$$

$$c := 0.138 + 0.126\cdot\alpha\_factor + 2.52\cdot\alpha\_factor^3$$

static shear stress correction factor

$$K_\alpha := a + b\cdot\exp\left(\frac{-\zeta_R}{c}\right) \qquad K_\alpha = 2.906$$

corrected cyclic stress ratio

$$CRR_{M\_\sigma effv} := CRR_{M7.5\_\sigma eff1}\cdot MSF\cdot K_\sigma\cdot K_\alpha$$

factor of safety for liquefaction

$$FS_{liq} := \frac{CRR_{M\_\sigma effv}}{CSR} \qquad FS_{liq} = 2.04\times 10^5$$

CDG

Engineering. Environmental. Answers.

ALBERTVILLE
417 Martling Road
PO Box 2079 [35950]
Albertville, AL 35951
256.891.3458 Phone
256.891.3459 FAX

ANDALUSIA
1840 E. Three Notch St.
PO Box 278 (36420)
Andalusia, AL 36421
334.222.9431Phone
334.222.4018 FAX

AUBURN
778 North Dean Road Ste. 200A
PO Box 2155 (36831)
Auburn, AL 36830
334.466.9431 Phone
334.466.9430 FAX

BIRMINGHAM
100 Concourse Parkway,
Ste. 170
Hoover, AL 35244
205.403.2600 Phone
205.403.2623 FAX

DOTHAN
1830 Hartford Hwy.
Dothan, AL 36301
334.677.9431 Phone
334.677.9450 FAX

HUNTSVILLE
612 Wheeler Ave. N.W.
Huntsville, AL 35801
256.539.7470 Phone
256.539.7473 FAX